

**HASAN KALYONCU UNIVERSITY
GRADUATE SCHOOL OF
NATURAL & APPLIED SCIENCES**

**MIX OPTIMIZATION AND EXPERIMENTAL
EVALUATION OF LIGHTWEIGHT GEOPOLYMER
MORTARS**

**Ph.D. THESIS
IN
CIVIL ENGINEERING**

**BY
SAFIE MAHDI OLEIWI
MARCH 2017**

**Mix Optimization and Experimental Evaluation of Lightweight
Geopolymer Mortars**

**Ph.D. Thesis
In
Civil Engineering**

**Mix Optimization and Experimental Evaluation of Lightweight
Geopolymer Mortars**

Ph.D. Thesis

In

Civil Engineering

Hasan Kalyoncu University

Supervisor

Assoc. Prof. Dr. Kasım MERMERDAŞ

By

Safie Mahdi Olewi

March 2017



© 2017 [Safie Mahdi Oleiwi]

T.C.
HASAN KALYONCU UNIVERSITY
GRADUATE SCHOOL OF NATURAL & APPLIED SCIENCES
CIVIL ENGINEERING DEPARTMENT

Name of the thesis: Mix Optimization and Experimental Evaluation of Lightweight Geopolymer Mortars


Name of the student: Safie Mahdi Olewi

Exam date: 30 - 03 -2017

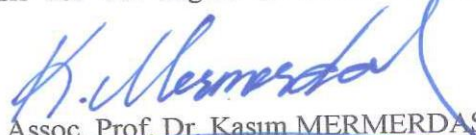
Approval of the Graduate School of Natural and Applied Sciences


Prof. Dr. Mehmet KARPUZCU
Director

I certify that this thesis satisfies all the requirements as a thesis for the degree of Ph.D. of Science.


Assist. Prof. Dr. Şafak Hengirmen TERCAN
Head of Civil Engineering Department

This is to certify that we have read this thesis and that in our opinion it is fully adequate, in scope and quality, as a thesis for the degree of Ph.D. in civil engineering.


Assoc. Prof. Dr. Kasım MERMERDAŞ
Supervisor

Examining Committee Members

Prof. Dr. Hanifi ÇANAKCI

Assoc. Prof. Dr. Kasım MERMERDAŞ

Assoc. Prof. Dr. M. Fatih HASOĞLU

Assist. Prof. Dr. Dia Eddin NASSANI

Assist. Prof. Dr. Hasan Selçuk SELEK

Signature







I hereby declare that all information in this document has been obtained and presented in accordance with academic rules and ethical conduct. I also declare that, as required by these rules and conduct, I have fully cited and referenced all material and results that are not original to this work.

Safie Mahdi OLEIWI

ABSTRACT
MIX OPTIMIZATION AND EXPERIMENTAL EVALUATION OF
LIGHTWEIGHT GEOPOLYMER MORTARS

OLEIWI, Safie Mahdi Oleiwi
Ph.D. in Civil Engineering

Supervisor: Assoc. Prof. Dr. Kasım MERMERDAŞ

March 2017, 163 pages

The main purpose of this thesis is to propose a comprehensive procedure to obtain optimum mixture proportions for lightweight geopolymer mortar (LWGM) through experimental evaluation and analytical optimization method. In the first stage of the study, the effect of binder content, curing temperature and curing time on the compressive strength of LWGM were investigated. The base materials used for LWGM are ground granulated blast furnace slag (GGBFS) and fly ash (FA). The main components of LWGM are lightweight pumice aggregate and alkali activated FA or GGBFS binder. Effectiveness of aforementioned parameters was examined in terms of variation of the compressive strengths of LWGMs. The experiments were performed on LWGM cubes under curing temperatures of 60, 80, 100 and 120 °C with curing period of 2, 6, 8, 24, 48 and 72 h. The alkaline activator is a mix of 12 M NaOH solution with sodium silicate in ratio of 1:2.5. The ratio of alkaline solution to binder was taken as 0.50. 7 binder contents were taken between 650 to 1250 kg/m³ with 100 kg/m³ increment. Full factorial experimental program was adopted to observe compressive strength development of LWGMs. Therefore, 336 data samples were obtained. The second stage of the study is to optimize those experimental parameters through response surface method (RSM). Test results indicate that the increment in the binder content increases the compressive strength of LWGM. The strength increases with the increase of curing temperature and curing period of LWGM. The experimental verification indicated a good agreement with optimized results. The third stage of the study is to examine the effect of different sodium hydroxide concentration and sodium silicate to sodium hydroxide (Na₂SiO₃/NaOH) ratio on the workability and strength properties of LWGMs. Moreover, this stage covers another optimization study by RSM. The experiments were performed on LWGM cubes under curing temperatures and curing periods obtained from optimization study in the second stage. The alkaline activator is a mix of 8, 10, 12 and 14 M NaOH solutions with sodium silicate in ratio of 1:0.5, 1:1, 1:1.5, 1:2 and 1:2.5. The ratio of alkaline solution to binder was taken as 0.50. A fixed binder contents were taken 950 kg/m³ for the base materials. Test results indicate that the increment in the Na₂SiO₃/NaOH ratio up to an optimum value increases the strength and decreases water absorption of LWGM. The increment in NaOH concentration from 8 to 14 M increases the strength and decreases water absorption of LWGM. The strength of GGBFS-based LWGM with different NaOH concentration and Na₂SiO₃/NaOH ratio is greater than that of FA-based LWGM.

Keywords: Curing regime, Geopolymer, Fly ash, Compressive strength, Lightweight mortar, Response surface method, Optimization

ÖZET

HAFİF GEOPOLİMER HARÇLARIN DENEYSSEL OLARAK İNCELENMESİ VE KARIŞIM OPTİMİZASYONU

OLEIWI, Safie Mahdi Olewi
İnşaat Mühendisliği Doktora Tezi
Danışman: Doç. Dr. Kasım MERMERDAŞ
Mart 2017, 163 sayfa

Bu tezin temel amacı, deneysel değerlendirme ve analitik optimizasyon tekniği ile hafif geopolimer harç (HGH) için optimum karışım oranlarını elde etmek için kapsamlı bir yöntem önermektir. Çalışmanın ilk aşamasında, bağlayıcı içeriğinin, kütleme sıcaklığının ve kütleme süresinin HGH'nin basınç dayanımına etkisi araştırıldı. Geopolimer bağlayıcı için kullanılan ana malzemeler, öğütülmüş yüksek fırın cürufu (YFC) ve uçucu küldür (UK). HGH'nin ana bileşenleri hafif pomza agregası ve alkali ile aktive edilmiş UK veya YFC bağlayıcısıdır. Bahsedilen parametrelerin etkinliği, HGH'lerin basınç dayanımlarının değişimi açısından incelenmiştir. Deneyler 2, 6, 8, 24, 48 ve 72 saatlik kür periyodu ile 60, 80, 100 ve 120 °C'lik kür sıcaklıklarında HGH küpleri üzerinde gerçekleştirilmiştir. Alkali aktivatör, 12 M NaOH çözeltisinin 1:2.5 oranında sodyum silikat ile karışımıdır. Alkali çözeltisinin bağlayıcıya oranı 0.50 olarak alınmıştır. 7 bağlayıcı içeriği 650 kg/m³ ile 1250 kg/m³ arasında 100 kg/m³ artışla alınmıştır. Tam faktöriyel deneysel bir program HGH'lerin basınç dayanımı gelişimini gözlemlemek için uygulanmıştır. Bu nedenle, 336 veri örneği elde edilmiştir. Çalışmanın ikinci aşaması tepki yüzey metodu (TYM) ile bu deneysel parametreleri optimize etmektir. Test sonuçları bağlayıcı içeriğinin artışı ile HGH basınç dayanımının arttığını göstermektedir. HGH'nin dayanımının kütleme süresi ve sıcaklığının artmasıyla arttığı tespit edilmiştir. Deneysel doğrulama, optimize edilmiş sonuçlarla iyi bir uyum olduğunu göstermektedir. Çalışmanın üçüncü aşaması, farklı sodyum hidroksit konsantrasyonu ve sodyum silikatın sodyum hidroksit (Na₂SiO₃/NaOH) oranının HGH'lerin işlenebilirliği ve mukavemet özelliklerine olan etkisini incelemektir. Ayrıca çalışmanın bu aşamasında TYM kullanılarak başka bir optimizasyon çalışması da verilmiştir. Bu aşamadaki deneyler, ikinci aşamadaki optimizasyon çalışmasından elde edilen kütleme sıcaklıkları ve kütleme süreleri alınarak HGH küpleri üzerinde gerçekleştirilmiştir. Alkali aktivatör 8, 10, 12 ve 14 M NaOH solüsyonunun 1:0.5, 1:1, 1:1.5, 1:2 ve 1:2.5 oranında sodyum silikat ile karışımıdır. Taban malzemeleri için sabit bir bağlayıcı içeriği 950 kg/m³ alınmıştır. Test sonuçları, optimum değere kadar Na₂SiO₃/NaOH oranındaki artışın dayanımı artıracağını ve HGH'nin su emilimini azalttığını göstermektedir. NaOH konsantrasyonunun 8'den 14 M değerine çıkması HGH'nin mukavemetini artırır ve su emmesini azaltır. Farklı NaOH konsantrasyonuna ve Na₂SiO₃/NaOH oranına sahip YFC tabanlı HGH'nin mukavemeti, UK esaslı HGH'den daha yüksektir.

Anahtar Kelimeler: Kür rejimi, Geopolimer, Uçucu kül, Basınç dayanımı, Hafif harç, Tepki yüzeyi yöntemi, Optimizasyon



To My Father

ACKNOWLEDGEMENT

In the name of Allah, the Entirely Merciful, the especially merciful. First of all, I want to express my gratitude and thankfulness to the God almighty who is creator, the sovereign, and the sustainer of the universe and creatures. It is only through his mercy and help this work could be completed and I am hoping that this little effort be accepted by him.

I would like to express my gratitude to my supervisor Assoc. Prof. Dr. Kasım MERMERDAŞ, for his invaluable help, advices and directions during this thesis.

Special thanks are reserved for Prof. Dr. Hanifi ÇANAKCI, Assoc. Prof. Dr. M. Fatih HASOĞLU, Assist. Prof. Dr. Dia Eddin NASSANI, and Assist. Prof. Dr. Hasan Selçuk SELEK for serving on the committee and their contributions and suggestions to improve the quality of the thesis. Moreover, contribution from Assist. Prof. Dr. Zeynep ALGIN is highly appreciated.

Special thanks to Diyala University – Iraq and its academic staff for giving me the opportunity to study in Turkey.

Finally, I would like to give special acknowledgment to my family, my mother, my brothers and my wife for having the management of family and taking care of my children while I was out of the country.

TABLE OF CONTENTS

ABSTRACT	V
ÖZET	VI
DEDICATION	VII
ACKNOWLEDGEMENT	VIII
TABLE OF CONTENTS	IX
CHAPTER 1	1
INTRODUCTION	1
1.1 General	1
1.2 Objectives and Scope of the Work	2
1.3 Thesis Layout	3
CHAPTER 2	5
LITERATURE REVIEW	5
2.1 Introduction	5
2.2 Mechanism of Geopolymerization	6
2.3 Structure of Geopolymer	8
2.4 Materials of Geopolymer Mortar	9
2.4.1 Alkali Activation of Fly Ash	9
2.2.2 Alkali Activation of Slag	10
2.4.3 Sodium Hydroxide, NaOH	11
2.4.3 Sodium Silicate, Na ₂ SiO ₃	13
2.5 Mixing Geopolymer Mortar	16
2.6 Curing of Geopolymer Mortar	16
2.7 Mechanical Properties of Geopolymer Mortar.....	21
2.7.1 Compressive Strength	21
2.7.2 Splitting Tensile Strength	25
2.7.3 Sorptivity and Water Absorption.....	28
2.8 Concluding Remarks	31
CHAPTER 3	32
MATERIALS AND EXPERIMENTAL WORK	32

3.1 Materials.....	32
3.1.1 Aggregate.....	32
3.1.2 Pozzolanic Materials.....	33
3.1.3 Sodium Hydroxide, NaOH	34
3.1.4 Sodium Silicate, Na ₂ SiO ₃	35
3.1.5 Superplasticizer	36
3.1.6 Distilled Water.....	37
3.2 Mix Proportions.....	37
3.3 Experimental Study	38
3.4 Stage I: Manufacturing GGBFS and FA Based Geopolymer Mortar and Studying the Compressive Strength Development under Different Curing Period, Curing Temperature and Binder Content	39
3.4.1 Preparation Alkaline Solution for Geopolymer	39
3.4.2 Mixing, Casting, and Curing Regime	40
3.4.3 Fresh Density Test	45
3.4.4 Compressive Strength Test of Geopolymer Mortar Cubes	45
3.5 Stage II: Studying the Optimization and Verification of Optimum Curing Period and Curing Temperature on the Compressive Strength.....	46
3.5.1 Fresh Density Test	46
3.5.2 Mortar Flow Test	46
3.5.3 Compressive Strength Test of Geopolymer Mortar Cubes	47
3.5.4 Splitting Tensile Strength Test	48
3.5.5 Saturated Water Absorption	49
3.5.6 Sorptivity	50
3.6 Stage II: Studying the Effect of Molarity and Different Ratios of Na ₂ SiO ₃ /NaOH on Mechanical Properties and Absorption of Fly Ash and GGBF Geopolymer Mortar	51
CHAPTER 4	52
TEST RESULTS AND DISCUSSION	52
4.1 General	52
4.2 Fresh Properties Tests	52
4.2.1 Flow Table Test	52
4.2.2 Fresh Density Test	54
4.3 Compressive Strength Test.....	55
4.3.1 Effect of the Binder Content on the Strength of Slag Based Geopolymer Mortar	55

4.3.2 Effect of the Binder Content on the Strength of Fly Ash Based Geopolymer Mortar	56
4.3.4 Effect of Curing Duration and Curing Temperature.....	58
4.3.4.1 GGBFS Based Geopolymer Mortar	58
4.3.4.2 Fly Ash Based Geopolymer Mortar	67
CHAPTER 5	75
OPTIMIZATION OF TEST PARAMETERS AND VERIFICATION	75
5.1 General	75
5.2 The Optimization Procedure Applied Experimental Data	75
5.3 Optimization Results	76
5.4 Additional Tests	84
5.4.1 Compressive Strength	84
5.4.2 Splitting Tensile Strength Test	86
5.4.2.1 Relationship between Compressive and Splitting Tensile Strength of LWGM.....	88
5.4.3 Sorptivity	92
5.4.4 Water Absorption	97
CHAPTER 6	101
EXPERIMENTAL STUDY AND OPTIMIZATION OF EFFECT OF MOLARITY AND Na₂SiO₃/NaOH RATIO	101
6.1 Introduction	101
6.2. Mix Proportions.....	101
6.3 Fresh Properties Tests	105
6.3.1 Flow Table Test	105
6.3.2 Fresh Density Test	108
6.4 Hardened Properties Tests.....	111
6.4.1 Compressive Strength.....	111
6.4.1.1 Effect of NaOH Concentration on The Strength of FA Geopolymer Mortar	111
6.4.1.2 Effect of Na ₂ SiO ₃ to NaOH Ratio on the Strength Development of FA Based LWGM.....	111
6.4.1.3 Effect of NaOH Concentration on The Strength of GGBFS Geopolymer Mortar	113
6.4.1.4 Effect of Na ₂ SiO ₃ to NaOH Mass Ratio on the Strength Development of GGBFS Based LWGM.....	114
6.4.2 Splitting Tensile Strength Test	116
6.4.3 Sorptivity	119

6.4.4 Water Absorption	123
6.5 Optimization Study	126
CHAPTER 7	136
STEP-WISE REGRESSION AND GENETIC MODELING	136
7.1 General	136
7.2 Step-Wise Regression Relationships of Compressive Strength vs. Binder and Temperature for Various Curing Periods	136
7.2.1 GGBFS-Based Geopolymer Mortar	137
7.2.2 Fly Ash-Based Geopolymer Mortar	140
7.3 Step-Wise Regression Models for Compressive Strength in Terms of Binder Content and Curing Time for Various Curing Temperatures.....	144
7.3.1 GGBFS-Based Geopolymer Mortar	144
7.3.2 Fly Ash-Based Geopolymer Mortar	146
7.4 Step-Wise Regression Relationships of Compressive Strength vs. Binder, Curing Temperature, and Curing Time	149
7.5 Compressive Strength Modeling of Geopolymer Mortar Based on Gene Expression Programming	152
7.5.1 Brief Review of GEP	152
7.5.2 Numerical Application of GEP.....	155
7.5.3 GEP-Based Formulas of Compressive Strength.....	155
CHAPTER 8	161
CONCLUSIONS AND RECOMMENDATIONS.....	161
8.1 Conclusions	161
8.2 Recommendation for Future Study	163
REFERENCES.....	164

LIST OF FIGURES

Figure 2.1 Geopolymerization process (Duxson et al., 2007).	7
Figure 2.2 Polymeric precursor that form geopolymer (Davidovits, 2011).....	8
Figure 2.3 Mechanism of gel formations in alkali activated fly ash binder (Fernandez-Jimenez et al., 2005).	9
Figure 2.4 Compressive strength of FAGP with various NaOH concentrations (Hanjitsuwan et al., 2014).	11
Figure 2.5 Relation between NaOH concentrations (Molar) with compressive strength at 60 days (Somna et al., 2011).	12
Figure 2.6 Effect of SS/SH and S/L ratio on compressive strength (Yahya et al., 2015).	13
Figure 2.7 Compressive strength at different ages (Helmy, 2016).	14
Figure 2.8 Compressive strength and density at different ratios of $\text{Na}_2\text{SiO}_3/\text{NaOH}$ (Patcharapol, 2015)	15
Figure 2.9 The compressive strength of geopolymer mortars (Görhan and Kürklü, 2014).	17
Figure 2.10 Effect of curing temperature on f_c development (Mijarsh et al., 2015).	18
Figure 2.11 Effect of curing type on compressive strength (Salih et al., 2015).	19
Figure 2.12 Effect of Ca/Si on compressive strength at different curing temperatures (Huseien et al., 2016).	20
Figure 2.13 Effect of Bottom Ash content on geopolymer compressive strength at 7 days and 28 days (Hardjito and Fung, 2010).	21
Figure 2.14 Relationship between compressive strength and Si/Al ratio with different percent of alkali %. (Sinha et al., 2013).....	22
Figure 2.15 The effect of GGBFS on the compressive strength of mortar mixed with POFA and FA at the age of 28-day (Islam et al., 2014).	23
Figure 2.16 Compressive strength of the unexposed and exposed geopolymers to the elevated temperatures 400, 600 and 800 °C (Abdulkareem et al., 2014).....	24
Figure 2.17 Splitting tensile strength with different of alkaline activator to FA (Yellaiah et al., 2014).....	25
Figure 2.18 Splitting tensile strength at different curing temperature (Zhang et al., 2016).	26
Figure 2.19 Effect of solution types and curing temperature on tensile strength of GPM (Huseien et al., 2016)	27

Figure 2.20 Splitting strength for different SS/SH ratio and GGBFS content (Partha et al., 2014).	27
Figure 2.21 Effect of silica fume on water absorption and sorptivity of FA based geopolymer (Thokchom et al., 2011).....	29
Figure 2.22 Effect of GGBFS and NaOH concentration on water absorption (Mazumder et al., 2016).....	29
Figure 2.23 Effect of nano-silica on sorptivity coefficient (Deb et al., 2016).....	30
Figure 3.1 Grading of the aggregates.....	33
Figure 3.2 Water absorption of LWFA.....	33
Figure 3.3 Sodium hydroxide flakes.....	35
Figure 3.4 Sodium silicate solution (water glass).....	36
Figure 3.5 Dry materials for geopolymer mortar.....	40
Figure 3.6 Saturation surface dry lightweight fine aggregate (LWFA).....	41
Figure 3.7 Mixer used for manufacturing geopolymer mortar.....	41
Figure 3.8 Fresh geopolymer mortar after mixing.....	42
Figure 3.9 Geopolymer compacting and placing.....	43
Figure 3.10 Mortar sealing with a heat resistant film.....	44
Figure 3.11 Mortar curing.....	44
Figure 3.12 Mortar cube compressive strength test.....	45
Figure 3.13 Flow table test apparatuses.....	46
Figure 3.14 Photographic view of mortar flow.....	47
Figure 3.15 Cube specimens after split tensile test.....	49
Figure 3.16 Sorptivity test setup.....	50
Figure 4.1 Flow table of GGBFS geopolymer mortar.....	53
Figure 4.2 Flow table of FA geopolymer mortar.....	54
Figure 4.3 Compressive strength development of GGBFS based geopolymer mortar cured at 60°C for 650,750, 850,950,1050,1150 and 1250 kg/m ³ binder.....	56
Figure 4.4 Compressive strength of fly ash geopolymer mortar cured at 60°C for 650,750,850,950, 1050, 1150 and 1250 kg/m ³ binder.....	57
Figure 4.5 Effect of binder content on the variations of maximum compressive strength and fresh unit weight of LWGMs.....	58
Figure 4.6 Compressive strength development of GGBFS based lightweight geopolymer mortar with 650 kg/m ³ binder content.....	60
Figure 4.7 Compressive strength development of GGBFS based lightweight geopolymer mortar with 750 kg/m ³ binder content.....	61
Figure 4.8 Compressive strength development of GGBFS based lightweight geopolymer mortar with 850 kg/m ³ binder content.....	62

Figure 4.9 Compressive strength development of GGBFS based lightweight geopolymer mortar with 950 kg/m ³ binder content.	63
Figure 4.10 Compressive strength development of GGBFS based lightweight geopolymer mortar with 1050 kg/m ³ binder content.	64
Figure 4.11 Compressive strength development of GGBFS based lightweight geopolymer mortar with 1150 kg/m ³ binder content.	65
Figure 4.12 Compressive strength development of GGBFS based lightweight geopolymer mortar with 1250 kg/m ³ binder content.	66
Figure 4.13 Compressive strength development of fly ash based geopolymer with 650 kg/m ³ binder content at different curing duration and curing temperature.	68
Figure 4.14 Compressive strength development of fly ash based geopolymer with 750 kg/m ³ binder content at different curing duration and curing temperature.	69
Figure 4.15 Compressive strength development of fly ash based geopolymer with 850 kg/m ³ binder content at different curing duration and curing temperature.	70
Figure 4.16 Compressive strength development of fly ash based geopolymer with 950 kg/m ³ binder content at different curing duration and curing temperature.	71
Figure 4.17 Compressive strength development of fly ash based geopolymer with 1050 kg/m ³ binder content at different curing duration and curing temperature.	72
Figure 4.18 Compressive strength development of fly ash based geopolymer with 1150 kg/m ³ binder content at different curing duration and curing temperature.	73
Figure 4.19 Compressive strength development of fly ash based geopolymer with 1250 kg/m ³ binder content at different curing duration and curing temperature.	74
Figure 5.1 Variation of desirability function for the response of compressive strength based on the light-weight geopolymer mortars incorporated with FA.	79
Figure 5.2 Variation of desirability function for the response of compressive strength based on the light-weight geopolymer mortars incorporated with GGBFS.	80
Figure 5.3 The variation of the factors in terms of the desirability and the response for the light-weight geopolymer mortars incorporated with FA.	83
Figure 5.4 The variation of the factors in terms of the desirability and the response for the light-weight geopolymer mortars incorporated with GGBFS.	83
Figure 5.5 Compressive strength of FA based geopolymer mortar at initial curing and 7 day ages.	85
Figure 5.6 Compressive strength of GGBFS based geopolymer mortar at initial curing and 7 day ages.	85
Figure 5.7 Splitting tensile strength of GGBFS based geopolymer mortar.	87
Figure 5.8 Splitting tensile strength of FA based geopolymer mortar.	87
Figure 5.9 Relationship between compressive and splitting tensile strength of GGBFS based geopolymer mortar.	88
Figure 5.10 Relationship between compressive and splitting tensile strength of FA based geopolymer mortar.	89

Figure 5.11 Comparison of splitting tensile strength of GGBFS geopolymer (experimental and theoretical).	90
Figure 5.12 Comparison of splitting tensile strength of FA geopolymer (experimental and theoretical).....	91
Figure 5.13 Water sorptivity of FA based geopolymer mortar without drying at 105 °C.....	94
Figure 5.14 Water sorptivity of FA based geopolymer mortar drying at 105 °C.	94
Figure 5.15 Water sorptivity of GGBFS based geopolymer mortar without drying at 105 °C.....	95
Figure 5.16 Water sorptivity of GGBFS based geopolymer mortar drying at 105 °C.	95
Figure 5.17 Relationship between compressive strength and sorptivity of GGBFS geopolymer.	96
Figure 5.18 Relationship between compressive strength and sorptivity of FA geopolymer.	97
Figure 5.19 Water absorption percentage of FA based geopolymer mortar with different binder content.....	98
Figure 5.20 Water absorption percentage of GGBFS based geopolymer mortar with different binder content.....	99
Figure 5.21 Relationship between compressive strength and water absorption of LWGM.....	100
Figure 6.1 Hardened LWGM during mixing in mixer.....	105
Figure 6.2 Flow table of FA geopolymer mortar.....	107
Figure 6.3 Flow table of GGBFS geopolymer mortar.....	108
Figure 6.4 Fresh unit weight of FA based geopolymer mortar.....	110
Figure 6.5 Fresh unit weight of GGBFS based geopolymer mortar.....	110
Figure 6.6 Effect of NaOH Concentration and NaOH to Na ₂ SiO ₃ ratio on FA geopolymer Compressive strength.....	113
Figure 6.7 Effect of NaOH Concentration and NaOH to Na ₂ SiO ₃ ratio on GGBFS geopolymer Compressive strength at 2 ages.....	116
Figure 6.8 Effect of NaOH concentration and NaOH to Na ₂ SiO ₃ ratio on FA geopolymer tensile strength.	118
Figure 6.9 Effect of NaOH concentration and NaOH to Na ₂ SiO ₃ ratio on GGBFS geopolymer tensile strength.	119
Figure 6.10 Sorptivity for FA based LWGMs without drying at 105 °C.....	121
Figure 6.11 Sorptivity for FA based LWGMs drying at 105 °C.....	121
Figure 6.12 Sorptivity for GGBFS based LWGMs without drying at 105 °C.....	122
Figure 6.13 Sorptivity for GGBFS based LWGMs drying at 105 °C.....	122
Figure 6.14 Water absorption results for FA based LWGMs.....	125

Figure 6.15 Water absorption results for GGBFS based LWGMs.	125
Figure 6.16 The influence of NaOH molarity and the ratio of $\text{Na}_2\text{SiO}_3/\text{NaOH}$ on the responses of (a) flow diameter, (b) fresh unit weight, (c) water absorption, (d) sorptivity, (e) compressive strength, (f) splitting tensile strength for FA based light-weight geopolymer mortar.	128
Figure 6.17 The influence of NaOH molarity and the ratio of $\text{Na}_2\text{SiO}_3/\text{NaOH}$ on the responses of (a) flow diameter, (b) fresh unit weight, (c) water absorption, (d) sorptivity, (e) compressive strength, (f) splitting tensile strength for GGBFS based light-weight geopolymer mortar.	129
Figure 6.18 Variation of desirability function in terms of the molarity of NaOH and the ratio of $\text{Na}_2\text{SiO}_3/\text{NaOH}$ for the case of FA utilisation as a base material.	131
Figure 6.19 Variation of desirability function in terms of the molarity of NaOH and the ratio of $\text{Na}_2\text{SiO}_3/\text{NaOH}$ for the case of GGBFS utilisation as a base material.	132
Figure 6.20 The variation of the factors in terms of the desirability and the responses for the light-weight geopolymer mortars incorporated with FA.	134
Figure 6.21 The variation of the factors in terms of the desirability and the responses for the light-weight geopolymer mortars incorporated with GGBFS.	135
Figure 7.1 Step-wise regression model for compressive strength of GGBFS based LWGMs exposed to 2 hrs of curing time.	137
Figure 7.2 Step-wise regression model for compressive strength of GGBFS based LWGMs exposed to 6 hrs of curing time.	138
Figure 7.3 Step-wise regression model for compressive strength of GGBFS based LWGMs exposed to 8 hrs of curing time.	138
Figure 7.4 Step-wise regression model for compressive strength of GGBFS based LWGMs exposed to 24 hrs of curing time.	139
Figure 7.5 Step-wise regression model for compressive strength of GGBFS based LWGMs exposed to 48 hrs of curing time.	139
Figure 7.6 Step-wise regression model for compressive strength of GGBFS based LWGMs exposed to 72 hrs of curing time.	140
Figure 7.7 Step-wise regression model for compressive strength of FA based LWGMs exposed to 2 hrs of curing time.	141
Figure 7.8 Step-wise regression model for compressive strength of FA based LWGMs exposed to 6 hrs of curing time.	141
Figure 7.9 Step-wise regression model for compressive strength of FA based LWGMs exposed to 8 hrs of curing time.	142
Figure 7.10 Step-wise regression model for compressive strength of FA based LWGMs exposed to 24 hrs of curing time.	142
Figure 7.11 Step-wise regression model for compressive strength of FA based LWGMs exposed to 48 hrs of curing time.	143
Figure 7.12 Step-wise regression model for compressive strength of FA based LWGMs exposed to 72 hrs of curing time.	143

Figure 7.13 Step-wise regression model for compressive strength of GGBFS based LWGMs exposed to 60 °C of curing temperature.	144
Figure 7.14 Step-wise regression model for compressive strength of GGBFS based LWGMs exposed to 80 °C of curing temperature.	145
Figure 7.15 Step-wise regression model for compressive strength of GGBFS based LWGMs exposed to 100 °C of curing temperature.	145
Figure 7.16 Step-wise regression model for compressive strength of GGBFS based LWGMs exposed to 120 °C of curing temperature.	146
Figure 7.17 Step-wise regression model for compressive strength of FA based LWGMs exposed to 60 °C of curing temperature.	147
Figure 7.18 Step-wise regression model for compressive strength of FA based LWGMs exposed to 80 °C of curing temperature.	147
Figure 7.19 Step-wise regression model for compressive strength of FA based LWGMs exposed to 100 °C of curing temperature.	148
Figure 7.20 Step-wise regression model for compressive strength of FA based LWGMs exposed to 120 °C of curing temperature.	148
Figure 7.21 Step-wise regression model for compressive strength of FA based LWGMs at different binder content, curing temperature, and curing time.	149
Figure 7.22 Step-wise regression model for compressive strength of GGBFS based LWGMs at different binder content, curing temperature, and curing time.	150
Figure 7.23 Flowchart of GEP (Ferreira C., 2001).	154
Figure 7.24 Expression trees of compressive strength prediction of fly ash-based geopolymer samples.....	157
Figure 7.25 GEP predicted vs experimental compressive strength of fly ash based LWGMs compressive strength of 168 specimens.....	158
Figure 7.26 Resulted expression trees of compressive strength of GGBFS-based geopolymer samples.....	159
Figure 7.27 GEP predicted vs experimental compressive strength of GGBFS based LWGMs compressive strength of 168 specimens.....	160

LIST OF TABLES

Table 1.1 CO ₂ emissions for OPC and blast furnace slag (Islam et al., 2014)	2
Table 2.1 Effect of Na ₂ SiO ₃ /NaOH ratio on compressive strength (Morsy et al., 2014).	15
Table 2.2 Compressive strength at different molarity and curing time (Manware et al., 2016).	23
Table 2.3 Water absorption and sorptivity at different silica and alkali content (Ghosh and Ghosh, 2012).	28
Table 3.1 Properties of FA and GGBFS.	34
Table 3.2 Composition of sodium hydroxide (%).	35
Table 3.3 Properties of sodium silicate.	36
Table 3.4 Properties of superplasticizer (SP1).	37
Table 3.5 Geopolymer lightweight mortar mix designs.	38
Table 3.6 Design expert results.	48
Table 4.1 Flow table of of LWGM.	53
Table 4.2 Fresh unit weight of LWGM.	54
Table 4.3 Compressive strength development of GGBFS based geopolymer with 650 kg/m ³ binder content at different curing duration and curing temperature.	60
Table 4.4 Compressive strength development of GGBFS based geopolymer with 750 kg/m ³ binder content at different curing duration and curing temperature.	61
Table 4.5 Compressive strength development of GGBFS based geopolymer with 850 kg/m ³ binder content at different curing duration and curing temperature.	62
Table 4.6 Compressive strength development of GGBFS based geopolymer with 950 kg/m ³ binder content at different curing duration and curing temperature.	63
Table 4.7 Compressive strength development of GGBFS based geopolymer with 1050 kg/m ³ binder content at different curing duration and curing temperature.	64
Table 4.8 Compressive strength development of GGBFS based geopolymer with 1150 kg/m ³ binder content at different curing duration and curing temperature.	65
Table 4.9 Compressive strength development of GGBFS based geopolymer with 1250 kg/m ³ binder content at different curing duration and curing temperature.	66
Table 4.10 Compressive strength development of fly ash based geopolymer with 650 kg/m ³ binder content at different curing duration and curing temperature.	68
Table 4.11 Compressive strength development of fly ash based geopolymer with 750 kg/m ³ binder content at different curing duration and curing temperature.	69

Table 4.12 Compressive strength development of fly ash based geopolymer with 850 kg/m ³ binder content at different curing duration and curing temperature.....	70
Table 4.13 Compressive strength development of fly ash based geopolymer with 950 kg/m ³ binder content at different curing duration and curing temperature.....	71
Table 4.14 Compressive strength development of fly ash based geopolymer with 1050 kg/m ³ binder content at different curing duration and curing temperature.....	72
Table 4.15 Compressive strength development of fly ash based geopolymer with 1150 kg/m ³ binder content at different curing duration and curing temperature.....	73
Table 4.16 Compressive strength development of fly ash based geopolymer with 1250 kg/m ³ binder content at different curing duration and curing temperature.....	74
Table 5.1 Response surface Parameters.....	76
Table 5.2 Definitions for the factors and the responses in the optimization problem.....	78
Table 5.3 Optimization results for the light-weight geopolymer mortars with FA and GGBFS.....	79
Table 5.4 The obtained optimum values and the results from the experimental verification tests for the light-weight geopolymer mortars incorporated with FA and GGBFS.....	82
Table 5.5 Compressive strength results from the experimental verification tests for the light-weight geopolymer mortars incorporated with FA and GGBFS.....	84
Table 5.6 Splitting tensile strength results, and their relationships with age and compressive strength.....	86
Table 5.7 Conversion for compressive and splitting tensile strength according to size and shape of the specimen (Neville, 2004).....	90
Table 5.8 Comparison of splitting tensile strength (experimental and theoretical)...	92
Table 5.9 Water sorptivity results from the experimental verification tests for the light-weight geopolymer mortars incorporated with FA and GGBFS.....	93
Table 5.10 Water absorption results from the experimental verification tests for the light-weight geopolymer mortars incorporated with FA and GGBFS.....	98
Table 6.1 Geopolymer lightweight mortar mix designs.....	103
Table 6.2 NaOH solids with different concentration (Hardjito and Rangan, 2005).	104
Table 6.3 Workability criteria of geopolymer mortar (Ghosh K. & Ghosh P., 2012).	106
Table 6.4 Flow table values of LWGM.....	107
Table 6.5 Fresh unit weight of LWGM.....	109
Table 6.6 Effect of NaOH concentration and NaOH to Na ₂ SiO ₃ ratio on FA geopolymer Compressive strength.....	112
Table 6.7 Compressive strength at different Molarity of NaOH and NaOH to Na ₂ SiO ₃ ratio for GGBFS geopolymer mortar.....	115
Table 6.8 Splitting tensile strength results of FA geopolymer mortar.....	117

Table 6.9 Splitting tensile strength results of GGBFS geopolymer mortar.	118
Table 6.10 Water sorptivity results for the LWGMs incorporated with FA and GGBFS.	120
Table 6.11 Water absorption results for the LWGMs incorporated with FA and GGBFS.	124
Table 6.12 The goals and the constraints used for each variable considered in the multi objective optimization analysis.	127
Table 6.13 Optimization results of FA and GGBFS light-weight geopolymer mortar.	130
Table 7.1 Comparison of step-wise regression formulations.	151



LIST OF SYMBOLS/ABBREVIATIONS

LWGM	Light-weight geopolymer mortar
GGBFS	Ground granulated blast furnace slag
FA	FLy ash
SS/SH	Sodium silicate to sodium hydroxide ratio
NaOH	Sodium hydroxide
Na ₂ SiO ₃	Sodium silicate
OPC	Ordinary Portland cement
CO ₂	Carbon dioxide
GP	Geopolymer
CaO	Calcium oxide
SiO ₂	Silica (silicon oxide)
ASTM	American Society for Testing and Materials
ACI	American Concrete Institute
MgO	Magnesium oxide
Al ₂ O ₃	Alumina (Aluminum oxide)
GFA	Ground fly ash
POFA	Palm oil fuel ash
FAGP	Fly ash geopolymer
GPMs	Geopolymer mortars
GPC	Geopolymer concrete
LWFA	Lightweight fine aggregate

LWAGC	Lightweight aggregate geopolymer concrete
f_c	Compressive strength
RSM	Response surface method
f_{sp}	Splitting tensile strength
P	Maximum load
a	Dimension of the cube
W_s	Weight of specimen at fully saturated condition
W_d	Weight of oven dried specimen
R^2	Determination coefficients
GEP	Gene Expression Programming
IC	Initial Curing
GAs	Genetic Algorithms
GP	Genetic Programming

CHAPTER 1

INTRODUCTION

1.1 General

The huge demand for concrete using Ordinary Portland Cement (OPC) has resulted in high volume of carbon dioxide (CO₂) emission, and lead to ecological imbalance due to continuous depletion of natural resources. The reality of air pollution through CO₂ emission into the atmosphere from the production of cement is well known. The contribution of OPC manufacturing to greenhouse gas emission is approximated as 6% of the total greenhouse gas emissions (Davidovits, 1995)

It is very important to develop alternative binders to minimize the carbon footprint of the construction industries and to utilize the industrial by-product materials. geopolymer (GP), a new environment friendly inorganic binder, is a developed alternative binder for concrete that utilizes industrial by-products. The geopolymer binder is produced by the reaction between the base materials which are affluent with silicon and aluminum with the alkaline solution. Many base materials such as FA, metakaolin and GGBFS could be utilized to produce GP. Blast furnace slag mixed with FA could also be used as base material for GP. Rice husk ash can be considered as base material as well. Product of the reaction between the base materials and the alkaline solution is the geopolymer concrete which bonds the concrete ingredients together.

The most commonly used source materials of these aluminosilicate binders are fly ash and ground granulated blast furnace slag, because of the presence of soluble silica and alumina species. When mixed with alkaline activators, these materials set and harden, delivering a material with very effective binding properties.

A huge amount of fly ash, produced by coal-fired power stations, could be used efficiently in manufacturing of geopolymer to minimize the carbon footprint of concrete productions. GGBFS is another waste material that is abundant worldwide.

GBFS is a by-product of the metallurgical industry and consists chiefly of lime and calcium–magnesium aluminosilicates.

The use of GGBFS as cement replacement material in geopolymer concrete reduces the CO₂ emission. Table 1.1 shows the comparison of CO₂ emission between the OPC and GGBFS and it shows that one ton of GGBFS releases only about 70 kg of CO₂ while it is 970 kg for OPC, the CO₂ emission of GGBFS is only 7 % of that of OPC for the same quantity of material produced (Islam et al. 2014).

The source materials, activating alkali, and the curing regime are the most influential factors on the properties of the resulting product. The focus of this study touches on all these aspects, by exploring the influence of binder content (fly ash, slag, or both), the effect of the alkali concentration of Sodium hydroxide and percentage of hydroxide to silicates moreover, the influence of curing regime.

Table 1.1 CO₂ emissions for OPC and blast furnace slag (Islam et al., 2014)

	CO ₂ emission/t OPC (kg)	CO ₂ emission/t GGBFS (kg)
Calcination of CaCO ₃	540	0
Fossil fuel (coal)	340	20 (drying)
Electricity generation	90	50
Total	970	70

1.2 Objectives and Scope of the Work

In this study, an experimental research was conducted to explore the effects of curing temperature levels and various curing periods on compressive strength of geopolymer based lightweight mortars. Two popular by-products, FA and GGBFS, were selected as base materials for alkali activation. Alkaline activator is a mix of Na₂SiO₃ and NaOH solutions. Benefiting from the available technical literature background, comprehensive ranges of curing temperatures and curing times were assigned for geopolymerization process. The performance criterion was selected as compressive strength of the mortars. The effects of binder content, curing temperature and curing duration on the compressive strength of LWGM were investigated. Furthermore, the optimization study on the parameters of binder content, curing temperature and curing time were conducted using response surface

method (RSM) to provide the maximized compressive strength for the LWGMs incorporated with FA and GGBFS.

The purpose of this work is to produce new binding material (geopolymer) that can bind components of light weight mortar (pumice and crushed limestone) instead of Portland cement depending on local materials (GGBFS and FA).

This was accomplished by studying:

- a) The effects of different binder content, binder type, curing temperature and curing duration on the compressive strength of LWGM samples.
- b) Identification and evaluation of the optimum compressive strength with minimum curing time and curing temperature of LWGMs.
- c) The short-term engineering properties of fresh and hardened fly ash and ground granulated blast furnace slag -based geopolymer mortars after optimized test parameters.
- d) The effect of sodium hydroxide concentration and SS/SH ratios on properties of LWGM. Additionally, the response surface method (RSM) is adopted in this study to optimize the parameters considered in the experimental analysis presented.

1.3 Thesis Layout

The thesis divides into eight chapters:

1. Chapter 1 presents an introduction to the subject and the objectives of this work.
2. Chapter 2 includes a literature review of previous researches on geopolymer mortar.
3. Chapter 3 deals with the materials mix proportions, methods of testing and experimental program details.
4. Chapter 4 discusses the findings of the studies with respect to the influence of binder content, curing temperature and curing duration on the compressive strength of light-weight geopolymer mortar (LWGM).
5. Chapter 5 includes the optimization by RSM and verification of optimum curing period and curing temperature on the compressive strength of GGBFS and FA based geopolymer mortar, including sorptivity, water absorption.

6. Chapter 6 discusses the findings of the studies with respect to the influence of NaOH concentration and Na₂SiO₃: NaOH ratio on the strength and absorption of LWGM. Moreover, this chapter covers another optimization study by RSM to evaluate the optimum values of above mentioned parameters.

7. Chapter 7 reports the study of the statistical analysis and modeling of test results.

8. Chapter 8 introduces the conclusions derived from this study and recommendations for further research work.



CHAPTER 2

LITERATURE REVIEW

2.1 Introduction

Portland cement production increases global greenhouse gas emissions through the calcination of clinker in coal heated furnaces. Traditionally, reduction in cement consumption has been attained by the use of industrial by products such as fly ash and ground granulated blast furnace slag (GGBFS) as partial cement replacement materials. Nowadays with the increasing importance on sustainability, researchers have tried to use industrial by-products such as fly ash and slag as the sole binding material in concretes instead of partial replacement of ordinary Portland cement. Alkali activated binder concretes, also known as geopolymer concretes is a result of this approach. Due to their excellent mechanical properties, the use of geopolymeric materials in construction is gaining importance. This class of materials was originally developed in France in the 1980's as the result of a search to develop new fire resistant building materials. In order to effectively apply these composites as engineering resources, it is essential to understand the properties, microstructure and performance characteristics of these materials. Numerous studies have been conducted over the last few decades to determine the composition-microstructure-property relationships in such systems. This research will assist in a better understanding of the material and provide valuable information to adapt the material for specific applications in the infrastructure sector.

2.2 Mechanism of Geopolymerization

Geopolymerization is an exothermic polycondensation reaction involving alkali activation by a cation in solution. Glukhovskiy (1994) suggests a model of alkali activated mechanism for the material having silica and alumina. This model was divided into three steps of geopolymerization:

- a) destruction–coagulation.
- (b) coagulation–condensation.
- (c) condensation–crystallization.

Figure 2.1 presents a highly simplified model of reaction mechanisms including converting solid particles to the gel by using high alkaline solution (Duxson et al., 2007).

Dissolution of the solid aluminosilicate source by the alkaline hydrolysis produces aluminate and silicate species. It starts when Si-Al from raw materials contacts alkaline solution, to produce Si and Al species, allowing for an ionic interface between species and breaking the covalent bonds to liberate the silicon, aluminum and oxygen atoms (Petermann, et al., 2010). Similar to OPC reactions, this step usually generates rapid and intense heat, and is directly proportional to the pH level and concentration of the activating solutions. The rate of dissolution is also a function of the amount and composition of the source material and pH of the activating solution (Fernández-Jiménez, et al., 2006).

Once dissolution is complete, the species released are incorporated into the aqueous phase, which may already contain free silicate from the activating solutions, providing a complete mixture of silicate, aluminate and aluminosilicate species. When activating solutions with a high pH are used, the dissolution is rapid and creates a supersaturated aluminosilicate solution. When the concentration reaches a substantial level, a gel starts to form as the oligomers in the aqueous phase form large networks consisting of Si-O-Al-O bonds through condensation. At this stage, water that was consumed during dissolution is released and plays the role of a reaction facilitator, residing within the pores of the gel. The formed gel is initially aluminum-rich and contains alkaline cations that compensate for the deficit charges produced with the aluminum-for-silicon substitution (Petermann, et al., 2010).

After gelation, the system continues to rearrange and reorganize as the connectivity of the gel network increases, resulting in a three-dimensional aluminosilicate network, as represented in Figure 2.1 with the presence of multiple “gel stages”. (Duxson et al., 2007).

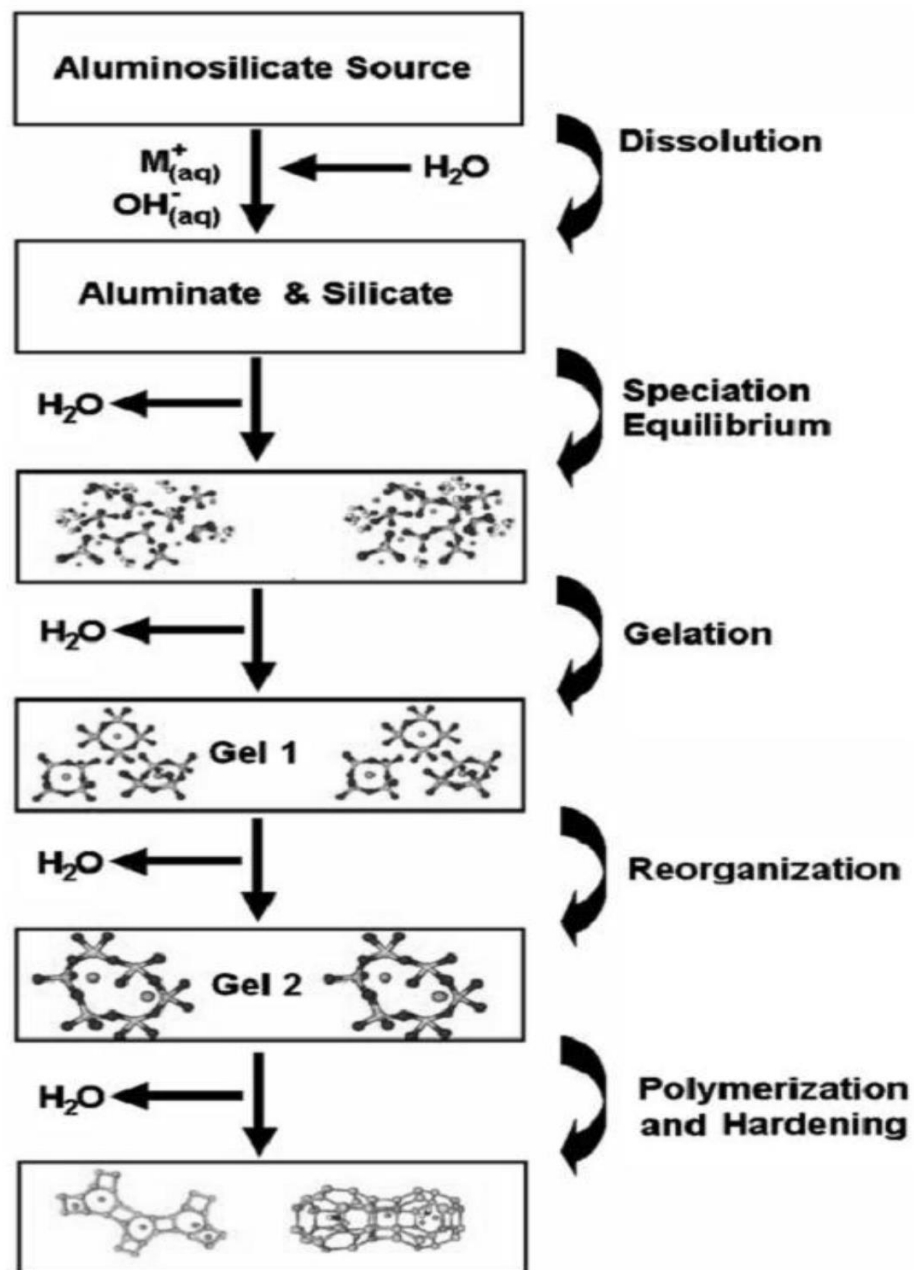


Figure 2.1 Geopolymerization process (Duxson et al., 2007).

2.3 Structure of Geopolymer

Structure of geopolymer is a poly (sialate) network consisting of silica (SiO_2) and alumina (Al_2O_3) tetrahedral connected together by sharing oxygen atoms (figure 2-3). Sialate is an abbreviation for silicon-oxo-aluminate (Si-O-Al) which form the basic polymeric precursor product (Davidovits, 2011; Bondar, 2013). Structure of the polymeric precursor formed depends on the ratio of silica to alumina (Si/Al) in the starting materials and can be classified according to this ratio:

- sialite, poly (sialite) $\text{Si:Al} = 1$
- sialate-siloxo, poly (sialate-siloxo) $\text{Si:Al} = 2$
- sialate-disiloxo, poly (sialate-disiloxo) $\text{Si:Al} = 3$
- Sialate link, poly (sialate-multisiloxo) ($\text{Si:Al} > 3$)

Figure 2.2 shows an illustration of the four polymeric structures that form geopolymer.

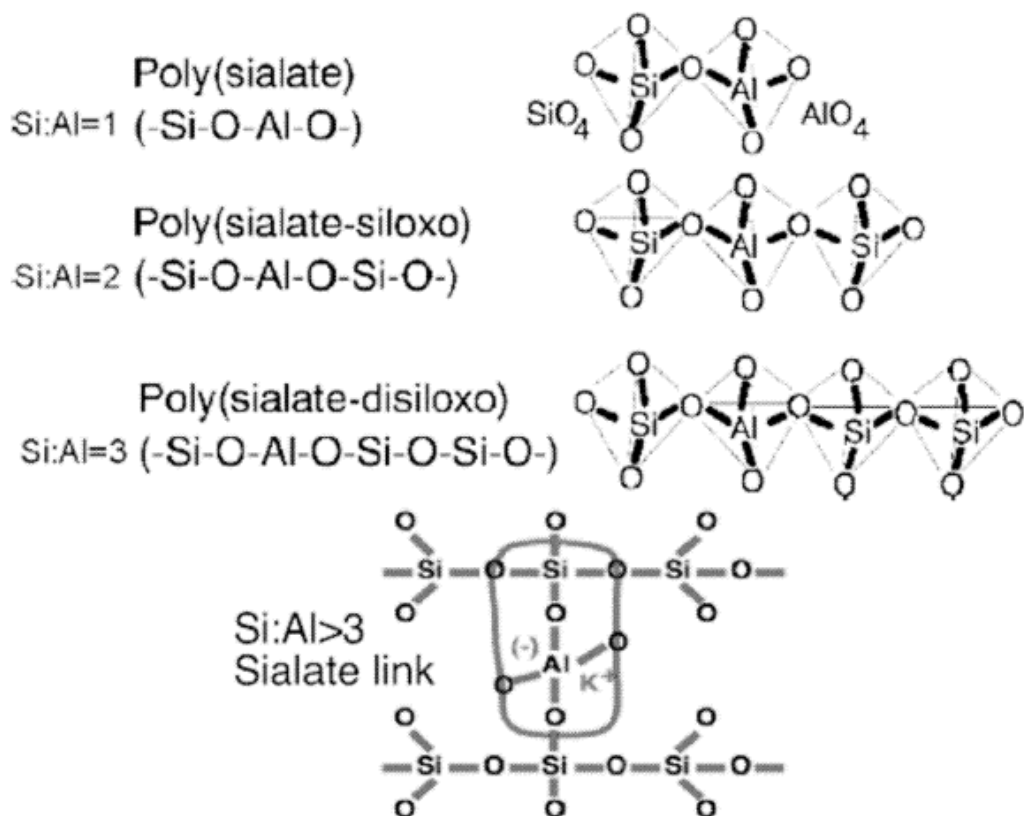


Figure 2.2 Polymeric precursor that form geopolymer (Davidovits, 2011).

2.4 Materials of Geopolymer Mortar

2.4.1 Alkali Activation of Fly Ash

Fly ash is a by-product of coal combustion, generally captured by electrostatic precipitators before the flue gases reach the chimneys of thermal power plants. It is the preferred supplementary cementitious material and has extensively been used to replace part of cement in concrete. Unused fly ash is usually disposed into landfills contributing to soil, water and air pollution (Duxon et al., 2007). Fly ash is usually classified as low-Ca fly ash or Class F fly ash and high Ca - FA or Class C fly ash. Class F fly ash is generally preferred for synthesis of GP concretes due to the high availability of reactive silica and alumina. Alkali activation of FA takes place through an exothermic reaction with dissolution during which the covalent bonds (Si-O-Si and Al-O-Al) in the glassy phase pass through the solution.

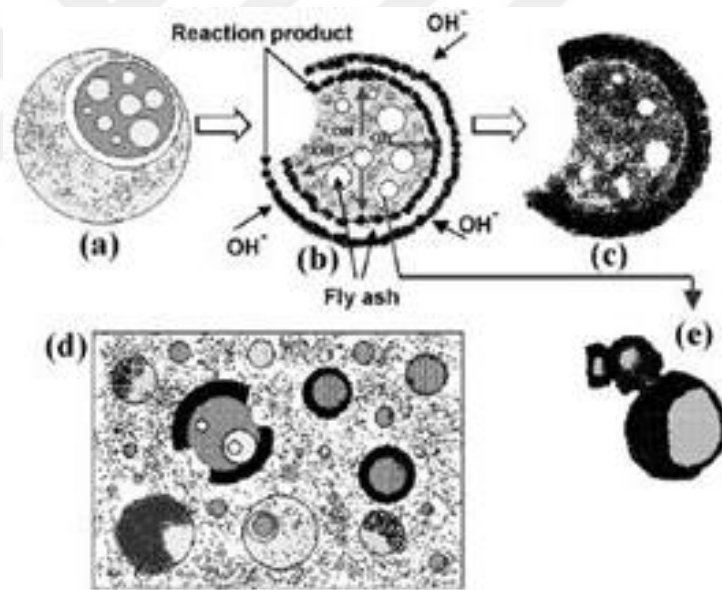


Figure 2.3 Mechanism of gel formations in alkali activated fly ash binder
(Fernandez-Jimenez et al., 2005).

The products generated from dissolution start to accumulate for a certain period of time (called the induction period) during which the heat release is really low.

Isothermal calorimetric studies (explained in a forthcoming section) are used to distinguish the extent of the induction period in systems proportioned using different activator and binder types, concentration, and dosages. A condensation of the structure is produced (a highly exothermal stage), which involves the creation of a

cementitious material with a poorly ordered structure, but high mechanical strength. The product is an amorphous alkali aluminosilicate gel having a structure similar to that of zeolitic precursors. This formation of reaction product as a layer around the fly ash particles is explained as the mechanism of geopolymerization and is depicted in Figure 2.3. Most research reveals that the activation of fly ash with alkalis requires heat curing to gain reasonable mechanical properties. The type of solution used for the activation of the fly ash is essential in the development of reactions. When the alkali solution contains soluble silicates (sodium or potassium silicate), the reactions occur at a higher rates than when hydroxides are used as the activators.

2.2.2 Alkali Activation of Slag

The aluminosilicates reaction mechanism containing a calcium bearing compound is different than the geopolymeric reaction as illustrated in the previous section. It was reported that the type of calcium bearing compound in the starting material is playing a major role in the alkali activation of the materials. An example of such is the alkali activation of slag. Alkalis first attack the slag particles breaking the outer layer and then a polycondensation of reaction products takes place. Wang et al. (1995) proposed that though the initial reaction products form due to dissolution and precipitation, at later ages, a solid state mechanism is followed where the reaction takes place on the surface of the formed particles, dominated by slow diffusion of the ionic species into the unreacted core. Alkali cation (R^+) acts as a mere catalyst for the reaction in the initial stages of hydration as shown in the following equations, via cation exchange with the Ca^{2+} ions (Glukhovsky, 1994).



The alkaline cations act as structure creators. The nature of the anion in the solution also plays a determining role in activation, particularly in early ages and especially with regard to paste setting (Fernández-Jiménez and Puertas, 2001; Fernández-Jiménez and Puertas, 2003).

2.4.3 Sodium Hydroxide, NaOH

Sodium hydroxide is the most commonly used alkali hydroxides in the production of geopolymer, due to its low price and wide availability of the alkali hydroxides. The concentration of sodium hydroxide is a significant factor in controlling the leaching of alumina and silica from source material particles, subsequent geopolymerization and mechanical properties of hardened geopolymer.

Hanjitsuwan et al. (2014) studied the effect of NaOH concentrations on high calcium FA geopolymer pastes. NaOH concentrations effect on geopolymer pastes was investigated using different concentration of NaOH (8, 10, 12, 14, 16 and 18M). Compressive strength of geopolymer cement increased with increasing NaOH concentration for 7 days age specimen. There results indicated in Figure 2.4, show that the compressive strength increases with NaOH concentration up to the studied value of 18 M.

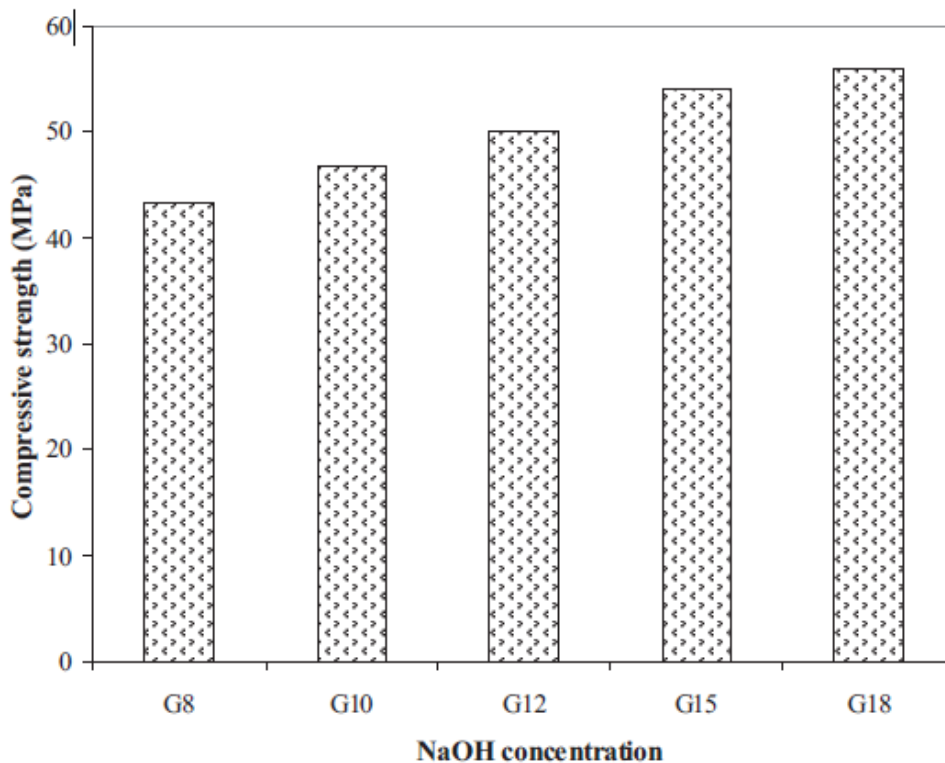


Figure 2.4 Compressive strength of FAGP with various NaOH concentrations (Hanjitsuwan et al., 2014).

Somna et al. (2011) reported the effect of NaOH concentration on properties of Ground fly ash (GFA), with a median particle size of 10.5 μm , was used as source material. The mass ratio of the solid material and liquid activator for the geosynthetic reaction is optimized as 3.3:1. The NaOH solution was used as an alkali activator. When concentration of NaOH increasing from 4.5 to 14 mol /L the compressive strength increased. The explanation is that NaOH solution has the ability to dissolve surface layer of GFA particulates, with the increase of NaOH concentration beyond this point resulted in a reduction in the paste strength due to early precipitation of aluminosilicate products. Figure 2.5 illustrates more details.

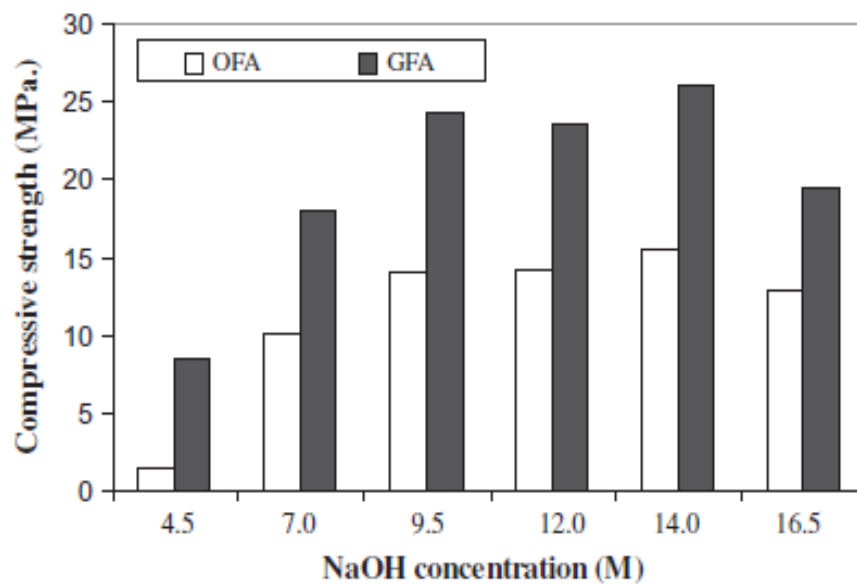


Figure 2.5 Relation between NaOH concentrations (Molar) with compressive strength at 60 days (Somna et al., 2011).

2.4.3 Sodium Silicate, Na_2SiO_3

Sodium silicates manufactured by fusing sand (SiO_2) with sodium or potassium carbonates (Na_2CO_3 or K_2CO_3) at temperatures ranging from 1100 to 1200°C and using steam pressure for dissolving the product to produce water glass (Jimenez et al., 2005).

Sodium silicate is usually mixed with sodium hydroxide to enhance its alkalinity to ensure increased dissolution and product formation. Sodium silicate is rarely used alone due to its weak ability to initiate reaction.

Yahya et al. (2015) studied the effect of $\text{Na}_2\text{SiO}_3/\text{NaOH}$ and solid/liquid ratios on compressive strength of Palm Oil Boiler Ash (POBA) based GP. The geopolymer samples were prepared with different S/L ratios (0.5, 1.0, 1.25, and 1.75) and SS/SH ratios (0.5, 1.0, 1.5, 2.0, and 3.0). The maximum compressive strength obtained with SS/SH and S/L ratio equal to 2.5 and 1.5, respectively. Figure 2.6 shows more details.

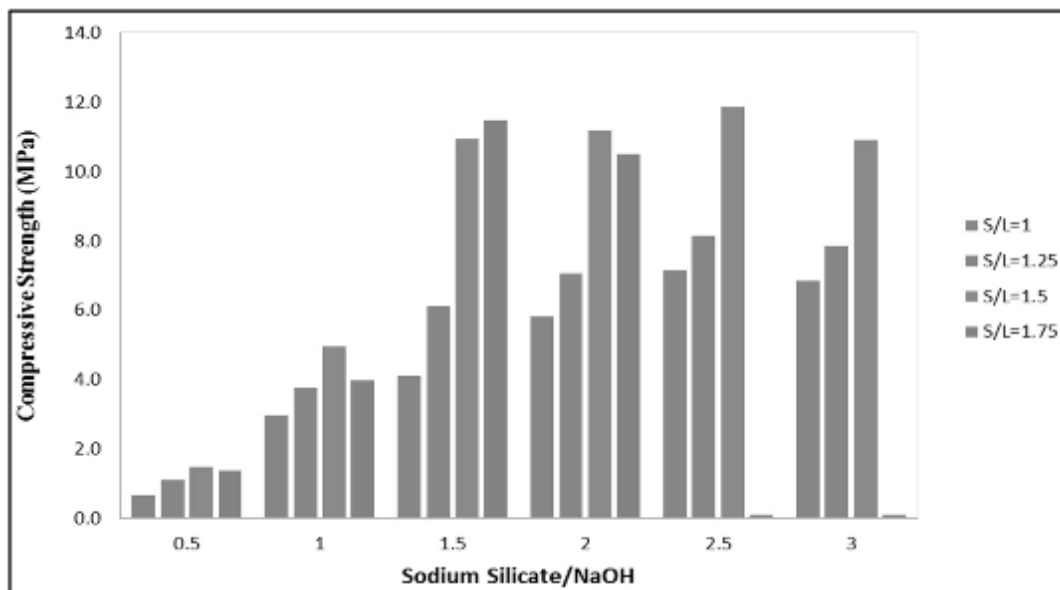


Figure 2.6 Effect of SS/SH and S/L ratio on compressive strength (Yahya et al., 2015).

Helmy (2016) studied the effect of two types of sodium silicate (low viscous and high viscous) on the fly ash geopolymer mortar compressive strength with different NaOH concentrations (8, 12 and 16M). For each NaOH concentration, the compressive strength increased as the total number of curing hours increased for both types of sodium silicate. At the end of any curing step specimens with low viscous sodium silicate showed lowering compressive strength as compared with high viscous sodium silicate at the same NaOH concentration (12M, 14 and 16M). This indicates that high viscous type sodium silicate is suitable for all molarity NaOH, because the low viscous sodium silicate having $\text{Na}_2\text{O} / \text{SiO}_2$ and $\text{SiO}_2 / \text{Al}_2\text{O}_3$ less than high viscous Sodium silicate, Figure 2.7 shows more details.

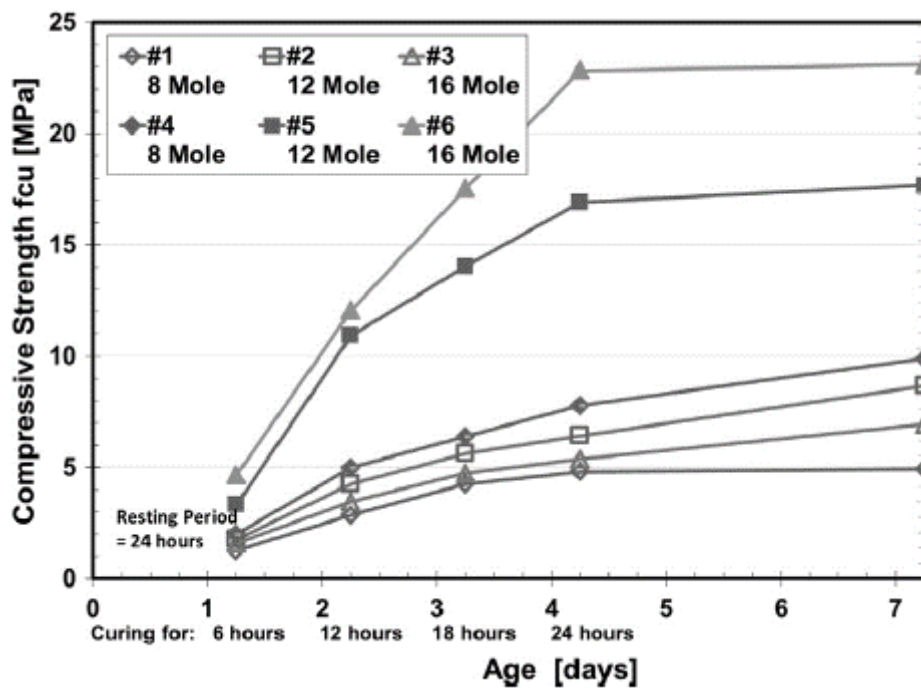


Figure 2.7 Compressive strength at different ages (Helmy, 2016).

Morsy et al. (2014) studied the effect of sodium silicate to sodium hydroxide ratios of 0.5, 1.0, 1.5, 2.0 and 2.5 on strength of fly ash geopolymer mortar. Maximum compressive strength value is reached when the ratio is 1.0, then the strength reduced. Table 2.1 shows compressive strength value at different ratios of $\text{Na}_2\text{SiO}_3/\text{NaOH}$.

Table 2.1 Effect of $\text{Na}_2\text{SiO}_3/\text{NaOH}$ ratio on compressive strength (Morsy et al., 2014).

Mixes	$\text{Na}_2\text{SiO}_3/\text{NaOH}$	Compressive strength MPa. at 3days
M1	0.5	34.7
M2	1.0	61.6
M3	1.5	40.4
M4	2.0	40.5
M5	2.5	22.3

Pacharapol et al. (2015) studied the effect of sodium silicate to sodium hydroxide ratio on compressive strength and density of lightweight high calcium fly ash geopolymer concrete. By increasing this ratio from 0.33 to 1.00, compressive strength increased to reach to the maximum. The sodium silicate to Sodium hydroxide ratio is 1.00, it causes increasing geopolymerization rate of geopolymer concrete due to the increased silica content of mixture. However, when the sodium silicate to sodium hydroxide ratio was increased to 1.5, the strength started to drop due to the difficulty in compaction Figure 2.8 shows compressive strength and density at different ratios of $\text{Na}_2\text{SiO}_3/\text{NaOH}$.

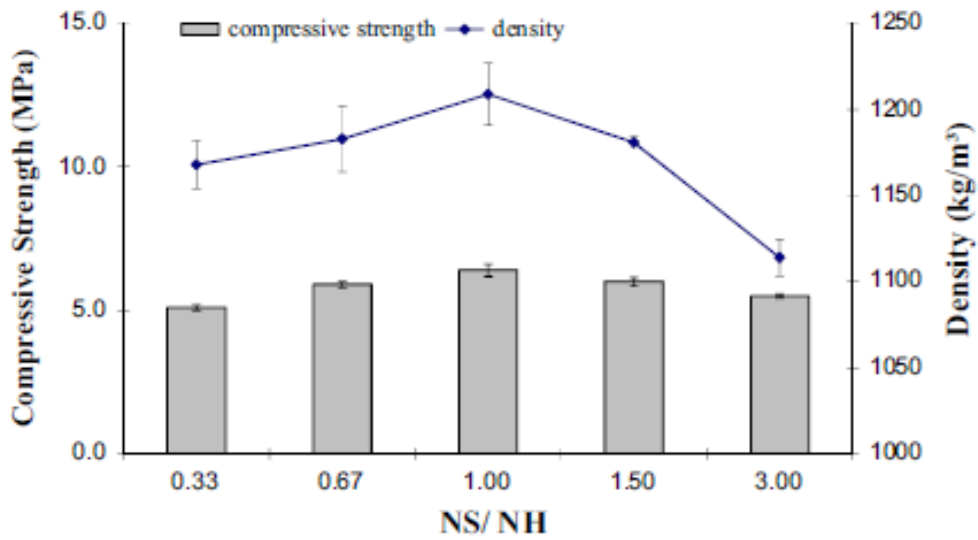


Figure 2.8 Compressive strength and density at different ratios of $\text{Na}_2\text{SiO}_3/\text{NaOH}$ (Pacharapol, 2015)

2.5 Mixing Geopolymer Mortar

There is not yet a standard method for mixing geopolymer components, and effect of mixing on its properties.

Huseien et al. (2016) used a procedure for mixing geopolymer mortar. It includes dry mixing of waste materials (FA, POFA and GBFS) homogenously in pan mixer, then fine aggregate added and mixed well. The alkaline liquid was prepared and mixed together before 24 hours, and then the liquid is added to solid components and mixed for another four minutes. The GPMs were synthesized by hand to achieve a homogeneous.

Helmy (2016) mentioned a procedure for mixing geopolymer mortar by using Fly ash. Mixing, the alkaline liquid activator and Fly ash to form the binder for 1.5 to 2 min in a pan mixer, then sand is added and mixed for at least 2 min or until a homogenous mortar mixture is formed.

Gorhan and Kurklu (2014) reported a new method for mixing fly ash geopolymer mortar, which include mixing fly ash powder with NaOH for 3 min to allow leaching of ions. Then sodium silicate solution was added to the mixture and mixed for 1 min. lastly, sand was added to the mixture and mixed for 3 min.

Patcharapol et al. (2015) stated mixing procedure for fly ash geopolymer concrete. The fly ash and NaOH solution are mixed in a pan mixer together for five minutes, then the Sand is added and mixed for another four minutes. After that, sodium silicate solution is added and mixed for five minutes, followed by added coarse aggregate and mixed for 1.5 min.

2.6 Curing of Geopolymer Mortar

The effect of curing temperatures on geopolymer behavior has been studied by many researchers. Heating is used to accelerate the geopolymerization reaction. Generally, high temperature curing is usually recommended.

Sindhunata et al. (2006) investigated the effect of curing temperatures on geopolymerization, they found that increasing the temperature from 30 to 50°C lowers the setting time and raises the nucleation rates and polycondensation of GP. Moreover, it has been observed that the ratio of silicon to aluminum decreased from 50 to 75°C, which indicate that the reactivity is low at 75°C comparing with 50°C.

Hardjito et al. (2008) studied the effect of curing temperature on the geopolymerization process of FA-based GP. They found that the elevated curing temperature accelerates the hardening of geopolymer mortar and increases the rate of geopolymerization process. However, above some critical elevated temperatures levels deterioration of compressive strength of geopolymer mortar can be observed. Gorhan and Kurklu (2014) studied the effect of curing temperature and curing time for Class F fly ash based geopolymer on the development of compressive strength. The specimens were cured at temperatures (65 and 80°C) using electrical oven for 2, 5, and 24hr and then kept at ambient temperature 20°C until the 7 day of testing. The compressive strength values of 21.3 MPa and 22 MPa were obtained from the sample cured at 65°C and from the sample cured at 85°C, respectively.

The influence of curing time at elevated temperatures on strength show that by increasing time of curing leads to accelerate the developing strength at 24 hours. Strength development of geopolymer cured at 65 and 80°C is too close. As shown in Figure 2.9.

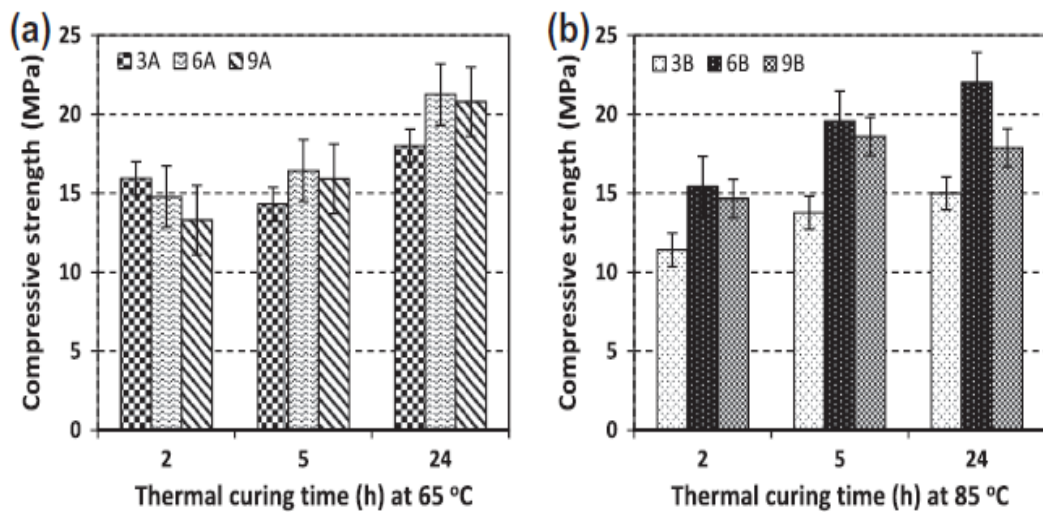


Figure 2.9 The compressive strength of geopolymer mortars (Görhan and Kürklu, 2014).

Mijarsh et al. (2015) reported the effect of curing temperatures of 65, 75 and 85 °C, for one day on compressive strength development of different geopolymer mortar the samples were keeping at ambient at 27°C temperature till the day of testing. Geopolymer mortar manufacturing by using treated palm oil fuel ash (TPOFA), they found that both curing time and curing temperature played a very important role in

compressive strength development. By increasing the temperature to 85°C, the initial compressive strength was increased, when compared to the temperatures 65 and 75 °C. However, for mixtures cured at 85°C for 28 days curing time, the compressive strength was lower than those cured at 65 and 75°C. The result of the compressive strength development at 28 days indicated that the best curing temperature was 75°C as shown in figure 2.10. The reduction in compressive strength by increased curing temperature for longer period time may be because of weakening the structure.

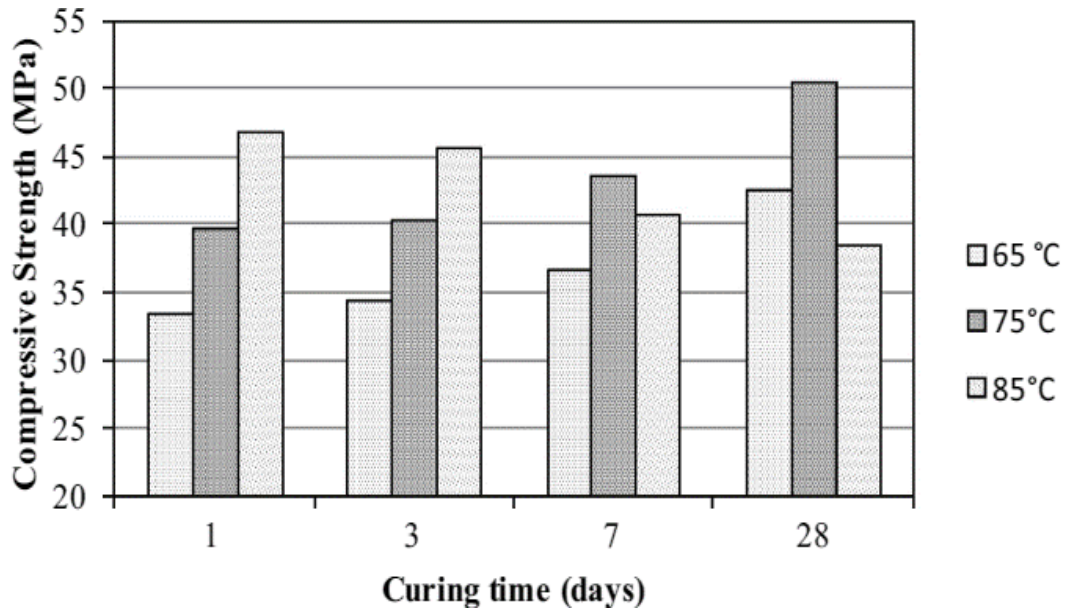


Figure 2.10 Effect of curing temperature on f_c development (Mijarsh et al., 2015).

Salih et al. (2015) studied the effect of curing conditions on strength of palm oil fuel ash paste. Two types of curing are used in this research: ambient curing at 25- 30°C and hot curing (in oven at 60°C, 70°C and 80°C for duration of 2 h). The compressive strength at 7days for ambient curing specimens was almost 15.8%, 17%, and 15% lower than that of oven cured specimens at 60°C, 70°C, and 80°C, respectively, this is attributable to a higher degree of geopolymerization due to heat which may increase the amount of reaction products. Figure 2.11 shows more details.

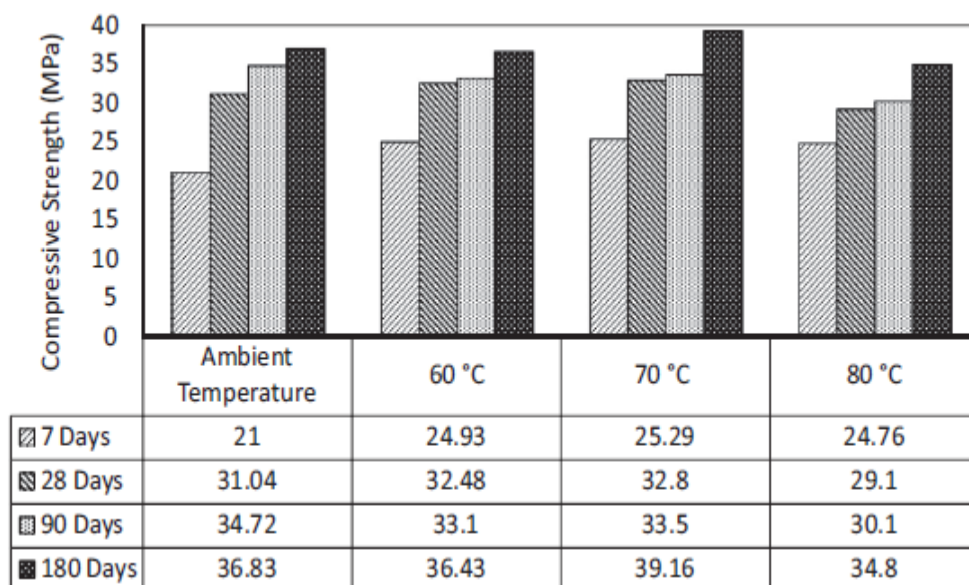


Figure 2.11 Effect of curing type on compressive strength (Salih et al., 2015).

Huseien et al. (2016) studied the effect of curing temperature and calcium content on geopolymer mortars. The specimens were cured at temperatures (27 °C ambient temperature, 60 °C and 90 °C) with curing periods 24 hours, then the specimens kept at room temperature with 21°C until testing day (1, 7 and 28 day). They found that compressive strength increase to 38.9, 46.3 and 50.0 MPa with increasing curing temperatures at 27, 60 °C and 90 °C, respectively. The binder activated with high amount of calcium showed lower strength at higher curing temperature compared with the strength results of samples cured at ambient temperature. The degradation in compressive strength occurred when increasing curing temperature led to the GPM microstructure much coarser, Porous with many cracks. Figure 2.12 illustrates compressive strength with different Ca/ Si ratio and curing temperature.

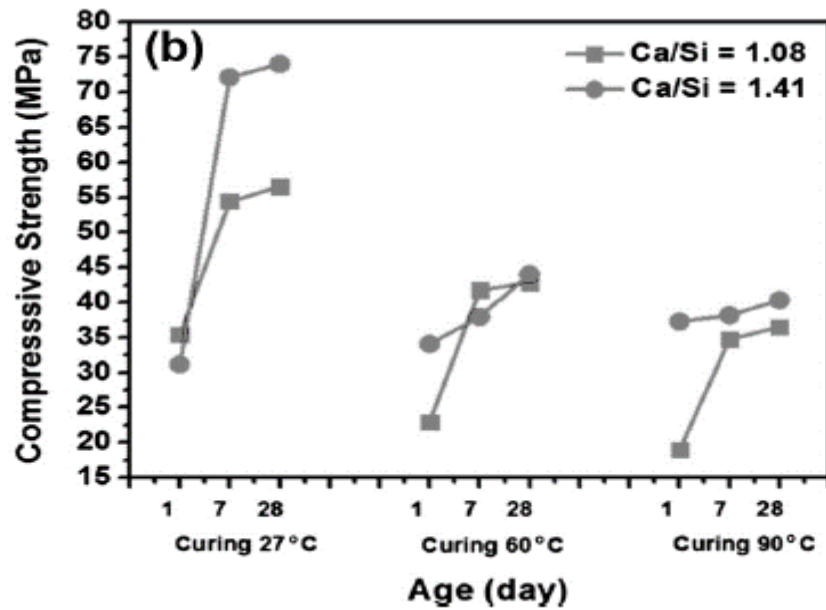


Figure 2.12 Effect of Ca/Si on compressive strength at different curing temperatures (Huseien et al., 2016).

Al Bakri et al. (2012) reported the effect of curing time and curing temperature on compressive strength of fly ash based geopolymer concrete. When curing temperature and time increase, compressive strength increases. The maximum strength value optioned with curing temperatures range from 60 - 90°C within a period from 24 - 72 hours.

2.7 Mechanical Properties of Geopolymer Mortar

2.7.1 Compressive Strength

Compressive strength is the most common property used to describe a concrete. Since other properties of concrete often correlate well with the compressive strength, it is used as an indicator of the other mechanical properties.

Hardjito and Fung (2010) studied the effect of bottom ash content on the compressive strength of fly based geopolymer mortar. The specimens are cured at 60 °C for 24 hours then kept in room temperature at 25°C to the day of testing. They found 10% of river sand can be replaced by bottom ash as fine aggregates in fly ash-based geopolymer mortar without any significant decrease in compressive strength. Further the compressive strength decreased with increase in bottom ash content. This refers to the higher porosity of the bottom ash caused the lower compressive strength to the geopolymer mortar. Also they found that the compressive strength of fly based geopolymer mortar at 7 and 28 days are very close. Figure 2.13 illustrate the effect of replaced river sand by bottom ash on compressive strength.

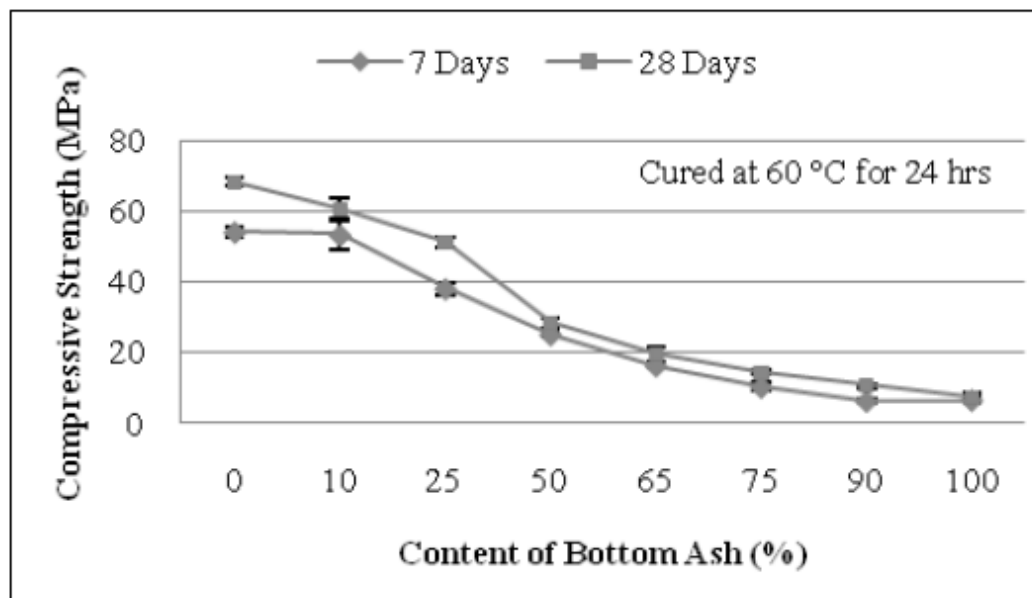


Figure 2.13 Effect of Bottom Ash content on geopolymer compressive strength at 7 days and 28 days (Hardjito and Fung, 2010).

Sinha et al. (2013) synthesis fly ash, bottom ash and granulated blast furnace slag (GBFS) with alkaline liquid. The alkaline liquid that been used in geopolymerisation is the combination of sodium hydroxide (NaOH) and sodium metasilicate (Na_2SiO_3). The specimens cured for 24hrs at 60°C with different percent of Si/Al ratios (2, 2.5 and 3) and NaOH (4, 6 and 8%). At Si/Al ratio 3 and alkali 8%, highest compressive strength was found for both Si/Al ratio and NaOH (alkali) as compared with other ratios. In general higher concentration of reactive Si in the geopolymerisation process typically leads to a higher compressive strength. With increase in NaOH %, the peak intensity of crystalline phases decreased. This is probably enhanced dissolution of crystalline peaks in higher alkali concentration. Figure 2.14 illustrates compressive strength with different Si/Al ratio and NaOH (alkali) %.

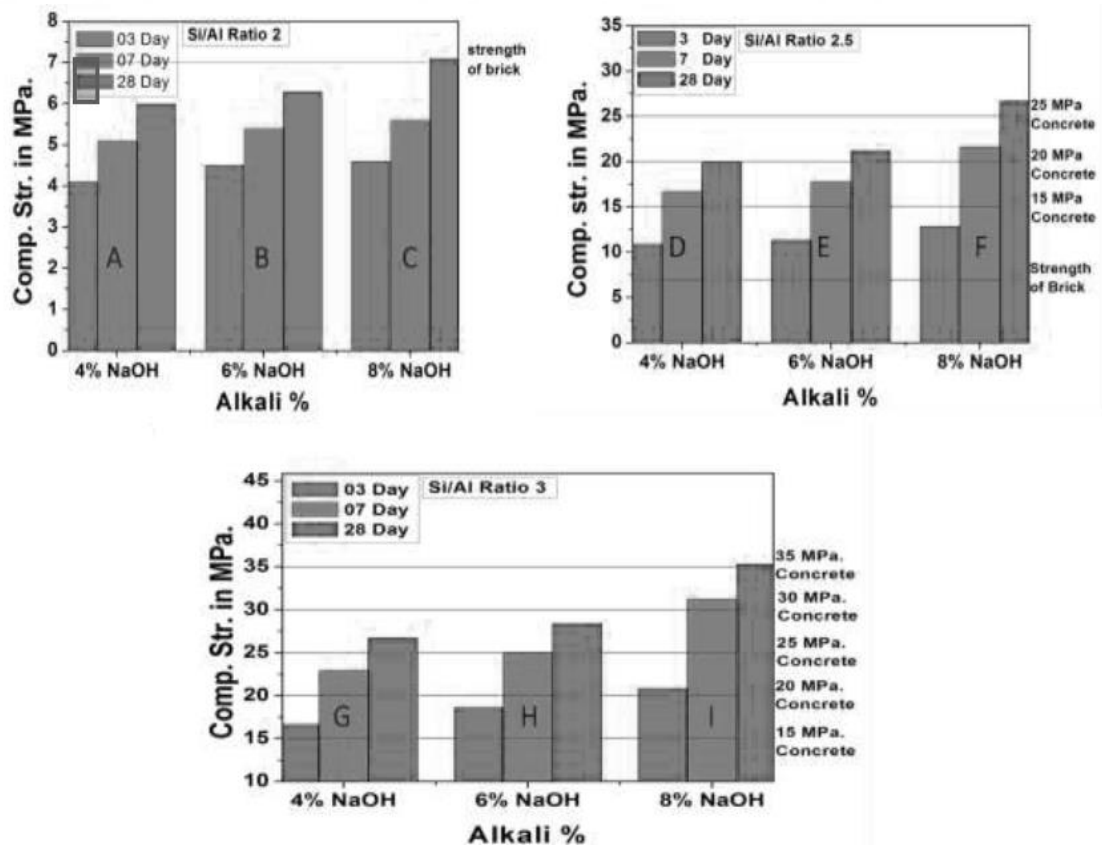


Figure 2.14 Relationship between compressive strength and Si/Al ratio with different percent of alkali %. (Sinha et al., 2013).

Manware et al. (2016) studied the effect of molarity, $\text{Na}_2\text{SiO}_3/\text{NaOH}$, and curing time on compressive strength of fly ash geopolymer mortar. The specimens used were (70.6×70.6×70.6 mm) cubes cured at 60°C for three different duration 24h, 48h, and 72 hours in hot air oven and tested at 7 days age.. They found that compressive

strength increase with increasing concentration of sodium hydroxide in alkaline solution and curing time. Table 2.2 shows effect of NaOH molarity and curing time on compressive strength of geopolymer mortar.

Table 2.2 Compressive strength at different molarity and curing time (Manware et al., 2016).

NaOH concentration (molar)	Na ₂ SiO ₃ /NaOH	Compressive strength for different durations (MPa)		
		24 hrs	48 hrs	72 hrs
6	0.5	12.43	15.1	15.65
8	1.0	14.52	18.25	19.20
10	1.5	19.82	21.38	22.86
12	2.0	24.12	28.72	30.32
14	2.5	25.6	30.10	33.18

Islam et al. (2014) studied the effect of GGBFS mixed with palm oil fuel ash (POFA) and FA on the compressive strength of the geopolymer mortar. The specimens cured in an oven at 65°C for 24 h. and tested at 7, 14, 21 and 28 days ages. The compressive strength increased by increasing GGBFS content till 70 percent, then reduction in strength occur by increasing GGBFS content, also the addition of POFA up to 30% with GGBS produced the highest strength and hence it is recommended for strength beyond 60 MPa. Figure 2.15 illustrates compressive strength with different GGBFS content.

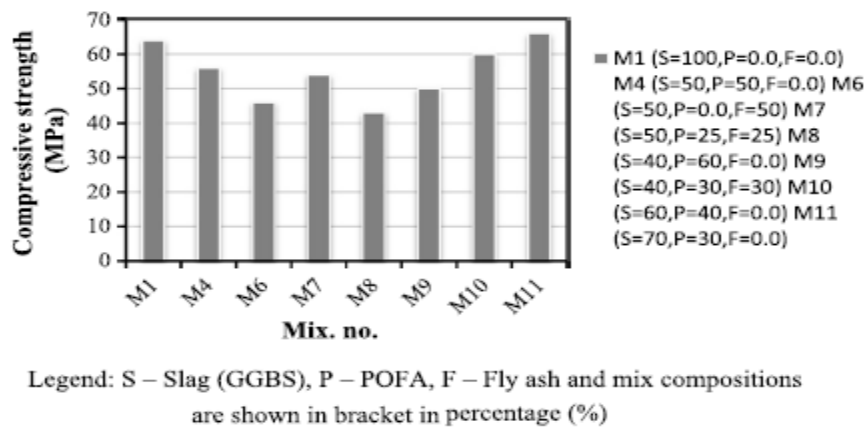


Figure 2.15 The effect of GGBFS on the compressive strength of mortar mixed with POFA and FA at the age of 28-day (Islam et al., 2014).

Abdulkareem et al. (2014) studied the effect of elevated temperature on compressive strength of fly ash geopolymer paste, mortars and lightweight aggregate geopolymer concrete (LWAGC). The unexposed FA geopolymer paste and mortar has higher compressive strength as compared to unexposed LWAGC. This is due to the high geopolymerization reaction rates. Also, they found that the compressive strength decreased after exposed to the elevated temperatures of 400, 600 and 800°C as shows in Figure 2.16.

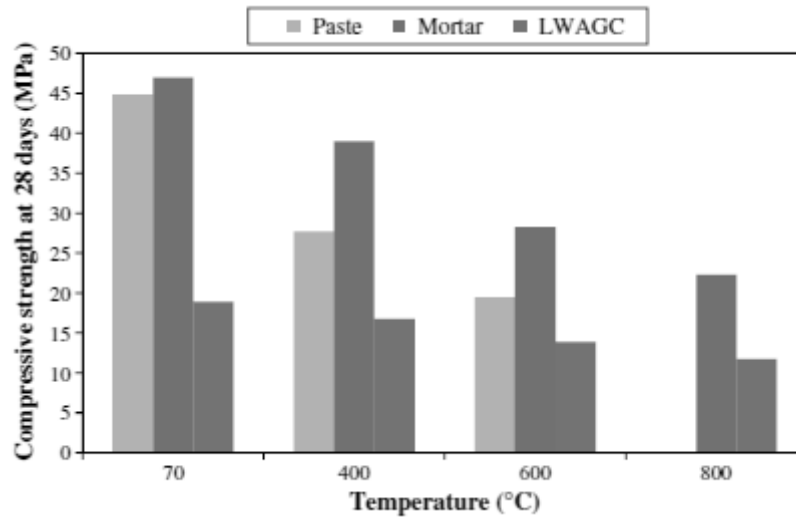


Figure 2.16 Compressive strength of the unexposed and exposed geopolymers to the elevated temperatures 400, 600 and 800 °C (Abdulkareem et al., 2014).

2.7.2 Splitting Tensile Strength

Hardjito and Rangan (2005) reported same to conventional OPC, tensile splitting strength of GPC was only a fraction of the compression strength. Actually, the tensile strength of FA based GPC is greater than the recommended values by Neville (1995) that it is $f_t = 0.23f_c^{2/3}$ for OPC concrete, and CEB-FIP (1990) which is $f_t = 0.3f_c^{2/3}$ and ACI Building Code which is $f_t = 0.59f_c^{1/2}$.

Yellaiah et al. (2014) studied the effect of curing temperature and alkaline activator to binder ratio on splitting tensile strength for geopolymer mortar using fly ash. They found that by increasing alkali activator to fly ash ratio from 0.3 to 0.4 the splitting tensile strength increased at 28 days from 3.03 to 3.44 MPa for curing at temperature of 30°C and from 3.15 to 4.91 MPa for curing at temperature of 60°C with constant curing period of 24 hour as shown in figure 2.17.

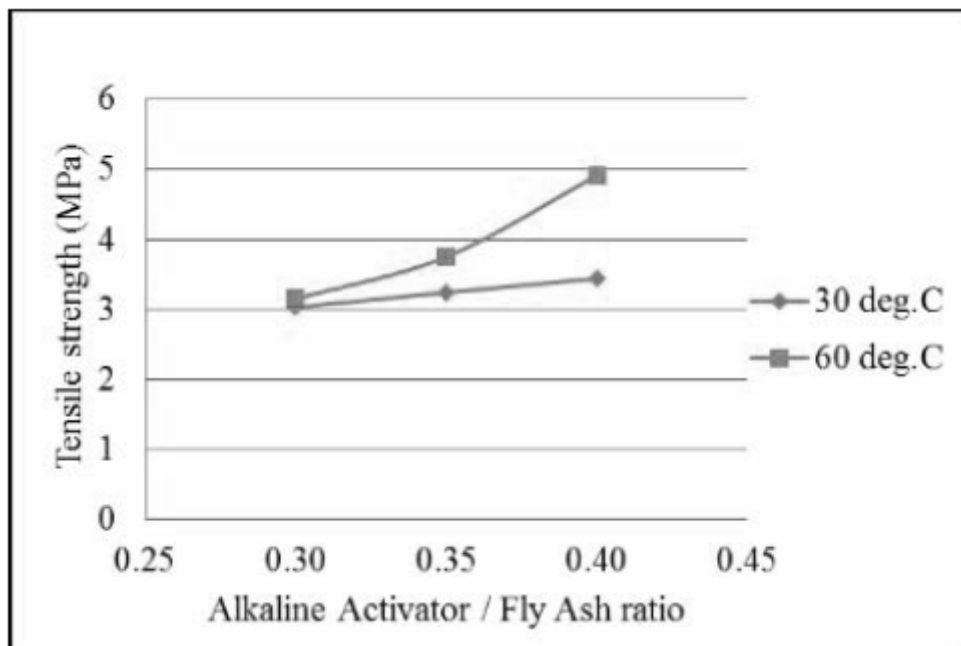


Figure 2.17 Splitting tensile strength with different of alkaline activator to FA (Yellaiah et al., 2014).

Zhang et al. (2016) studied the effect of curing temperature on splitting strength of geopolymer mortar (GM) and compare it with Portland cement mortar (CM) and polymer modified cement mortar (PMCM). The specimens cured at constant temperatures (22°C) for 6 days, after that exposure to 100, 300, 500 and 700 °C). They found the optimum temperature was 100°C that give maximum strength of GM.

Splitting tensile strength of geopolymer mortar increases over cement mortar by 1.85 times at ambient temperature, after that, the difference in tensile strength between GM and CM decreases with increase in temperature. Figure 2.18 shows the effect of curing temperature on splitting strength.

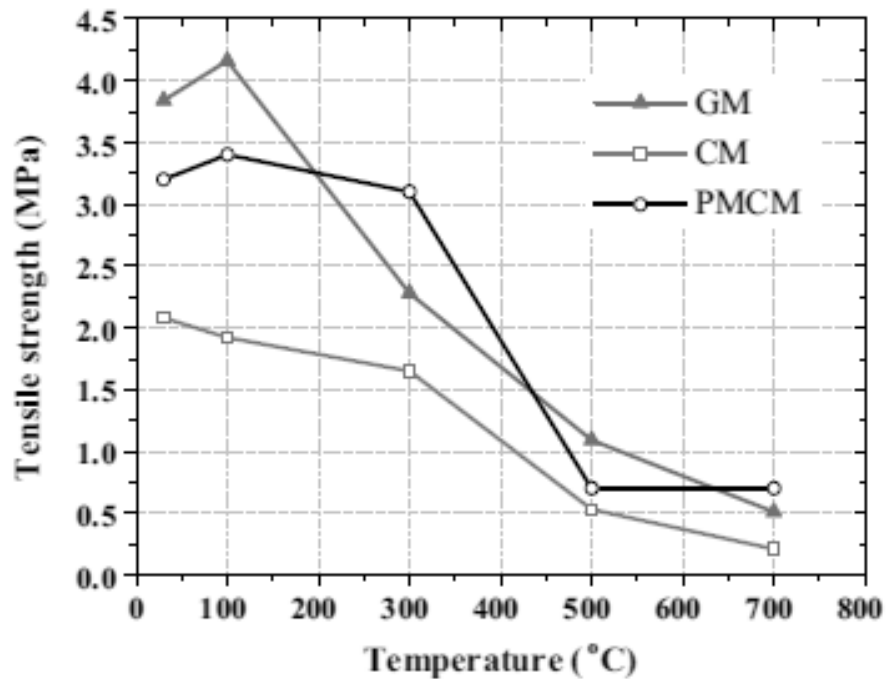


Figure 2.18 Splitting tensile strength at different curing temperature (Zhang et al., 2016).

Huseien et al. (2016) studied the effect of solution types and curing temperature on tensile strength of GPM at 7 days of age using FA, POFA and GGBFS. The result referred to the tensile strength increased when the specimens were activated with Sodium silicate and cured in oven up to 60°C for 24hrs, while the specimens activated by combination of Sodium hydroxide and Sodium silicate and cured at curing temperature above 27°C results in a decrease in the tensile strength, moreover the GPM activated by Sodium silicate has higher tensile strength than GPM activated by Sodium hydroxide and Sodium silicate as shown in Figure 2.19.

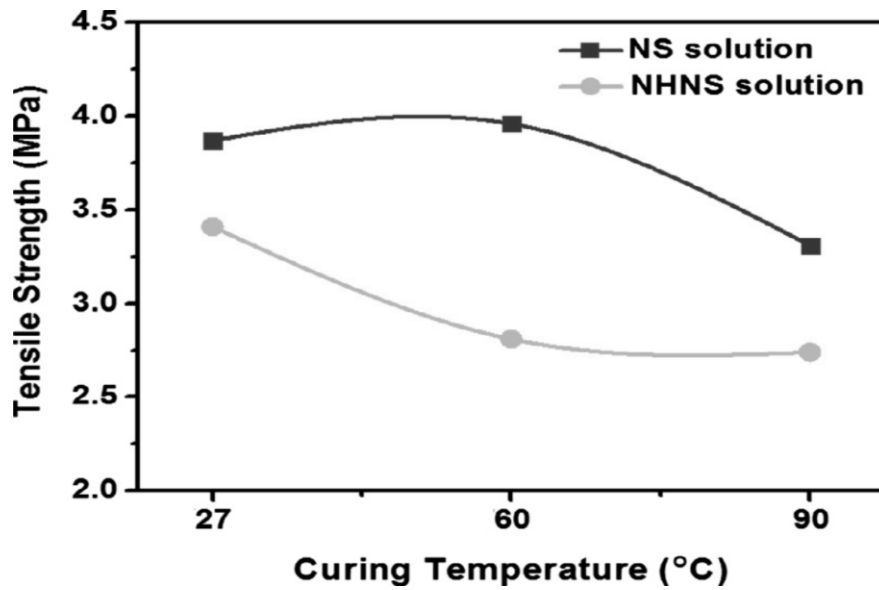


Figure 2.19 Effect of solution types and curing temperature on tensile strength of GPM (Huseien et al., 2016)

Partha et al. (2014) studied the effect of mixing GGBFS with class F Fly ash on splitting strength. They found that maximum splitting strength occurs when mixing 20 percent GGBFS with 80 percent Fly ash, also by decreasing of SS/SH ratio from 2.5 to 1.5 where splitting strength increased by 55 percent with 20% GGBFS and SS/SH ratio of 1.5 when compared with mixes that have 10% GGBFS and SS/SH ratio of 2.5 at 28 days. Figure 2.20 shows splitting tensile strength for different percentage of GGBFS and SS/SH ratio at different ages.

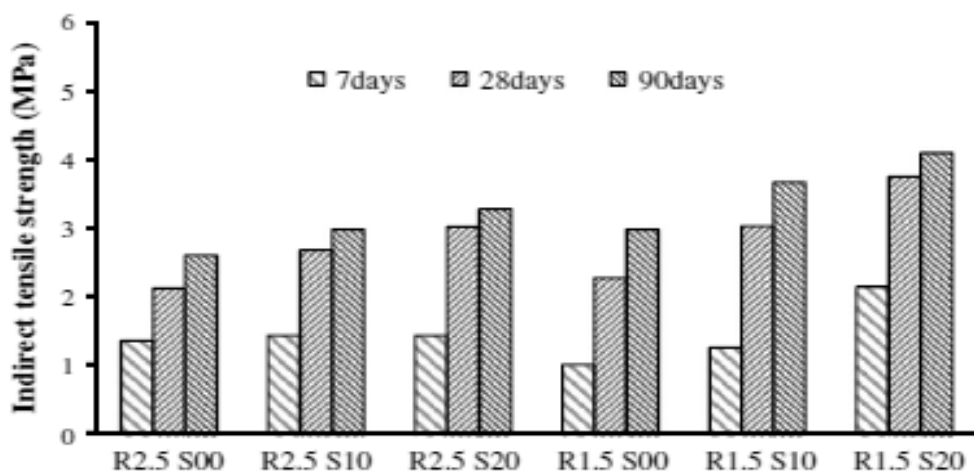


Figure 2.20 Splitting strength for different SS/SH ratio and GGBFS content (Partha et al., 2014).

2.7.3 Sorptivity and Water Absorption

Ghosh and Ghosh (2012) studied the effect of %Na₂O and %SiO₂ on water absorption and sorptivity of fly ash based geopolymer mortar. The specimens used were cured in ambient temperature and humidity in ranging from 25°C to 40°C and 75% to 90% respectively. They found that water absorption and sorptivity decrease with increasing of alkali and silica content. Tables 2.3 shows effect of %Na₂O and %SiO₂ on water absorption and sorptivity of fly ash based geopolymer mortar.

Table 2.3 Water absorption and sorptivity at different silica and alkali content
(Ghosh and Ghosh, 2012).

%SiO ₂	% Na ₂ O	% water absorption	Sorptivity mm/min ^{1/2} , x10 ⁻⁴
0.00	8.00	11.23	5.80
4.25	8.00	9.02	5.00
8.50	8.00	8.11	4.10
12.75	8.00	7.41	3.84
17.00	8.00	7.23	3.62
8.00	4.25	11.70	7.34
8.00	6.25	10.10	6.84
8.00	8.25	7.30	4.12
8.00	10.25	6.90	3.96

Thokchom et al. (2011) studied the Sorptivity and water absorption of geopolymer paste and mortar produced using fly ash with different range of silica fume from 2.5% to 5% and cured for 48hrs at 85 °C. They found that the Addition of silica fume decreased the water absorption and sorptivity for geopolymer mortar while it caused an increase in case of paste specimens. This is because the addition of silica fume enhances pore characteristics for mortar specimens whereas it reduces in the paste specimens. Figure 2.21 shows the effect of silica fume on water absorption and sorptivity.

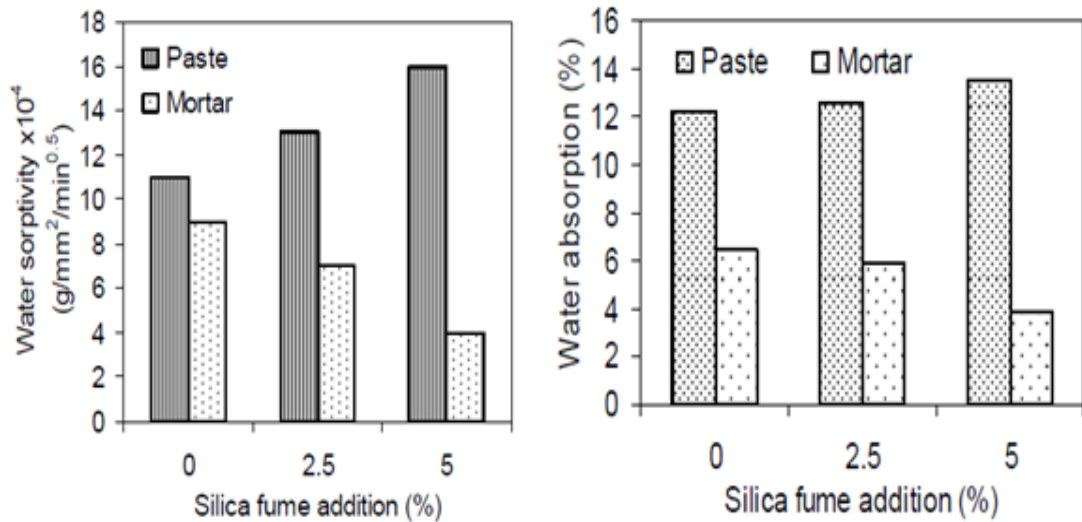


Figure 2.21 Effect of silica fume on water absorption and sorptivity of FA based geopolymer (Thokchom et al., 2011).

Mazumder et al. (2016) studied the effect of replacement GGBFS from 0 percent to 30 percent with FA to produce geopolymer mortar with different sodium hydroxide concentration from 2M to 8M. When replaced GGBFS to 30 percent the water absorption decrease by 17 percent at 7 days as compared with 0 percent GGBFS, due to the increase GGBFS in matrix lead to increase amount of calcium content. The Ca⁺ ions may act as a charge balancer of aluminum atoms. While unreacted GGBFS particles may act as reinforcing agent. Figure 2.22 shows the effect of GGBFS percent on water absorption.

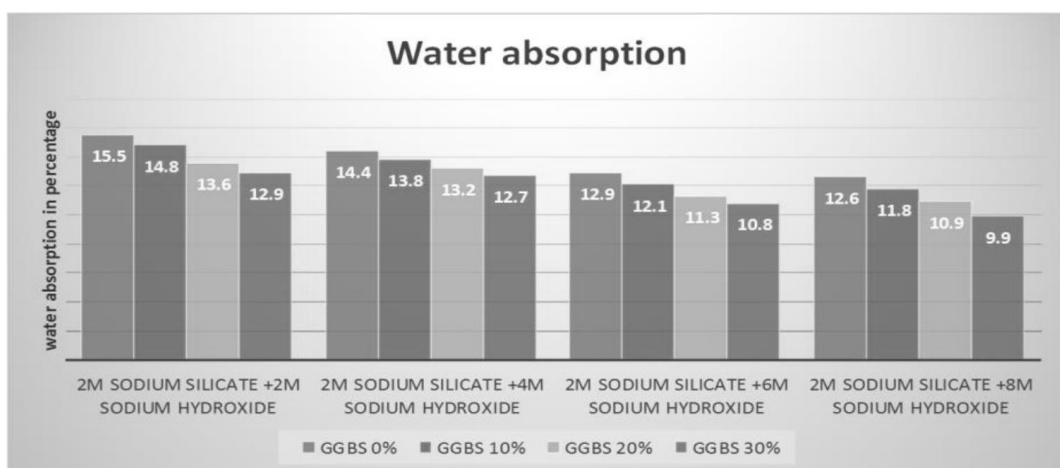


Figure 2.22 Effect of GGBFS and NaOH concentration on water absorption (Mazumder et al., 2016).

Deb et al. (2016) investigated the effect of nano-silica on sorptivity of the fly ash only, OPC and GGBFS blended fly ash geopolymer mortars cured at 20 °C. They found sorptivity coefficient of the mixes without nano-silica was in the range of $3.575 \times 10^{-3} \text{ mm/s}^{1/2}$ to $3.980 \times 10^{-3} \text{ mm/s}^{1/2}$ and that of the mixes with 2% nano-silica was in the range of $1.247 \times 10^{-3} \text{ mm/s}^{1/2}$ to $2.157 \times 10^{-3} \text{ mm/s}^{1/2}$. Thus, it is apparent from the results that the sorptivity coefficient decreased with 2% nano-silica in the all mortar mixes in addition to increasing compressive strength, as shown in Figure 2.23. That is due to the particle packing of nano-silica in the wide distribution of binder particle sizes resulted in a denser matrix and the reaction of nano-silica in geopolymerization process produced further amount of aluminosilicate gel along with the reaction products from the main source materials.

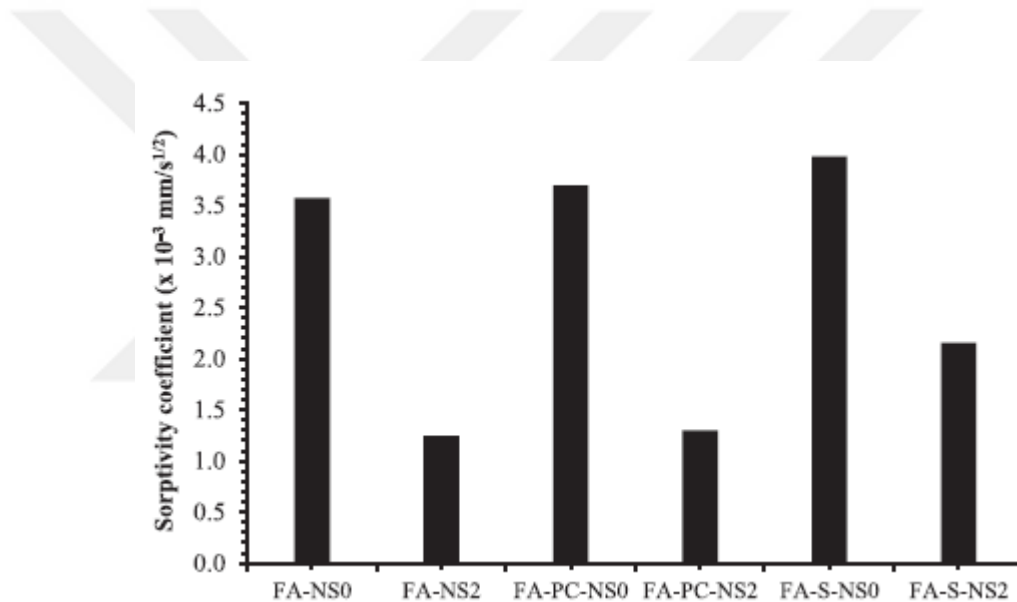


Figure 2.23 Effect of nano-silica on sorptivity coefficient (Deb et al., 2016).

2.8 Concluding Remarks

From the previous studies the following remarks can be concluded:

1. The better geopolymerization and higher reactivity can be achieved for curing temperatures lie between 60 and 90 °C. Curing of GP for more time at high temperature weakens its microstructure.
2. Increasing NaOH concentration lead to improve the properties of geopolymer concrete and mortar.
3. The properties of sodium silicate (Na_2SiO_3) depending on the percent of SiO_2 to Na_2O and water.
4. The presence of calcium in the GGBFS performs hydration and forms C–S–H gel that develops the strength properties.
5. The ratio of Na_2SiO_3 to NaOH plays important role in the properties of geopolymer concrete and mortar.

CHAPTER 3

MATERIALS AND EXPERIMENTAL WORK

This chapter includes the detailed description of properties of materials used in this work, mix proportions, mixing procedure, curing, and various testing procedures.

3.1 Materials

3.1.1 Aggregate

During preliminary study it was found out that using lightweight fine aggregate (LWFA) alone caused no workability and uniformity of the mix. Moreover, the other problems such as segregation, demolding of the samples and very low compressive strength values measured led the authors to decide on utilization of crushed limestone aggregate in production of the mortar samples. Therefore, 70% and 30% of the volume of aggregates were comprised of locally available LWFA and crushed limestone aggregate, respectively. The specific gravity of 1.48 and 2.42 were measured for the former and the latter. The aggregates were sieved from 4 mm sieve to obtain maximum particle size of 4 mm. Figure 3.1 indicates the grading of the aggregates. From the grading curves it is understood that the LWFA is coarser than crushed limestone aggregate. The aggregates were immersed in water to obtain 100% saturation. The excessive moisture on the surface of the aggregates was dried to get SSD condition. 24 hours immersion decided to be enough for full saturation. The result of the experimental study on the water absorption capacity of LWFA was shown in Figure 3.2. It was observed that maximum saturation level (26.6%) can be reached at the end of 24 hours.

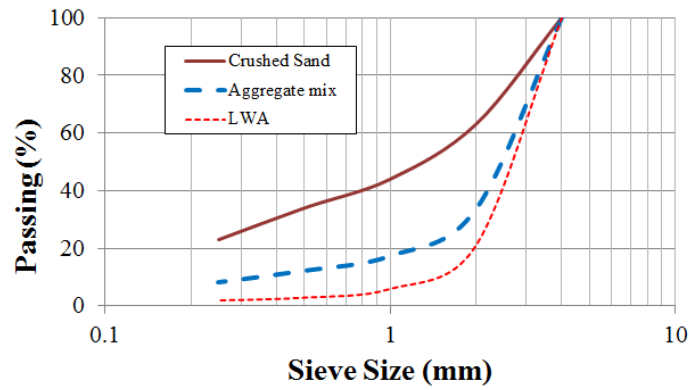


Figure 3.1 Grading of the aggregates.

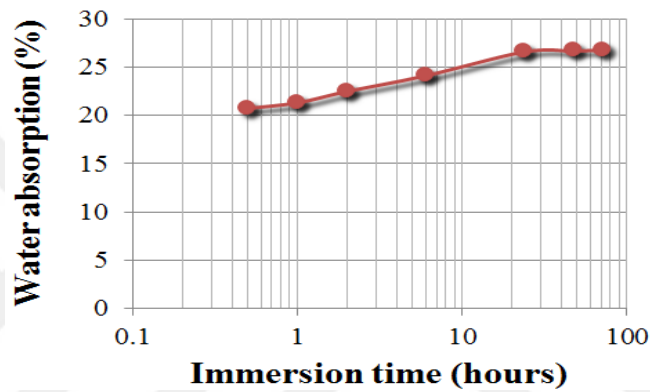


Figure 3.2 Water absorption of LWFA.

3.1.2 Pozzolanic Materials

Two pozzolanic materials, FA and GGBFS, were utilized as binding materials to develop lightweight geopolymer mortar in an alkaline environment. Fly ash (FA) of class F according to ASTM C618 (ASTM C618-08, 2002) was supplied from Ceyhan Sugozy thermal power plant, and ground granulated blast furnace slag (GGBFS) conformed to ASTM C 989 were used. The physical and chemical properties of FA and GGBFS are given in Table 3.1 as obtained by X-ray fluorescence (XRF).

Table 3.1 Properties of FA and GGBFS.

Physical and chemical analysis (%)	FA	GGBFS
CaO	2.2	34.12
SiO ₂	57.2	36.41
Al ₂ O ₃	24.4	10.39
Fe ₂ O ₃	7.1	0.69
MgO	2.4	10.26
SO ₃	0.3	
K ₂ O	3.4	0.97
Na ₂ O	0.4	0.35
Loss of ignition	1.5	1.64
Specific gravity	2.25	2.61
Specific surface area (m ² /kg)	379	418

3.1.3 Sodium Hydroxide, NaOH

The sodium hydroxide, with 98 percent purity, in flake form is local available. The solids must be dissolved in distilled water to make a solution with the required concentration. Sodium hydroxide is used to prepare solution of geopolymer mortar. NaOH in flakes form with 98% purity shown in figure 3.3 was purchased from local chemical supplier has been used to produce NaOH solution. Table 3.2 shows more details for the used sodium hydroxide solution in the present work according to ASTM E291-09. The reaction of sodium hydroxide with water was exothermic (it should take care) therefore, it recommended to cooling by water especially during mix.



Figure 3.3 Sodium hydroxide flakes.

Table 3.2 Composition of sodium hydroxide (%).

Item	Specification ASTM E291-09	Results
Sodium hydroxide (NaOH), min.	97.5≤	98.14
Sodium carbonate (Na ₂ CO ₃), max	0.40	0.36
Sodium chloride (NaCl), max.	0.15	0.07
Iron oxides (Fe ₂ O ₃), max.	0.01	0.005

3.1.4 Sodium Silicate, Na₂SiO₃

The concentration of sodium silicate is depending on the ratio of Na₂O to SiO₂ and H₂O. This type of sodium silicate shown in figure 3.4 was manufactured in Turkey. The composition of sodium silicate solution (water glass) is 29.4% SiO₂, 14.7% Na₂O, and 55.99% water (by mass). Table 3.3 illustrates the properties of used sodium silicate.

Table 3.3 Properties of sodium silicate.

Description	Value
Ratio of SiO ₂ to Na ₂ O	2.0 ± 0.05
Na ₂ O percent by weight	14.7
SiO ₂ percent by weight	29.4
Density - 20°	51± 0.5
Specific Gravity	1.48
Viscosity (CP) at 20°C	600-1200
Appearance	Hazy

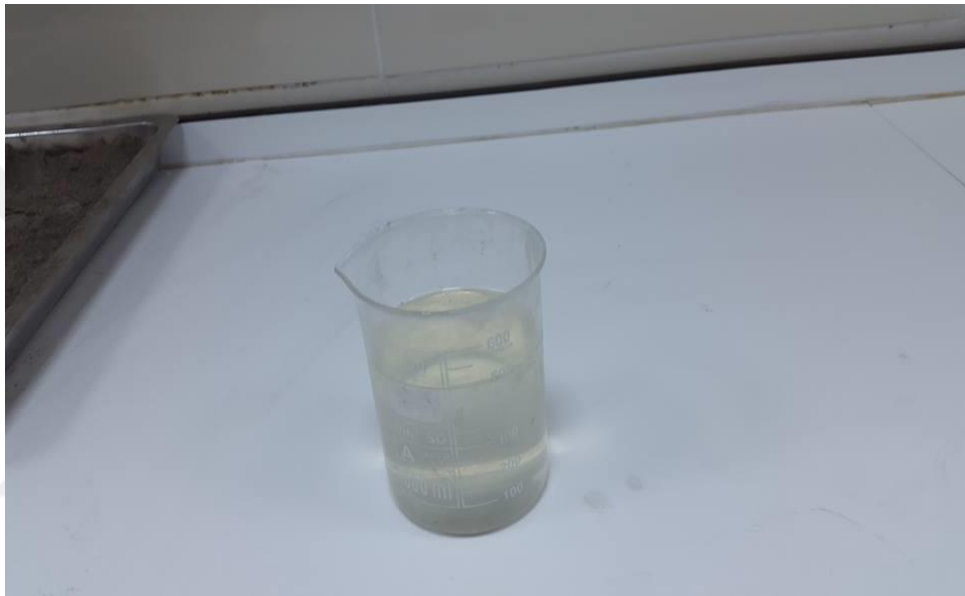


Figure 3.4 Sodium silicate solution (water glass).

3.1.5 Superplasticizer

The plasticizer is utilized to improve the workability of geopolymer mortar without adding water and it is taken as 5% of binder, a polycarboxylic ether based high range water reducing super plasticizer, supplied by Master Builders Technologies, Perth, Turkey, under the brand name of Glenium 51, was used in all of the mixtures. This type of superplasticiser is a liquid and complies with the ASTM C494-2005. Table 3.4 shows the main properties of superplasticizer SP1.

Table 3.4 Properties of superplasticizer (SP1).

Property	Description
Color	Dark brown / black liquid
Specific gravity	1.07 at 25 ⁰ C
Air entrainment	Maximum 1%
Chloride content	< 0.1%
Alkaline content	< 3%
Freezing point	0%

3.1.6 Distilled Water

This type of water is used to dissolve sodium hydroxide to make NaOH solution.

3.2 Mix Proportions

Fourteen LWGM mixtures were designed with varying GGBFS and FA content to study the compressive strength response of LWGM under different curing period, curing temperature and binder content. The binder content in the mixtures is total amount of alkaline solutions and the base material (FA or GGBFS). The selected binder contents are 650, 750, 850, 950, 1050, 1150, and 1250 Kg/m³. The experiments were conducted on LWGM cubes under curing temperature of 60, 80, 100 and 120 °C with curing period of 2, 6, 8, 24, 48 and 72 hrs. The mixture proportions of LWGM are presented in Table 3.5. The alkaline solution was the only liquid component in all mixtures (without adding water). Super-plasticizer with specific gravity of 1.07 is added to the mix to improve the workability and to make GP mix homogeneous.

Table 3.5 Geopolymer lightweight mortar mix designs.

Designation LWGM	Pumice agg. (kg/m ³)	Crushed limestone (kg/m ³)	GGBFS (kg/m ³)	FA (kg/m ³)	Na ₂ SiO ₃ solution (kg/m ³)	Solution of NaOH (kg/m ³)	S.P. (kg/m ³)
MS650*	624.03	415.45	433.29	---	154.7	61.88	21.66
MS750	574.45	382.44	499.95	---	178.5	71.40	24.99
MS850	524.88	349.44	566.61	---	202.3	80.92	28.33
MS950	475.30	316.43	633.27	---	226.1	90.44	31.66
MS1050	425.72	283.42	699.93	---	249.9	99.96	34.99
MS1150	376.14	250.41	766.59	---	273.7	109.48	38.32
MS1250	326.56	217.41	833.25	---	297.5	119.00	41.66
MF650**	598.94	398.74	---	433.29	154.7	61.88	21.66
MF750	545.50	363.16	---	499.95	178.5	71.40	24.99
MF850	492.06	327.59	---	566.61	202.3	80.92	28.33
MF950	438.62	292.01	---	633.27	226.1	90.44	31.66
MF1050	385.18	256.43	---	699.93	249.9	99.96	34.99
MF1150	331.74	220.85	---	766.59	273.7	109.48	38.32
MF1250	278.30	185.28	---	833.25	297.5	119.00	41.66

*MS650: GGBFS based mixture with geopolymer binder 650 kg/m³

**MF650: Fly ash based mixture with geopolymer binder 650 kg/m³

3.3 Experimental Study

Experimental investigation is primarily focused on three stages. The first stage is devoted to manufacture of geopolymer mortar by using local GGBFS and FA-based geopolymer mortar and the compressive strength development under different curing period, curing temperature and binder content. The alkaline activator is a mix of 12M NaOH solution with sodium silicate in ratio of 1:2.5. The ratio of alkaline solution to binder equal to 0.50.

The second stage studies the optimization and verification of optimum curing period and curing temperature on the compressive strength, splitting tensile strength, water absorption and sorptivity.

The systems “A Central Composite Experimental Test” was designed to find the optimum parameters for geopolymer mortar made with this type of fly ash and GGBFS. There were 24 tests that were set up for one binder content and 168 tests for all levels of fly ash bind and the same of GGBFS with the following three fixed factors: Alkali type: Sodium silicate and sodium hydroxide , sodium hydroxide to silicate ratio: 1 to 2.5 and activator solution-to-fly ash or GGBFS ratio 1 to 2. Finally, investigates the effect of molarity and different ratios of $\text{Na}_2\text{SiO}_3/\text{NaOH}$ on mechanical properties and absorption of Fly ash and GGBF geopolymer mortar.

3.4 Stage I: Manufacturing GGBFS and FA Based Geopolymer Mortar and Studying the Compressive Strength Development under Different Curing Period, Curing Temperature and Binder Content

3.4.1 Preparation Alkaline Solution for Geopolymer

The solution of geopolymer mortar is constituted of sodium hydroxide and sodium silicate. Sodium hydroxide, in flakey form and high purity, more than 98 percent, can be dissolved in distilled water to make a solution with the appropriate concentration. Sodium hydroxide is a mix of 12M solution. The mass of sodium hydroxide solids in a solution with a concentration of 12 Molar consists of $12 \times 40 = 480$ grams of NaOH solids per liter of the solution, where 40 is the molecular weight of NaOH; Na=23, O=16, and H=1. The mass of NaOH solids is measured as 361 grams per kg of NaOH solution.

The sodium silicate solution is commercially available in different grades. Throughout this work, the used sodium silicate solution has a ratio of SiO_2 to Na_2O by mass which equals 2.0. The proportions, by mass of components, are 29.4%, 14.7% and 55.99% for SiO_2 , Na_2O , and water, respectively.

After preparing NaOH as a solution, it is added to the Na_2SiO_3 solution. The combination of sodium hydroxide (NaOH) solution and sodium silicate solution is considered as the alkaline liquid. It is recommended that the alkaline liquid is prepared by mixing both the solutions together at least 24 hours before using (Rangan, 2011).

3.4.2 Mixing, Casting, and Curing Regime

The binder is the main difference between geopolymer Mortar and Portland cement Mortar. The silica and aluminum oxide in FA and GGBFS react with alkaline liquid solution (Na_2SiO_3 and NaOH) to form a paste of geopolymer that binds the coarse and fine aggregates with other materials together to form the geopolymer mortar. The procedure of mixing has a major effect on workability and strength of geopolymer mortar. Many researchers stated that geopolymer Mortar and concrete can be manufactured by adopting the conventional techniques used in the manufacture of Portland cement concrete (Lloyd and Rangan, 2009; Sanni and Khadiranaikar, 2013). Base material and fine aggregate first are mixed together in dry form in a mixer for three minutes (Figure 3.5). The aggregates are prepared in saturated surface dry, SSD condition (Figure 3.6).

The alkaline liquid was mixed with the superplasticiser without water for not less than two minutes. Then the liquid component of the mixture is added to the dry materials in the pan of the mixer (Fig. 3.7) and the mixing continued usually for another four minutes (Huseien et al., 2016). Figure 3.8 show homogenous geopolymer mortar.



Figure 3.5 Dry materials for geopolymer mortar.



Figure 3.6 Saturation surface dry lightweight fine aggregate (LWFA).



Figure 3.7 Mixer used for manufacturing geopolymer mortar.



Figure 3.8 Fresh geopolymer mortar after mixing.

The fresh FA-based geopolymer mortar was dark in colour and shiny in appearance (Figure 3.11). The mixtures were usually cohesive. The workability of the fresh mortar was measured by means of the conventional flow table test.

The fresh LWGM was poured in two layers in the moulds (mould size is 50 x 50 x 50 mm). After casting LGWM in the specimen moulds and to remove the air voids, the moulds were vibrated using vibrating table for 30s. Figure 3.9 shows compaction table. The specimens were wrapped with thin plastic film (heat resistant) as shown in Figure 3.10 to avoid loss of water due to evaporation.



Figure 3.9 Geopolymer compacting and placing.



Figure 3.10 Mortar sealing with a heat resistant film.

Next, all the mixtures were cured in an oven under curing temperature of 60, 80, 100 and 120 °C for 2, 6, 8, 24, 48 and 72 h. Figure 3.11 shows the specimens curing in the oven. Then specimens were demolded after the curing process and the specimens were tested. Considering full factorial combination of 2 base materials, 4 curing temperatures, 6 curing periods, and 7 binder contents; a total of 336 data samples were obtained.



Figure 3.11 Mortar curing.

3.4.3 Fresh Density Test

Fresh density conducted for geopolymer mortar according to ASTM C 138– 01a.

3.4.4 Compressive Strength Test of Geopolymer Mortar Cubes

The compressive strengths of the mortars are determined in accordance with ASTM C 109. The compressive strengths of the all the mixtures were cured in an oven under curing temperature of 60, 80, 100 and 120 °C for 2, 6, 8, 24, 48 and 72 h. After the specimen has been cured for the proper length of time in the oven, remove and let to cool down before testing. Place the specimen in the compressive strength machine, as seen in Figure 3.12. The compressive strength tests are usually performed on three specimens for better accuracy and the average value is taken as the final result.



Figure 3.12 Mortar cube compressive strength test.

3.5 Stage II: Studying the Optimization and Verification of Optimum Curing Period and Curing Temperature on the Compressive Strength

Several standardized tests of fresh geopolymer mortars properties were followed to evaluate the properties of the raw materials and hardened geopolymer mortars properties followed to study optimization. These tests included:

3.5.1 Fresh Density Test

Fresh density conducted for geopolymer mortar according to ASTM C 138– 01a.

3.5.2 Mortar Flow Test

The flow of the geopolymer mortars was determined using a flow table and flow mold conforming to the requirement of specification ASTM C 230 (2003). The flow test was conducted on each geopolymer mixture following ASTM C 109 (2002).



Figure 3.13 Flow table test apparatuses.



Figure 3.14 Photographic view of mortar flow.

3.5.3 Compressive Strength Test of Geopolymer Mortar Cubes

The compressive strength of the specimens in the response surface method (RSM) was determined after the different curing period and one curing temperature of 60°C as show in Table 3.6 get from optimization program. Additional 2" cube specimens were cast as required to determine the effect of age on the compressive strength of the GPM mixtures. Measurements were recorded at 7 days. Compressive testing was performed with a compressive machine in accordance with ASTM C109 (2005).

Table 3.6 Design expert results.

Designation LWGM	Curing temperature (°C.)	Curing time (hours)	Compressive strength (MPa)	Desirability
MS650*	60	21.547	27.712	0.784
MS750	60	20.908	29.171	0.805
MS850	60	20.391	30.432	0.823
MS950	60	19.949	31.47	0.837
MS1050	60	19.634	32.315	0.849
MS1150	60	19.372	32.935	0.857
MS1250	60	19.228	33.363	0.862
MF650**	60	21.856	10.767	0.669
MF750	60	22.381	11.904	0.689
MF850	60	22.823	13.05	0.708
MF950	60	23.244	14.218	0.727
MF1050	60	23.590	15.386	0.745
MF1150	60	23.926	16.573	0.761
MF1250	60	24.208	17.759	0.778

3.5.4 Splitting Tensile Strength Test

The tensile strength is important because it determines the ability of concrete to resist to cracking. Several tests can be used to determine indirect tensile strength but the one used in this study is the ASTM C 39, 2012: “Methods for Splitting Tensile Strength of Cube Concrete Specimens”. The mortar cube is placed on its side . It is then subjected to diametrical compressive force along its length. This test can be performed on the same machine as the compressive strength test but a bearing bar can be added. The load is then applied; the value at which a longitudinal failure occurs is then recorded. The following equation is used to calculate the value of the Split tensile strength:

$$\text{Equation: } f_{sp} = \frac{2P}{\pi a^2}$$

Where:

f_{sp} is the split tensile strength value in MPa

P is the maximum load during test in N

a is the dimension of the cube in mm.



Figure 3.15 Cube specimens after split tensile test.

3.5.5 Saturated Water Absorption

Saturated water absorption test was conducted on 50 x 50 x 50 mm cubes at the age of 7 days. The specimens were weighed before drying in hot air oven at 105° C. The drying process was continued, until the difference in mass between two successive measurements at 24 hours interval closely agreed. The dried specimens were cooled at room temperature and then immersed in water. The specimens were taken out at regular intervals of time, surface dried and weighed. The differences between the saturated mass and the oven dried mass expressed as the percentage of oven dried mass gives the saturated water absorption. (Thokchom et al., 2009).

$$\text{Saturated Water Absorption} = [(W_s - W_d) / W_d] \times 100$$

Where

W_s = weight of specimen at fully saturated condition.

W_d = weight of oven dried specimen.

3.5.6 Sorptivity

The sorptivity test is a simple and rapid test to determine the tendency of concrete to absorb water by capillary suction. The test was developed by Hall (1989) and is based on Darcy's law of unsaturated flow.

The samples were pre-conditioned for 7 days in hot air oven at curing temperature 60 C and drying temperature 100 C. The sides of the specimen were sealed in order to achieve unidirectional flow. Locally available silicon resin was used as sealant. Weights of the specimen after sealing were taken as initial weight. The initial mass of the sample was taken and at time 0 it was immersed to a depth of 3-5 mm in the water. At selected times (typically 1, 4, 9, 16, 25, 36, 49, and 64 minutes) the sample was removed from the water, the stop watch stopped, excess water blotted off with a damp paper towel or cloth and the sample weighed. It was then replaced in water and stop watch was started again. The gain in mass per unit area over the density of water is plotted versus the square root of the elapsed time. The slope of the line of best fit of these points (ignoring the origin) is reported as the sorptivity. ASTM C1585 were followed to conduct the test.

The experimental set up for the sorptivity test as conducted on mortar is shown in Figure 3.16.



Figure 3.16 Sorptivity test setup.

3.6 Stage II: Studying the Effect of Molarity and Different Ratios of $\text{Na}_2\text{SiO}_3/\text{NaOH}$ on Mechanical Properties and Absorption of Fly Ash and GGBF Geopolymer Mortar

The tests conducted in this stage were fresh density measurement, flow table test, compressive strength test, splitting tensile strength test, sorptivity and water absorption test for the mixtures of FA and GGBFS geopolymer mortars cured in an oven under curing temperature of 60 °C for initial curing (IC) of 23.2 hr. and 19.9 hr. respectively.

Moreover, this stage covers new combinations of alkaline solutions with different molarities and $\text{Na}_2\text{SiO}_3/\text{NaOH}$ ratios. The details of the mixtures are given in Chapter 6.

After examining the LWGMs experimentally, a new optimization study was conducted to find optimum molarity and $\text{Na}_2\text{SiO}_3/\text{NaOH}$ ratio for the optimum curing time and curing temperature predefined in Stage II.

CHAPTER 4

TEST RESULTS AND DISCUSSION

4.1 General

In this chapter, the results are presented and discussed for all the experimental work described in first part in chapter three. The discussion presents the results of geopolymer mortar which are fresh density and flow table in addition to hard state tests including compressive strength have been studied and discussed. The effects of binder content, curing temperature and curing duration on the compressive strength of LWGM were investigated.

4.2 Fresh Properties Tests

4.2.1 Flow Table Test

Table 4.1 and Figures (4.1 and 4.2) shows the results of the workability tests (flow table) for different mortar mixes used in this investigation.

The results show that it is possible to have a homogeneous mix for all the studied mixes using fly ash geopolymer binder (750-1250 kg/m³) and GGBFS mix with geopolymer binder content (950-1250 kg/m³) except for M1 of fly ash which was (650 kg/m³) and M1,M2&M3 of GGBFS. Flow percentage increase with the increment of binder content in the mixture due to lesser friction between particles. On the other hand, Workability is high for fly ash geopolymer mortar when compared to GGBFS geopolymer mortar.

Fly ash has smooth spherical particles whereas slag is composed of angular particles of varying sizes (Figure 3.5) combined with the lubricating effect of sodium silicate solution increase the flow ability and leads to increase the flow diameter of the fresh mortar specimens during the flow table test.

Table 4.1 Flow table of of LWGM.

Mix no.	Binder content (kg/m ³)	Flow table of GGBFS (mm)	Flow table of FA (mm)
M1	650	0	110
M2	750	0	162
M3	850	121	178
M4	950	155	185
M5	1050	164	200
M6	1150	190	220
M7	1250	200	225

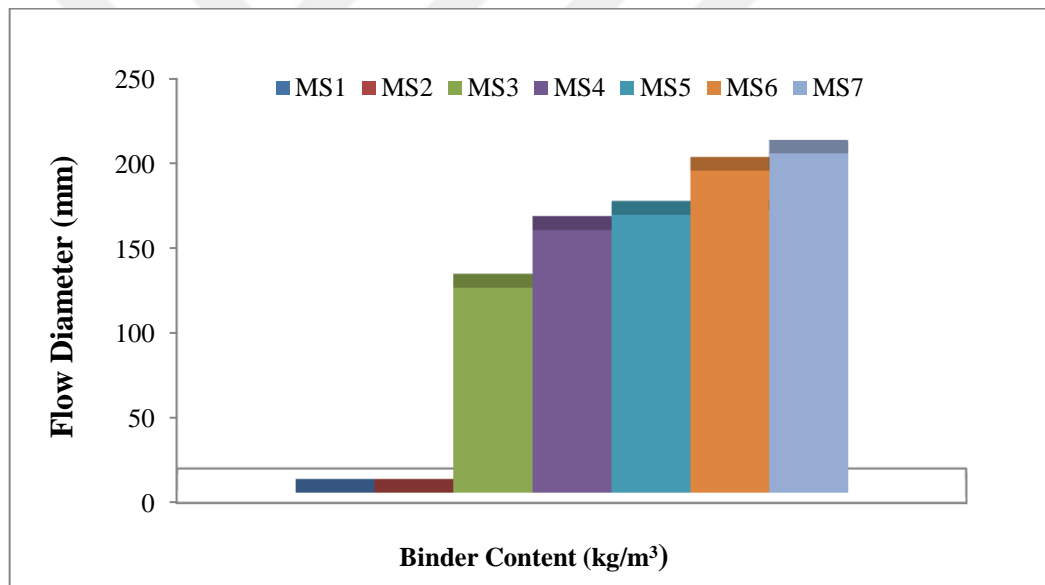


Figure 4.1 Flow table of GGBFS geopolymer mortar.

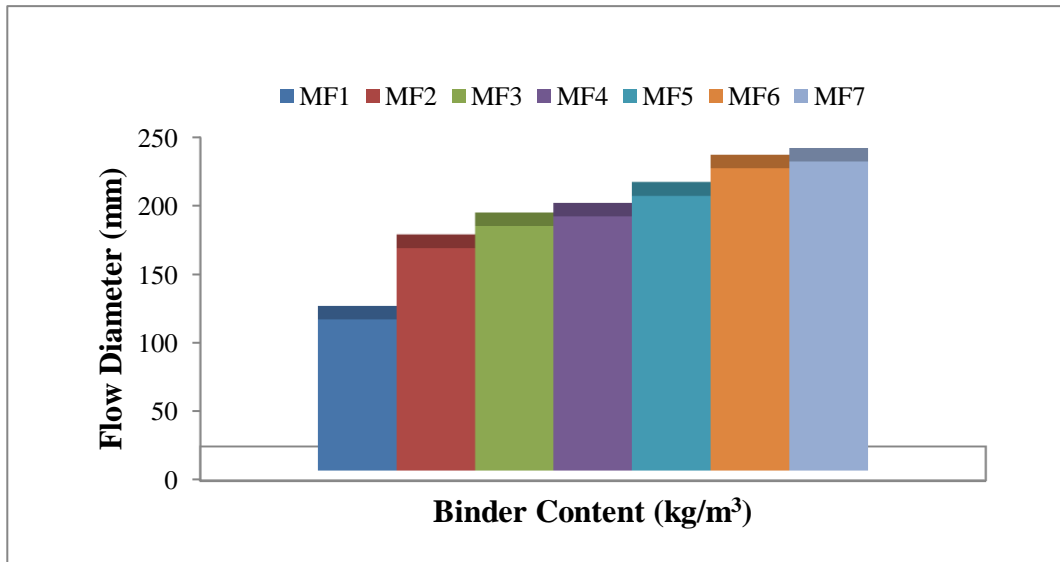


Figure 4.2 Flow table of FA geopolymer mortar.

4.2.2 Fresh Density Test

Fresh density of GGBFS and FA based geopolymer mortar was conducted directly after mixing. The measured density was for the all mixtures Table 4.2 presents the density of the fresh unit weight of LWGM. As shown in Table 4.2 there was insignificant increase in mortar unit weight with the increase of binder content because the LWFA has less specific gravity than binder. On the other hand, the fly ash based geopolymer mortar exhibits a reduction in fresh unit weight density compared with GGBFS based geopolymer mortar.

Table 4.2 Fresh unit weight of LWGM.

Mix no.	Binder content (kg/m ³)	Fresh unit weight of GGBFS (kg/m ³)	Fresh unit weight of FA(kg/m ³)
M1	650	1726.6	1685.3
M2	750	1760.8	1702.6
M3	850	1800.6	1722.0
M4	950	1830.2	1739.6
M5	1050	1844.0	1749.3
M6	1150	1868.0	1760.0
M7	1250	1885.1	1771.3

4.3 Compressive Strength Test

Compressive Strength is the most important physical property of mortar. In many ways compressive strength predicts the behavior of mortar in gross. The obtained results from compressive strength test are presented here. The strength obtained at different binder content of mortar with different curing temperature and curing duration.

4.3.1 Effect of the Binder Content on the Strength of Slag Based Geopolymer Mortar

Figures 4.3 show the results of compressive strength developed in GGBFS-based LWGM with variable geopolymer binder content. It could be concluded that the compressive strength raised proportionally with the increment of binder content. Compressive strength of GGBFS-based LWGM at 24 hours increased gradually from 26.02, 27.81, 24, and 22.5 MPa to 34.1, 32.71, 30.6 and 28.8 MPa for binder contents of 650 Kg/m³ and 1250 kg/m³, respectively. Similar trend was observed at 48 hours as increasing from 27.5, 29.8, 29.8, and 22.71 MPa to 38.01, 35.54, 32.51 and 31.2MPa for 650 kg/m³ and 1250 kg/m³ binder content.

Compressive strength at the end of 2, 6, 8, 24, 48 and 72 hours thermal curing is shown in Figures no. 4.1 which clearly show that strength increases with increase in binder content. At lower ground granulated blast furnace slag content, the quantity of the geopolymer gel formed during the process of geopolymerization may not be adequate to bind all loose aggregates and reduction in compressive strength was observed.

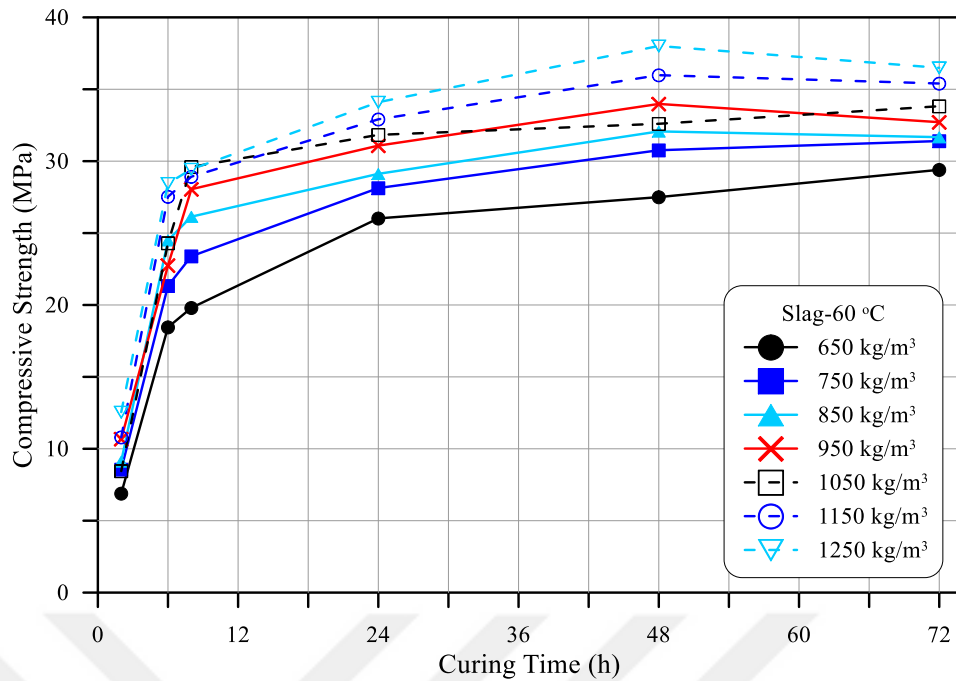


Figure 4.3 Compressive strength development of GGBFS based geopolymer mortar cured at 60°C for 650,750, 850,950,1050,1150 and 1250 kg/m³ binder.

4.3.2 Effect of the Binder Content on the Strength of Fly Ash Based Geopolymer Mortar

Figure 4.4 show the compressive strength of fly ash geopolymer mortars cured at 60 °C., 80 °C, and 100 °C. and 120 °C after 2, 6, 8, 24, 48 and 72 hours, respectively The results show that the increase in content of fly ash from 650 to 1250 kg/m³ no effect on compressive strength at 2 hour curing time but leads to a slight increase in compressive strength (4.7–6.81 MPa) at 60°C for 6 hour. There is a 50 percent difference in strength between mixes MF1 and MF7 at 8 and 24 hours for 60°C and about 50 percent at 6 to 24 hours for another curing temperatures . Increasing the fly ash content could lead to an increase in (Si) and (Al) content and may increase geopolymer gel that binds aggregate and increase compressive strength (Djobo and Tchakoute, 2014). On the other hand, lowering the fly ash content leads to a reduction in compressive strength because of the deficiency in Si and Al content. The lowering of fly content from 1250 to 650 kg/m³ leads to a decrease in compressive strength by (45.3,26.8,32.08 and 30.9 percent) at 72 hours and (39.7,23,43.9 and 39.2 percent) at 48 hours for (60,80,100 and 120) °C., respectively. Increasing fly ash to 1250 kg/m³ lead to improving in compressive strength while the cost will be higher.

Compressive strength is high for GGBFS geopolymer mortar when compared to fly ash geopolymer mortar because of the presence of lower amounts of reactive glassy phases in fly ash as compared to slag (Kumar et al., 2010).

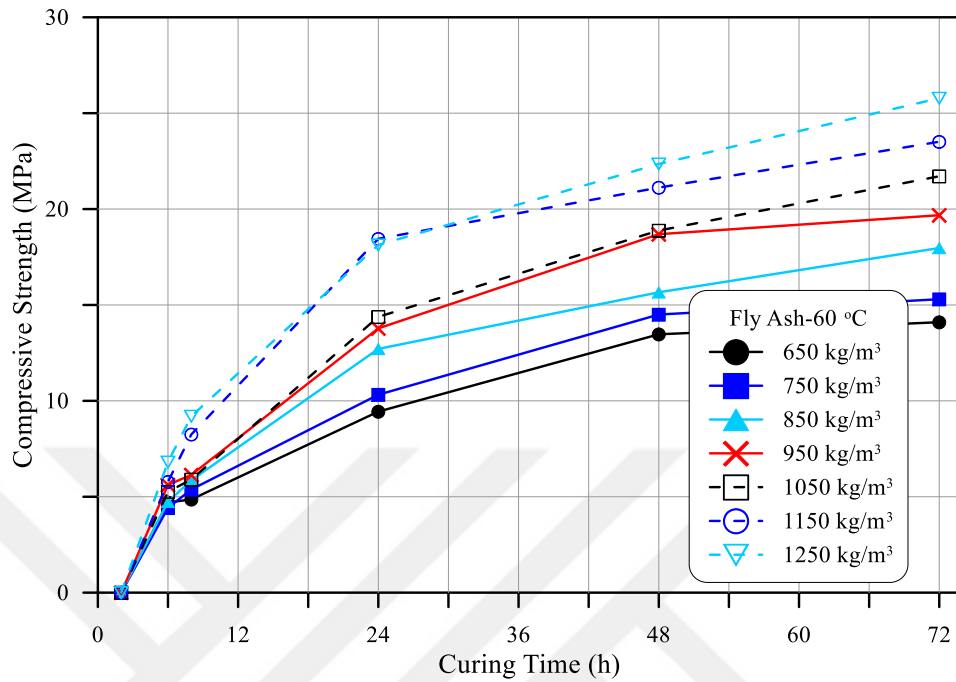


Figure 4.4 Compressive strength of fly ash geopolymer mortar cured at 60°C for 650,750,850,950, 1050, 1150 and 1250 kg/m³ binder.

Figure 4.5 indicates the variation binder content and the highest compressive strength value mainly depend on curing temperature and duration. The figure also indicates change in the fresh unit weights of LWGMs. Since the LWFA has less specific gravity than binder, as the amount of binder increases in the mix the fresh unit weight increased accordingly. Accordingly, higher density causes a higher compressive strength (Aguilar et al., 2010). The highest unit weight measured 1885 Kg/m³ for GGBFS based LWGM while the lowest value was 1685 Kg/m³ for FA based one. The most critical observation of Figure 4.5 is that almost all of the mixtures satisfy the definition of structural lightweight concrete specified by American Concrete Institute. ACI 213R committee report defines structural lightweight concrete as 28 day compressive strength value of higher than 17.2 MPa and dry density of 1850 Kg/m³.

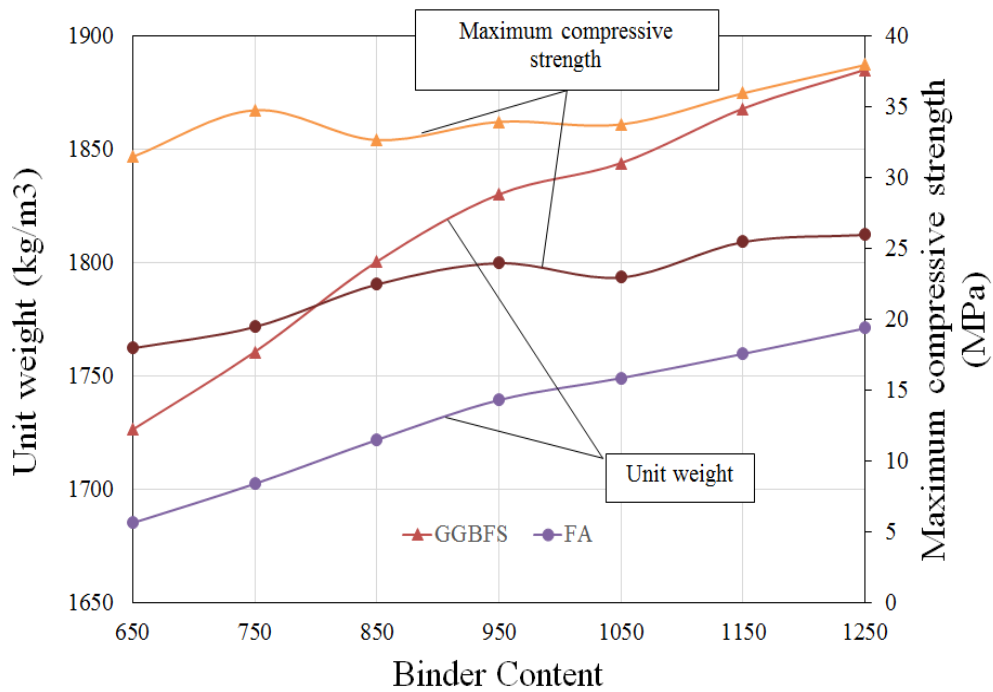


Figure 4.5 Effect of binder content on the variations of maximum compressive strength and fresh unit weight of LWGMs.

4.3.4 Effect of Curing Duration and Curing Temperature

4.3.4.1 GGBFS Based Geopolymer Mortar

It is important to increase the curing temperature for the samples to gain strength quickly when higher strengths are intended to be achieved during a shorter period of time (De Vargas et al., 2011). The thermal curing process applied for more than a few hours at high temperatures had a positive effect on compressive strength of the material (Van Jaarsveld et al., 2007). The strengths of the samples increased as a result of the curing times and the reactions between silica and alumina in the alkaline ions (Somna et al., 2011).

The compressive strength response of GGBFS-based LWGM under different curing period and curing temperature is shown in Figure 4.6 -4.12 and Table 4.3-4.9. It could be concluded from Figure 5 that the compressive strength increases with the increase in curing duration. The samples gained the maximum strength at the first six hours of curing as can be clearly observed from Figure 5; however, the gain in strength beyond 8 h is not important.

The highest compressive strength was observed at samples cured at 60°C for 48 h with different GGBFS content except for mixture of 650 kg/m³ GGBFS content produced the highest compressive strength at 80°C for 72 h. At the first 2 and 4 h of curing, the maximum compressive strength was noticed in the specimens cured at 100 and 120 °C. It can be concluded that the strength of LWGM can be obtained quickly by increasing the curing temperature with reduced duration of heating.

Considering the results, the compressive strength increased when the curing temperature was increased. However, the value of compressive strength decreased when the curing temperature greater than 60 °C for 24 h. (Hardjito et al., 2004) concluded that the increase in curing temperature for more than 60 °C doesn't increase the compressive strength. So that, some researches recommended that the curing temperature for geopolymers must be 60° C.

Table 4.3 Compressive strength development of GGBFS based geopolymer with 650 kg/m³ binder content at different curing duration and curing temperature.

Mix No.	Binder content (kg/m ³)	Curing temp. °C.	Compressive strength of geopolymer mortar (MPa)					
			2 h.	6 h.	8 h.	24 h.	48 h.	72 h.
MS1	650	60	6.89	18.45	19.80	26.02	27.50	29.40
		80	11.16	20.28	23.28	27.81	29.80	31.47
		100	14.74	21.51	23.39	24.00	26.10	26.69
		120	18.37	20.22	21.00	22.50	22.71	21.20

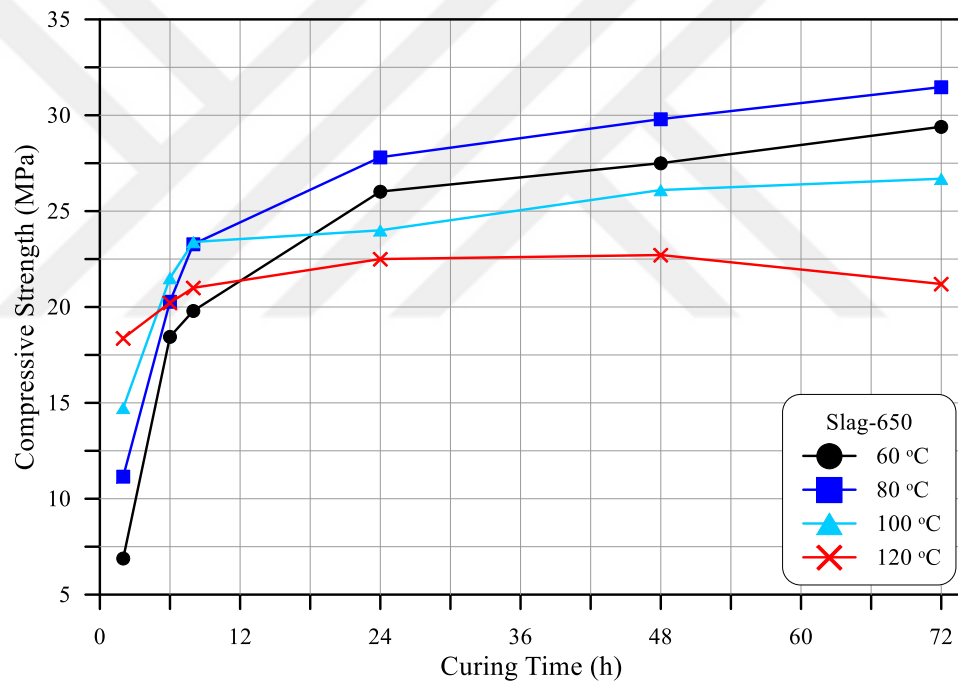


Figure 4.6 Compressive strength development of GGBFS based lightweight geopolymer mortar with 650 kg/m³ binder content.

Table 4.4 Compressive strength development of GGBFS based geopolymer with 750 kg/m³ binder content at different curing duration and curing temperature.

Mix No.	Binder content (kg/m ³)	Curing temp. °C.	Compressive strength of geopolymer mortar (MPa)					
			2 h.	6 h.	8 h.	24 h.	48 h.	72 h.
MS2	750	60	8.56	21.33	23.39	28.13	30.76	31.40
		80	12.00	23.70	24.74	28.41	29.30	30.88
		100	20.92	26.29	27.21	29.36	29.79	30.08
		120	21.39	23.71	24.00	24.47	24.62	23.98

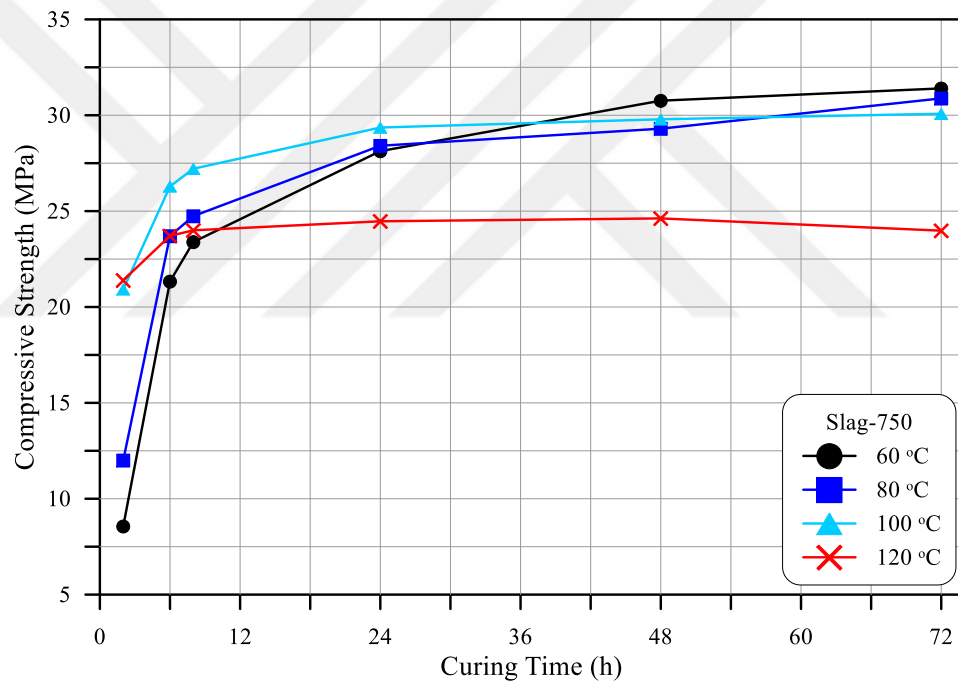


Figure 4.7 Compressive strength development of GGBFS based lightweight geopolymer mortar with 750 kg/m³ binder content.

Table 4.5 Compressive strength development of GGBFS based geopolymer with 850 kg/m³ binder content at different curing duration and curing temperature.

Mix No.	Binder content (kg/m ³)	Curing temp. °C.	Compressive strength of geopolymer mortar (MPa)					
			2 h.	6 h.	8 h.	24 h.	48 h.	72 h.
MS3	850	60	9.12	24.50	26.14	29.12	32.07	31.67
		80	12.63	21.27	27.00	30.16	31.00	30.32
		100	22.00	27.00	29.00	30.00	30.60	30.10
		120	23.19	25.42	26.73	27.00	27.49	26.97

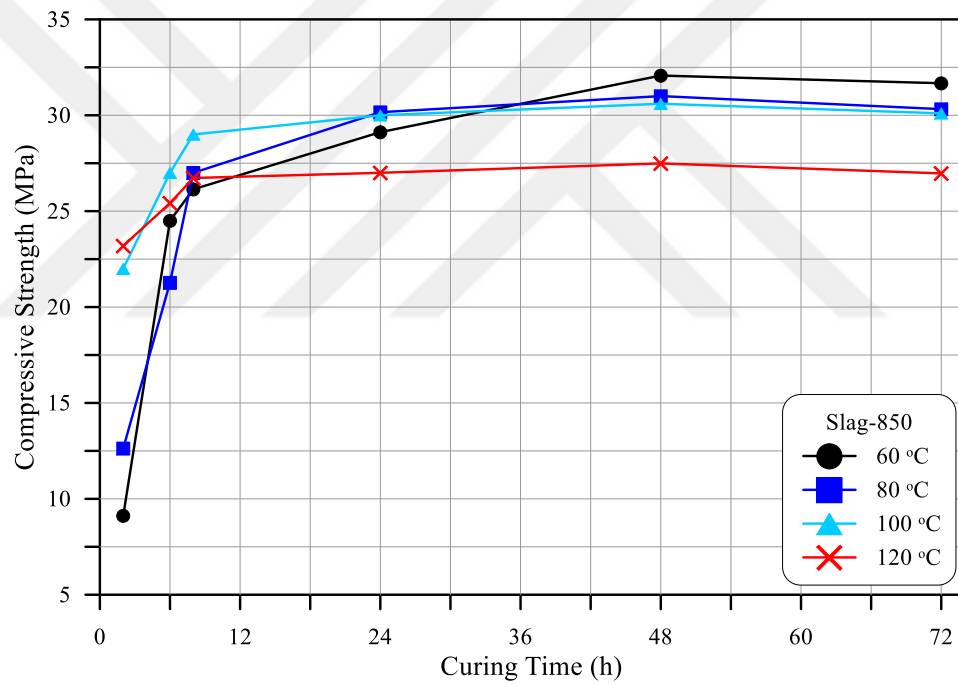


Figure 4.8 Compressive strength development of GGBFS based lightweight geopolymer mortar with 850 kg/m³ binder content.

Table 4.6 Compressive strength development of GGBFS based geopolymer with 950 kg/m³ binder content at different curing duration and curing temperature.

Mix No.	Binder content (kg/m ³)	Curing temp. °C.	Compressive strength of geopolymer mortar (MPa)					
			2 h.	6 h.	8 h.	24 h.	48 h.	72 h.
MS4	950	60	10.68	22.75	28.05	31.08	33.98	32.71
		80	11.08	24.34	27.33	29.52	30.88	30.20
		100	22.51	29.96	30.04	30.72	31.00	31.04
		120	22.47	25.34	24.82	25.00	26.57	24.94

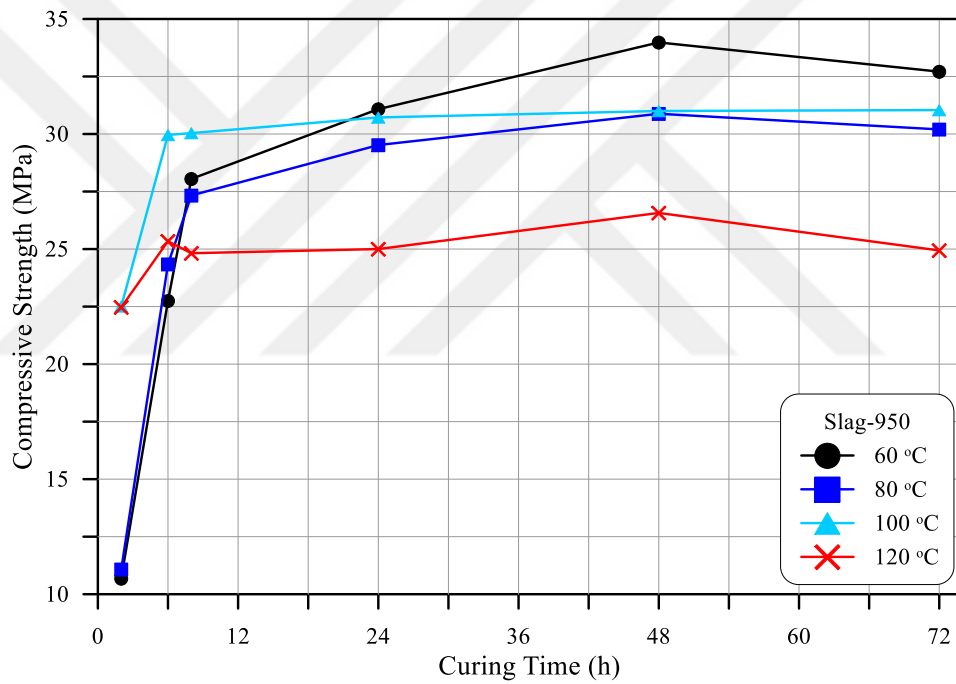


Figure 4.9 Compressive strength development of GGBFS based lightweight geopolymer mortar with 950 kg/m³ binder content.

Table 4.7 Compressive strength development of GGBFS based geopolymer with 1050 kg/m³ binder content at different curing duration and curing temperature.

Mix No.	Binder content (kg/m ³)	Curing temp. °C.	Compressive strength of geopolymer mortar (MPa)					
			2 h.	6 h.	8 h.	24 h.	48 h.	72 h.
MS5	1050	60	8.45	24.30	29.60	31.83	32.6	33.82
		80	16.73	27.93	29.40	31.83	32.27	33.42
		100	25.62	27.97	29.32	30.35	30.90	31.40
		120	27.16	27.73	26.93	27.33	28.00	30.32

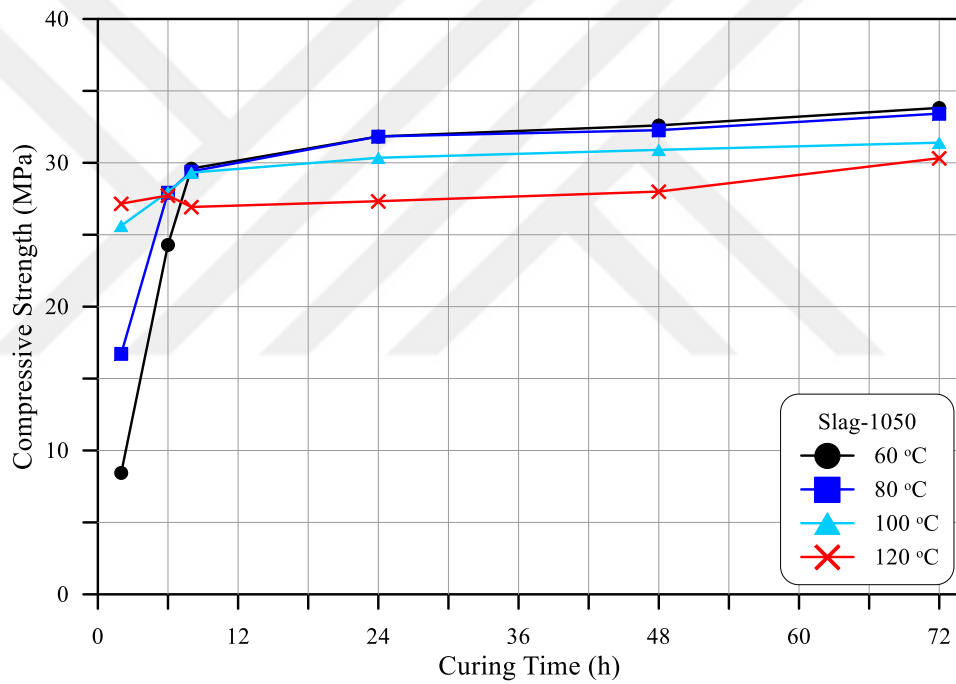


Figure 4.10 Compressive strength development of GGBFS based lightweight geopolymer mortar with 1050 kg/m³ binder content.

Table 4.8 Compressive strength development of GGBFS based geopolymer with 1150 kg/m³ binder content at different curing duration and curing temperature.

Mix No.	Binder content (kg/m ³)	Curing temp. °C.	Compressive strength of geopolymer mortar (MPa)					
			2 h.	6 h.	8 h.	24 h.	48 h.	72 h.
MS6	1150	60	10.80	27.53	28.92	32.91	35.98	35.40
		80	11.35	26.93	28.25	32.91	34.10	35.26
		100	26.39	29.40	29.72	31.27	31.95	32.83
		120	27.37	27.77	27.49	28.00	28.50	29.46

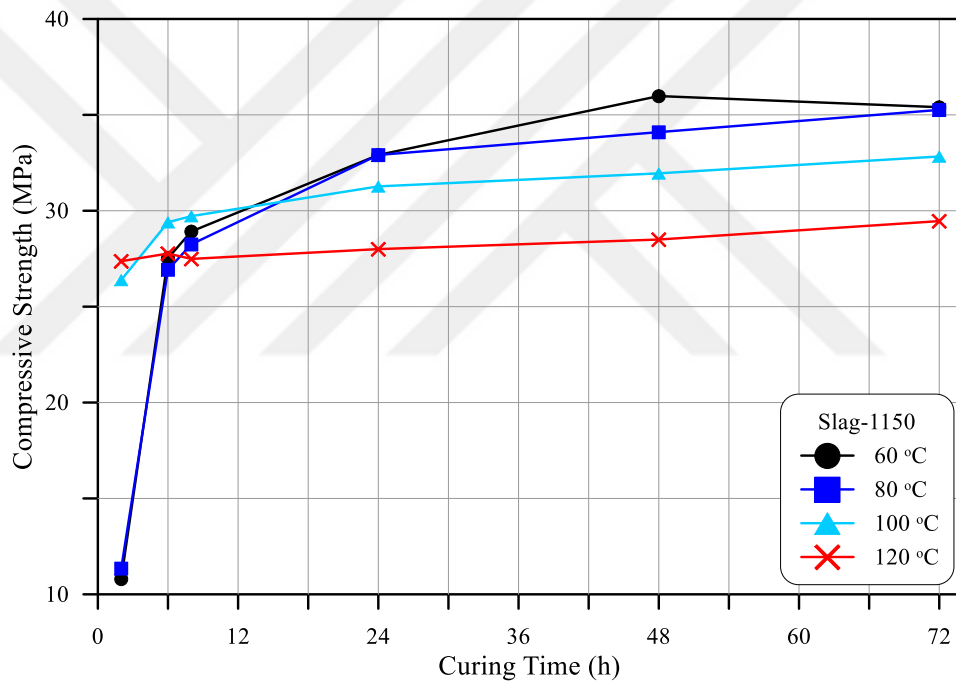


Figure 4.11 Compressive strength development of GGBFS based lightweight geopolymer mortar with 1150 kg/m³ binder content.

Table 4.9 Compressive strength development of GGBFS based geopolymer with 1250 kg/m³ binder content at different curing duration and curing temperature.

Mix No.	Binder content (kg/m ³)	Curing temp. °C.	Compressive strength of geopolymer mortar (MPa)					
			2 h.	6 h.	8 h.	24 h.	48 h.	72 h.
MS7	1250	60	12.55	28.45	29.44	34.10	38.01	36.49
		80	16.37	30.16	31.12	32.71	35.54	36.06
		100	23.89	27.86	29.96	30.60	32.51	29.64
		120	28.25	27.85	28.61	28.80	31.2	28.65

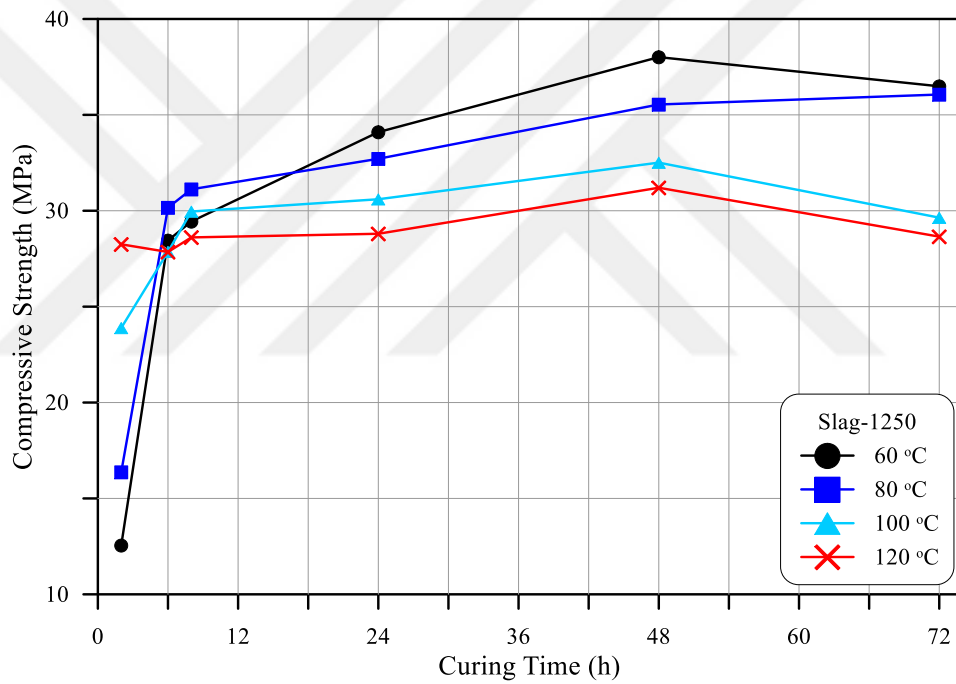


Figure 4.12 Compressive strength development of GGBFS based lightweight geopolymer mortar with 1250 kg/m³ binder content.

4.3.4.2 Fly Ash Based Geopolymer Mortar

The compressive strength response of FA-based LWGM under different curing period and curing temperature is shown in Figures 4.13 to 4.19 and Tables 4.10 to 4.16. It was noticed that for the same temperature of curing, compressive strength increases with the increase of heating duration. At 60, 80, 100 and 120 °C, the rate of gain of strength is constant up to 24 hrs of the curing duration, but after that the strength increases with reduced rate. At curing temperature of 120 °C, it is also observed that LWGM gained more strength at just 24 hours of heating than strength achieved after 72 hours.

The results indicate that longer curing time did not decrease the compressive strength of fly ash geopolymer mortar as claimed by van Jaarsveld et al (2002).

As shown in figures 4.13 to 4.19 and tables 4.12 to 4.18, it was noticed that for the same period of curing, compressive strength increases with the increase of heating temperature. There is considerably small difference in 48 hours and 72 hours beyond 80 °C of curing. Hence, maximum compressive strength can be achieved within 24 hour of curing at 120°C, 48 hour of curing at 80°C, 100°C and 72 hour of curing at 60 °C.

High curing temperature is essential for FA-based geopolymers as increasing the temperature leads to an increase in the extent and rate of reaction however it becomes less significant after the geopolymers have set.

It is demonstrated that the strength of GGBFS-based LWGM with different temperature and duration is greater than that of FA-based LWGM. It can be attributed due to lower $\text{SiO}_2/\text{Al}_2\text{O}_3$ ratio of the binder mix. General range for $\text{SiO}_2/\text{Al}_2\text{O}_3$ is 3.3-4.5 as mentioned by Islam et al., (2014). It has been reported that Al_2O_3 dissolves faster than SiO_2 and the reaction between aluminate and silicate types is faster than the reaction between only silicate types (Silva et al., 2007). The Ca presented in the GGBFS performs hydration and forms C–S–H gel that develops the strength properties (Kumar et al., 2010).

Table 4.10 Compressive strength development of fly ash based geopolymer with 650 kg/m³ binder content at different curing duration and curing temperature.

Mix No.	Binder content (kg/m ³)	Curing temp. °C.	Compressive strength of geopolymer mortar (MPa)					
			2 h.	6 h.	8 h.	24 h.	48 h.	72 h.
MF1	650	60	0.00	4.70	4.86	9.44	13.47	14.10
		80	4.62	5.97	6.50	11.28	17.68	18.08
		100	4.58	8.05	9.32	11.6	13.75	17.29
		120	4.69	9.82	11.45	15.00	15.15	16.50

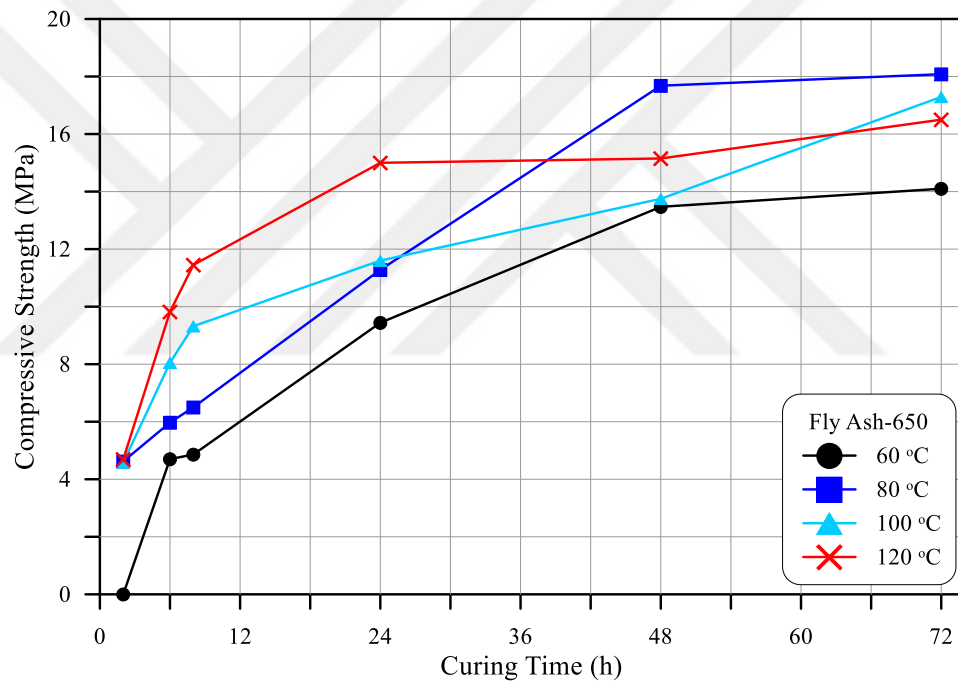


Figure 4.13 Compressive strength development of fly ash based geopolymer with 650 kg/m³ binder content at different curing duration and curing temperature.

Table 4.11 Compressive strength development of fly ash based geopolymer with 750 kg/m³ binder content at different curing duration and curing temperature.

Mix No.	Binder content (kg/m ³)	Curing temp. °C.	Compressive strength of geopolymer mortar (MPa)					
			2 h.	6 h.	8 h.	24 h.	48 h.	72 h.
MF2	750	60	0.00	4.42	5.38	10.32	14.50	15.30
		80	4.06	6.61	8.37	14.70	18.00	19.00
		100	5.50	9.40	10.20	14.10	15.58	18.65
		120	5.46	11.12	12.00	17.80	18.29	18.90

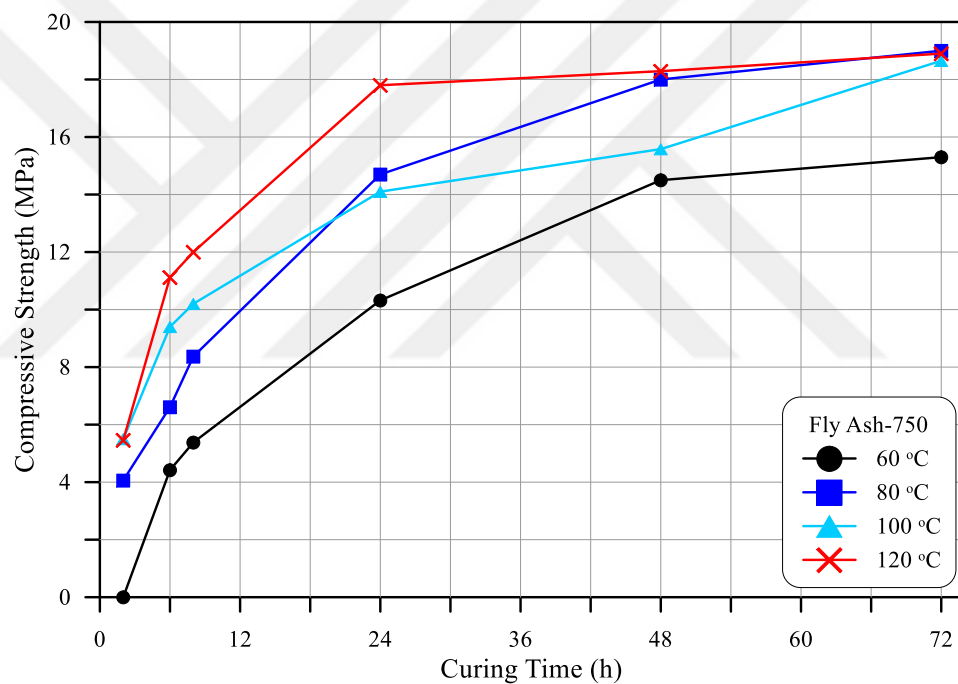


Figure 4.14 Compressive strength development of fly ash based geopolymer with 750 kg/m³ binder content at different curing duration and curing temperature.

Table 4.12 Compressive strength development of fly ash based geopolymer with 850 kg/m³ binder content at different curing duration and curing temperature.

Mix No.	Binder content (kg/m ³)	Curing temp. °C.	Compressive strength of geopolymer mortar (MPa)					
			2 h.	6 h.	8 h.	24 h.	48 h.	72 h.
MF3	850	60	0.00	4.74	5.86	12.71	15.66	17.97
		80	4.02	9.12	9.48	15.34	18.50	21.56
		100	5.14	13.07	14.50	16.02	18.84	22.47
		120	6.49	12.43	14.02	18.76	20.72	21.12

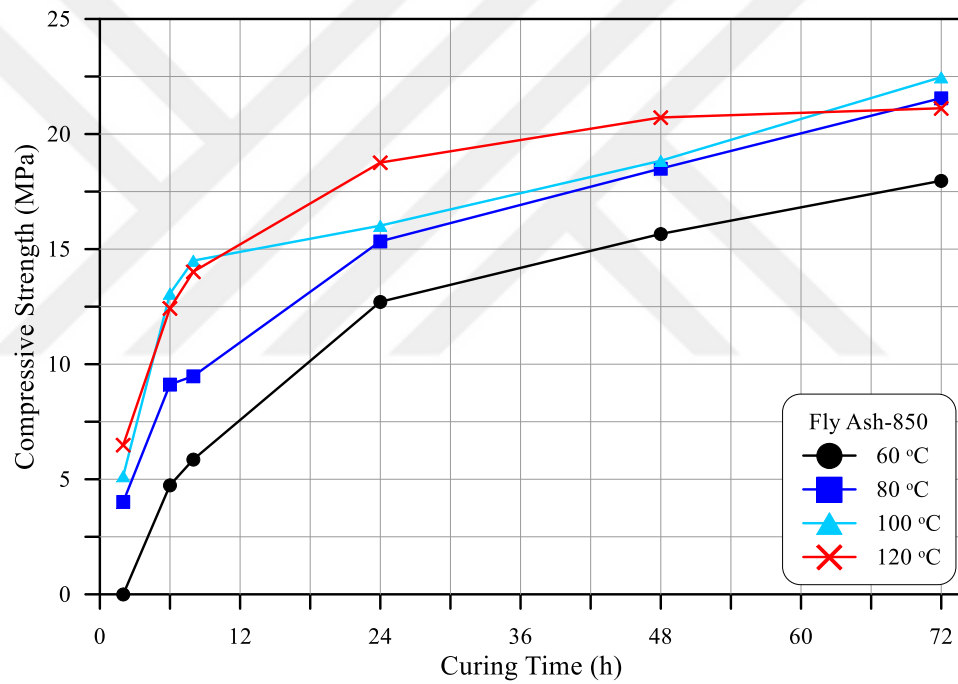


Figure 4.15 Compressive strength development of fly ash based geopolymer with 850 kg/m³ binder content at different curing duration and curing temperature.

Table 4.13 Compressive strength development of fly ash based geopolymer with 950 kg/m³ binder content at different curing duration and curing temperature.

Mix No.	Binder content (kg/m ³)	Curing temp. °C.	Compressive strength of geopolymer mortar (MPa)					
			2 h.	6 h.	8 h.	24 h.	48 h.	72 h.
MF4	950	60	0.00	5.62	6.14	13.78	18.69	19.68
		80	4.50	10.44	12.15	17.21	20.32	22.76
		100	5.46	13.75	14.65	18.00	23.43	23.94
		120	7.41	13.82	14.86	20.00	19.08	19.84

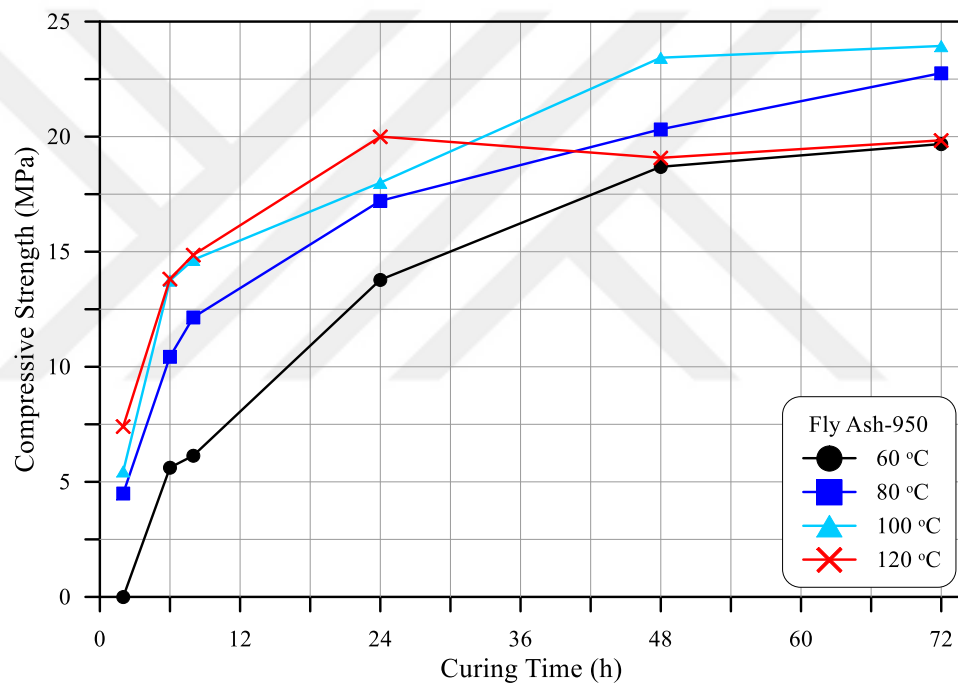


Figure 4.16 Compressive strength development of fly ash based geopolymer with 950 kg/m³ binder content at different curing duration and curing temperature.

Table 4.14 Compressive strength development of fly ash based geopolymer with 1050 kg/m³ binder content at different curing duration and curing temperature.

Mix No.	Binder content (kg/m ³)	Curing temp. °C.	Compressive strength of geopolymer mortar (MPa)					
			2 h.	6 h.	8 h.	24 h.	48 h.	72 h.
MF5	1050	60	0.00	5.26	5.90	14.38	18.88	21.71
		80	4.14	13.03	14.14	19.28	21.00	22.8
		100	5.98	14.86	15.18	18.97	22.11	23.15
		120	8.41	14.06	17.53	22.43	20.52	21.31

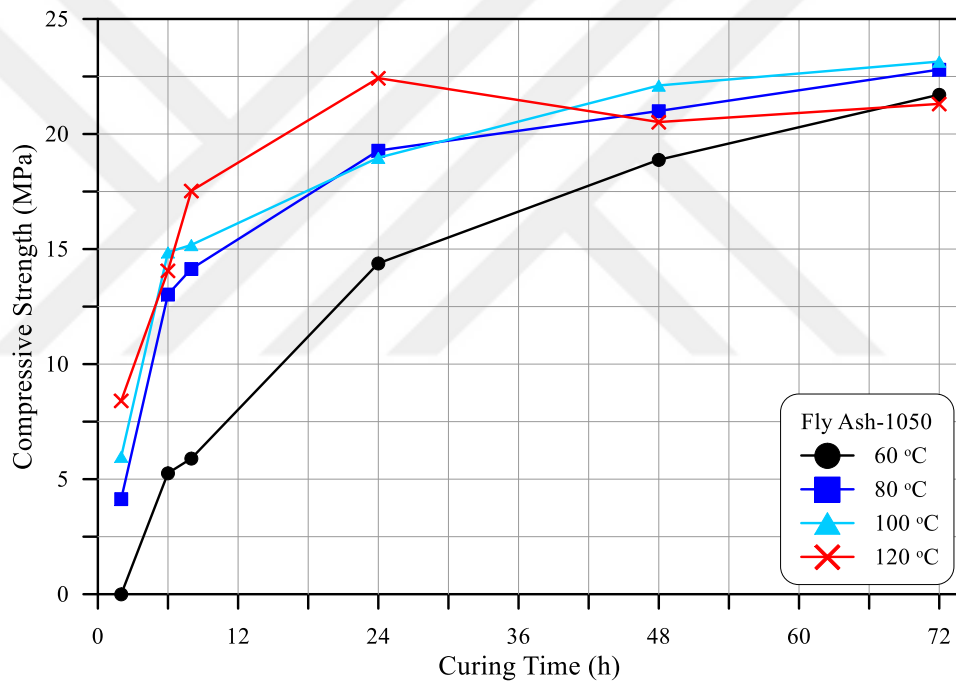


Figure 4.17 Compressive strength development of fly ash based geopolymer with 1050 kg/m³ binder content at different curing duration and curing temperature.

Table 4.15 Compressive strength development of fly ash based geopolymer with 1150 kg/m³ binder content at different curing duration and curing temperature.

Mix No.	Binder content (kg/m ³)	Curing temp. °C.	Compressive strength of geopolymer mortar (MPa)					
			2 h.	6 h.	8 h.	24 h.	48 h.	72 h.
MF6	1150	60	0.00	5.78	8.25	18.45	21.12	23.51
		80	4.74	13.85	14.40	19.50	22.10	24.3
		100	7.85	17.37	18.53	19.84	24.22	25.34
		120	11.00	16.77	17.93	23.9	23.55	21.91

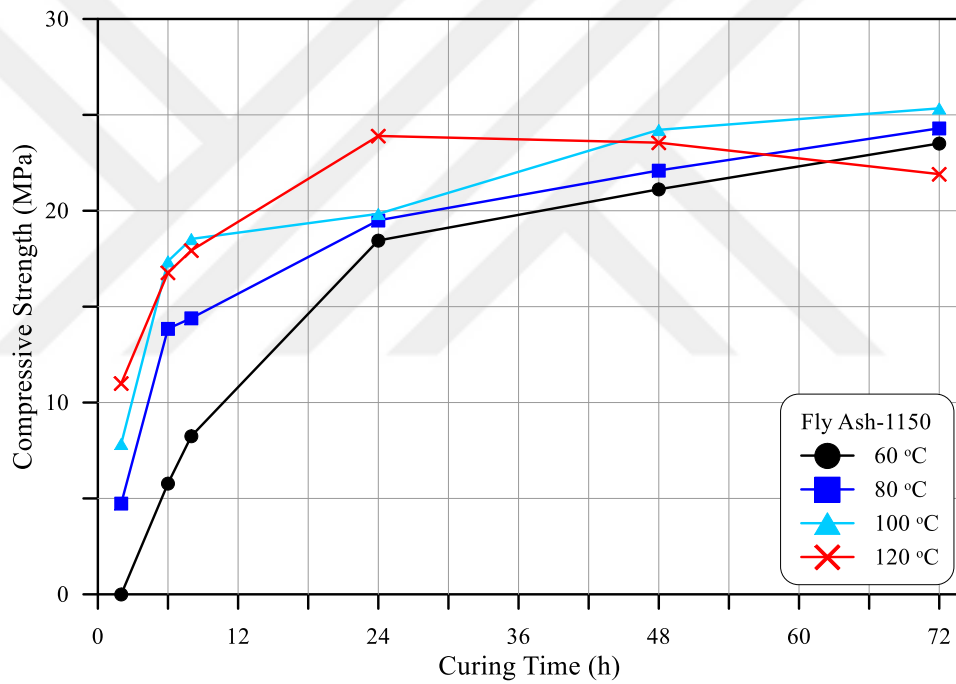


Figure 4.18 Compressive strength development of fly ash based geopolymer with 1150 kg/m³ binder content at different curing duration and curing temperature.

Table 4.16 Compressive strength development of fly ash based geopolymer with 1250 kg/m³ binder content at different curing duration and curing temperature.

Mix No.	Binder content (kg/m ³)	Curing temp. °C.	Compressive strength of geopolymer mortar (MPa)					
			2 h.	6 h.	8 h.	24 h.	48 h.	72 h.
MF6	1250	60	0.00	6.81	9.20	18.13	22.35	25.78
		80	4.82	14.60	15.60	21.64	23.00	24.72
		100	10.92	17.50	18.90	21.43	24.54	25.46
		120	13.86	18.05	20.32	23.71	24.94	23.90

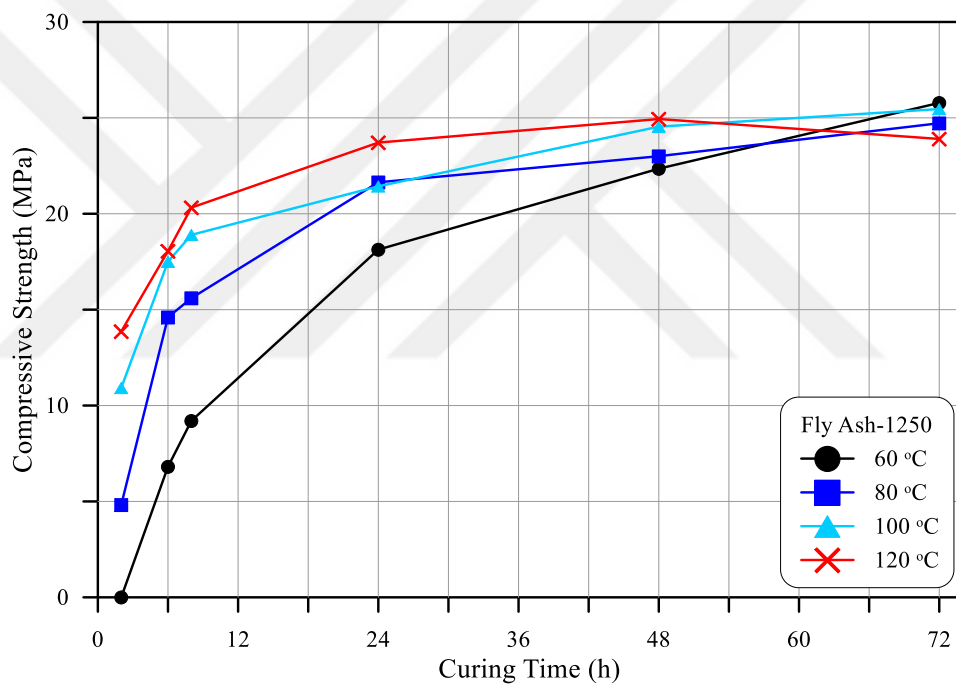


Figure 4.19 Compressive strength development of fly ash based geopolymer with 1250 kg/m³ binder content at different curing duration and curing temperature.

CHAPTER 5

OPTIMIZATION OF TEST PARAMETERS AND VERIFICATION

5.1 General

The response surface method (RSM) (Whitcomb P.J. and Anderson M.J., 2004) is an optimization procedure that combines statistical and mathematical methods of experiment design, regression analysis and optimization. RSM has been conducted on the 3 independent and 1 dependent variables considered in the presented experimental study. These three independent variables (or factors) are binder content, curing temperature and curing time, and the dependent variable (or response) is considered as compressive strength. RSM is useful to visually analyse the effect of factors on the responses. The procedure is initiated with the response surface modelling in which a proper model is selected to fit the collection of data by considering the adequacy of the chosen model. This stage is followed by the optimisation process subjected to determine the required best solution using the response surface of the chosen model.

5.2 The Optimization Procedure Applied Experimental Data

The response surface design for 24 tests of one binder content ran is shown in Table 5.1.

Table 5.1 Response surface Parameters.

Run No.	Factor 1	Factor 1	Factor 1	Response
	Curing Temperature	Curing Time	Binder content	Compressive strength
Unit	°C	hours	kg/m ³	MPa
1	60	2	650	6.89
2	60	6	650	18.45
3	60	8	650	19.80
4	60	24	650	26.02
5	60	48	650	27.50
6	60	72	650	29.40
7	80	2	650	11.16
8	80	6	650	20.28
9	80	8	650	23.28
10	80	24	650	27.81
11	80	48	650	29.80
12	80	72	650	31.47
13	100	2	650	14.74
14	100	6	650	21.51
15	100	8	650	23.39
16	100	24	650	24.00
17	100	48	650	26.10
18	100	72	650	26.69
19	120	2	650	18.37
20	120	6	650	20.22
21	120	8	650	21.00
22	120	24	650	22.50
23	120	48	650	22.71
24	120	72	650	21.20

5.3 Optimization Results

The optimization study aims to identify the optimum values of binder content, curing temperature and curing time while maximizing the compressive strength of lightweight geopolymer mortar. For this purpose, the response influenced by the multiple factors was optimized using the procedure of RSM in which the desirability function is defined for the target response to optimize the response (e.g. [Whitcomb P.J.& Anderson M.J., 2004 and Pradeep G., 2008]). After establishing relationship between the factors and the response and building the regression model, the factors are varied simultaneously and independently to optimise the objective functions. The

desirability functions (d_i) are defined in the process of RSM for each response and they are used to optimize the responses simultaneously (e.g. [Pradeep G., 2008, Myers R.H., 2009]). A desirability function (d_i) is quantified within the range of $0 \leq d_i \leq 1$. When the response or the factors falls outside the desirability range, the overall function becomes zero.

The desirability is defined by the following expressions for maximising and minimising the individual response, (Eqs. 1 and 2), respectively.

$$d_i = \begin{cases} 0 & Y_i \leq \min f_i \\ \left[\frac{Y_i - \min f_i}{\max f_i - \min f_i} \right]^{wt_i} & \text{and } 0 < d_i < 1 \\ 1 & Y_i \geq \max f_i \end{cases} \quad (5.1)$$

$$d_i = \begin{cases} 1 & Y_i \leq \min f_i \\ \left[\frac{\max f_i - Y_i}{\max f_i - \min f_i} \right]^{wt_i} & \text{and } 0 < d_i < 1 \\ 0 & Y_i \geq \max f_i \end{cases} \quad (5.2)$$

Where,

$d_i, Y_i, \min f_i$ and $\max f_i$ are the desirability function, the fitted value, and minimum and maximum actual values of i th response, respectively. The power value wt_i is a weighting factor for the i th response.

Desirability is an objective function that ranges from zero to one which respectively indicates that the optimisation is outside the range and the goal of optimisation is satisfied. The desirability is targeted to be maximized to achieve a point in the numerical optimization. The weighting factor of a response may be altered to define the important characteristics of a goal. The target response was defined as a desirability function by using the procedure provided by Myers and Montgomery (Myers et al., 2009). The characteristic goals of the factors and the response for the simultaneous optimization process are shown in Table 5.2.

As shown in Table 5.2, two optimisation processes were conducted separately on the responses of compressive strength data obtained from the light-weight geopolymers

mortars incorporated with FA and GGBFS. The characteristic goals of these responses are maximized. Since the performed optimisations tend to identify the optimum binder content, curing temperature and curing time for the light-weight geopolymer mortars incorporated with FA and GGBFS separately, the characteristic goals for the factors of binder content, curing temperature and curing time were minimized. Accordingly, the numerical optimization with the defined desirability function on the target response was performed to optimize the responses.

Table 5.2 Definitions for the factors and the responses in the optimization problem.

Name of factors and response	Goal	Lower limit	Upper limit
Binder content (kg/m ³)	minimize	650	1250
Curing temperature (oC)	minimize	2	72
Curing time (h)	minimize	60	120
Compressive strength for FA (MPa)	maximize	0	25.78
Compressive strength for GGBFS (MPa)	maximize	6.89	38.01

Figs. 5.1 and 5.2 demonstrate the variation of desirability function obtained from the optimisation analyses performed on the responses of the light-weight geopolymer mortar incorporated with FA and GGBFS, respectively. The obtained optimum solutions for these two separate optimisations are provided in Table 5.3 which indicates that the defined upper and lower limits are satisfied and the desirability values are in the acceptable range. If the comparison is made between the light-weight geopolymer mortars incorporated with FA and GGBFS as shown in Table 5.3, the optimum results for the factors of binder content, curing temperature and curing time are similar and the maximum compressive strength values are obtained as 10.8 MPa and 27.7 MPa, respectively.

Table 5.3 Optimization results for the light-weight geopolymer mortars with FA and GGBFS.

Factors and response	FA	GGBFS
Binder content (kg/m ³)	650	650
Curing temperature (oC)	60	60
Curing time (h)	21.856	21.566
Compressive strength (MPa)	10.767	27.712
Desirability	0.740	0.833

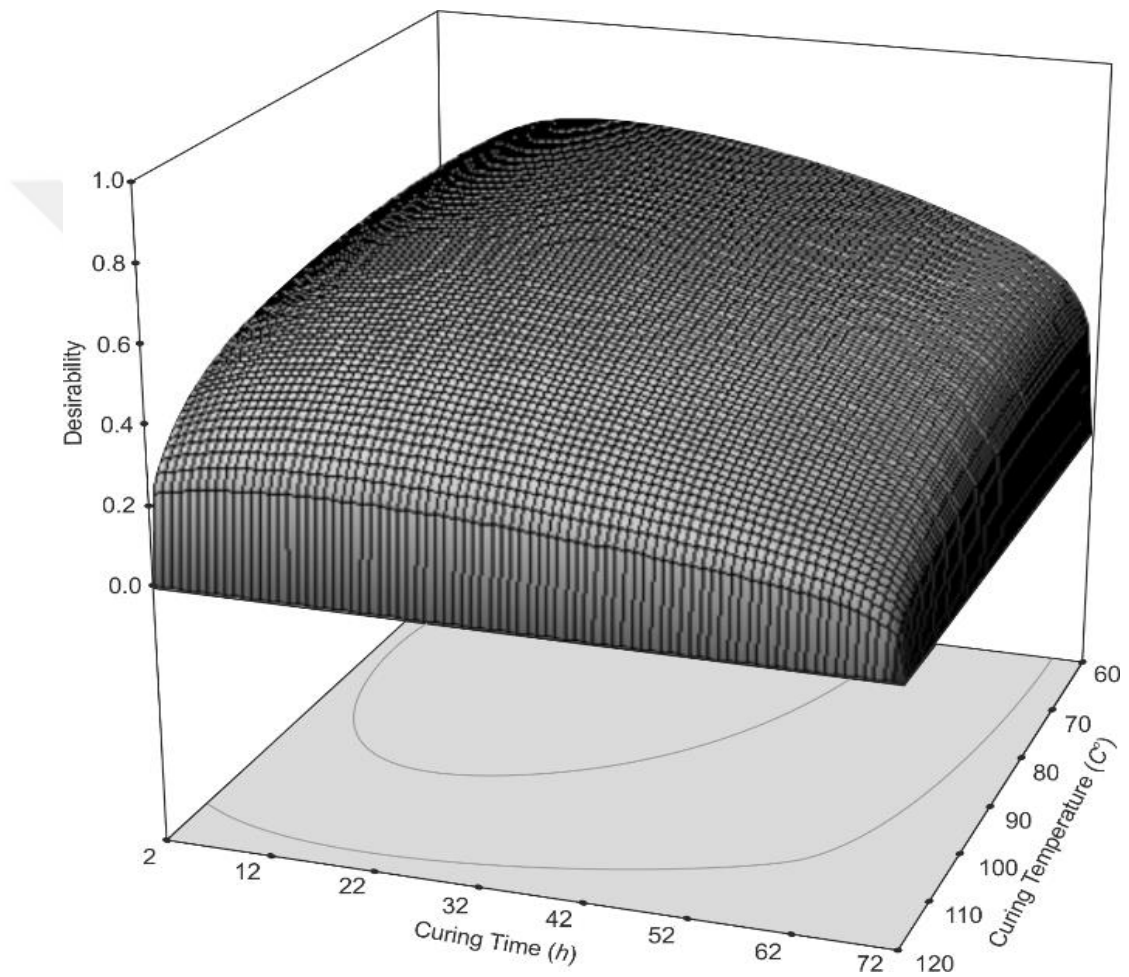


Figure 5.1 Variation of desirability function for the response of compressive strength based on the light-weight geopolymer mortars incorporated with FA.

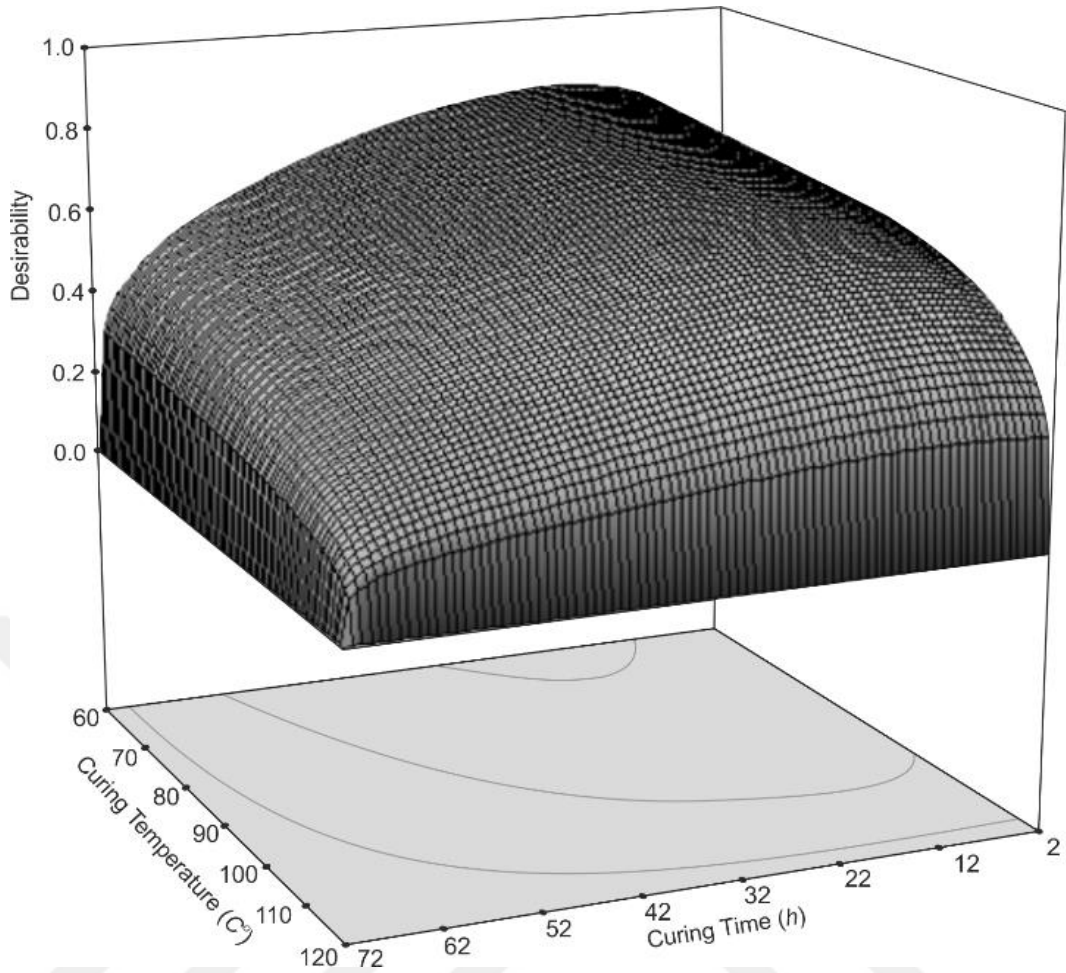


Figure 5.2 Variation of desirability function for the response of compressive strength based on the light-weight geopolymer mortars incorporated with GGBFS.

Figures 5.3 and 5.4 demonstrate the variation of the considered factors in terms of the desirability and the responses of the compressive strength for the light-weight geopolymer mortars incorporated with FA and GGBFS, respectively. Figure 5.3 shows that the increase in the binder content decreases the desirability value and the dramatic reduction is observed especially beyond the binder content of approximately 1150 kg/m^3 , this increase corresponds a slight increase in the compressive strength for the light-weight geopolymer mortars incorporated with FA. Figure 5.3 shows that generally the compressive strength has an increasing tendency in terms of the increasing curing time, but this increase is almost negligible between the curing times of approximately 22 h and 52 h. There is a dramatic increase in the compressive strength up to 22 h and the slight increase in the compressive strength is observed beyond the curing time of 52 h. In the considered range of curing time, the

desirability is increased dramatically up to the curing time of 22 h, the desirability decreases gradually up to the curing time of 62 h, and the dramatic reduction in the desirability is observed beyond this curing time. Figure 5.3 demonstrates that the increase in the curing temperature has a decreasing tendency on the desirability. While a slight decrease is observed in the desirability up to the curing temperature of 110 °C, a dramatic reduction in the desirability is observed beyond this value. The increase in the curing temperature slightly increases the compressive strength up to the curing temperature of 110 °C and beyond this temperature the increase in the compressive strength is negligible. Although, Figure 5.4 demonstrates the similar behaviour of the factors on the desirability for the light-weight geopolymer mortar incorporated with GGBFS, their effect on the variation of the compressive strength response is varied compared to Figure 5.3. Figure 5.4 shows that a slight increase in the compressive strength is observed up to the binder content of 1150 kg/m³ and beyond this value the increase in the compressive strength is negligible. The compressive strength is gradually increased up to the curing time of 32 h and a slight reduction is observed beyond this value of curing time. Figure 5.4 shows that the compressive strength is almost not affected by the curing temperature up to 100 C° and the curing temperature slightly causes a reduction in the compressive strength beyond this value.

Further experimental study is conducted to verify the obtained optimum results for the factors obtained from the performed optimisations in order to identify whether in reality they could provide the maximized compressive strength responses for the light-weight geopolymer mortars incorporated with FA and GGBFS. By using the same materials and mixture proportions with the implementation of the identical experimental conditions, the additional adequate numbers of mortar specimens were prepared and tested to obtain the compressive strength values. The results obtained from these experimental tests are given in Table 5.4. Table 5.4 shows that the obtained compressive strength results indicate that the proposed optimum curing time and temperature provide relatively good results compared to the experimental results which suggest that the proposed optimisation results are valid.

Table 5.4 The obtained optimum values and the results from the experimental verification tests for the light-weight geopolymer mortars incorporated with FA and GGBFS.

Binder type	Binder content (kg/m ³)	Optimum values and expected response			Experimental results for optimum values
		Curing time (h)	Curing temperature (°C)	Compressive strength (MPa)	Compressive strength (MPa)
FA	650	21.856	60	10.76	8.17
	750	22.381	60	11.90	9.56
	850	22.823	60	13.05	12.95
	950	23.244	60	14.21	13.19
	1050	23.590	60	15.38	15.66
	1150	23.926	60	16.57	16.45
	1250	24.208	60	17.75	17.97
GGBFS	650	21.547	60	27.70	26.36
	750	20.908	60	29.17	27.29
	850	20.391	60	30.43	27.77
	950	19.949	60	31.47	30.0
	1050	19.634	60	32.31	31.08
	1150	19.372	60	32.93	32.55
	1250	19.228	60	33.36	33.27

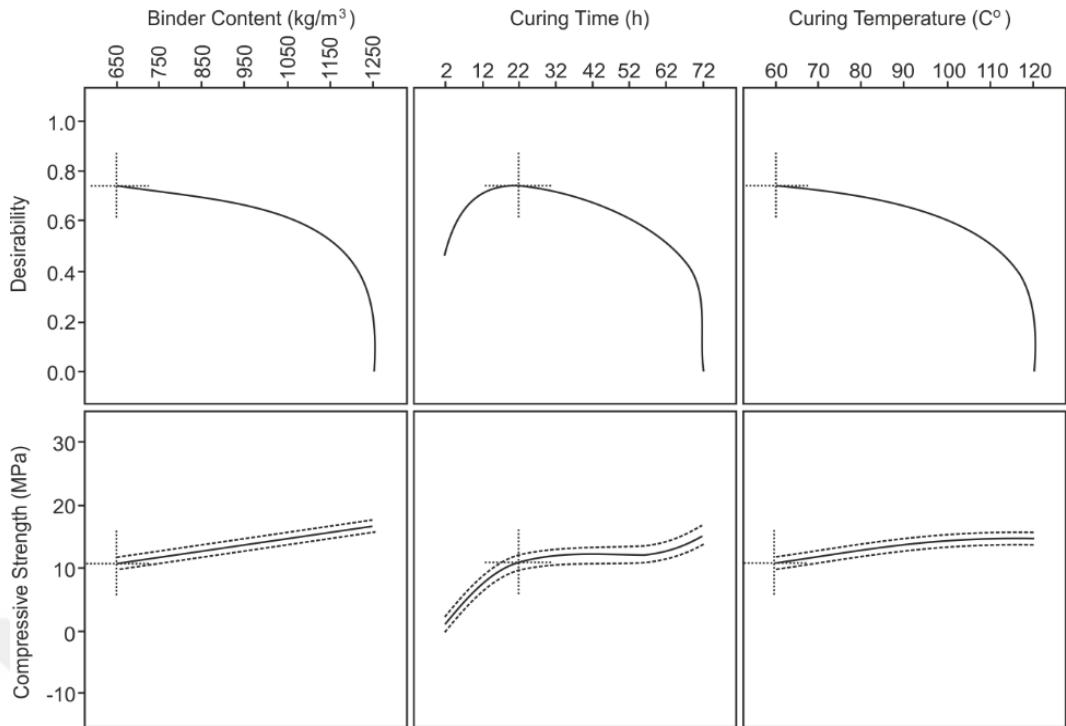


Figure 5.3 The variation of the factors in terms of the desirability and the response for the light-weight geopolymer mortars incorporated with FA.

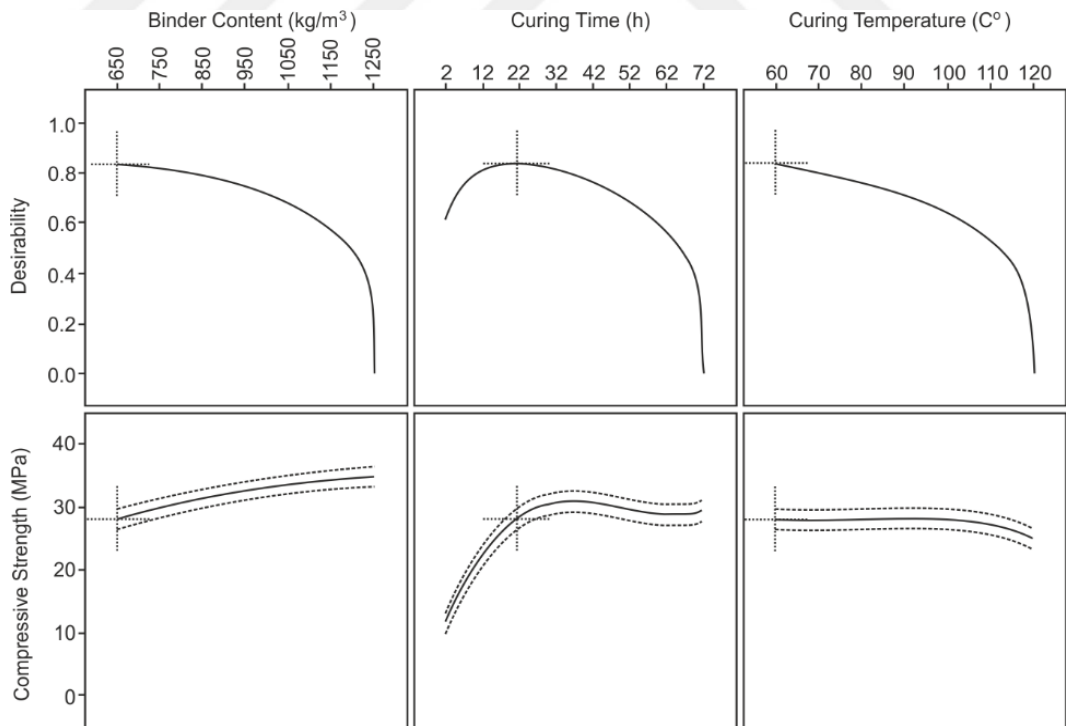


Figure 5.4 The variation of the factors in terms of the desirability and the response for the light-weight geopolymer mortars incorporated with GGBFS.

5.4 Additional Tests

5.4.1 Compressive Strength

This section will discuss the effect of the age 7 day on the development of the geopolymer mortars compressive strength. Figures (5.5 and 5.6) and Table 5.5 show the results of compressive strength developed in GGBFS-based LWGM prepared with variable curing period and one curing temperature of 60 °C get from the response surface method (RSM). As shown in both Figures (5.5 and 5.6), the geopolymer lightweight mortars showed no major change in compressive strength after the initial curing. The increase in strength at the age of 7 days was less than 8% and 5.8% for all the light-weight geopolymer mortars incorporated with FA and GGBFS tested in this study. This seems to agree with the finding of previous studies by Kong and Sanjayan (2008); Lloyd and Rangan (2009).

Table 5.5 Compressive strength results from the experimental verification tests for the light-weight geopolymer mortars incorporated with FA and GGBFS.

Binder type	Binder content (kg/m ³)	Optimum values and expected response		Experimental results for optimum values	
		Curing time (h)	Curing temperature (°C)	Compressive strength after curing (MPa)	Compressive strength after 7 day (MPa)
FA	650	21.856	60	8.17	8.69
	750	22.381	60	9.56	10.36
	850	22.823	60	12.95	13.98
	950	23.244	60	13.19	14.94
	1050	23.590	60	15.66	15.98
	1150	23.926	60	16.45	18.69
	1250	24.208	60	17.97	18.76
GGBFS	650	21.547	60	26.36	27.64
	750	20.908	60	27.29	28.51
	850	20.391	60	27.77	29.15
	950	19.949	60	30.00	32.31
	1050	19.634	60	31.08	33.23
	1150	19.372	60	32.55	34.40
	1250	19.228	60	33.27	35.04

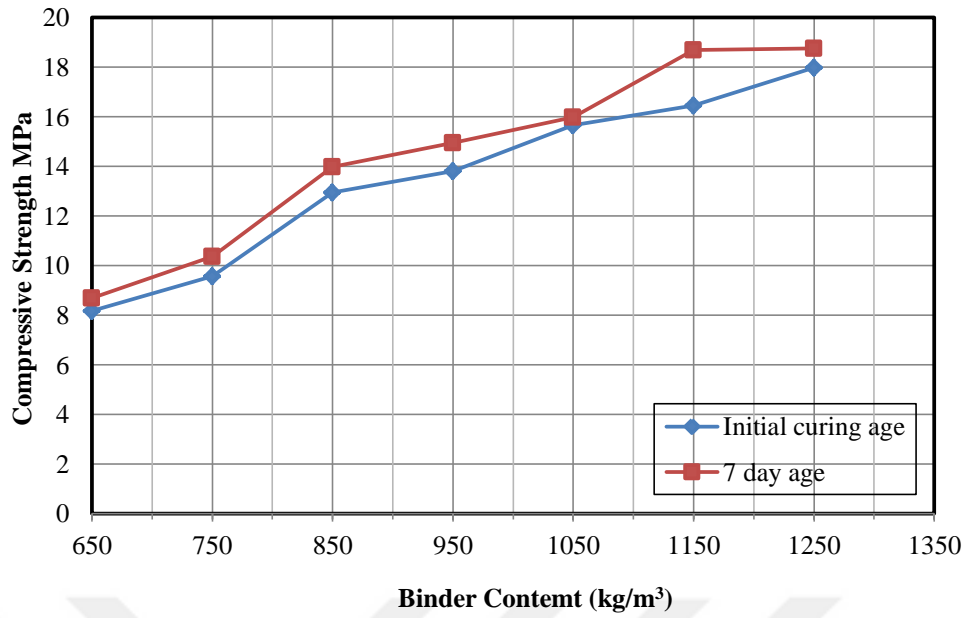


Figure 5.5 Compressive strength of FA based geopolymer mortar at initial curing and 7 day ages.

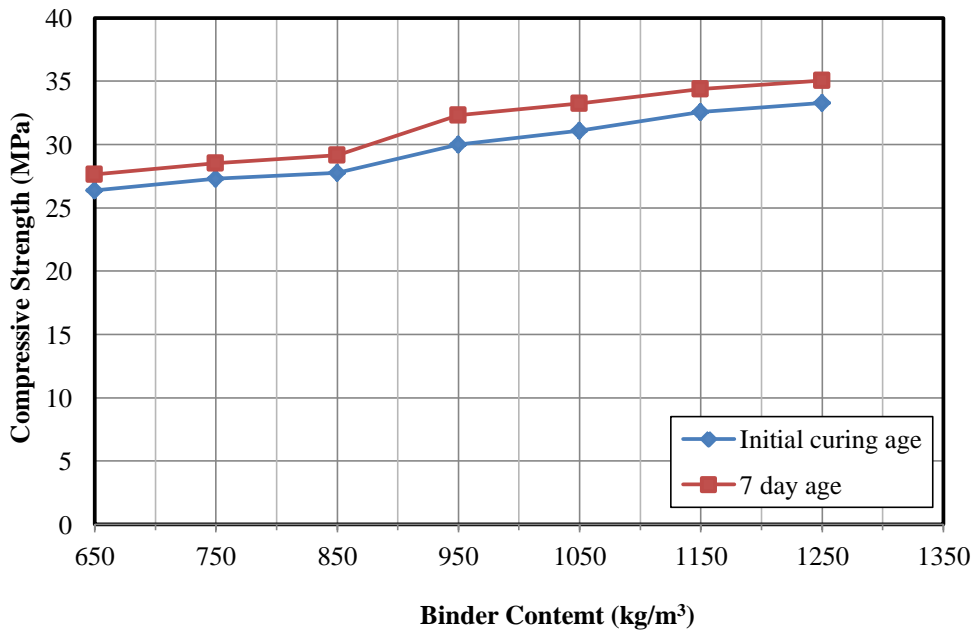


Figure 5.6 Compressive strength of GGBFS based geopolymer mortar at initial curing and 7 day ages.

5.4.2 Splitting Tensile Strength Test

Splitting tensile strength conducted by using cube of (50×50) mm tests at age 7day according to ASTM C-39. The results summarized in. The experimental results of splitting tensile strength and compressive strength are shown in Table 5.6, from which is clear that increasing compressive strength will lead to an increase in splitting tensile strength.

It can be seen from the figures 5.7 and 5.8 that tensile strength increased with the increase of binder content for all the mixtures. This trend is similar to the trend shown by the development of compressive strength. In GGBFS and FA based geopolymer mortar mixture M7 with 1250 kg/m³ binder content gained 34% and 44% higher 7-day tensile strength than M1 with 650 kg/m³ binder content, the strength increased gradually during geopolymer formation.

Generally the value of splitting tensile strength of FA based geopolymer mortar was low. That refers to lowering geopolymerization process and which may reflect ineffective the lightweight aggregate.

On the other hand, the average splitting tensile strength is found to be 0.11 and 0.16 times the compressive strength of GGBFS and FA based geopolymer mortar.

The experimental results of splitting tensile strength and compressive strength are shown in Table 5.6, from which is clear that increasing compressive strength will lead to an increase in splitting tensile strength.

Table 5.6 Splitting tensile strength results, and their relationships with age and compressive strength.

Mix no.	Binder content (kg/m ³)	Tensile strength of GGBFS at 7 day(MPa)	Compressive strength of GGBFS at 7 day(MPa)	Tensile strength of FA at 7 day(MPa)	Compressive strength of FA at 7 day(MPa)
M1	650	2.85	27.64	1.80	8.69
M2	750	3.23	28.51	2.00	10.36
M3	850	3.36	29.15	2.30	13.98
M4	950	3.56	32.31	2.41	14.94
M5	1050	3.64	33.23	2.60	15.98
M6	1150	3.77	34.40	2.80	18.69
M7	1250	3.82	35.04	2.90	18.76

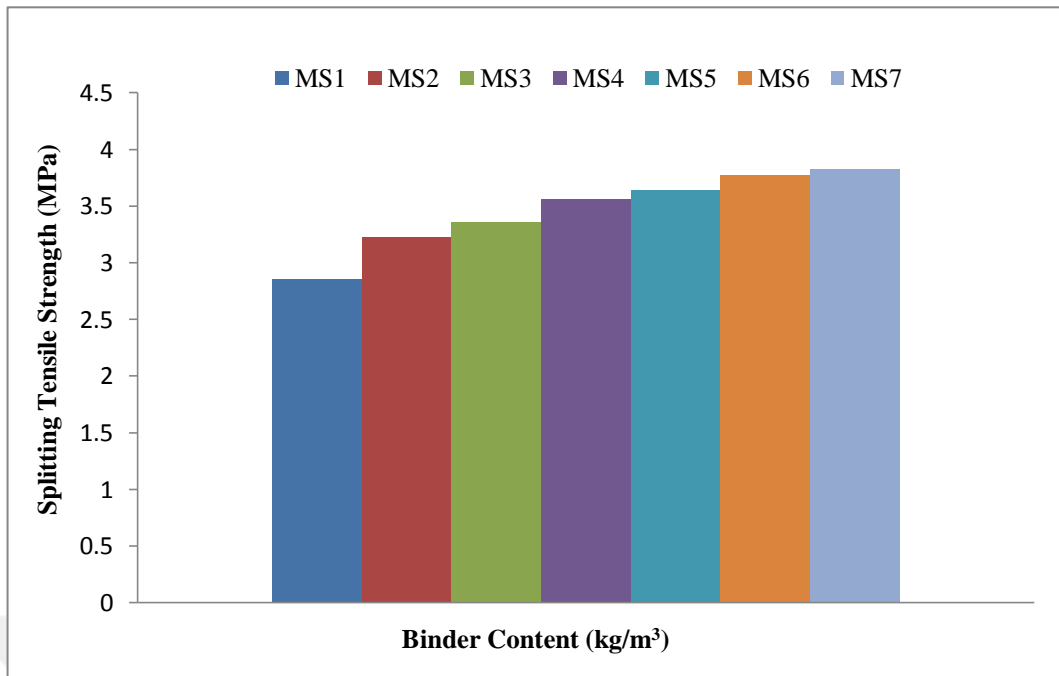


Figure 5.7 Splitting tensile strength of GGBFS based geopolymer mortar.

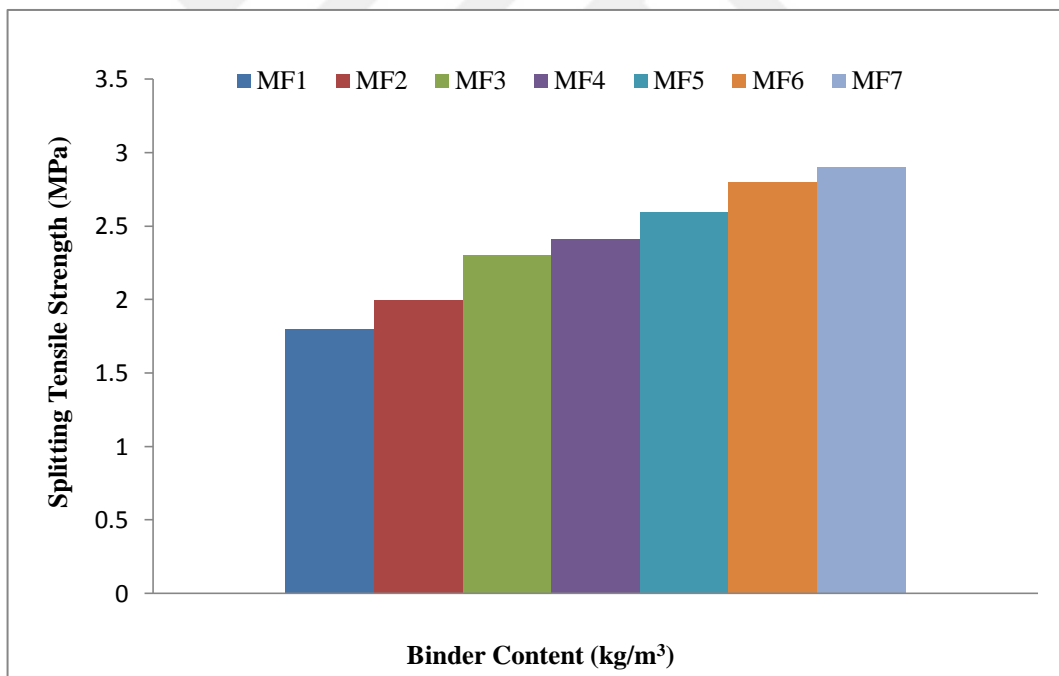


Figure 5.8 Splitting tensile strength of FA based geopolymer mortar.

5.4.2.1 Relationship between Compressive and Splitting Tensile Strength of LWGM

The following two equations may be suggested to fit the relationship between compressive strength and splitting tensile strength for GGBFS and FA geopolymer mortar but with low accuracy for these equations because of a little number of models that gives higher value of (R²) as shown in Figures 5.9 and 5.10. The relevant empirical expression obtained from this study is;

1. $f_s = 0.1083 f_c + 1.0528$ (with $R^2 = 0.90$ for GGBFS).

2. $f_t = 0.1042 f_c + 1.8919$ (with $R^2 = 0.9889$ for FA).

Where:

f_s : Predicted splitting tensile strength in MPa.

f_c : Compressive strength in MPa.

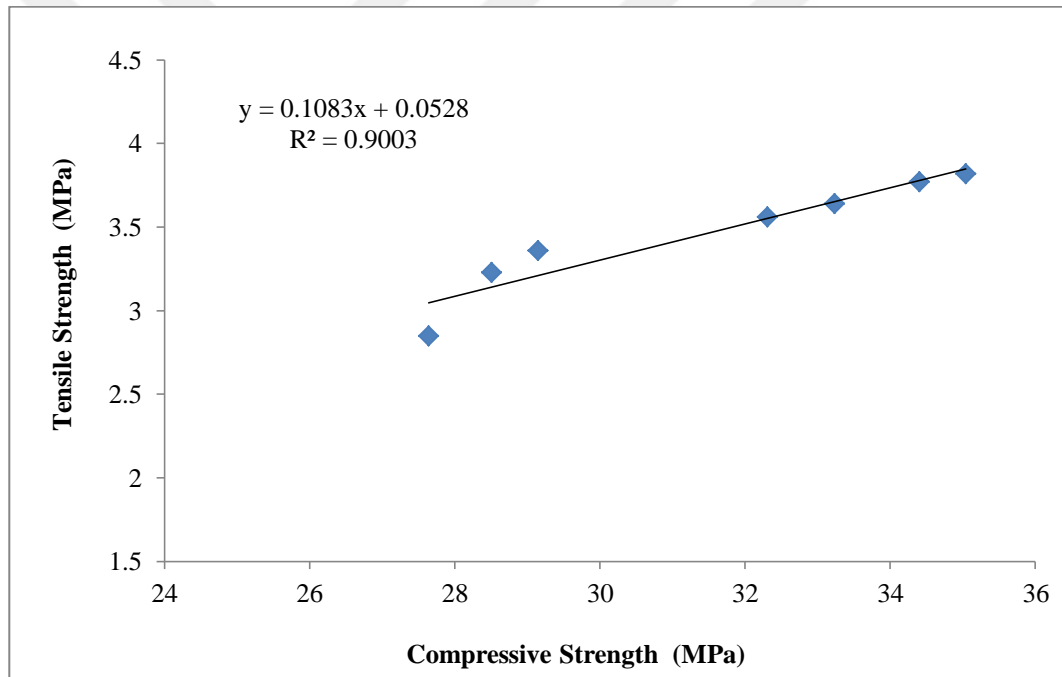


Figure 5.9 Relationship between compressive and splitting tensile strength of GGBFS based geopolymer mortar.

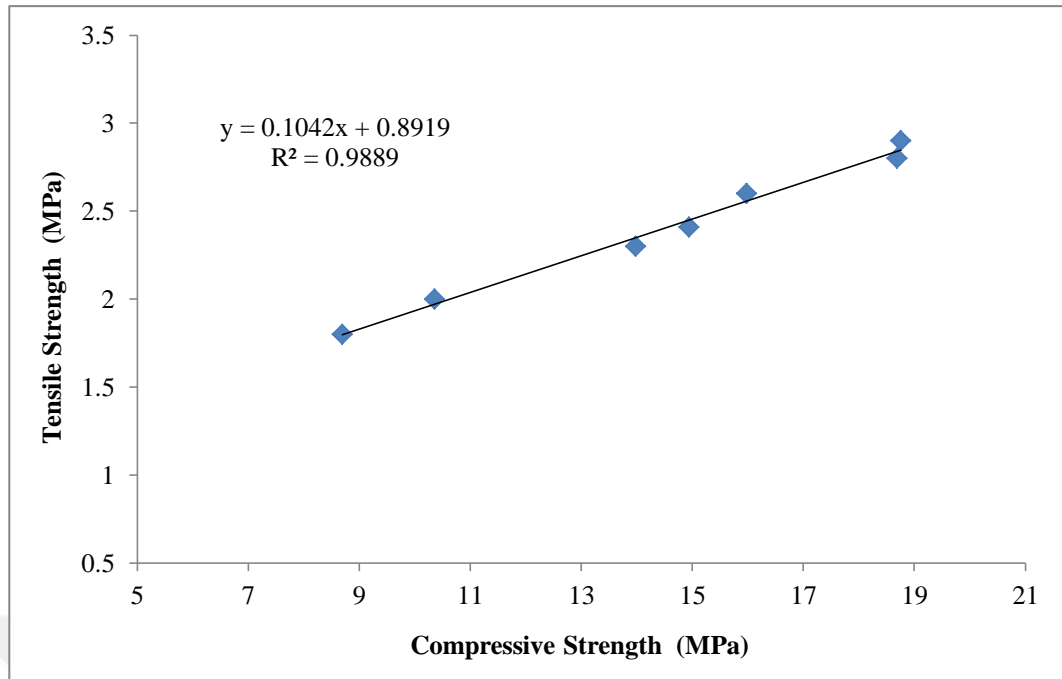


Figure 5.10 Relationship between compressive and splitting tensile strength of FA based geopolymer mortar.

The conversion table from the strength of 50 mm cubic specimen to standard cylindrical specimen ($\varnothing 150 \times 300$ mm) is given in Table 5.7 (Neville, 2004). As for comparison, Figures 5.11 and 5.12 showed relationship obtained by other study and this study for GGBFS and FA after Converted. Based on the figures, the best regression line from this study approximates to the empirical relation suggested by ACI Building Code (ACI 363R-92). The empirical relation is expressed as;

$$f_s = 0.59f_c^{0.5} \quad (5.1)$$

Eq. 2, 3 and 4 are made by CEB-FIP (1990), TS 500 (2000) and Neville (2004), respectively;

$$f_s = 0.3 f_c^{2/3} \quad (5.2)$$

$$f_s = 0.5 f_c^{0.5} \quad (5.3)$$

$$f_s = 0.23f_c^{0.67} \quad (5.4)$$

Table 5.7 Conversion for compressive and splitting tensile strength according to size and shape of the specimen (Neville, 2004).

From	TO	conversion
50*50*50 compressive strength specimen	150*300 cylindrical compressive strength	$f_{c, \phi 150} = 0.752 f_{c, 50}$
50*50*50 splitting tensile strength specimen	150*300 cylindrical splitting tensile strength	$f_{s, \phi 150} = 0.1083 f_{c, \phi 150} + 0.0528$ from fig. 5.9 $f_{s, \phi 150} = 0.1042 f_{c, \phi 150} + 0.8919$ from fig. 5.10

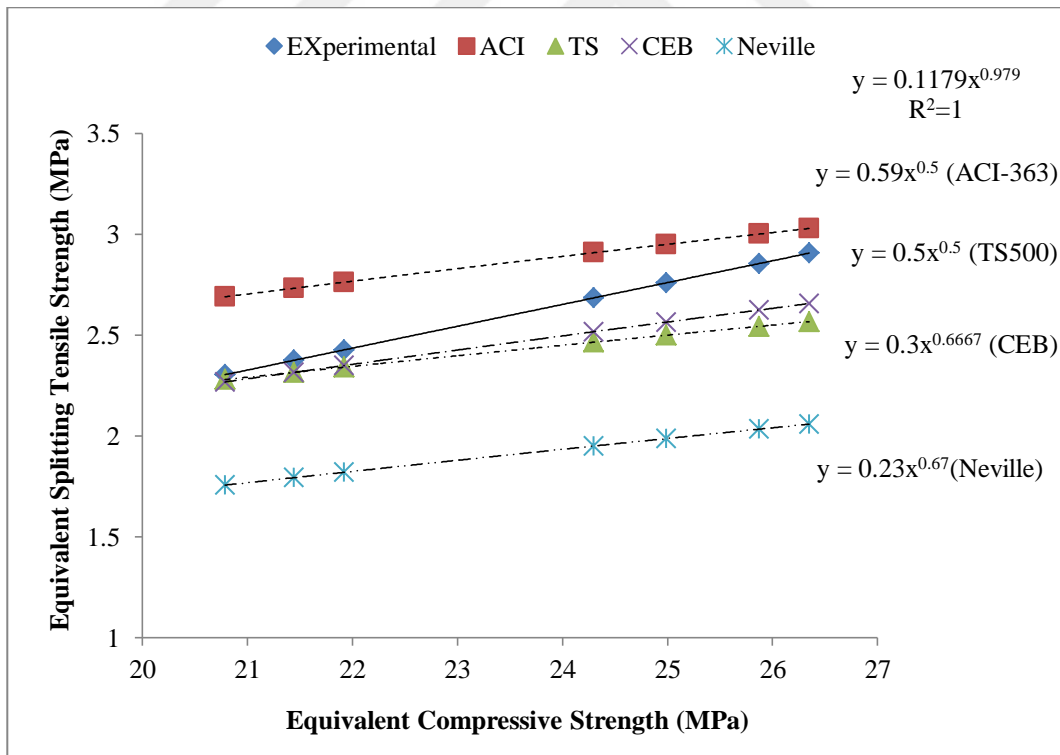


Figure 5.11 Comparison of splitting tensile strength of GGBFS geopolymer (experimental and theoretical).

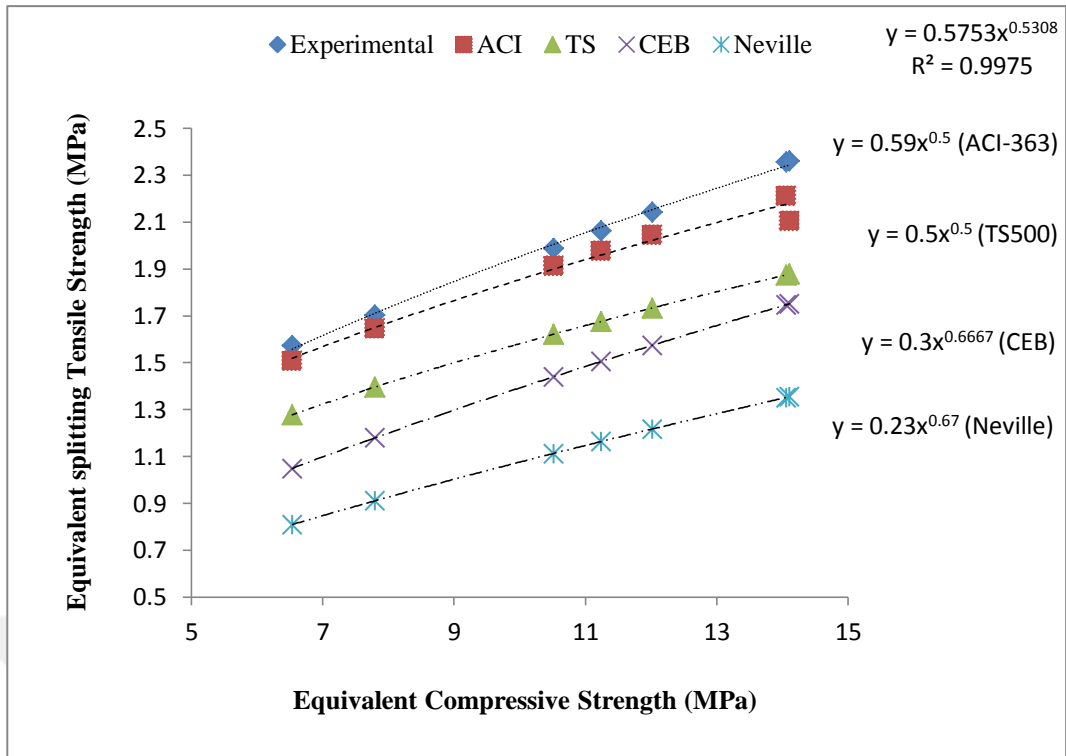


Figure 5.12 Comparison of splitting tensile strength of FA geopolymer (experimental and theoretical).

The results of experimental and predicted splitting tensile strength from Eq. 1 to 4 listed in Table 5.7. Based on the table, the average experimental/predicted splitting tensile strength is calculated. Significantly, the empirical expression from Eq.1 (ACI Building Code, 1992) is approximately give a closer value to the experimental result of FA geopolymer, while, the experimental result of GGBFS geopolymer obtained in this study is in agreement with the value for empirical expression from Eq.2 (TS500, 2000) and the value from Eq.1. Meanwhile, Eq. 4 that proposed by Neville significantly underestimates all the split tensile strength.

Table 5.8 Comparison of splitting tensile strength (experimental and theoretical).

Mix no.	Experimental for GGBFS & FA (MPa)				Predicted fst (MPa)				Experimental/predicted ratio			
	$f_{c,50}$	$f_c, \varnothing 150$	$f_{s,50}$	$f_s, \varnothing 150$	Eq (1)	Eq (2)	Eq (3)	Eq (4)	Eq (1)	Eq (2)	Eq (3)	Eq (4)
MS1	27.64	20.78	2.85	2.30	2.68	2.26	2.27	1.75	0.85	1.01	1.01	1.31
MS2	28.51	21.44	3.23	2.37	2.73	2.31	2.31	1.79	0.86	1.02	1.02	1.32
MS3	29.15	21.92	3.36	2.42	2.76	2.34	2.34	1.82	0.87	1.03	1.03	1.33
MS4	32.31	24.29	3.56	2.68	2.90	2.51	2.46	1.95	0.92	1.06	1.08	1.37
MS5	33.23	24.98	3.64	2.75	2.94	2.56	2.49	1.98	0.93	1.07	1.10	1.38
MS6	34.4	25.86	3.77	2.85	3.00	2.62	2.54	2.03	0.95	1.08	1.12	1.40
MS7	35.04	26.35	3.82	2.90	3.02	2.65	2.56	2.05	0.95	1.09	1.13	1.41
MF1	8.69	6.53	1.8	1.57	1.50	1.04	1.27	0.80	1.04	1.49	1.23	1.94
MF2	10.36	7.79	2	1.70	1.64	1.17	1.39	0.91	1.03	1.44	1.22	1.87
MF3	13.98	10.51	2.3	1.98	1.91	1.43	1.62	1.11	1.03	1.38	1.22	1.78
MF4	14.94	11.23	2.41	2.06	1.97	1.50	1.67	1.16	1.04	1.37	1.23	1.77
MF5	15.98	12.01	2.6	2.14	2.04	1.57	1.73	1.21	1.04	1.36	1.23	1.76
MF6	18.69	14.05	2.8	2.35	2.21	1.747	1.87	1.35	1.06	1.34	1.25	1.74
MF7	18.76	14.10	2.9	2.36	2.21	1.75	1.87	1.35	1.12	1.34	1.25	2.14

5.4.3 Sorptivity

The measurement of sorptivity has primary importance in durability assessment of geopolymer. The experimental results on water sorptivity are shown in Table 5.9, generally for all the light-weight geopolymer mortars incorporated with FA and GGBFS tested in this study has low water sorptivity and increased by the conditioning of specimens at 105°C.

From Figures 5.13 and 5.14 the water sorptivity of FA geopolymer mortar decreased with increasing binder content because fly ash acts as a filler material which fills the pores and there by reduces the water sorptivity. Also the sorptivity for all samples of LWGM was slightly low that could be attributed to increased silica content formed

higher quantity of aluminosilicate gel and the silicate occupies the void spaces between the binder particles resulting in lower water sorptivity.

It could be concluded that the water sorptivity of geopolymer lightweight mortar specimens are significantly affected by binder content and source material of geopolymer mix. The water sorptivity value of GGBFS geopolymer mortar increased with increasing binder content as shown in Figure (5.15 and 5.16) and was significantly larger than FA geopolymer mortar at higher level of binder. This could be because the GGBFS geopolymer mortar is more porous of fly ash geopolymer mortar.

Table 5.9 Water sorptivity results from the experimental verification tests for the light-weight geopolymer mortars incorporated with FA and GGBFS.

Mix no.	Binder content (kg/m ³)	Sorptivity value of GGBFS (mm/min ^{1/2})		Sorptivity value of FA (mm/min ^{1/2})	
		drying at 60 °C	drying at 105 °C	drying at 60 °C	drying at 105 °C
M1	650	0.0027	0.0967	0.0640	0.1880
M2	750	0.0040	0.1040	0.0320	0.1336
M3	850	0.0060	0.1236	0.0180	0.0696
M4	950	0.0073	0.1963	0.0047	0.0680
M5	1050	0.0085	0.2400	0.0039	0.0660
M6	1150	0.0087	0.2923	0.0030	0.0610
M7	1250	0.0093	0.3730	0.0027	0.0587

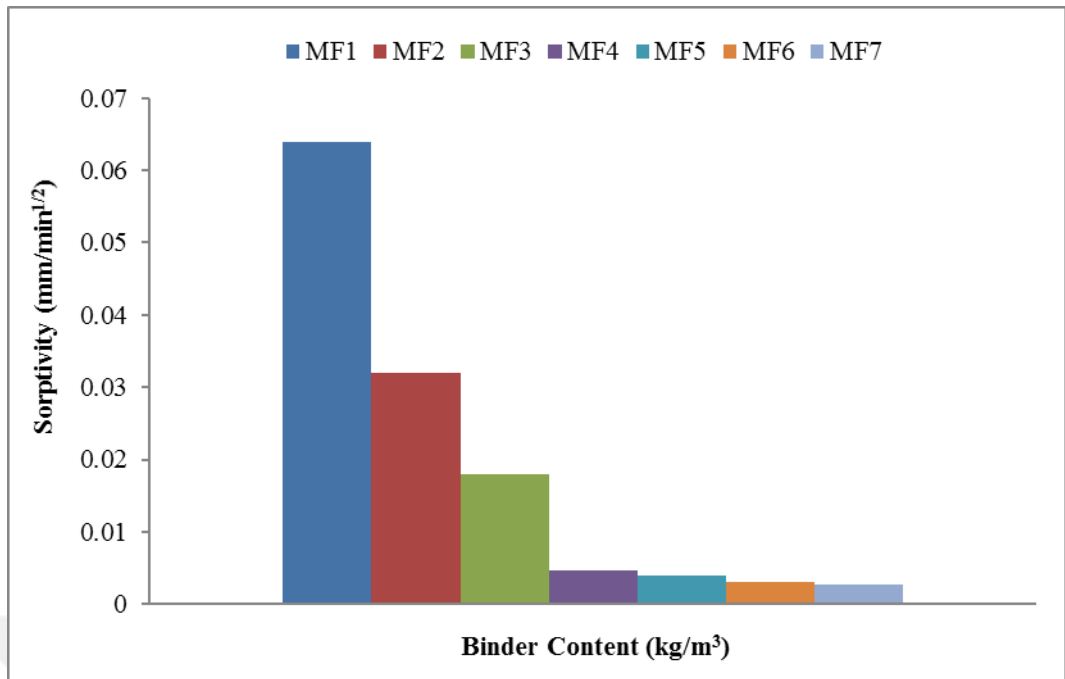


Figure 5.13 Water sorptivity of FA based geopolymer mortar without drying at 105 °C.

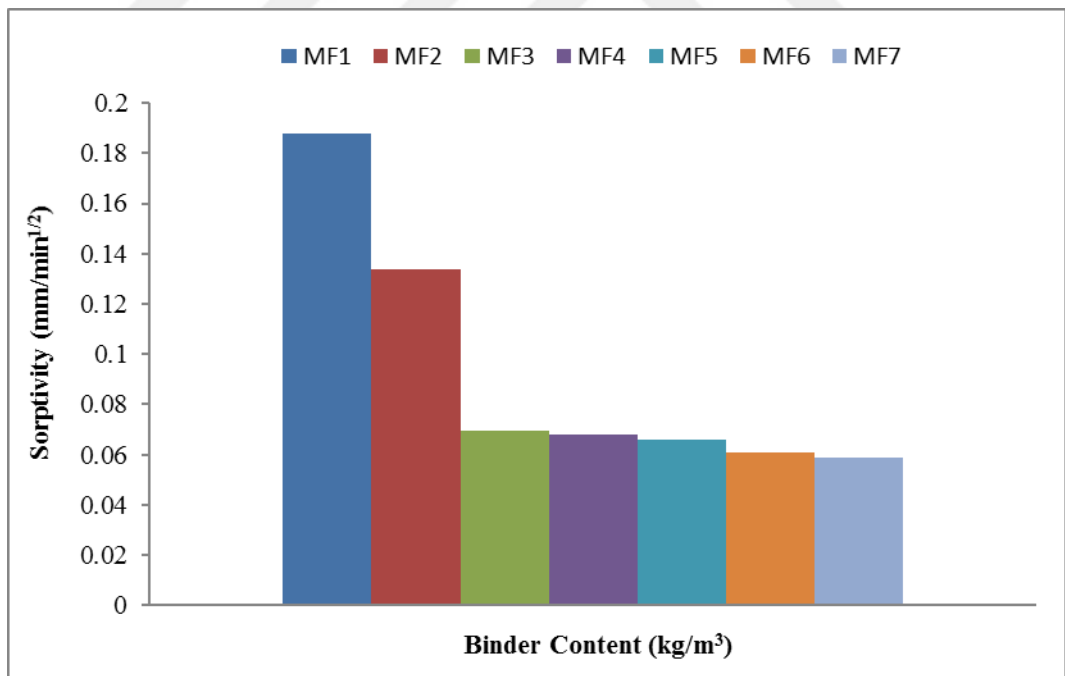


Figure 5.14 Water sorptivity of FA based geopolymer mortar drying at 105 °C.

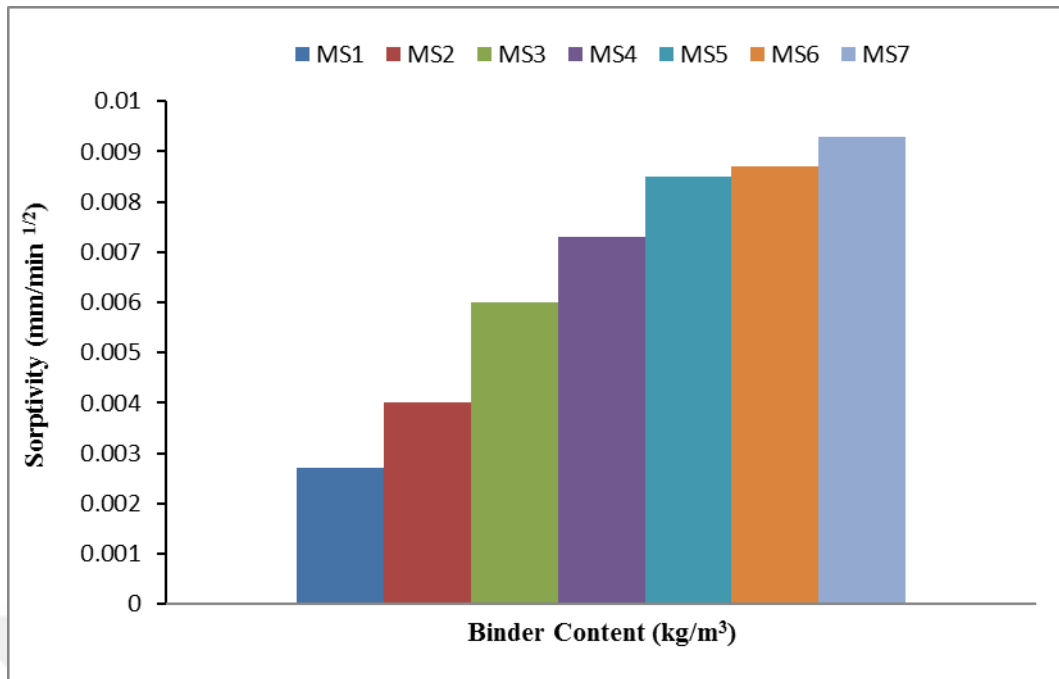


Figure 5.15 Water sorptivity of GGBFS based geopolymer mortar without drying at 105 °C.

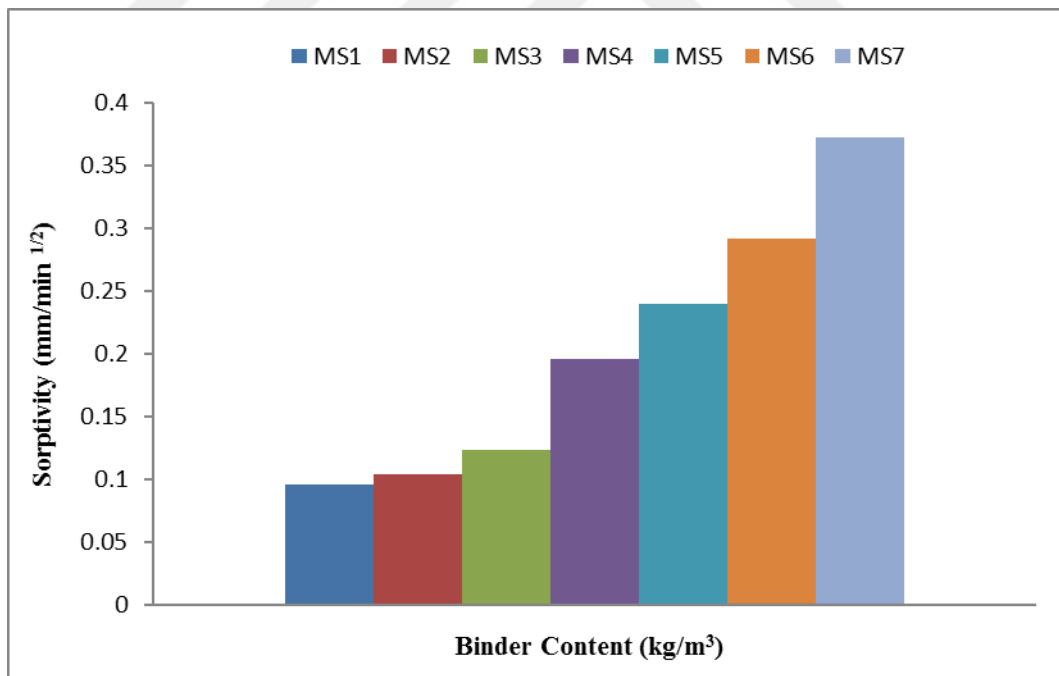


Figure 5.16 Water sorptivity of GGBFS based geopolymer mortar drying at 105 °C.

The following equations may be suggested to fit the relationship between compressive strength and sorptivity for FA and GGBFS based geopolymer mortar .The equation of the GGBFS mortar has a coefficient of determination $R^2 = 0.927$ and 0.93 for drying specimens at 105 °C in oven and without drying, respectively . This coefficient of determination is superior to that suggested from linear regression (0.81 and 0.82) for FA mortar at the same condition with GGBFS. As shown in Figures 5.17 and 5.18.

$Y=0.0336X- 0.8536$ ($R^2=0.92$) for GGBFS with drying specimens.

$Y=0.0008X- 0.189$ ($R^2=0.93$) for GGBFS without drying specimens.

$Y=0.0116X+ 0.2608$ ($R^2=0.81$) for FA with drying specimens .

$Y=0.0054X+ 0.0962$ ($R^2=0.82$) for FA without drying specimens.

where:

X: Compressive strength in MPa.

Y: Sorptivity in $\text{mm}/\text{min}^{1/2}$.

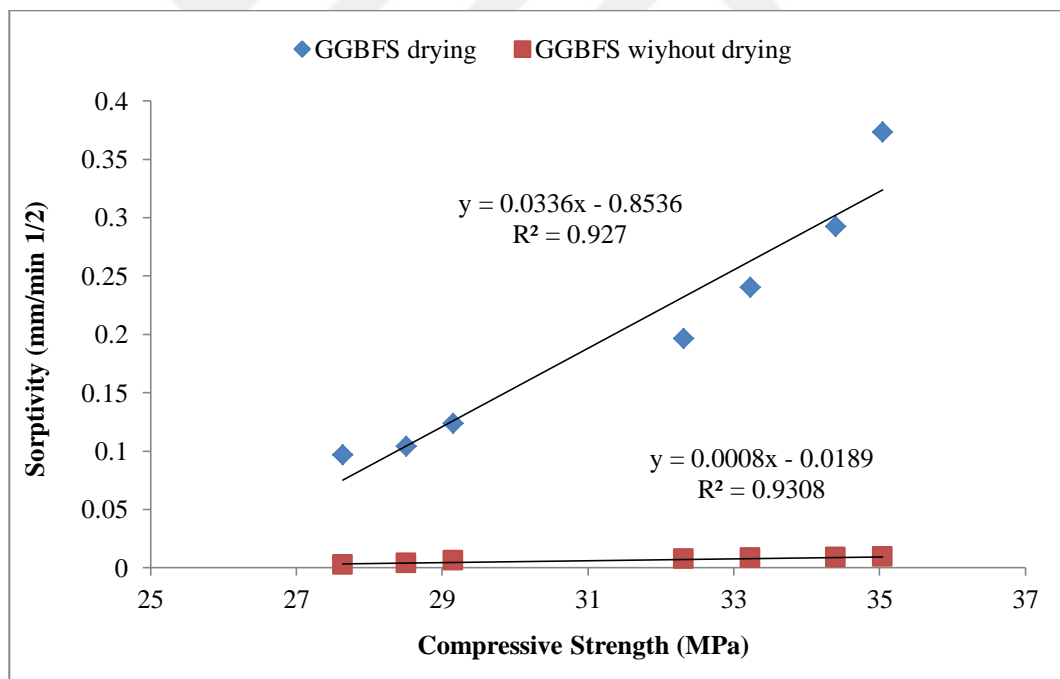


Figure 5.17 Relationship between compressive strength and sorptivity of GGBFS geopolymer.

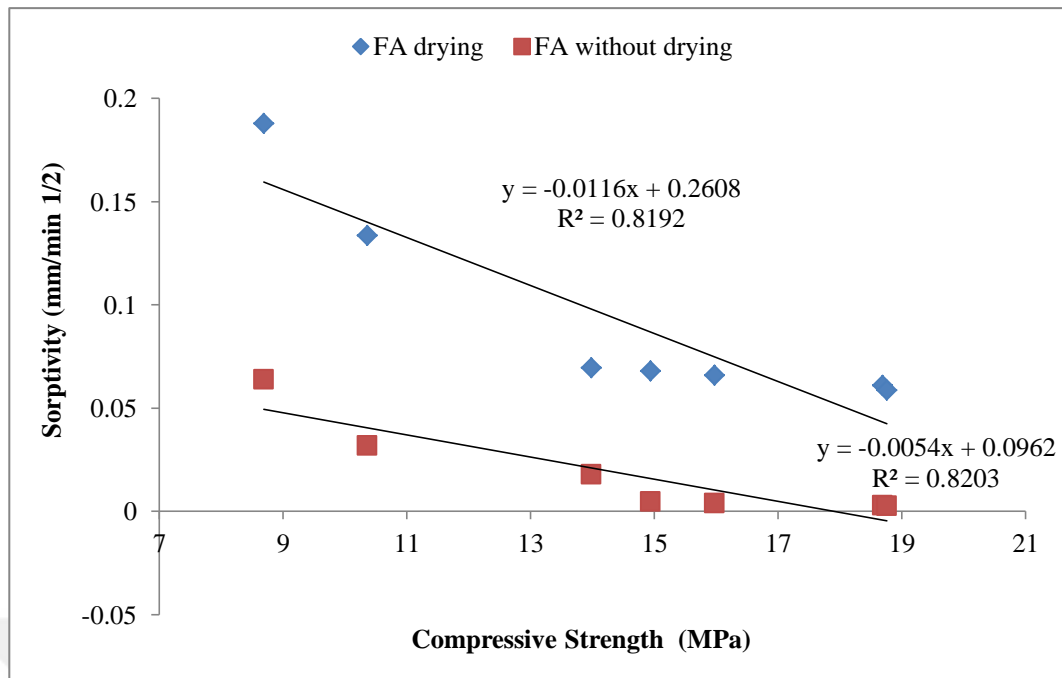


Figure 5.18 Relationship between compressive strength and sorptivity of FA geopolymer.

5.4.4 Water Absorption

The specimens for water absorption test were cubes (50×50×50 mm). The test was conducted at age 7 days. The optimum curing temperature 60 °C was adopted in this study for the light-weight geopolymer mortars incorporated with FA and GGBFS.

The results of water absorption on the binder content from 650 to 1250 kg/m³ are presented in table 5.10 and figures (5.19 and 5.20). From the table 5.10 it was noted that the water absorption percentage of fly ash based geopolymer mortar is higher than GGBFS based geopolymer mortar. From the table it is clear that M1 is showing better result than M7. Water absorption value increases as the binder content of mortar increases that may be because of a higher volume of paste is observed as the mixture containing the lower volume of aggregate has the higher absorption (Javier et al., 2011).

On the other hand, the percentage of water absorption for all samples was slightly higher. The physical properties of lightweight fine aggregate (LWFA) itself and a lot of embedded network capillary in the particle are the main reason behind the increasing magnitudes of water absorption. The irregularity in shape and the highly porous surface contributed to the increment of water absorption percentage.

Table 5.10 Water absorption results from the experimental verification tests for the light-weight geopolymer mortars incorporated with FA and GGBFS.

Mix no.	binder content (kg/m ³)	% water absorption value of GGBFS	% water absorption value of FA
M1	650	10.81	13.10
M2	750	11.24	13.80
M3	850	11.36	14.20
M4	950	11.59	14.60
M5	1050	11.71	14.80
M6	1150	11.87	15.54
M7	1250	12.00	15.83

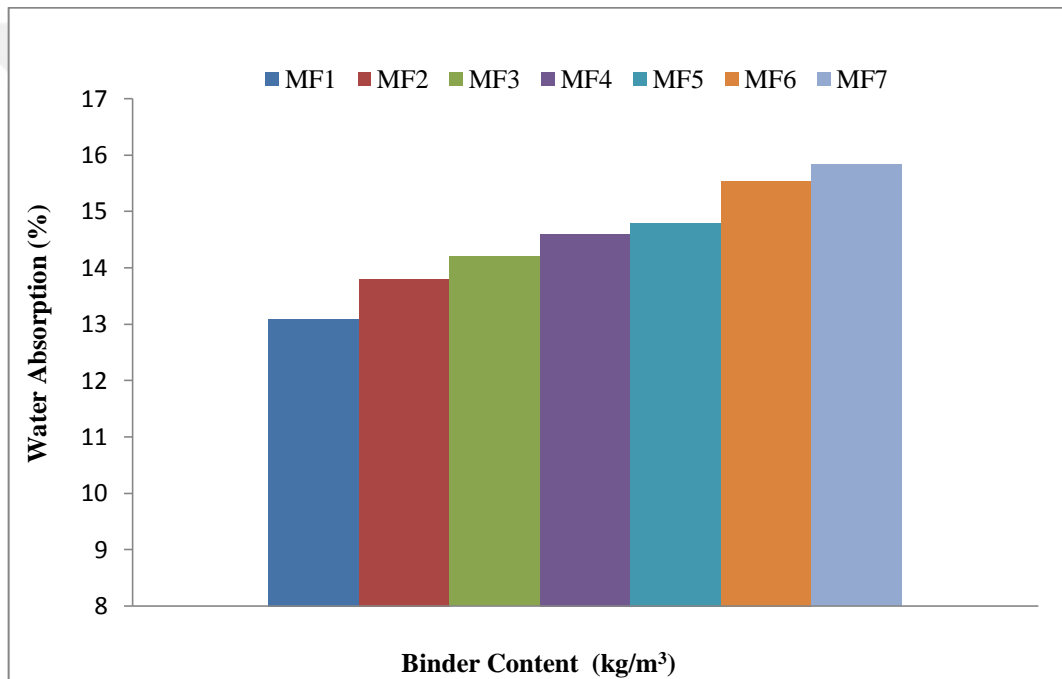


Figure 5.19 Water absorption percentage of FA based geopolymer mortar with different binder content.

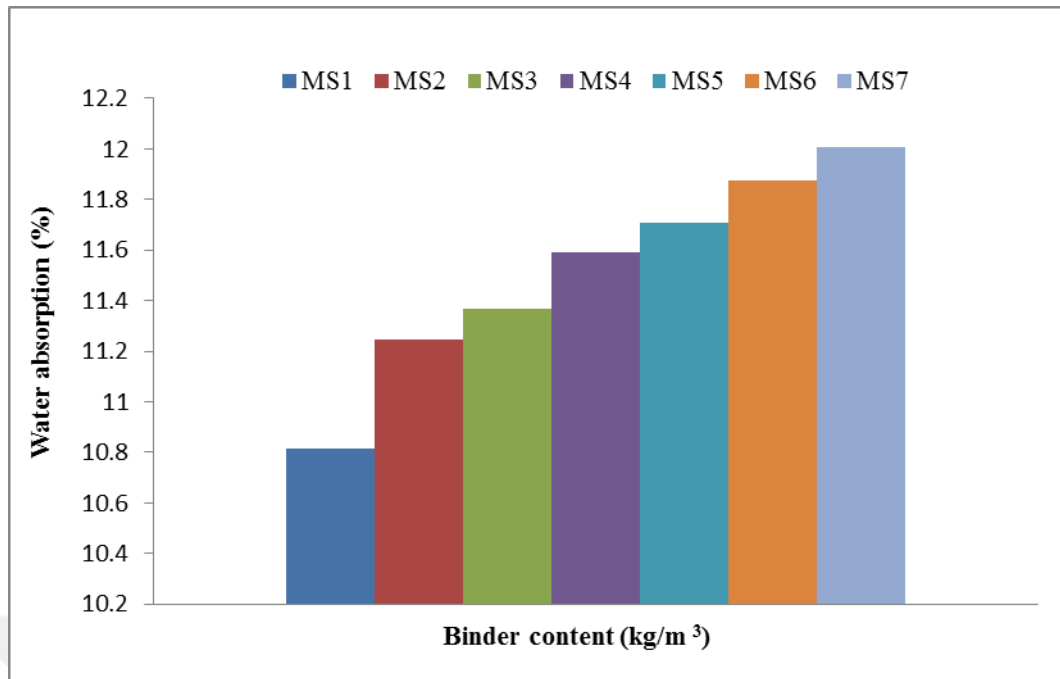


Figure 5.20 Water absorption percentage of GGBFS based geopolymer mortar with different binder content.

The following equations may be suggested to fit the relationship between compressive strength and water absorption for FA and GGBFS based geopolymer, this equations gives higher value of (R^2), as shown in Figure 5.21.

$$Y=0.2432X+11.03 \quad (R^2=0.9648 \text{ for GGBFS}).$$

$$Y=0.13X+7.4261 \quad (R^2=0.918 \text{ for FA}).$$

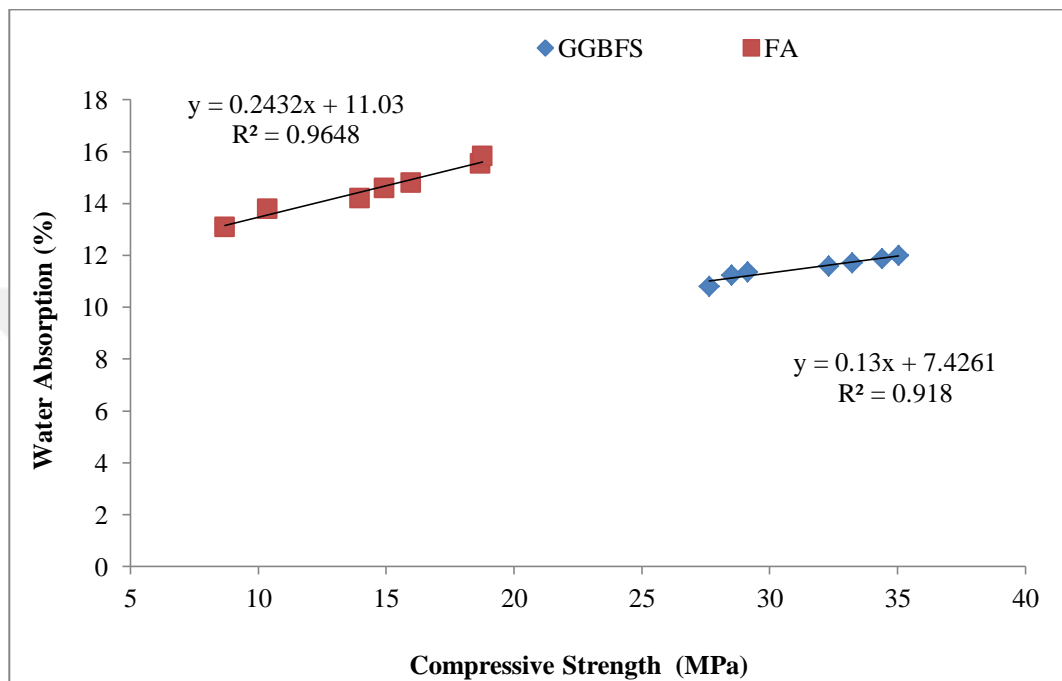


Figure 5.21 Relationship between compressive strength and water absorption of LWGM.

CHAPTER 6

EXPERIMENTAL STUDY AND OPTIMIZATION OF EFFECT OF MOLARITY AND $\text{Na}_2\text{SiO}_3/\text{NaOH}$ RATIO

6.1 Introduction

In this chapter, an experimental research was conducted to explore the effects of NaOH concentration and various SS/SH ratio on fresh flow table diameter, fresh unit weight, compressive strength, tensile strength, water absorption and sorptivity of geopolymer based lightweight mortars. Two popular by-products, FA and GGBFS, were selected as base materials for alkali activation

One of governing factors on properties of the gel and its formation is type and dosage of alkali activators. So far, liquid sodium silicate (water glass) (Na_2SiO_3) and liquid NaOH were the most used activating solutions in geopolymer. According to (Komnitsas and Zaharaki, 2007) alkali hydroxide is required for dissolution of aluminosilicate sources while water glass solution acts as a binder, alkali activator and dispersant or plasticizer. However, because of the soluble silicate available in the liquid water glass, it is a preferred activating solution, which tends to increase the rate of the polymerization reaction. Alkaline solutions induce a certain amount of Si and Al atoms to dissolve the aluminosilicate sources, forming monomers in solutions, and then poly-condense to form a rigid framework (Singh et al., 2005).

6.2. Mix Proportions

Forty LWGM mixtures were designed with constant GGBFS and FA content to study the fresh and hardened properties response of LWGM with different concentration of the solution expressed in terms of molar, M. (8,10,12 and 14) and sodium silicate to sodium hydroxide ratio (0.5,1.0,1.5,2.0,and 2.5) under constant curing temperature and curing duration. The binder content in the mixtures is total amount of alkaline solutions and the base material (FA or GGBFS). The selected binder content is 950 Kg/m^3 . The experiments were conducted on LWGM cubes

under curing temperature of 60°C with curing period 23.244 hr. for FA and 19.949 hr. for GGBFS, this optimum values obtained from chapter five.

The mixture proportions of LWGM are presented in Table 6.1. The alkaline solution was the only liquid component in all mixtures (without adding water). Superplasticizer with specific gravity of 1.07 is added to the mix to improve the workability and to make GP mix homogeneous. The mass of sodium hydroxide solids in a solution with a concentration of 8 Molar consists of $8 \times 40 = 360$ grams of NaOH solids per liter of the solution, where 40 is the molecular weight of NaOH; Na=23, O=16, and H=1. The mass of NaOH solids is measured as 260 grams per kg of NaOH solution. . Similarly, the mass of NaOH solids per kg of the solution for other concentrations were measured as 10M: 314 grams, 12M: 361 grams, and 14M: 404 grams (Hardjito and Rangan, 2005). The above calculations are tabulated in Table 6.2 .The LWGM were prepared as explained in Chapter 3.

It was observed that the mixes activated with high level of NaOH concentration (14M) and lower ratio of $\text{Na}_2\text{SiO}_3/\text{NaOH}$ (0.5and1.0) hardened during mixing in mixer specifically in the third minute as shown in figure 6.1 .That may be because of high percentage of (Na) that have ability to dissolve of (Si) in the source material and the increase in OH- ions due to the increase in alkali hydroxide content result in increased source material dissolution, this allows to form reaction products earlier. However if the $\text{Na}_2\text{SiO}_3/\text{NaOH}$ ratio is too low, the increased solid content of the paste starts to become a destabilizing factor while most added Na ion cannot be accommodated in the final structure (van Jaarsveld & van Deventer, 1999).

Table 6.1 Geopolymer lightweight mortar mix designs.

Designation LWGM	Pumice agg. (kg/m ³)	Crushed limestone (kg/m ³)	GGBFS (kg/m ³)	FA (kg/m ³)	Na ₂ SiO ₃ solution (kg/m ³)	Solution of NaOH (kg/m ³)	S.P. (kg/m ³)
MF8-0.5	413.27	286.424		633.27	105.45	210.9	31.66
MF8-1.0	422.27	281.127		633.27	158.27	158.27	31.66
MF8-1.5	428.37	285.191		633.27	190	126.635	31.66
MF8-2.0	431.61	287.345		633.27	210.9	105.45	31.66
MF8-2.5	434.12	289.021		633.27	226.1	90.44	31.66
MF10-0.5	418.75	278.787		633.27	105.45	210.9	31.66
MF10-1.0	426.39	283.874		633.27	158.27	158.27	31.66
MF10-1.5	431.07	286.986		633.27	190	126.635	31.66
MF10-2.0	434.39	289.201		633.27	210.9	105.45	31.66
MF10-2.5	436.46	290.577		633.27	226.1	90.44	31.66
MF12-0.5	423.79	282.138		633.27	105.45	210.9	31.66
MF12-1.0	430.17	286.388		633.27	158.27	158.27	31.66
MF12-1.5	434.03	288.961		633.27	190	126.635	31.66
MF12-2.0	436.915	290.877		633.27	210.9	105.45	31.66
MF12-2.5	438.62	292.014		633.27	226.1	90.44	31.66
MF14-0.5	428.46	285.251		633.27	105.45	210.9	31.66
MF14-1.0	433.67	288.722		633.27	158.27	158.27	31.66
MF14-1.5	436.82	290.817		633.27	190	126.635	31.66
MF14-2.0	439.25	292.433		633.27	210.9	105.45	31.66
MF14-2.5	440.60	293.450		633.27	226.1	90.44	31.66
MS8-0.5	449.95	299.555	633.27		105.45	210.9	31.66
MS8-1.0	458.97	305.564	633.27		158.27	158.27	31.66
MS8-1.5	464.42	309.191	633.27		190	126.635	31.66
MS8-2.0	468.31	311.782	633.27		210.9	105.45	31.66
MS8-2.5	470.83	313.458	633.27		226.1	90.44	31.66
MS10-0.5	455.45	303.222	633.27		105.45	210.9	31.66
MS10-1.0	463.10	308.311	633.27		158.27	158.27	31.66

MS10-1.5	467.77	311.423	633.27		190	126.635	31.66
MS10-2.0	471.10	313.638	633.27		210.9	105.45	31.66
MS10-2.5	473.17	315.014	633.27		226.1	90.44	31.66
MS12-0.5	460.49	306.574	633.27		105.45	210.9	31.66
MS12-1.0	466.87	310.825	633.27		158.27	158.27	31.66
MS12-1.5	470.74	313.398	633.27		190	126.635	31.66
MS12-2.0	473.62	315.313	633.27		210.9	105.45	31.66
MS12-2.5	475.32	316.450	633.27		226.1	90.44	31.66
MS14-0.5	465.17	309.687	633.27		105.45	210.9	31.66
MS14-1.0	470.38	313.159	633.27		158.27	158.27	31.66
MS14-1.5	473.53	315.253	633.27		190	126.635	31.66
MS14-2.0	475.95	316.869	633.27		210.9	105.45	31.66
MS14-2.5	477.30	317.767	633.27		226.1	90.44	31.66

Table 6.2 NaOH solids with different concentration (Hardjito and Rangan, 2005).

Molarity	Mass of NaOH solids(grams)
8	260
10	314
12	361
14	404



Figure 6.1 Hardened LWGM during mixing in mixer.

6.3 Fresh Properties Tests

6.3.1 Flow Table Test

The workability of LWGM was evaluated using mini slump cone according to ASTM C-124. The flow diameter of mini slump can be defined as the diameter of LWGM after spreading. The flow diameter was measured immediately after completion of mixing of LWGM in mixer. The following tests were designed to study the effect of NaOH concentration and Na_2SiO_3 to NaOH ratio on workability of geopolymer mix. The workability of a mix could be classified based on the flow diameter as shown in the Table 6.3 (Ghosh K. & Ghosh P., 2012). The minimum flow diameter of 150 ± 10 mm could be considered as required as the LWGM could be easily placed in the moulds.

Table 6.3 Workability criteria of geopolymer mortar (Ghosh K. & Ghosh P., 2012).

Sl. No.	Flow Diameter	Workability
1	Above 250	Very High
2	180 to 250 mm	High
3	150 to 180 mm	Moderate
4	150 to 120 mm	Stiff
5	Below 120 mm	Very Stiff

The workability, as presented in Table 6.4 and Figures (6.2 & 6.3) shows that for FA and GGBFS geopolymer mortar, the flow decreased with an increase of SS/SH ratio from 1 to 2.5 in FA and GGBFS geopolymer mortar. It may be safe to state that the flow ability depends on the ratio of SS/SH by mass. It can be explained by nature of sodium silicate as a suspension liquid (Liew, et al., 2011) .while the flow of 0.5 ratio for all mixture less than another ratio that it may be because a higher concentration of OH- ions increases the reaction rate (van Jaarsveld & van Deventer, 1999).

On the other hand, it has been noticed that, the flow diameter decreases with the increase in in the NaOH concentration. This is due to increases viscosity of LWGM and resulted in reduction in flow diameter (Ariffin et al., 2015). The results for all mixtures showed that GGBFS geopolymer mortars had lower workability than FA geopolymer mortars. This is generally because of the accelerated reaction of the calcium and the angular shape of GGBFS as compared to the spherical shape of FA particles.

Table 6.4 Flow table values of LWGM.

Mix name	Molarity	Na ₂ SiO ₃ to NaOH ratio	Flow table values of FA (mm)	Flow table values of GGBFS (mm)
M 8-0.5	8	0.5	225	140
M 8-1.0		1.0	220	178
M 8-1.5		1.5	215	173
M 8-2.0		2.0	207	163
M 8-2.5		2.5	200	160
M 10-0.5	10	0.5	190	NA*
M 10-1.0		1.0	214	163
M 10-1.5		1.5	210	180
M 10-2.0		2.0	198	175
M 10-2.5		2.5	187	170
M 12-0.5	12	0.5	NA*	NA*
M 12-1.0		1.0	207	NA*
M 12-1.5		1.5	198	170
M 12-2.0		2.0	188	166
M 12-2.5		2.5	185	155
M 14-0.5	14	0.5	NA*	NA*
M 14-1.0		1.0	NA*	NA*
M 14-1.5		1.5	120	152
M 14-2.0		2.0	180	157
M 14-2.5		2.5	177	145

* NA: Not available due to rapid setting during mixing.

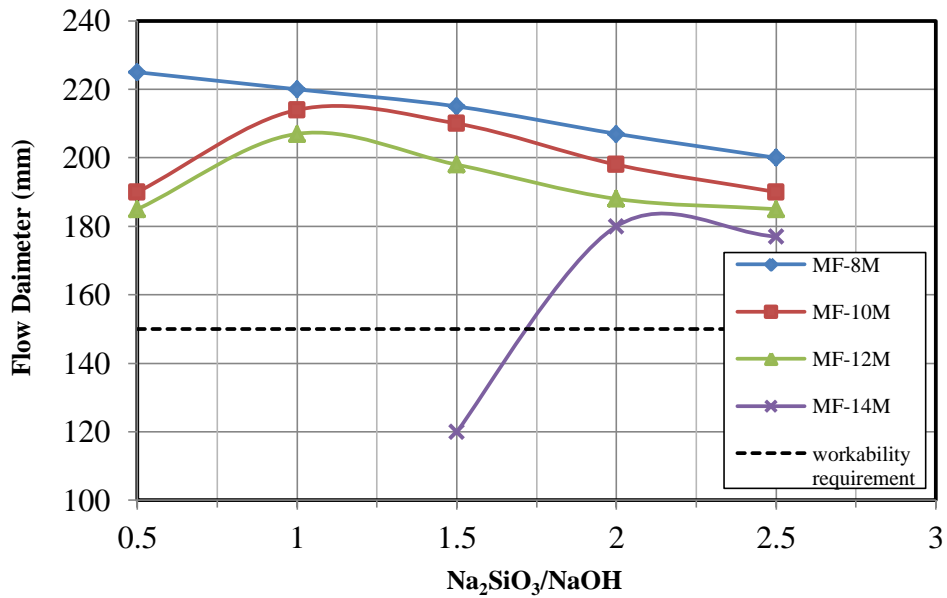


Figure 6.2 Flow table of FA geopolymer mortar.

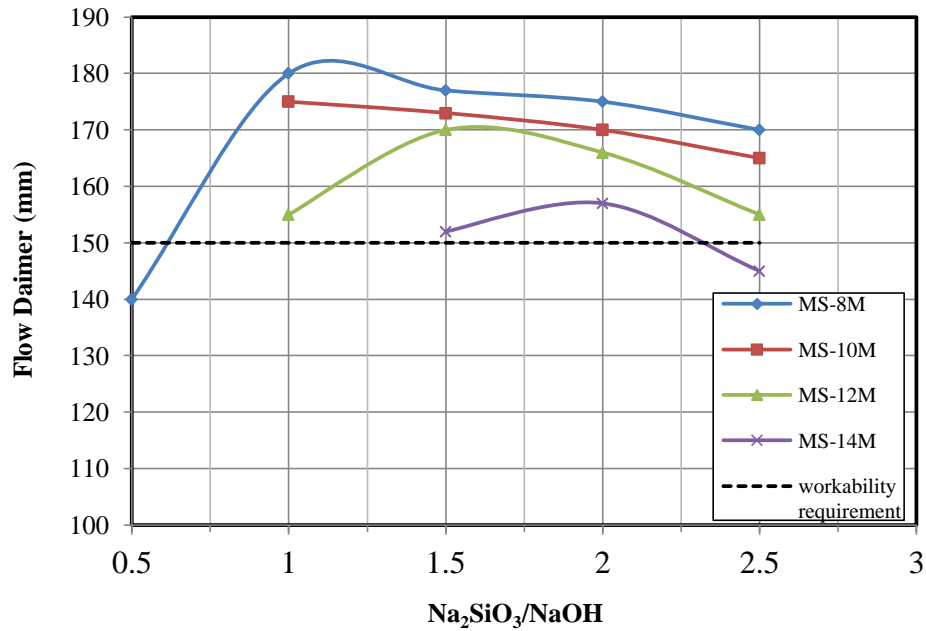


Figure 6.3 Flow table of GGBFS geopolymer mortar.

6.3.2 Fresh Density Test

Fresh density of GGBFS and FA based geopolymer mortar was conducted directly after mixing. The measured density was for the all mixtures Table 6.5 and figures (6.4& 6.5) presents the density of the fresh unit weight of LWGM. As shown in Table 6.5 there was slightly increase in mortar unit weight with the increase of Na₂SiO₃ to NaOH ratio but it was observed increase in unit weight of FA and GGBFS based geopolymer mortar with increasing NaOH concentration. On the other hand, FA-based geopolymer mortar exhibits a reduction in fresh unit weight density compared with GGBFS-based geopolymer mortar.

Table 6.5 Fresh unit weight of LWGM.

Mix name	Molarity	Na ₂ SiO ₃ to NaOH ratio	Fresh unit weight values of FA (kg/m ³)	Fresh unit weight values of GGBFS (kg/m ³)
M 8-0.5	8	0.5	1696.37	1786.38
M 8-1.0		1.0	1711.83	1802.09
M 8-1.5		1.5	1722.25	1811.56
M 8-2.0		2.0	1727.44	1817.95
M 8-2.5		2.5	1731.89	1822.48
M 10-0.5	10	0.5	1705.68	NA*
M 10-1.0		1.0	1718.81	1809.19
M 10-1.5		1.5	1726.82	1817.32
M 10-2.0		2.0	1732.16	1822.75
M 10-2.5		2.5	1735.85	1826.50
M 12-0.5	12	0.5	1714.20	NA*
M 12-1.0		1.0	1725.20	1815.68
M 12-1.5		1.5	1731.84	1822.42
M 12-2.0		2.0	1736.42	1827.07
M 12-2.5		2.5	1739.50	1830.21
M 14-0.5	14	0.5	NA*	NA*
M 14-1.0		1.0	NA*	NA*
M 14-1.5		1.5	1736.55	1827.21
M 14-2.0		2.0	1740.37	1831.09
M 14-2.5		2.5	1742.97	1833.61

* NA: Not available due to rapid setting during mixing.

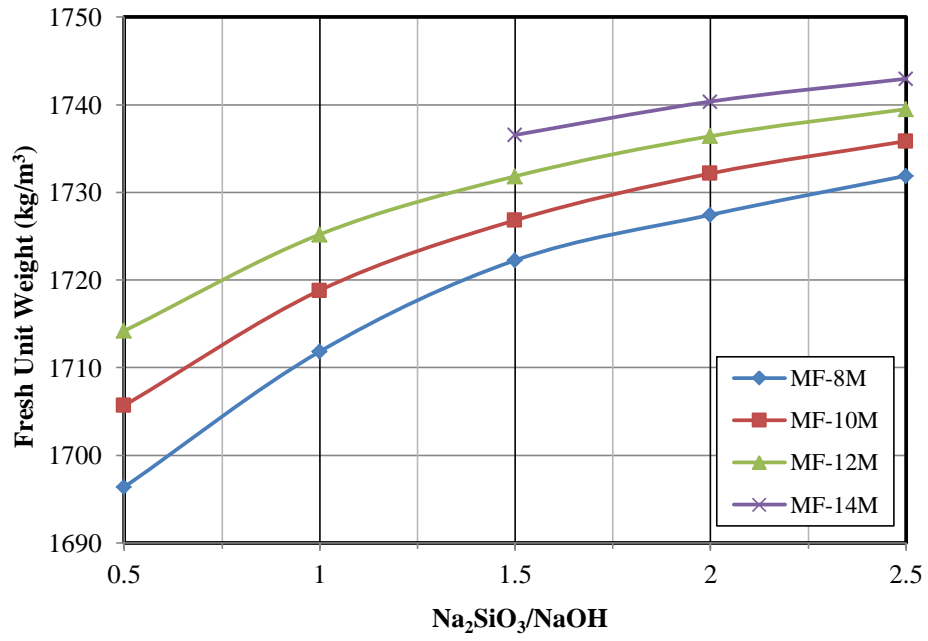


Figure 6.4 Fresh unit weight of FA based geopolymer mortar.

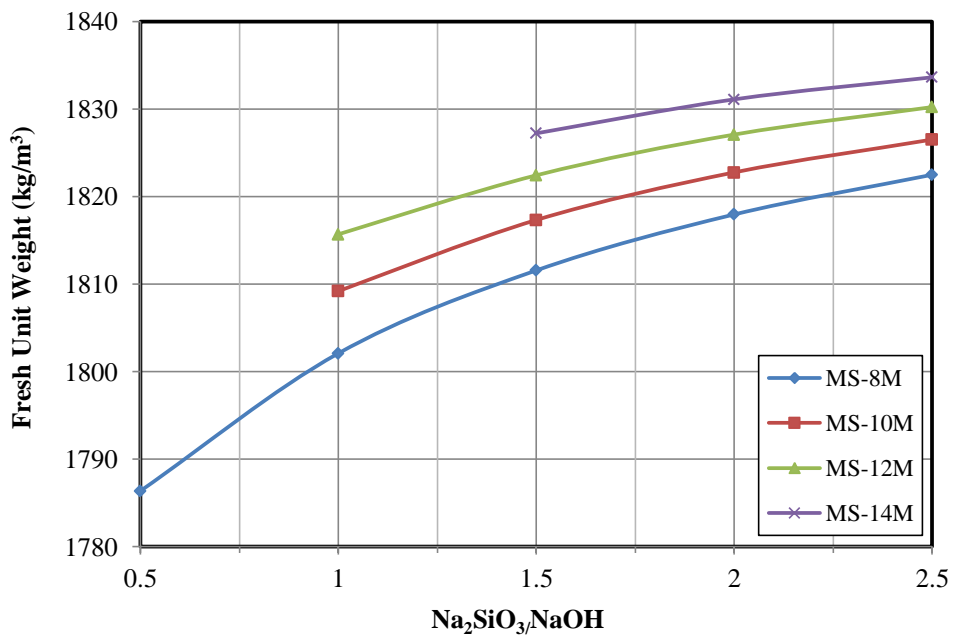


Figure 6.5 Fresh unit weight of GGBFS based geopolymer mortar.

6.4 Hardened Properties Tests

6.4.1 Compressive Strength

6.4.1.1 Effect of NaOH Concentration on The Strength of FA Geopolymer Mortar

The concentration of NaOH had one of a major effect on the compressive strength development of FA geopolymer mortars. The concentration of NaOH acts on the dissolution process in the aqueous phase of geopolymeric system, in addition to bonding of solid particles in the final structure (Panias, 2007). High concentration of NaOH increases the dissolution of solid materials and leads to greater geopolymerization reactions and consequently increases the compressive strength (Temuujin et al., 2009).

Table 6.6 and Figure 6.6 show the effect of NaOH concentration on compressive strength in FA-based LWGM with variable SS/SH. It could be concluded that the compressive strength raised proportionally with the increment of NaOH concentration from 8 to 14 M at the same SS/SH ratio at 23.244 hours and 7 days. geopolymerization process needs strong alkali to activate the (Si) and (Al) in FA. By increasing NaOH concentration, ability of solution to leach (Si) and (Al) in FA is improved due to the formation of alumino-silicate gel at an early stage that resulted from increasing NaOH concentration (Rattanasak, 2009).

6.4.1.2 Effect of Na₂SiO₃ to NaOH Ratio on the Strength Development of FA Based LWGM

The increase in Na₂SiO₃ to NaOH ratio leads to an increase in compressive strength of FA based LWGM up to an optimum value 1.0, at which strength reaches 13.75, 17.17 and 20.72 MPa at 8 M, 10M and 12 M, respectively. After that limit, the strength decreases, as shown in Figure 6.6 and Table 6.6.

The ratio of silicate to hydroxide affects the compressive strength development of activated systems. In general, an increase in the concentration of the alkali (or decreasing the added soluble silicate) results in an increase of the compressive strength. This is because an excess of soluble silicates retards setting (through the delayed release of water and the polycondensation) and structure formation (Khale, 2007 and Morsy, 2014). Thus, care must be taken to regulate the molar ratio of

hydroxides to silicates. Therefore the optimum ratio of NaOH Concentration and Na_2SiO_3 to NaOH were 12M and 1:1 by mass for the FA based LWGM, which gives maximum compressive strength (20.72MPa).

Table 6.6 Effect of NaOH concentration and NaOH to Na_2SiO_3 ratio on FA geopolymer Compressive strength.

Mix name	Molarity	Na_2SiO_3 to NaOH ratio	Compressive strength after curing (MPa)	Compressive strength after 7 day (MPa)
MF8-0.5	8	0.5	11.55	12.47
MF8-1.0		1.0	13.75	14.42
MF8-1.5		1.5	12.75	13.67
MF8-2.0		2.0	12.50	12.67
MF8-2.5		2.5	11.51	12.19
MF10-0.5	10	0.5	13.31	13.55
MF10-1.0		1.0	17.17	17.40
MF10-1.5		1.5	14.76	16.18
MF10-2.0		2.0	14.10	14.62
MF10-2.5		2.5	13.63	14.26
MF12-0.5	12	0.5	13.63	13.90
MF12-1.0		1.0	20.72	21.08
MF12-1.5		1.5	16.41	18.20
MF12-2.0		2.0	14.14	16.57
MF12-2.5		2.5	13.80	14.94
MF14-0.5	14	0.5	NA*	NA*
MF14-1.0		1.0	NA*	NA*
MF14-1.5		1.5	18.57	19.48
MF14-2.0		2.0	16.02	17.60
MF14-2.5		2.5	15.62	16.65

* NA: Not available due to rapid setting during mixing.

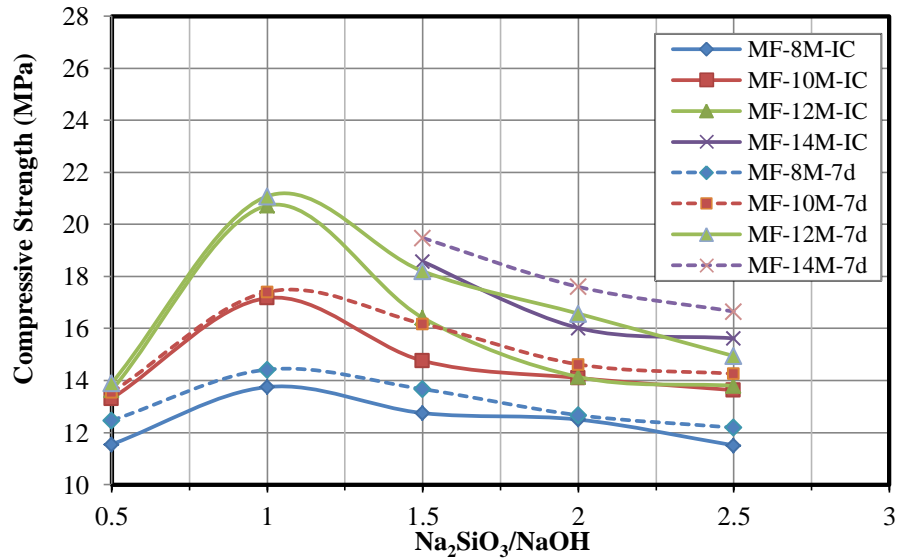


Figure 6.6 Effect of NaOH Concentration and NaOH to Na₂SiO₃ ratio on FA geopolymer Compressive strength.

6.4.1.3 Effect of NaOH Concentration on The Strength of GGBFS Geopolymer Mortar

Figure 6.7 and table 6.7 show NaOH concentration effect on compressive strength in GGBFS-based LWGM at two ages, namely 19.949 hours and 7 days. The results showed that the compressive strength raised with the increment of NaOH concentration from 8 to 12 M at the same SS/SH ratio. The maximum compressive strength with NaOH concentrations of 12 M were 30.4 and 31.2 MPa after initial curing (19.949 hours) and 7 day respectively. While compressive strength decreases with the further increase in NaOH concentration. The increase in alkali concentration developed the geopolymerization process which resulted to an increase in the compressive strength of GGBFS-based LWGM. However, the increase in concentration of hydroxide ion caused aluminosilicate gel precipitation at early stages, and subsequent geopolymerization was hindered, resulting in lower strength geopolymer (Lee, 2002).

6.4.1.4 Effect of Na₂SiO₃ to NaOH Mass Ratio on the Strength Development of GGBFS Based LWGM

The GGBFS-based LWGM prepared with various Na₂SiO₃/NaOH mass ratios display dissimilar strength developments at initial curing age and after 7 days. Figure 12 show the compressive strength of GGBFS based LWGM at five Na₂SiO₃ to NaOH ratios and four NaOH molarity.

The maximum strength of 31.2 MPa was obtained at 7 days. It can be concluded from results that compressive strength and SS/SH ratio were related proportionally. The compressive strength was increased by increasing SS/SH ratio up to an optimum value. This behavior may be attributed to the joint effect of Na₂SiO₃ and NaOH. The increment in the SS/SH ratio would result in increasing Na₂SiO₃ and hence an increase in geopolymerization (Hardjito, 2005). It is shown that the maximum compressive strength was obtained at SS/SH ratio of 1.1.5, 2 and 2.5 for 8, 10, 12 and 14 M, respectively. It can be concluded that SS/SH ratio represents the optimum ratio for the applied activators in this study.

However, increased SS/SH ratio greater than the optimum ratio there was a little decrease in the strength which can be interpreted because of extra amount of activating solution delaying the geopolymerization process. Previous researches mentioned that the increase in sodium silicate hinders the geopolymerization reaction through Al-Si phase precipitation which block contact between the activator solution and reacting materials and decrease activator concentration (Lee, 2002 and Villa, 2010).

It is demonstrated that the strength of GGBFS-based LWGM with different molarity and SS/SH ratio is greater than that of FA-based LWGM, the compressive strength results indicated that this type of more calcined source materials had higher mechanical strength by improving the microstructure of geopolymer matrix resulted in the formation of more compact microstructure of the binder (Van Jaarsveld, 2002). The highest compressive strength value reached nearly 31.2 MPa at 7th days. It can be attributed due to the utilized of slag. The content of slag in the system, the more hydration products of CSH and hydrated aluminates calcium were obtained.

Table 6.7 Compressive strength at different Molarity of NaOH and NaOH to Na_2SiO_3 ratio for GGBFS geopolymer mortar.

Mix name	Molarity	Na_2SiO_3 to NaOH ratio	Compressive strength after curing (MPa)	Compressive strength after 7 day (MPa)
MS8-0.5	8	0.5	22.70	23.20
MS8-1.0		1.0	26.93	27.90
MS8-1.5		1.5	26.81	27.70
MS8-2.0		2.0	26.35	27.40
MS8-2.5		2.5	26.57	27.80
MS10-0.5	10	0.5	NA*	NA*
MS10-1.0		1.0	27.10	28.00
MS10-1.5		1.5	27.80	28.70
MS10-2.0		2.0	26.90	27.90
MS10-2.5		2.5	27.23	28.20
MS12-0.5	12	0.5	NA*	NA*
MS12-1.0		1.0	28.00	28.90
MS12-1.5		1.5	29.76	30.30
MS12-2.0		2.0	30.40	31.20
MS12-2.5		2.5	30.00	30.70
MS14-0.5	14	0.5	NA*	NA*
MS14-1.0		1.0	NA*	NA*
MS14-1.5		1.5	25.90	26.61
MS14-2.0		2.0	27.72	28.50
MS14-2.5		2.5	28.90	29.45

* NA: Not available due to rapid setting during mixing.

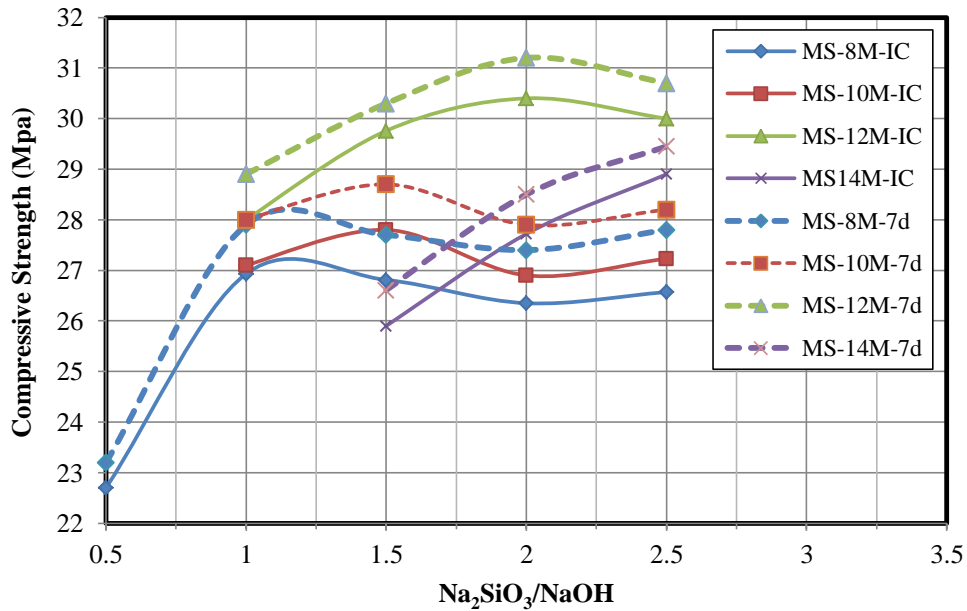


Figure 6.7 Effect of NaOH Concentration and NaOH to Na_2SiO_3 ratio on GGBFS geopolymer Compressive strength at 2 ages.

6.4.2 Splitting Tensile Strength Test

Splitting tensile test was performed on LWGM specimens after initial curing and after 7 days. Test results are shown in Table 6.8 and 6.9. The tensile strengths of geopolymer mortar after initial curing and 7 day are plotted in Figures 6.8 and 6.9. It could be concluded from these figures that tensile strength very slightly increased with the increase of age for all the mixtures. The results show that the tensile strength of mortar increased with the increase of sodium concentration and with optimum of SS/SH ratio in the mixtures of both FA and GGBFS based LWGM. This trend is similar to the trend shown by the development of compressive strength. In activator fly ash after initial curing, geopolymer mortar mixtures with (8, 10 and 12 M) and optimal SS/SH ratio of 1.0 gained 10.2%, 10.18% and 13.5% higher tensile strength than mixtures with SS/SH ratio of 2.5, while after 7 day gained 8.7% ,12.8% and 12.06%.

In activator GGBFS, the tensile strength of geopolymer mortar was relatively greater than geopolymer mortar with fly ash as a binder. As shown in Figs. 6.8 and 6.9, tensile strength increased with the increase of NaOH concentration in the mortar. After initial curing, mixtures having 12M, achieved 15% higher strength than

mixtures having 8M., it can be seen that tensile strength was enhanced with the reduction of SS/SH ratio from 2.5 to optimal values.

Table 6.8 Splitting tensile strength results of FA geopolymer mortar.

Mix name	Molarity	Na ₂ SiO ₃ to NaOH ratio	Splitting tensile strength after curing (MPa)	Splitting tensile strength after 7 day (MPa)
MF8-0.5	8	0.5	2.57	2.62
MF8-1.0		1.0	2.80	2.85
MF8-1.5		1.5	2.59	2.65
MF8-2.0		2.0	2.42	2.57
MF8-2.5		2.5	2.54	2.62
MF10-0.5	10	0.5	2.67	2.72
MF10-1.0		1.0	3.05	3.16
MF10-1.5		1.5	2.90	3.03
MF10-2.0		2.0	2.85	2.93
MF10-2.5		2.5	2.75	2.80
MF12-0.5	12	0.5	2.75	2.85
MF12-1.0		1.0	3.18	3.25
MF12-1.5		1.5	3.00	3.15
MF12-2.0		2.0	2.92	3.10
MF12-2.5		2.5	2.80	2.90
MF14-0.5	14	0.5	NA*	NA*
MF14-1.0		1.0	NA*	NA*
MF14-1.5		1.5	3.28	3.46
MF14-2.0		2.0	3.18	3.40
MF14-2.5		2.5	3.08	3.28

* NA: Not available due to rapid setting during mixing.

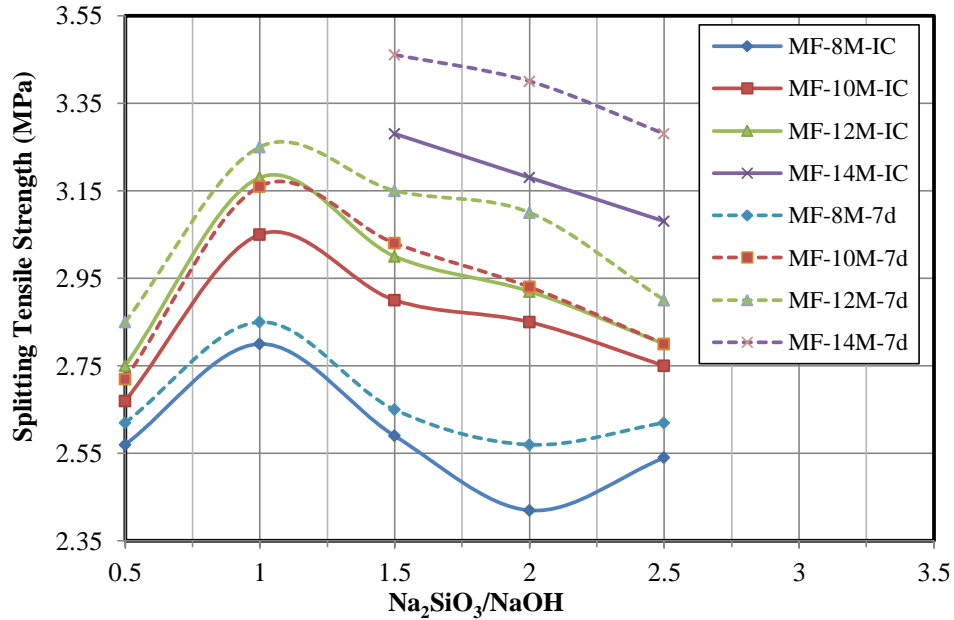


Figure 6.8 Effect of NaOH concentration and NaOH to Na_2SiO_3 ratio on FA geopolymer tensile strength.

Table 6.9 Splitting tensile strength results of GGBFS geopolymer mortar.

Mix name	Molarity	$\text{Na}_2\text{SiO}_3:\text{NaOH}$ ratio	Splitting tensile strength after curing (MPa)	Splitting tensile strength after 7 day (MPa)
MS8-0.5	8	0.5	2.70	2.90
MS8-1.0		1.0	2.87	3.05
MS8-1.5		1.5	3.41	3.48
MS8-2.0		2.0	3.30	2.90
MS8-2.5		2.5	3.20	3.43
MS10-0.5	10	0.5	NA*	NA*
MS10-1.0		1.0	2.98	3.28
MS10-1.5		1.5	3.43	3.61
MS10-2.0		2.0	3.35	3.74
MS10-2.5		2.5	3.26	3.56
MS12-0.5	12	0.5	NA*	NA*
MS12-1.0		1.0	3.25	3.28
MS12-1.5		1.5	3.59	3.74
MS12-2.0		2.0	3.71	3.61
MS12-2.5		2.5	3.48	3.56
MS14-0.5	14	0.5	NA*	NA*
MS14-1.0		1.0	NA*	NA*
MS14-1.5		1.5	2.95	2.97
MS14-2.0		2.0	3.41	3.45
MS14-2.5		2.5	3.40	3.50

* NA: Not available due to rapid setting during mixing.

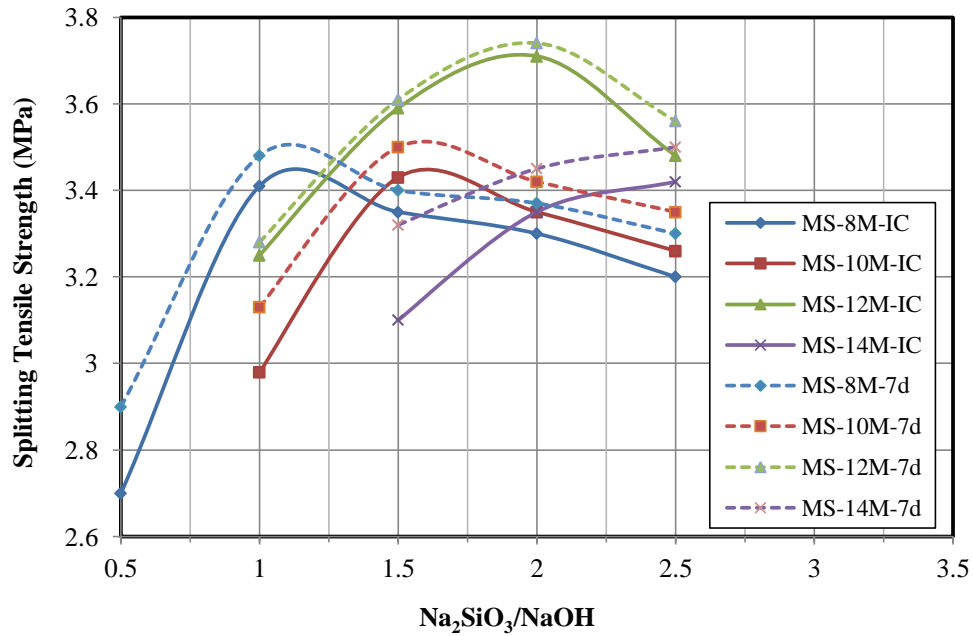


Figure 6.9 Effect of NaOH concentration and NaOH to Na_2SiO_3 ratio on GGBFS geopolymer tensile strength.

6.4.3 Sorptivity

Sorptivity test is one of the most important tests that evaluate the durability of LWGM. Table 6.10 and Figures 6.10 to 6.13 show the experimental results on water sorptivity at age 7 day drying at 2 conditions (60 °C. and 105 °C.). It was observed from above results that, the rate of water absorption through capillary absorption is decreased with increasing NaOH concentration. It decreased with increasing SS/SH ratio. It is observed that the water sorptivity is more at lower alkali content. However, the specimens with lower sorptivity yielded higher compressive strength (Thokchom, 2009) as can be observed in the current study. The water sorptivity decreased almost linearly with increasing silicate ratio. Results indicated that addition of soluble silicate has positive effect on water sorptivity. The pore structure of the geopolymer composite becomes more compact and homogeneous with increasing silicate content resulted in decreasing water sorptivity. From the discussion it can be concluded that water sorptivity of geopolymer mortar specimen is significantly affected by alkali content and silicate ratio of geopolymer mix. Addition of soluble silica has positive effect on sorptivity as pore structure becomes more dense and compact at higher dosage of soluble silicate.

Table 6.10 Water sorptivity results for the LWGMs incorporated with FA and GGBFS.

Mix name	Molarity	Na ₂ SiO ₃ to NaOH ratio	Sorptivity value of FA (mm/min ^{1/2})		Sorptivity value of GGBFS (mm/min ^{1/2})	
			Without drying at 105 °C.	drying at 105 °C	Without drying at 105°C.	drying at 105°C
M 8-0.5	8	0.5	0.052	0.167	0.0207	0.274
M 8-1.0		1.0	0.008	0.085	0.0190	0.245
M 8-1.5		1.5	0.015	0.080	0.0170	0.257
M 8-2.0		2.0	0.029	0.099	0.0159	0.239
M 8-2.5		2.5	0.020	0.110	0.0151	0.229
M 10-0.5	10	0.5	0.0413	0.130	NA*	NA*
M 10-1.0		1.0	0.006	0.047	0.0173	0.252
M 10-1.5		1.5	0.012	0.058	0.0155	0.233
M 10-2.0		2.0	0.020	0.082	0.0147	0.226
M 10-2.5		2.5	0.011	0.051	0.0143	0.210
M 12-0.5	12	0.5	0.035	0.115	NA*	NA*
M 12-1.0		1.0	0.004	0.035	0.0150	0.233
M 12-1.5		1.5	0.009	0.036	0.0140	0.225
M 12-2.0		2.0	0.016	0.051	0.0131	0.223
M 12-2.5		2.5	0.004	0.068	0.0093	0.196
M 14-0.5	14	0.5	NA*	NA*	NA*	NA*
M 14-1.0		1.0	NA*	NA*	NA*	NA*
M 14-1.5		1.5	0.0027	0.033	0.0120	0.197
M 14-2.0		2.0	0.006	0.020	0.0113	0.210
M 14-2.5		2.5	0	0.009	0.0085	0.205

* NA: Not available due to rapid setting during mixing.

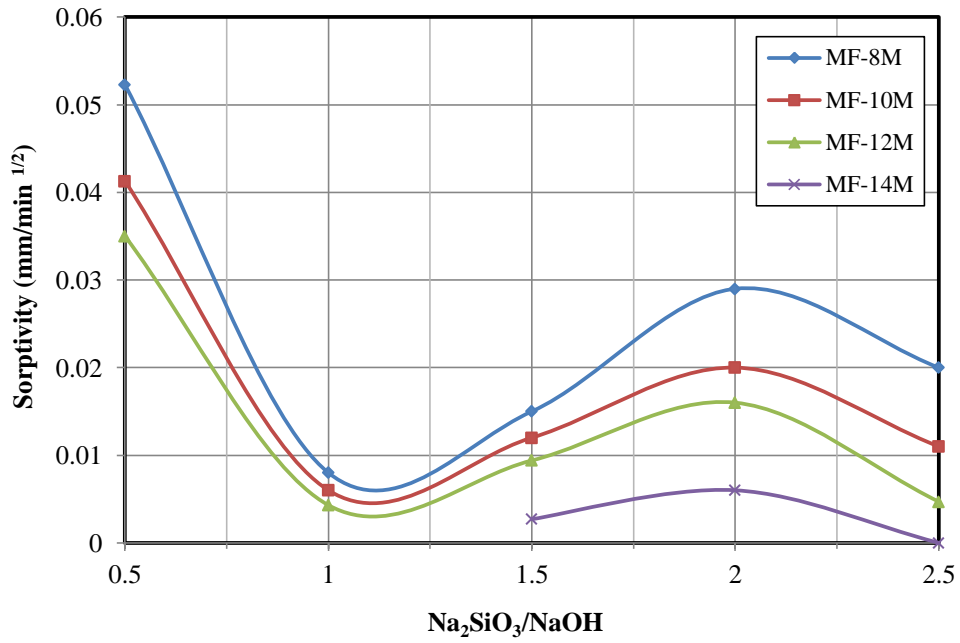


Figure 6.10 Sorptivity for FA based LWGMs without drying at 105 °C.

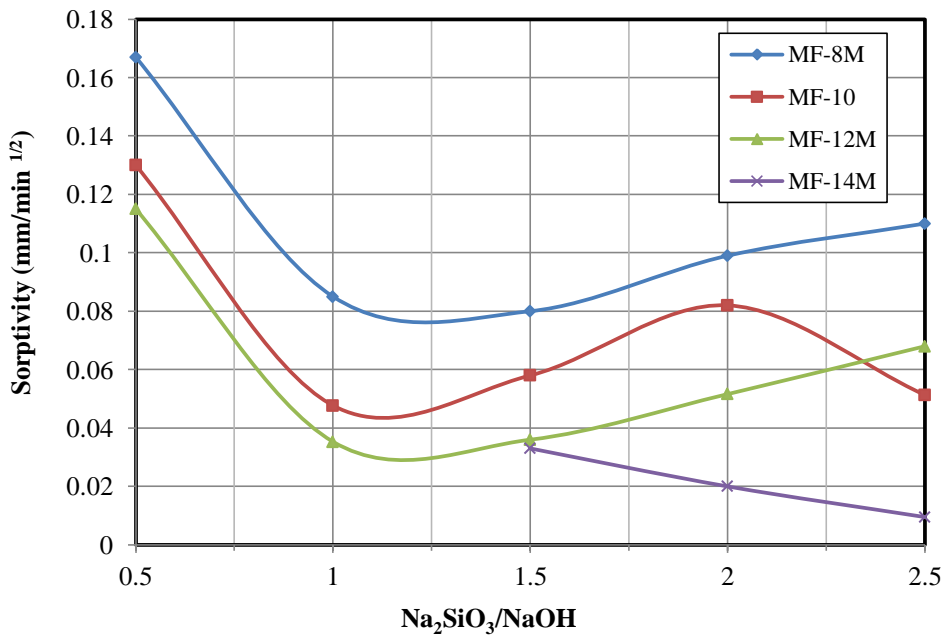


Figure 6.11 Sorptivity for FA based LWGMs drying at 105 °C.

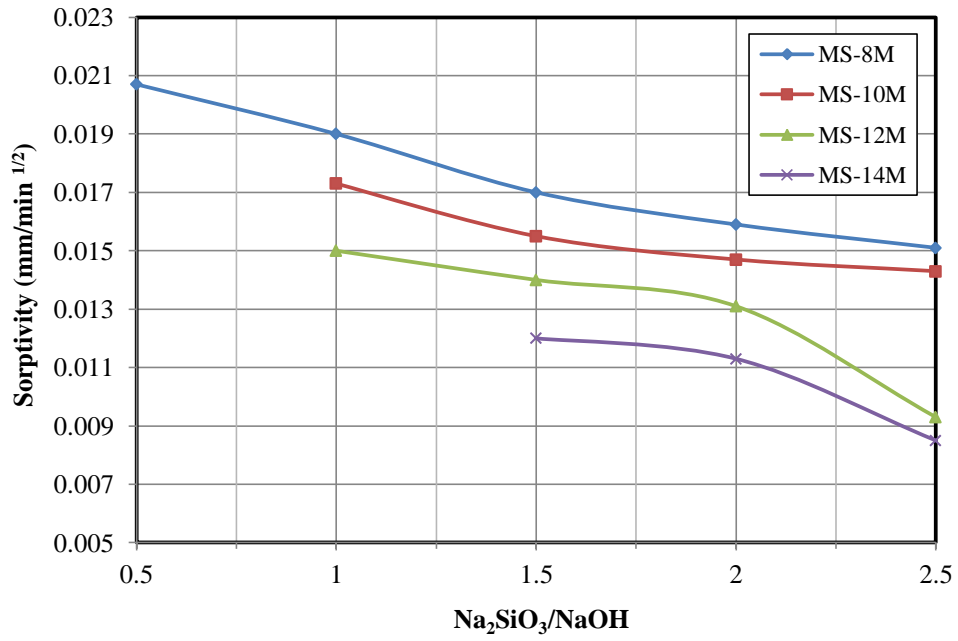


Figure 6.12 Sorptivity for GGBFS based LWGMs without drying at 105 °C.

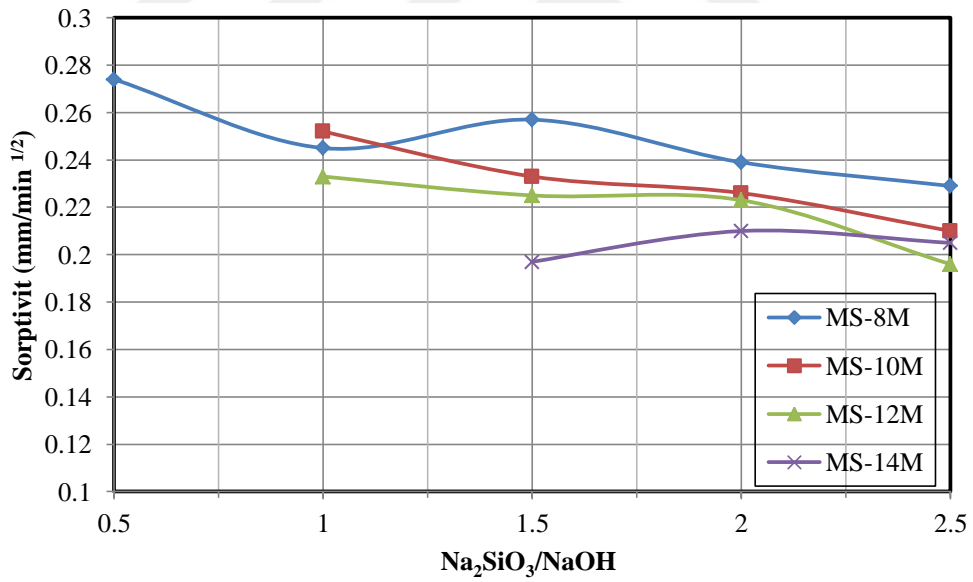


Figure 6.13 Sorptivity for GGBFS based LWGMs drying at 105 °C.

6.4.4 Water Absorption

The measurement of water absorption was taken by calculating the difference in specimen weight under oven dried and fully saturated conditions. The specimen of water absorption was cube (50×50×50) mm, the water absorption tested conducted at age 7 day.

Table 6.11 and Figures (6.14& 6.15) presents water absorption of the FA and GGBFS based geopolymer mortar for change in NaOH Concentration and Na₂SiO₃ to NaOH ratio.

It has been observed from the Table 6.11, that the geopolymer mortar specimen having NaOH Concentration of 8M and Na₂SiO₃ to NaOH ratio of 0.5, showed maximum water absorption of 17.54% and 12.991% for FA and GGBFS geopolymer mortar. Whereas, specimen having NaOH concentration of 14 M revealed minimum water absorption of 12.8% and 11.149%. It is also observed that water absorption decreased with increasing molarity in the geopolymer mix. At lower molarity the water absorption was more indicating higher void content in the geopolymer specimen. Moreover, the geopolymerization reaction is not complete at lower alkali content and large number of unreacted fly ash particles also present in the geopolymer matrix. The fly ash particles content nano pores and adsorb additional water. At higher alkali content the water absorption is less due to lower void spaces by more quantity of fly ash particles dissolved forming higher quantity of gel which reduces void space in the matrix resulted in decreasing water absorption.

In addition to that, almost the absorption has relationship with optimal Na₂SiO₃ to NaOH ratio and that is a good indication to the continuous geopolymerization process. Optimal silica content involved formation of higher quantity of aluminosilicate gel and provides very good interparticle bonding.

It could be concluded that the water absorption of geopolymer lightweight mortar specimens are significantly affected by source material of geopolymer mix. The water absorption value of GGBFS geopolymer mortar very slightly decreased with increasing molarity and Na₂SiO₃ to NaOH ratio as shown in Table 6.11 and was significantly less than FA geopolymer mortar, that may be because the lower porosity of GGBFS than FA geopolymer mortar.

On the other hand, the percentage of water absorption for all samples was slightly higher. The physical properties of lightweight fine aggregate (LWFA) itself and a lot of

embedded network capillary in the particle are the main reason behind the increasing magnitudes of water absorption. The irregularity in shape and the highly porous surface contributed to the increment of water absorption percentage.

Table 6.11 Water absorption results for the LWGMs incorporated with FA and GGBFS.

Mix name	Molarity	Na ₂ SiO ₃ to NaOH ratio	Water absorption value of FA (%)	Water absorption value of GGBFS (%)
M 8-0.5	8	0.5	17.54	12.99
M 8-1.0		1.0	16.34	12.34
M 8-1.5		1.5	15.60	12.00
M 8-2.0		2.0	15.38	11.87
M 8-2.5		2.5	14.95	11.86
M 10-0.5	10	0.5	16.90	NA*
M 10-1.0		1.0	14.90	12.12
M 10-1.5		1.5	15.30	11.63
M 10-2.0		2.0	15.00	11.81
M 10-2.5		2.5	14.93	11.75
M 12-0.5	12	0.5	15.80	NA*
M 12-1.0		1.0	13.40	12.00
M 12-1.5		1.5	15.05	11.55
M 12-2.0		2.0	14.80	11.40
M 12-2.5		2.5	14.60	11.59
M 14-0.5	14	0.5	NA*	NA*
M 14-1.0		1.0	NA*	NA*
M 14-1.5		1.5	12.80	11.40
M 14-2.0		2.0	13.50	11.28
M 14-2.5		2.5	13.73	11.15

* NA: Not available due to rapid setting during mixing.

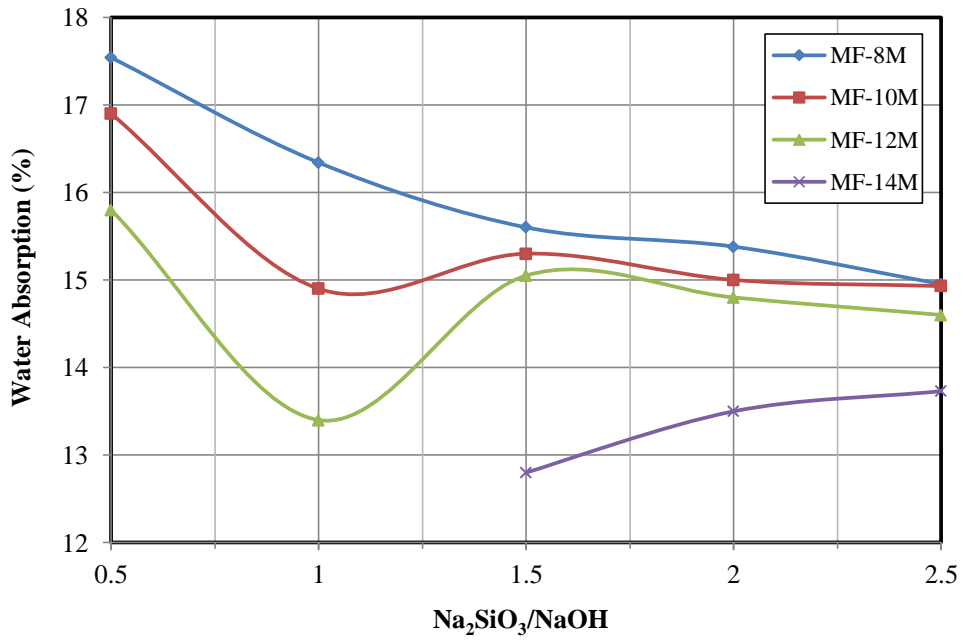


Figure 6.14 Water absorption results for FA based LWGMs.

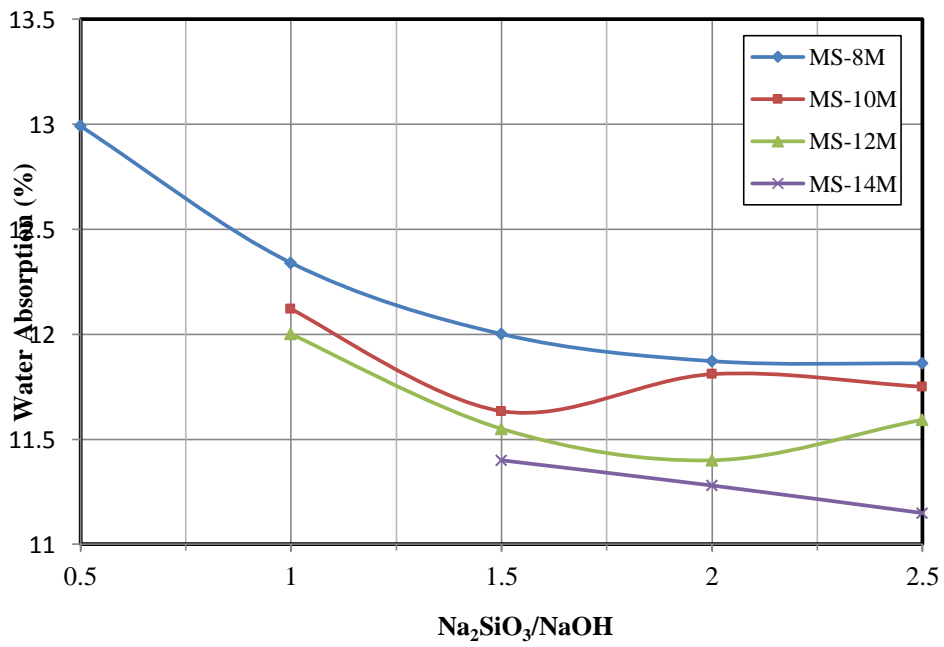


Figure 6.15 Water absorption results for GGBFS based LWGMs.

6.5 Optimization Study

The response surface method (RSM) (Whitcomb and Anderson, 2004) is adopted in this study to optimize the parameters considered in the experimental analysis presented. RSM has gained immense popularity not only because of its ease of use but also it provides reliable results in the case of having amount of data less than required by the alternative optimisation techniques. The optimisation analysis presented in this study has been undertaken using the three independent variables namingly the molarity of NaOH, the ratio of $\text{Na}_2\text{SiO}_3/\text{NaOH}$ and the incorporated base materials (i.e. FA and GGBFS). Additionally, in this process the six dependent variables are employed, specifically the numerical results obtained from the presented experimental study (i.e. fresh unit weight, water absorption, sorptivity, flow diameter, compressive strength and splitting tensile strength). RSM provides the graphs to visualize the effects of the dependent variables on the responses and it involves the statistical process to select the proper model fitting the data that includes the accuracy check for the chosen model. This process follows the numerical optimisation procedure of RSM involves defining the desirability function (d_i) for each response (e.g. [Whitcomb PJ, Anderson M.J., Pradeep G., Myers R.H. et al., Algin H.M.]). The objective functions are then optimised numerically using the regression models link on the factors and responses. The desirability function (d_i) varies between zero and one ($0 \leq d_i \leq 1$) which implies that the function becomes zero if the considered dependent or independent variables provide the desirability that falls outside the range. The desirability is defined by the equations (Eqs. 5.1 and 5.2 as explained in section 5.3) indicate as the individual response to be maximised and minimised, respectively.

Desirability as an objective function ranges from zero to one indicating the achievement of the defined goals (i.e. one indicates that the defined goals are fully achieved) and it is aimed to be maximized in the process of optimization. If a response is required to be set to have a higher importance, the weight of a response can be altered regarding the characteristics of a goal. This optimisation procedure defined by Myers and Montgomery (Myers R.H. et al., 2009) is utilised in the presented study to identify the optimum values for the molar concentration of sodium hydroxide (NaOH) and the ratio of sodium silicate to sodium hydroxide

($\text{Na}_2\text{SiO}_3/\text{NaOH}$) in terms of two types of base materials namely FA and GGBFS used in the light-weight geopolymer mortar mixes.

The molar concentration of sodium hydroxide (NaOH) and the ratio of sodium silicate to sodium hydroxide ($\text{Na}_2\text{SiO}_3/\text{NaOH}$) are optimized simultaneously in the case of minimizing the responses of fresh unit weight, water absorption, sorptivity in the meanwhile maximizing the responses of flow diameter, compressive strength and splitting tensile strength. All of the objective functions and the defined constraints for this optimisation are given in Table 6.12. Figures 6.16 and 6.17 show the relationship between the parameters considered in the multi objective optimization analysis conducted in this research.

Table 6.12 The goals and the constraints used for each variable considered in the multi objective optimization analysis.

Name of factors and response	Goal	Lower limit	Upper limit
NaOH molarity	in range	8.00	14.00
$\text{Na}_2\text{SiO}_3/\text{NaOH}$	In range	0.50	2.50
Base Material	equal to	FA or GGBFS	
Flow diameter (mm)	maximize	100.00	225.00
Fresh unit weight (kg/m^3)	minimize	1696.37	1833.61
Water absorption (%)	minimize	11.149	17.54
Sorptivity ($\text{mm}/\text{min}^{1/2}$)	minimize	0.0095	0.274
Compressive strength (MPa)	maximize	11.51	30.40
Splitting tensile strength (MPa)	maximize	2.42	3.71

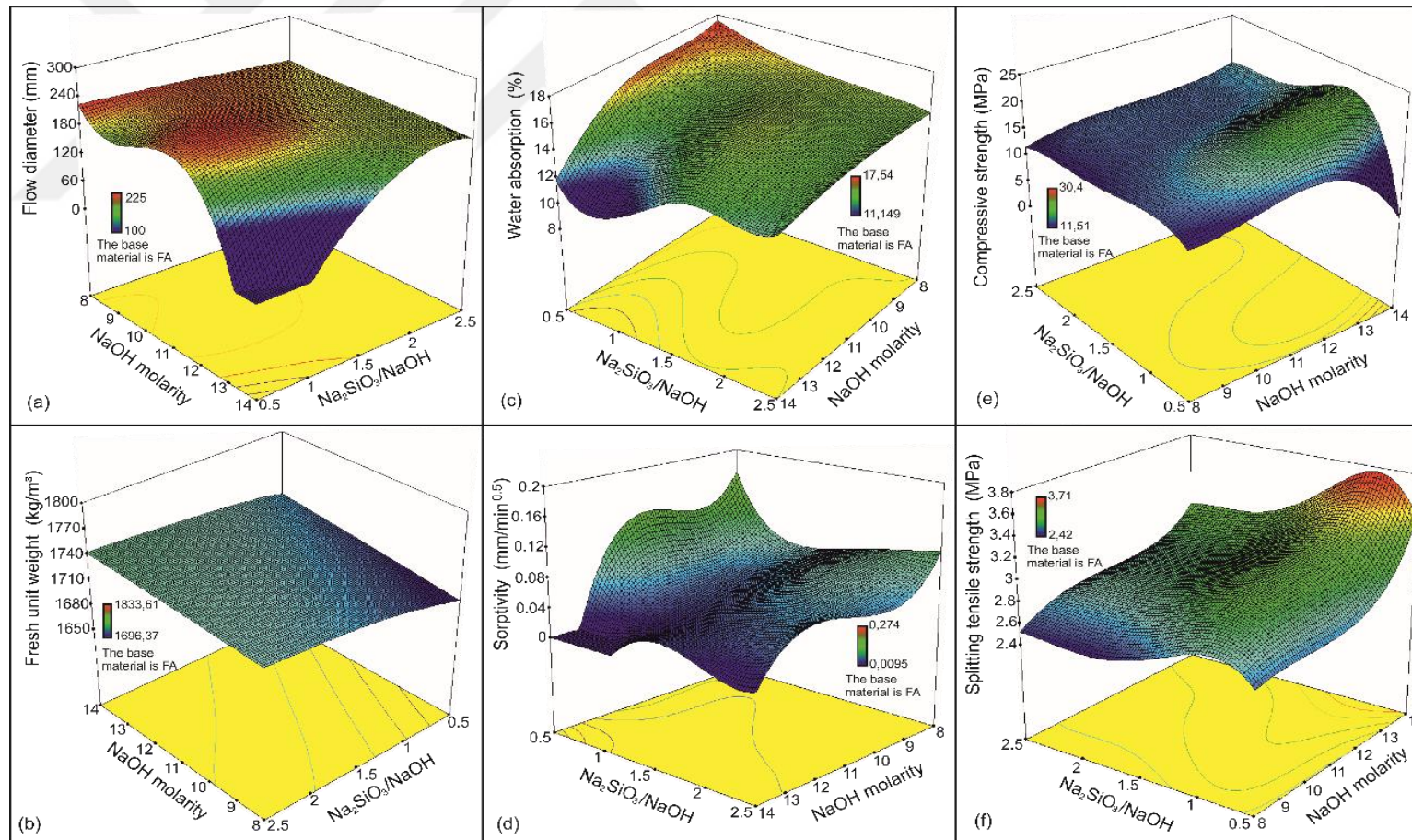


Figure 6.16 The influence of NaOH molarity and the ratio of $\text{Na}_2\text{SiO}_3/\text{NaOH}$ on the responses of (a) flow diameter, (b) fresh unit weight, (c) water absorption, (d) sorptivity, (e) compressive strength, (f) splitting tensile strength for FA based light-weight geopolymer mortar.

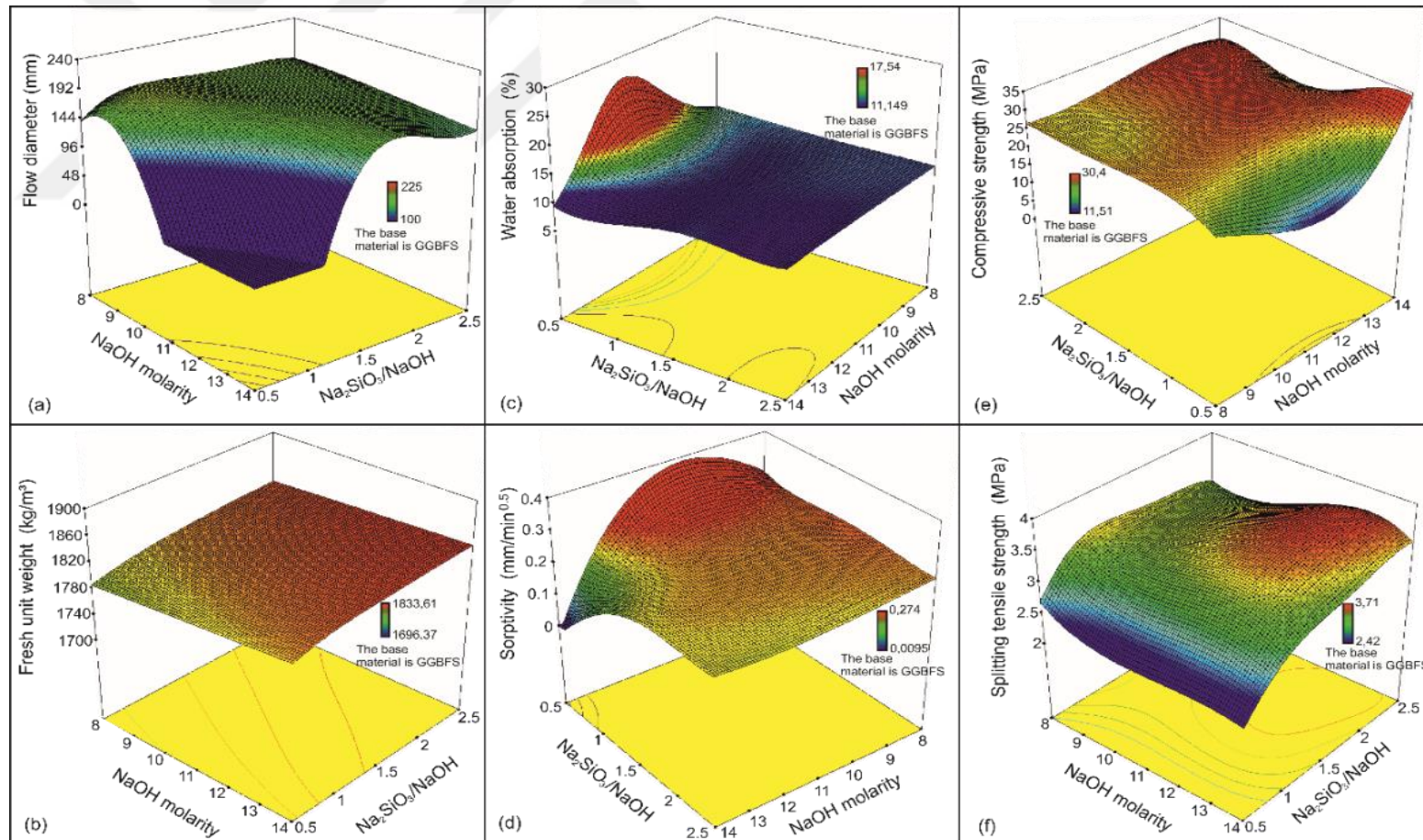


Figure 6.17 The influence of NaOH molarity and the ratio of $\text{Na}_2\text{SiO}_3/\text{NaOH}$ on the responses of (a) flow diameter, (b) fresh unit weight, (c) water absorption, (d) sorptivity, (e) compressive strength, (f) splitting tensile strength for GGBFS based light-weight geopolymer mortar.

Figures 6.18 and 6.19 demonstrate the variation of the desirability function obtained from the presented optimisation analysis for the utilisation of FA or GGBFS as a base material in the light-weight geopolymer mortar mixes, respectively. The obtained optimum solutions given in Table 6.13 satisfy the defined upper and lower limits in Table 6.12, and provide the desirability values of 0.703 and 0.440 for the base materials of FA and GGBFS, respectively. Table 6.13 demonstrates that the optimum results with the highest desirability value is obtained from the utilisation of FA and in this optimum solution the values for the molarity of NaOH and the ratio of $\text{Na}_2\text{SiO}_3/\text{NaOH}$ are of 12.280 and 0.944, respectively.

Table 6.13 Optimization results of FA and GGBFS light-weight geopolymer mortar.

Factors and response	FA	GGBFS
NaOH molarity	12.280	10.797
$\text{Na}_2\text{SiO}_3/\text{NaOH}$ ratio	0.944	1.388
Flow diameter (mm)	193.949	172.495
Fresh unit weight (kg/m ³)	1725.214	1817.942
Water absorption (%)	12.951	11.576
Sorptivity (mm/min ^{1/2})	0.033	0.230
Compressive strength (MPa)	21.126	28.920
Splitting tensile strength (MPa)	3.213	3.409
Desirability	0.703	0.440

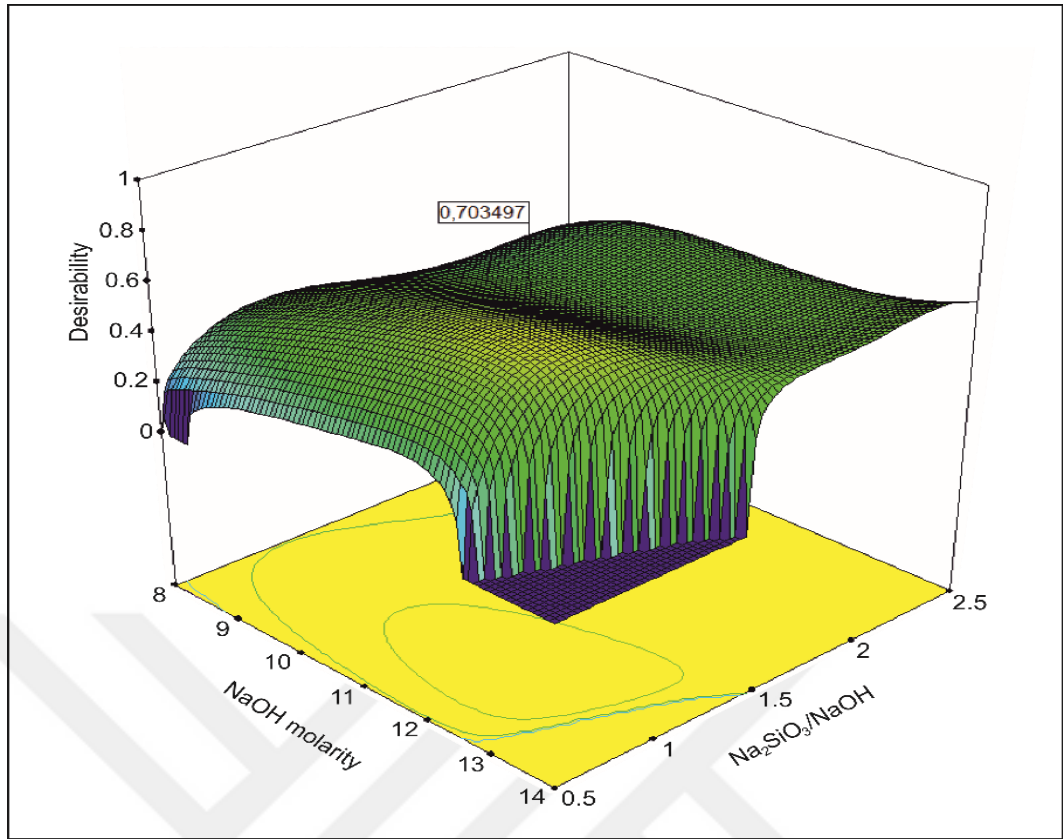


Figure 6.18 Variation of desirability function in terms of the molarity of NaOH and the ratio of Na₂SiO₃/ NaOH for the case of FA utilisation as a base material.

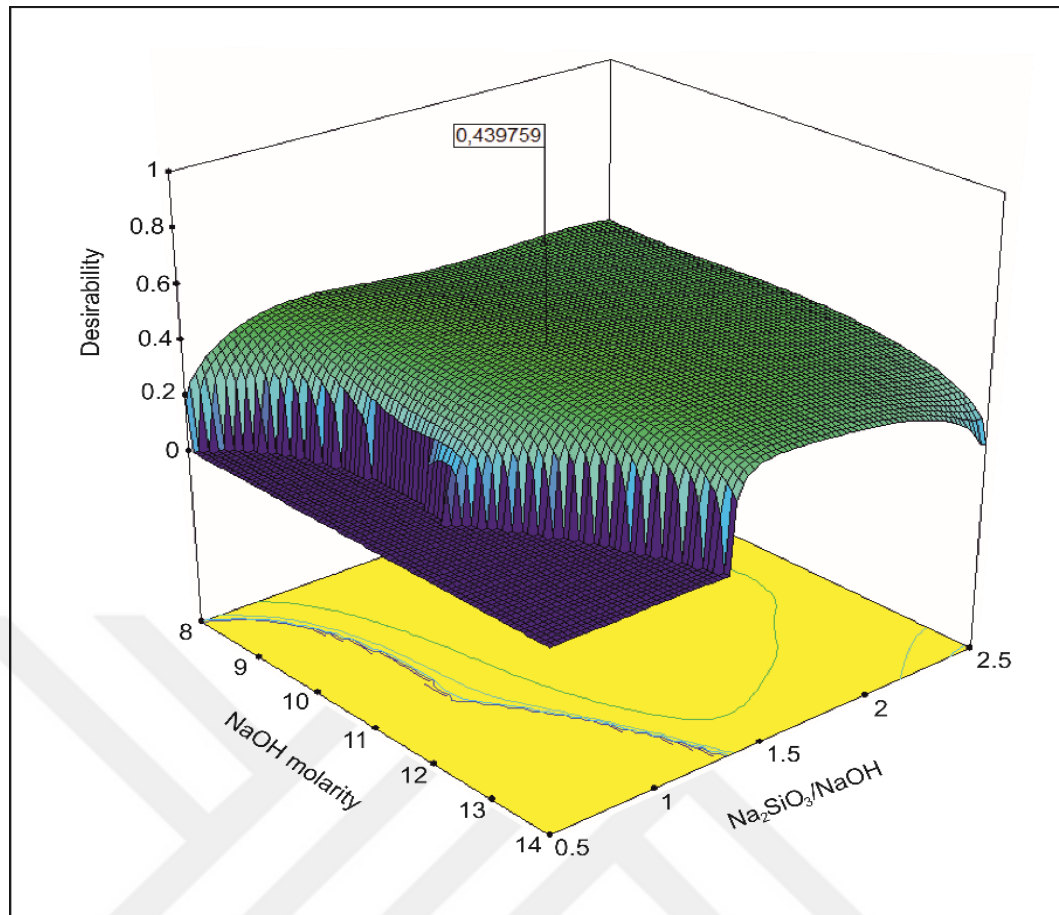


Figure 6.19 Variation of desirability function in terms of the molarity of NaOH and the ratio of $\text{Na}_2\text{SiO}_3/\text{NaOH}$ for the case of GGBFS utilisation as a base material.

Figures 6.20 and 6.21 demonstrate the variation of the considered factors in terms of the desirability and the responses of flow diameter, fresh unit weight, water absorption, sorptivity, compressive strength, and splitting tensile strength for the light-weight geopolymer mortars incorporated with FA and GGBFS, respectively. Figure 6.20 shows that the increase in the molarity increases the desirability value and the dramatic reduction is observed especially beyond the molarity of approximately 12M, this increase corresponds a slight increase in the compressive strength and splitting tensile strength for the light-weight geopolymer mortars incorporated with FA. Figure 6.20 shows that generally the compressive strength and splitting tensile strength has an increasing tendency in terms of the increasing SS/SH ratio up to 1 and decreasing beyond this ratio, the desirability is increased dramatically up to the SS/SH ratio to 1. Figure 6.21 demonstrates the similar behaviour of the factors on the desirability for the light-weight geopolymer mortar

incorporated with GGBFS. Figure 4 shows that a slight increase in the compressive strength and splitting tensile strength is observed up to the NaOH concentration of approximately 11M and $\text{Na}_2\text{SiO}_3/\text{NaOH}$ ratio approximately 1.5 and beyond this value the increase in the compressive strength and splitting tensile strength is negligible. The fresh unit weight is gradually increased up to the molarity and SS/SH ratio increasing. Figure 6.21 shows that the sorptivity is almost not affected by the NaOH concentration and the $\text{Na}_2\text{SiO}_3/\text{NaOH}$ ratio. The desirability is increased dramatically up to the SS/SH ratio to 1.5



Design-Expert® Software
 Factor Coding: Actual
 All Responses

Actual Factors
 A: NaOH molarity = 12.1
 B: Na₂SiO₃/NaOH = 0.9
 C: Base material = FA

X2: Desirability = 0.7034
 X2: Flow diameter (mm)
 X2: Fresh unit weight (kg/m³)
 X2: Water absorption (%)
 X2: Sorptivity (mm²/min)
 X2: Compressive strength (MPa)
 X2: Splitting tensile strength (MPa)

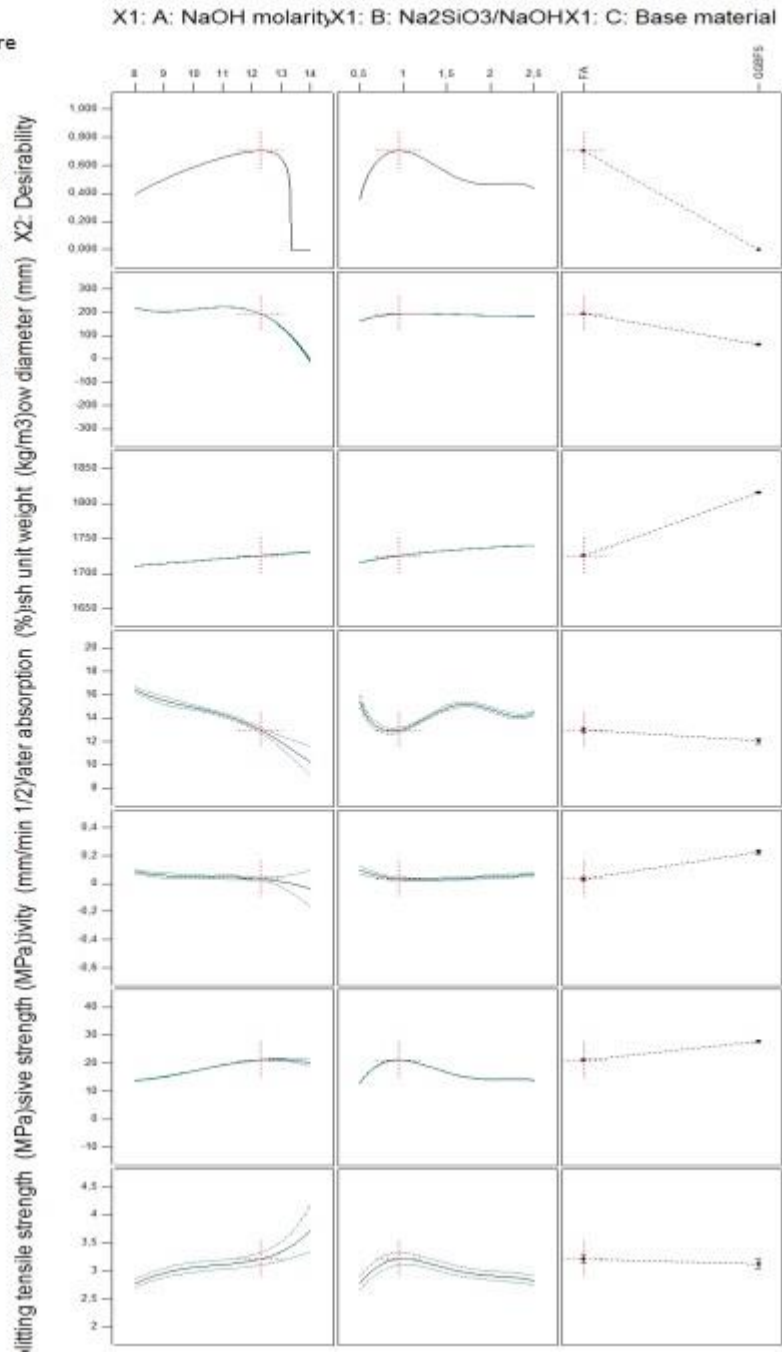


Figure 6.20 The variation of the factors in terms of the desirability and the responses for the light-weight geopolymer mortars incorporated with FA.

Design-Expert® Software
 Factor Coding: Actual
 All Responses

Actual Factors
 A: NaOH molarity = 10.1
 B: Na₂SiO₃/NaOH = 1.1
 C: Base material = GGE

X2: Desirability = 0,439;
 X2: Flow diameter (mm)
 X2: Fresh unit weight (kg/m³)
 X2: Water absorption (%)
 X2: Sorptivity (mm²/min)
 X2: Compressive strength (MPa)
 X2: Splitting tensile strength (MPa)

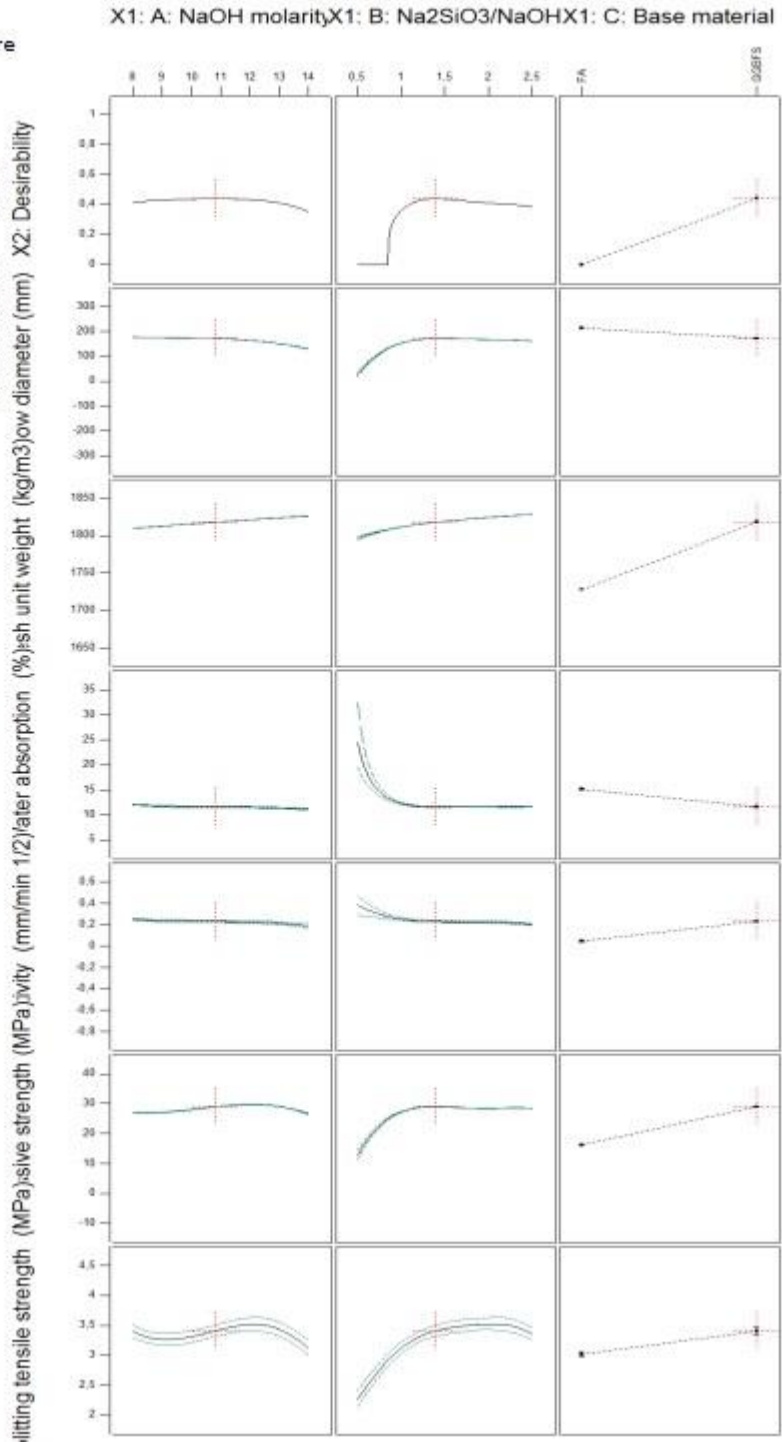


Figure 6.21 The variation of the factors in terms of the desirability and the responses for the light-weight geopolymer mortars incorporated with GGBFS.

CHAPTER 7

STEP-WISE REGRESSION AND GENETIC MODELING

7.1 General

In this chapter, the data from the experimental work conducted in this study are used to introduce modeling formulas for the compressive strength of geopolymer mortar. Two methods are used to generate these formulas. The first is the simplified linear step-wise regression, while the second method is the genetic expression programming. Step-wise is a regression tool that uses the impact of each factor to evaluate its effect on the equation. This impact is calculated based on the probability effect based on the F-distribution and the null-hypothesis. The default value of probability that refers to the significance of each factor is 0.05. Thus, the software calculates the probability of each of the independent variables and includes only those with probability values less than 0.05. Based on the included independent variables, simplified linear regression equation is introduced. The genetic programming on the other hand, is much more sophisticated method that uses the principles of gene evolution. This method will be discussed in more details in section 7.5. The modeling is separated for each type of binder. Thus, two sets of formulas are obtained from each modeling, one for the GGBFS-based geopolymer, while the second is for the fly ash-based geopolymer.

7.2 Step-Wise Regression Relationships of Compressive Strength vs. Binder and Temperature for Various Curing Periods

In this section, the compressive strength is correlated with both of the binder content and the curing temperature for different curing periods. Figures 7.1 to 7.12 show the conducted linear step-wise regressions for curing periods of 2, 6, 8, 24, 48, and 72 hours for both GGBFS and fly ash binders.

7.2.1 GGBFS-Based Geopolymer Mortar

Figures 7.1 through 7.6 show the correlations of the compressive strength of GGBFS geopolymer with binder content and curing temperature for different curing periods. In the formulas shown in Figures 7.1 through 7.6, the binder contents vary from 650 kg/m³ to 1250 kg/m³, with steps of 100 kg/m³. On the other hand, the included curing temperatures were 60, 80, 100, and 120 °C. As shown in the figures, although the regression is linear, the determination coefficients were good for all curing periods. The determination coefficients (R²) for curing periods of 2, 6, 8, 24, 48, and 72 hours were approximately 0.88, 0.72, 0.68, 0.79, 0.88, and 0.8, respectively.

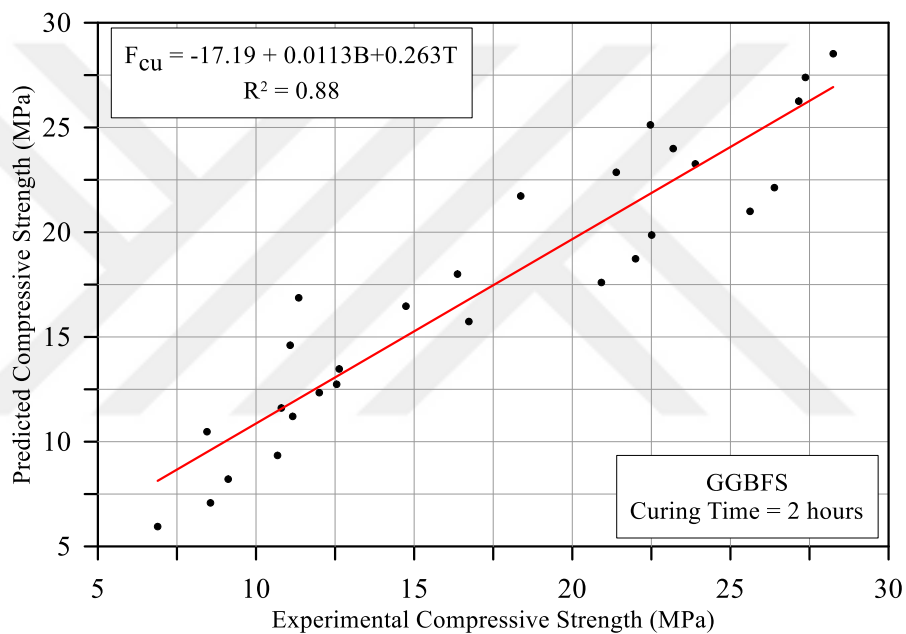


Figure 7.1 Step-wise regression model for compressive strength of GGBFS based LWGMs exposed to 2 hrs of curing time.

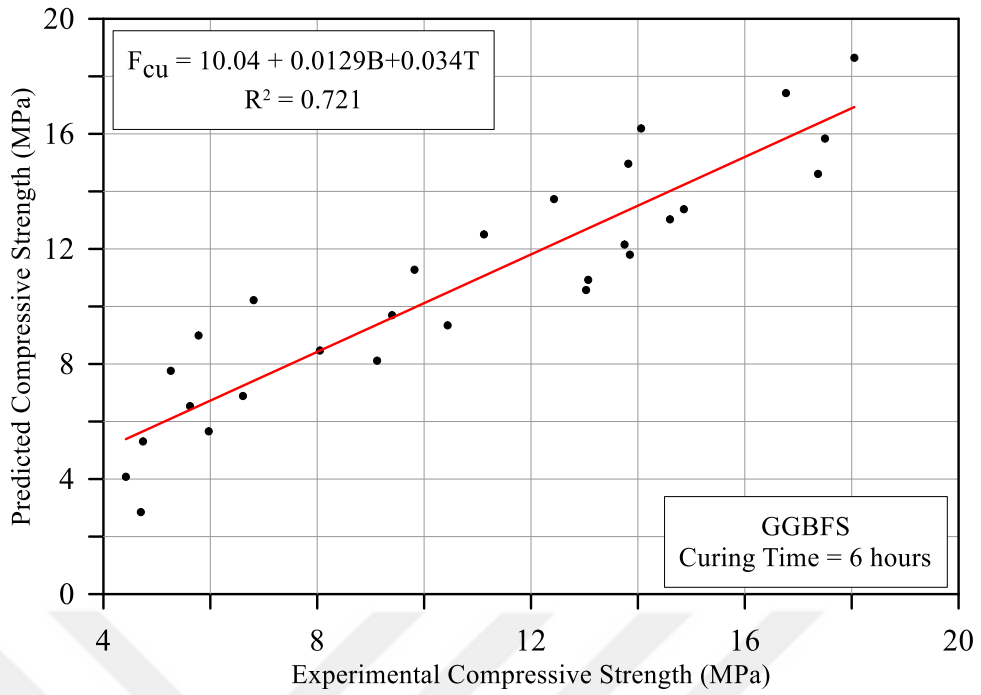


Figure 7.2 Step-wise regression model for compressive strength of GGBFS based LWGMs exposed to 6 hrs of curing time.

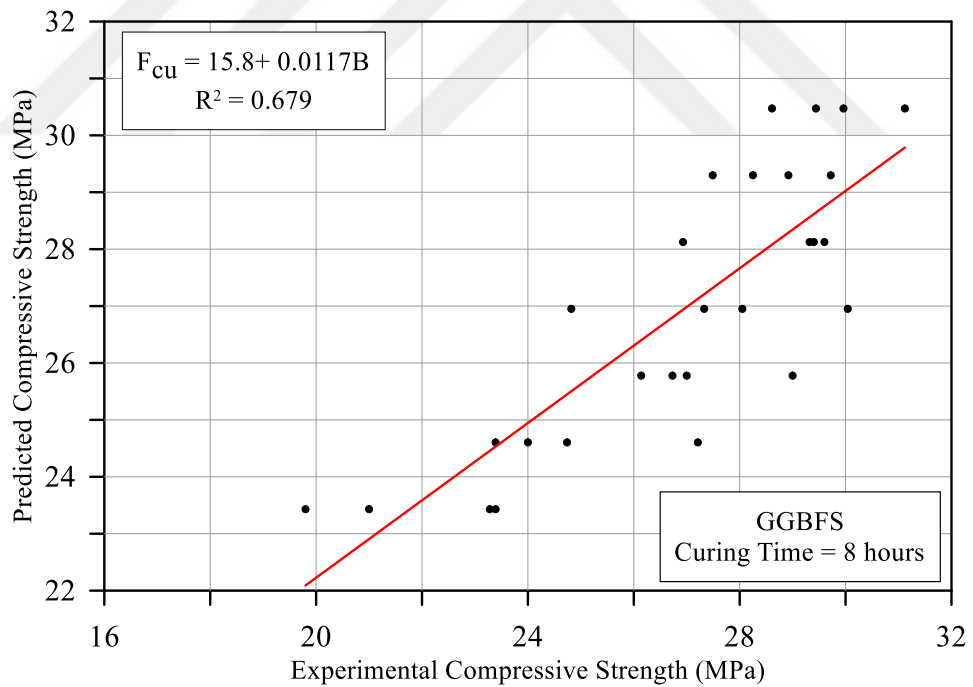


Figure 7.3 Step-wise regression model for compressive strength of GGBFS based LWGMs exposed to 8 hrs of curing time.

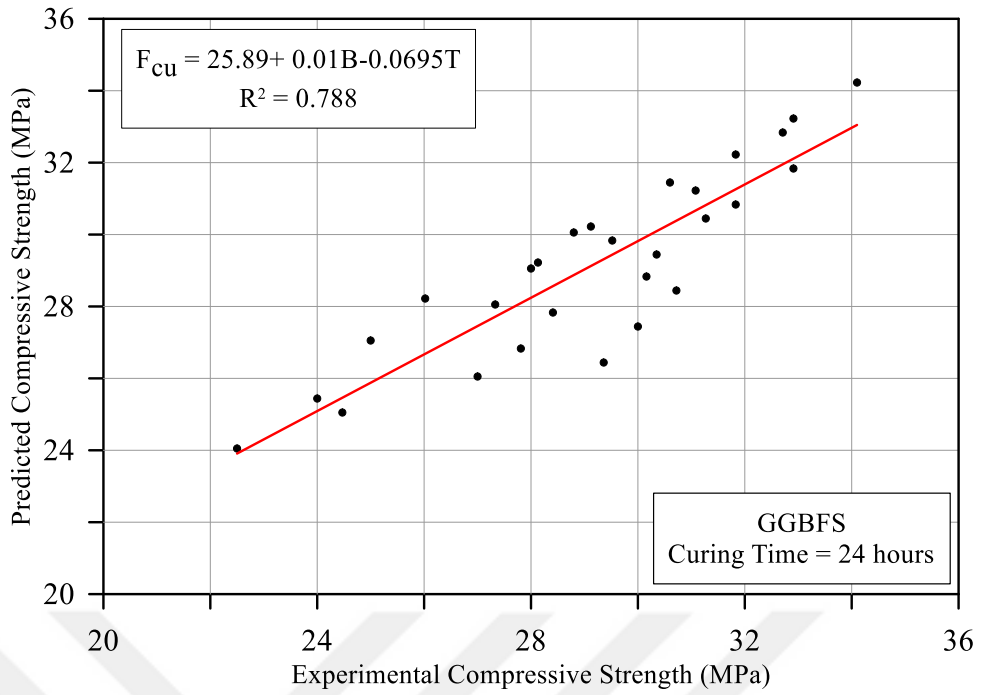


Figure 7.4 Step-wise regression model for compressive strength of GGBFS based LWGMs exposed to 24 hrs of curing time.

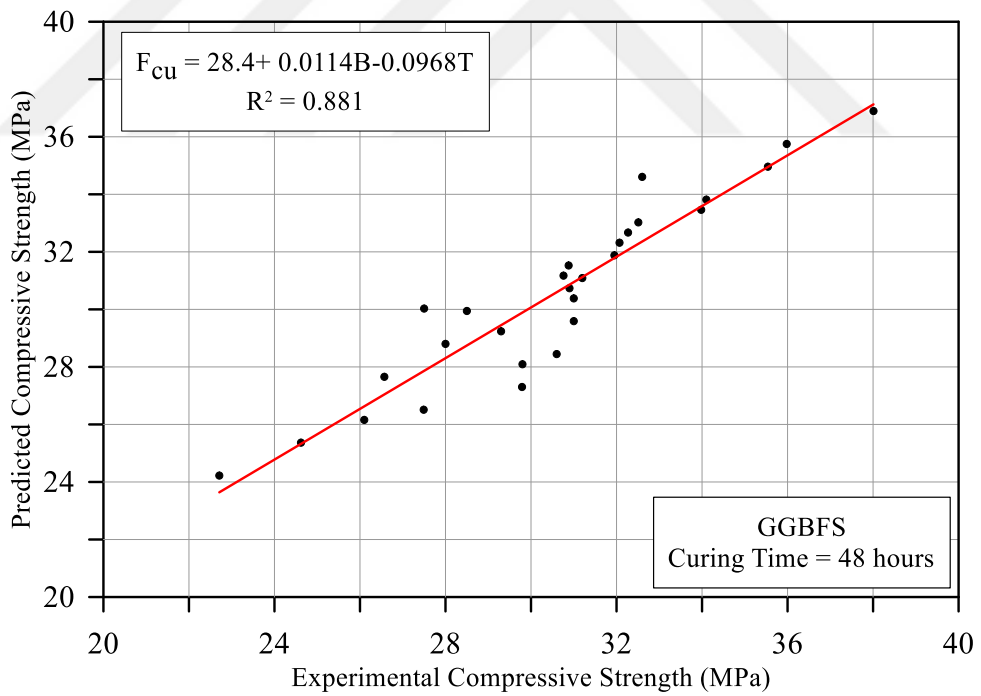


Figure 7.5 Step-wise regression model for compressive strength of GGBFS based LWGMs exposed to 48 hrs of curing time.

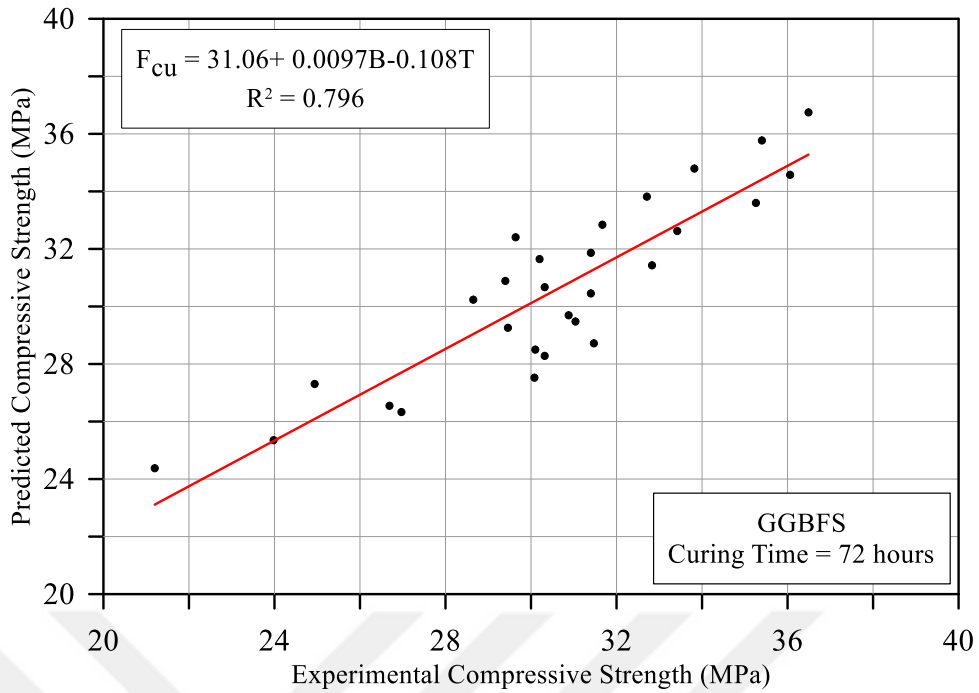


Figure 7.6 Step-wise regression model for compressive strength of GGBFS based LWGMs exposed to 72 hrs of curing time.

7.2.2 Fly Ash-Based Geopolymer Mortar

The correlations between predicted and experimental compressive strength of fly ash-based LWGMs are shown in Figures 7.7 through 7.12 for curing periods of 2, 6, 8, 24, 48, and 72 hours. It is clear that these relations have better determination coefficients than those of GGBFS-based geopolymer. The determination coefficients for curing periods of 2, 6, 8, 24, 48, and 72 hours range from approximately 0.78 to approximately 0.94, while those of GGBFS were in the range of 0.68 to 0.88.

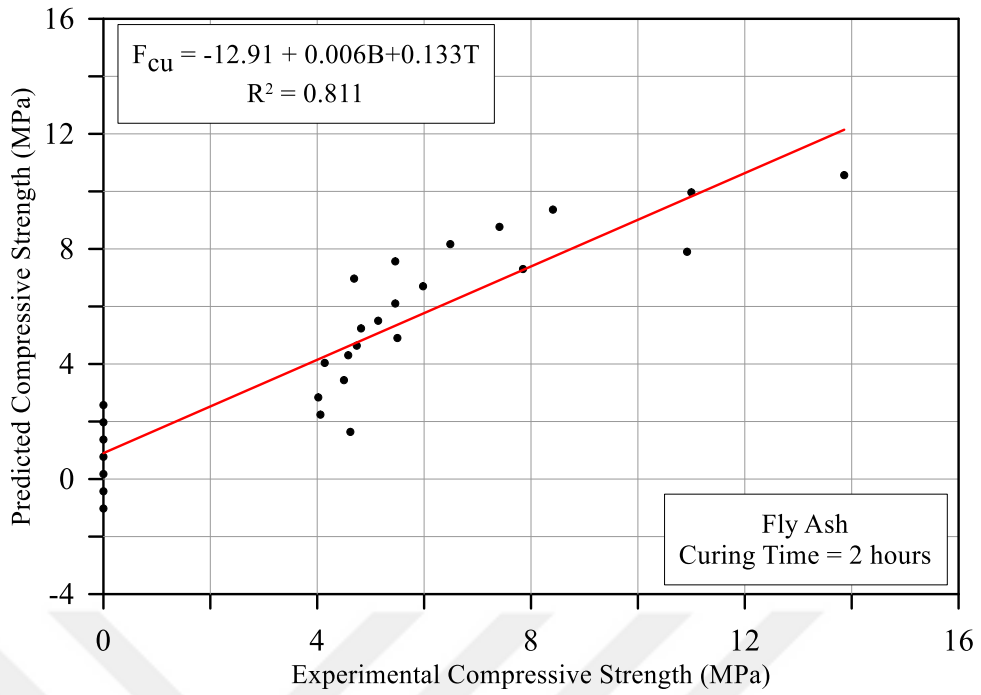


Figure 7.7 Step-wise regression model for compressive strength of FA based LWGMs exposed to 2 hrs of curing time.

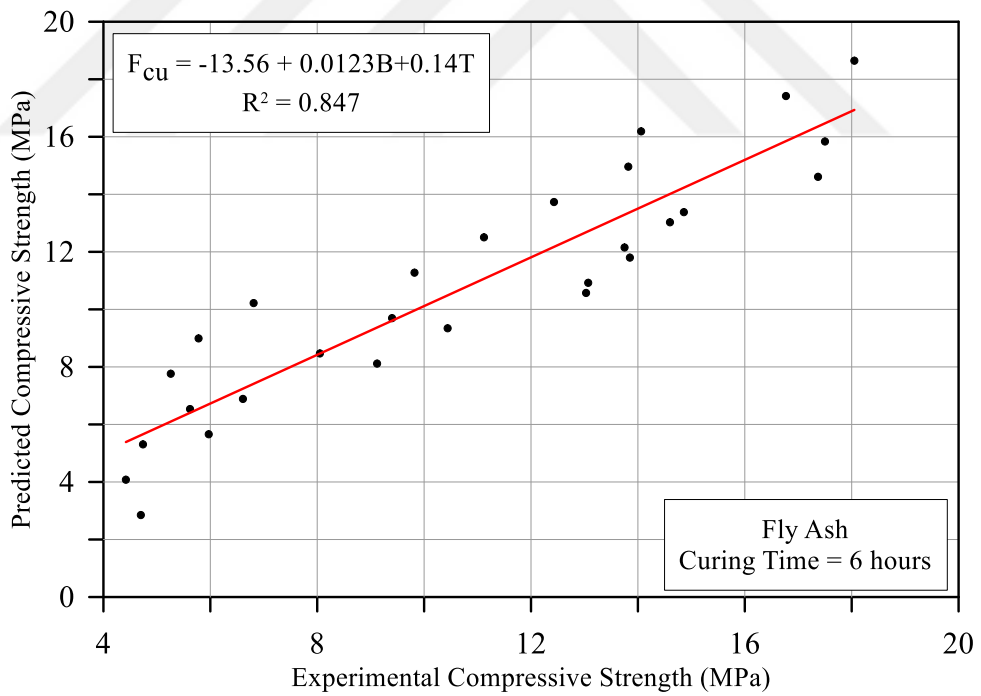


Figure 7.8 Step-wise regression model for compressive strength of FA based LWGMs exposed to 6 hrs of curing time.

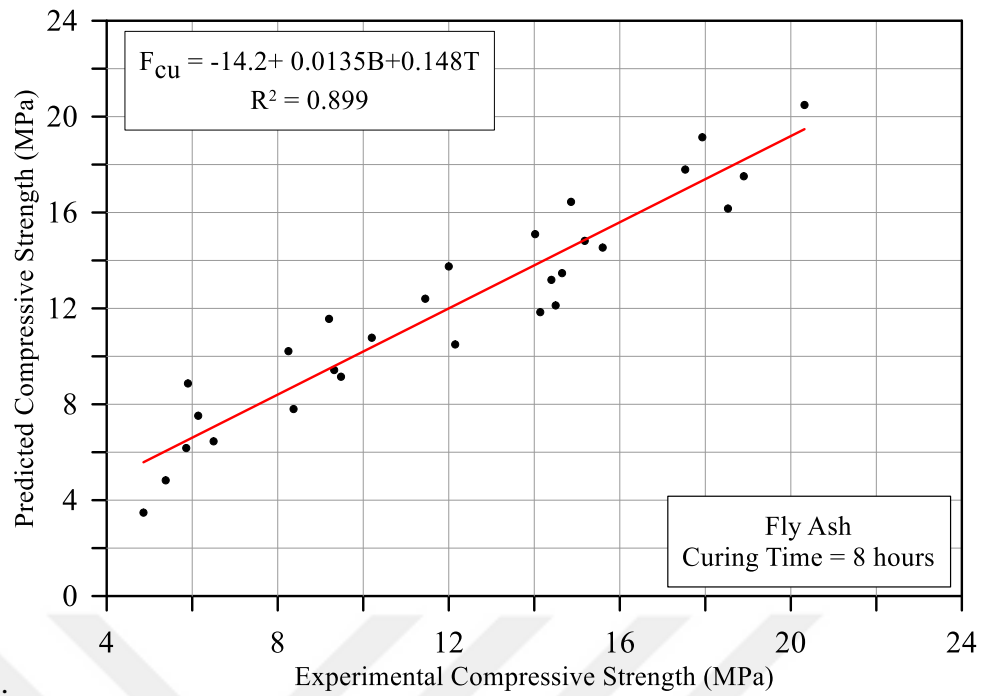


Figure 7.9 Step-wise regression model for compressive strength of FA based LWGMs exposed to 8 hrs of curing time.

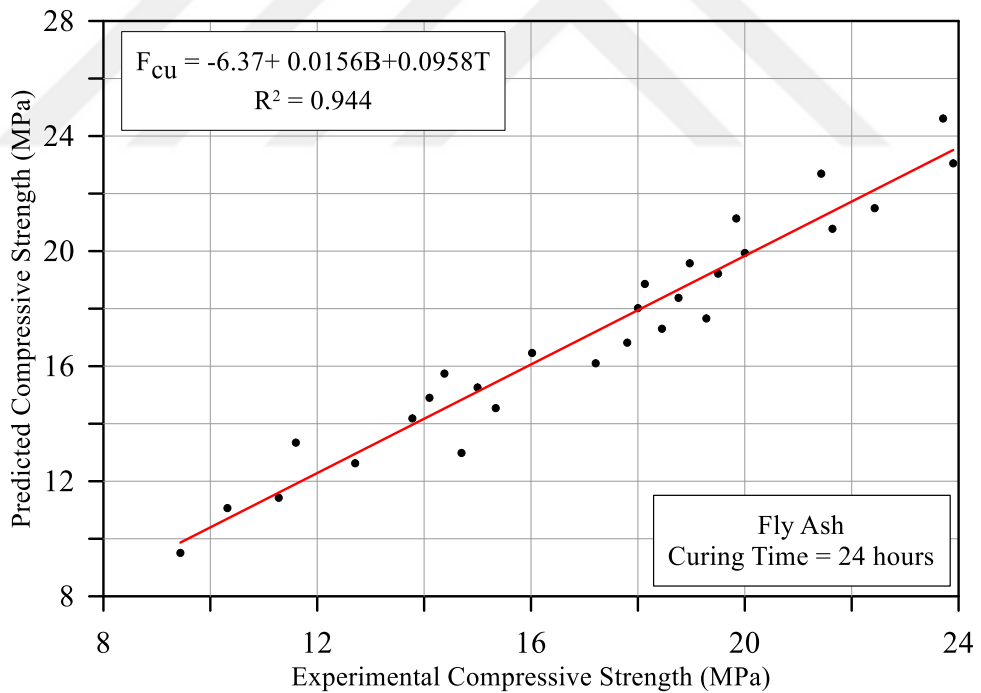


Figure 7.10 Step-wise regression model for compressive strength of FA based LWGMs exposed to 24 hrs of curing time.

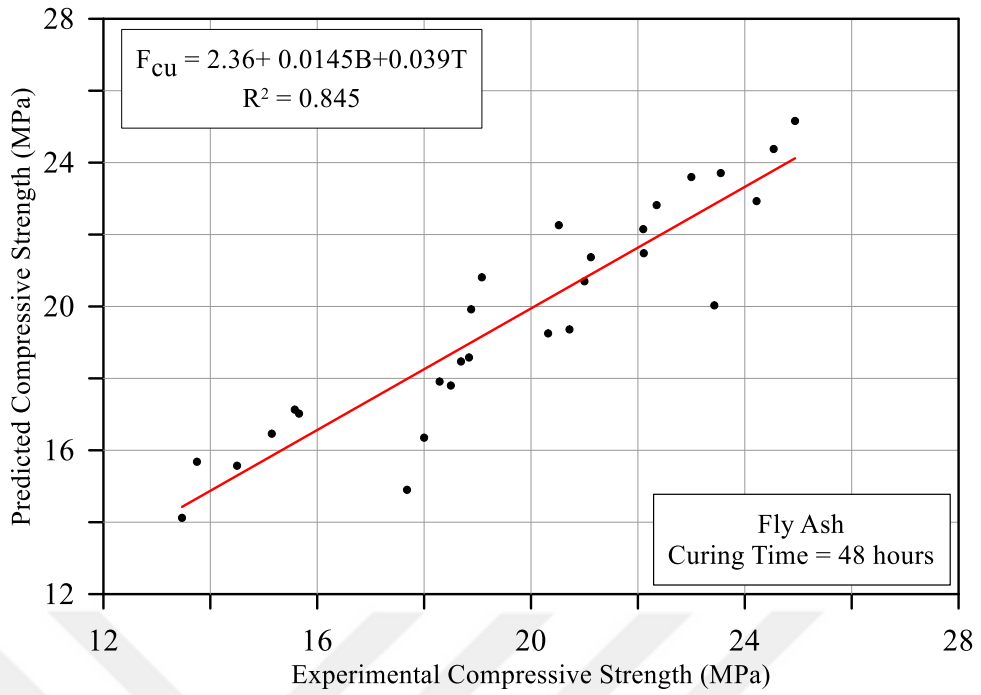


Figure 7.11 Step-wise regression model for compressive strength of FA based LWGMs exposed to 48 hrs of curing time.

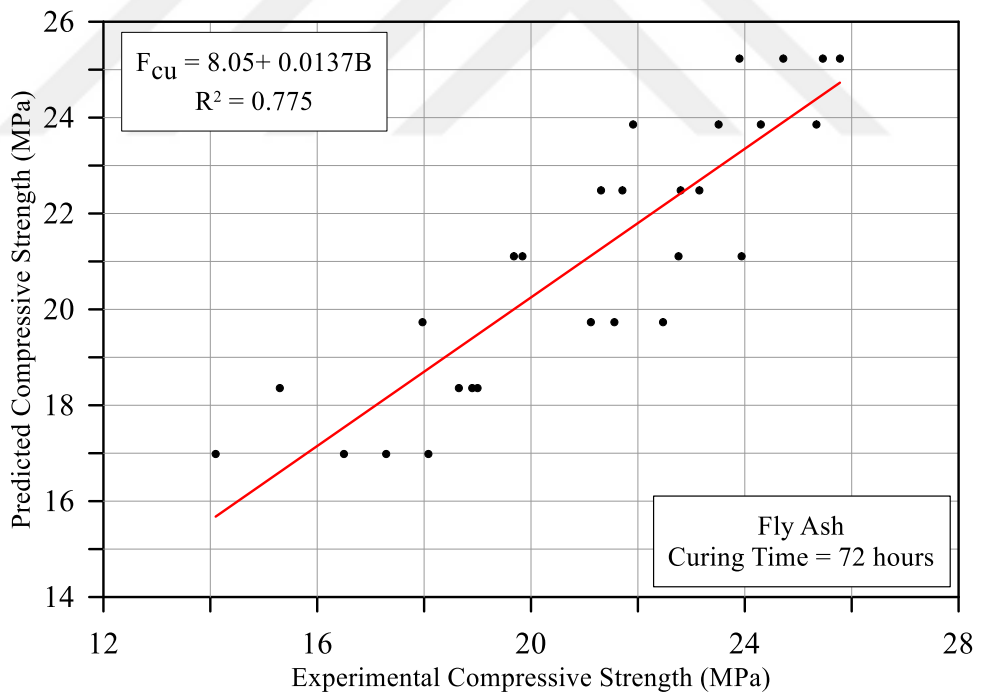


Figure 7.12 Step-wise regression model for compressive strength of FA based LWGMs exposed to 72 hrs of curing time.

7.3 Step-Wise Regression Models for Compressive Strength in Terms of Binder Content and Curing Time for Various Curing Temperatures

In this section, for each curing temperature, the compressive strength of geopolymer mortar is predicted by means of binder content and curing period for different curing temperatures. The curing temperatures are 60, 80, 100, and 120 °C. Similar to the previous section, all formulas were found based on the binder content. The regression equations for GGBFS-based geopolymer are shown in Figures 7.13 to 7.16, while Figures 7.17 to 7.20 shows the regression equations of fly ash-based geopolymer.

7.3.1 GGBFS-Based Geopolymer Mortar

It is obvious that the degree of confidence of this set of equations (see figs. 7.13-7.16) is much lower than of that for different curing periods. In the prediction equations for different curing temperatures the coefficients of determination are mostly lower than 0.6, while for those of different curing periods (figs. 7.1-7.6), the lowest R^2 is 0.67. The values of R^2 for compressive strength of GGBFS-based LWGMs for curing temperatures of 60, 80, 100, and 120 °C are approximately 0.56, 0.54, 0.53 and 0.79, respectively, as shown in Figs. 7.13 - 7.16.

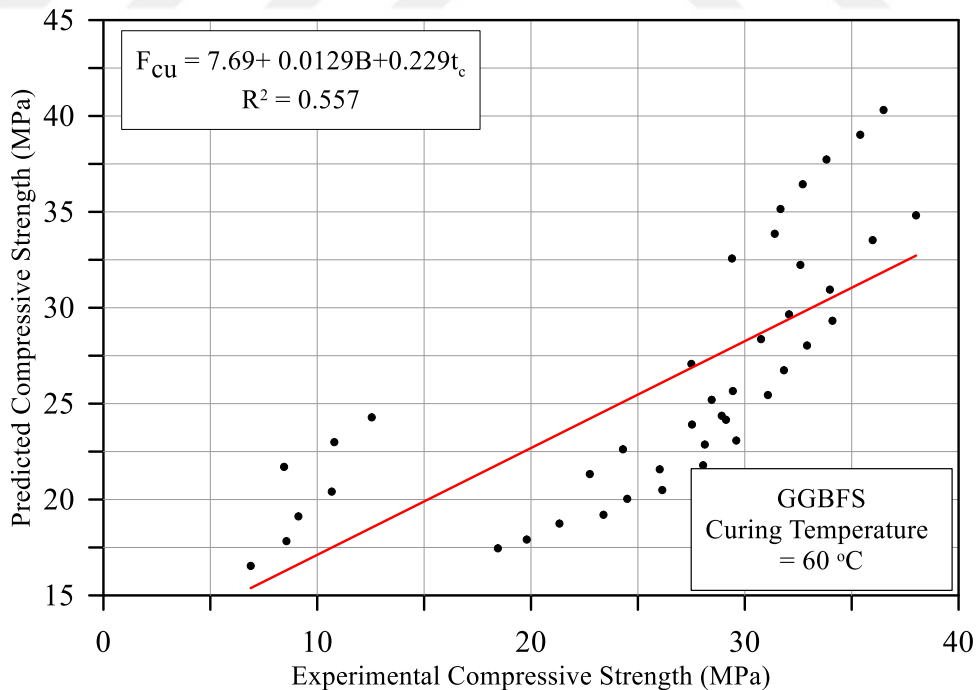


Figure 7.13 Step-wise regression model for compressive strength of GGBFS based LWGMs exposed to 60 °C of curing temperature.

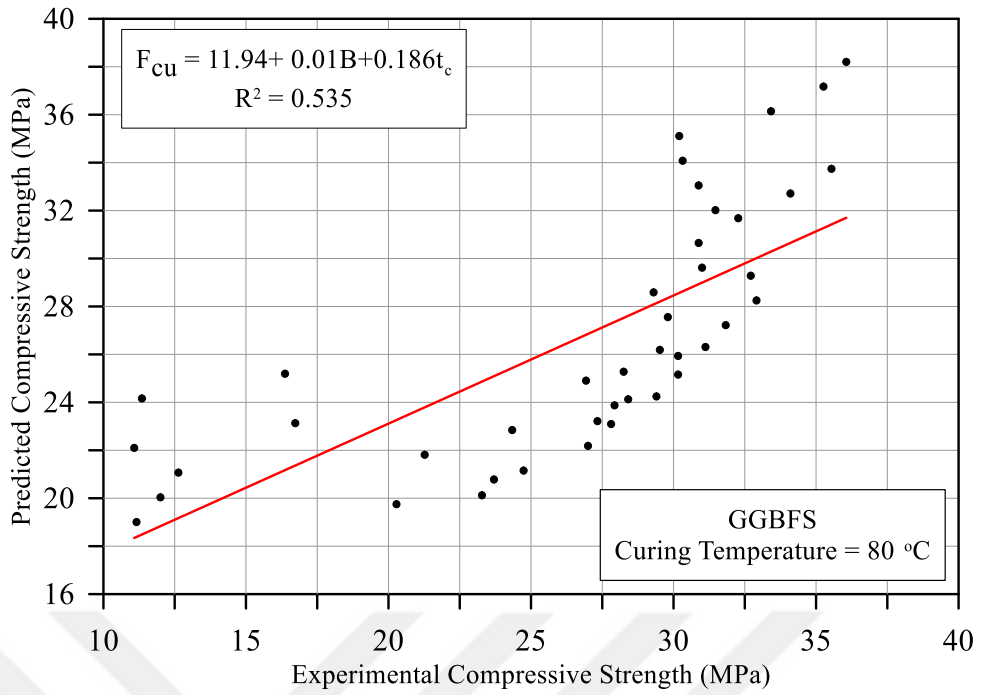


Figure 7.14 Step-wise regression model for compressive strength of GGBFS based LWGMs exposed to 80 °C of curing temperature.

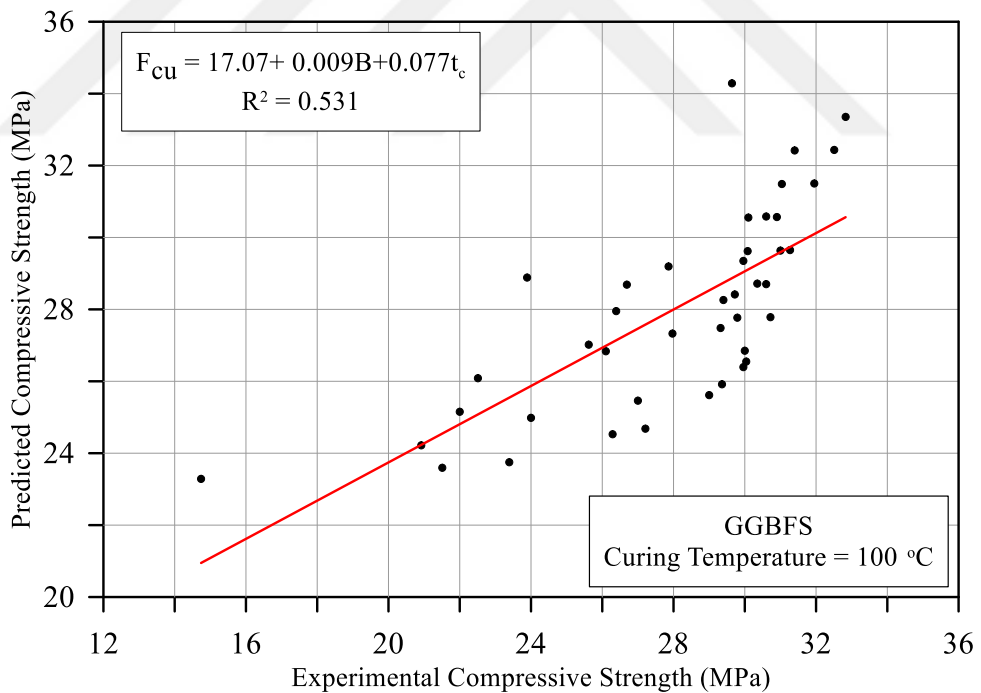


Figure 7.15 Step-wise regression model for compressive strength of GGBFS based LWGMs exposed to 100 °C of curing temperature.

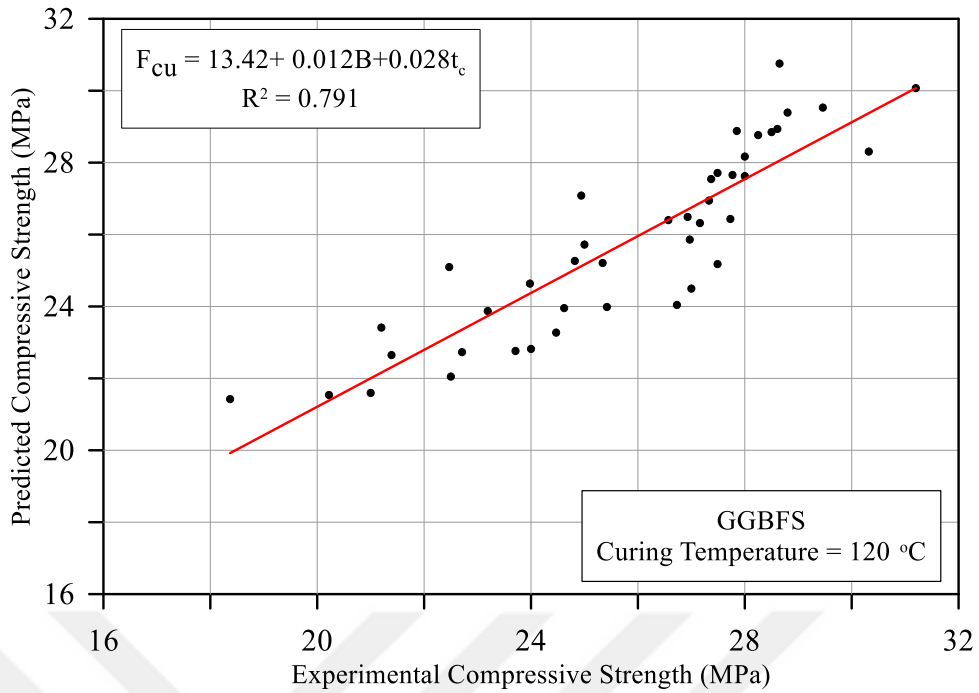


Figure 7.16 Step-wise regression model for compressive strength of GGBFS based LWGMs exposed to 120 °C of curing temperature.

7.3.2 Fly Ash-Based Geopolymer Mortar

As it is clear in Figures 7.17 to 7.20, the coefficients of determination the compressive strength of fly ash-based LWGMs for different curing temperatures are better than their corresponding values with GGBFS binder. The coefficients of determination of compressive strength versus binder content and curing time for curing temperatures of 60, 80, 100, and 120 °C are approximately 0.83, 0.81, 0.8, and 0.69, respectively.

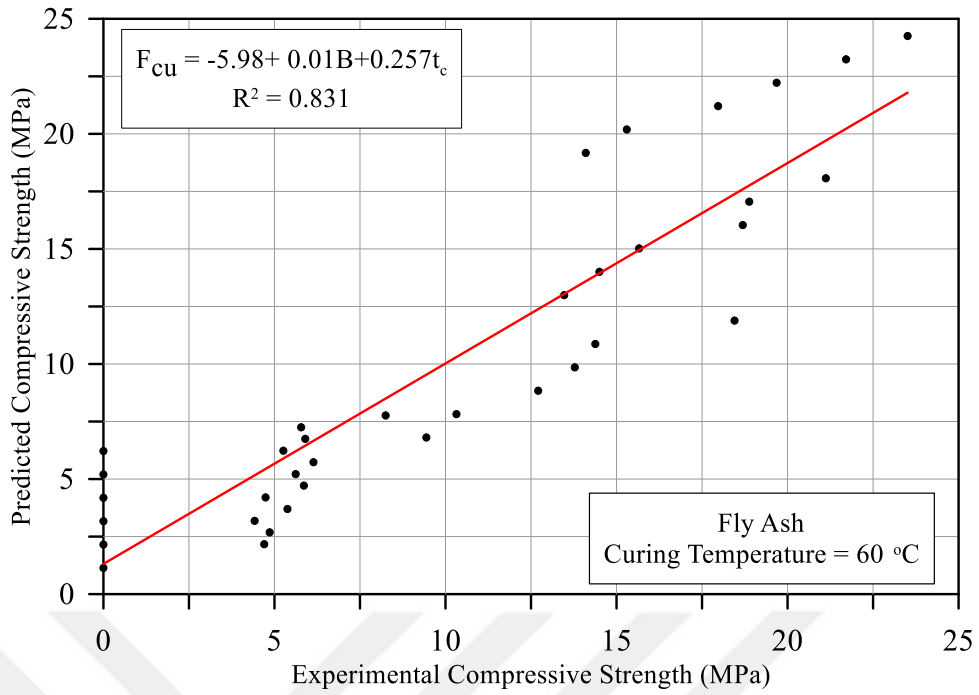


Figure 7.17 Step-wise regression model for compressive strength of FA based LWGMs exposed to 60 °C of curing temperature.

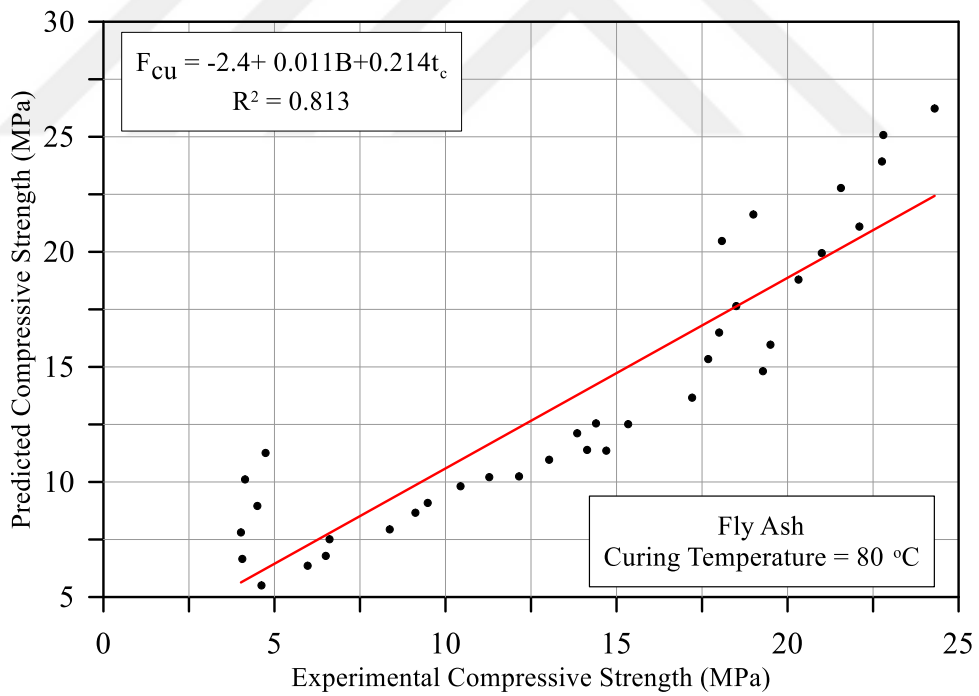


Figure 7.18 Step-wise regression model for compressive strength of FA based LWGMs exposed to 80 °C of curing temperature.

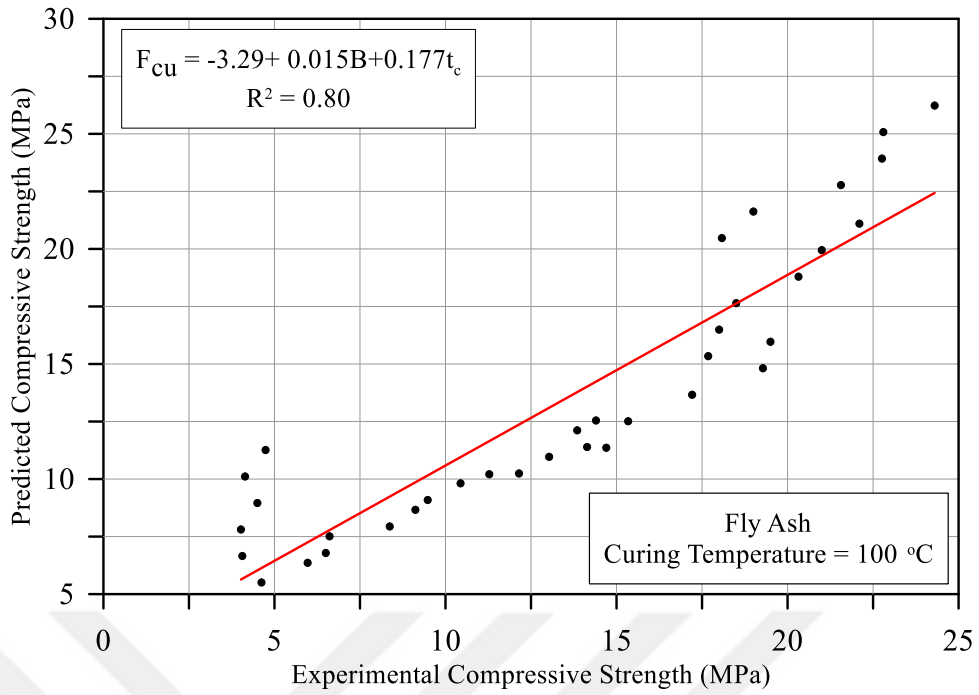


Figure 7.19 Step-wise regression model for compressive strength of FA based LWGMs exposed to 100 °C of curing temperature.

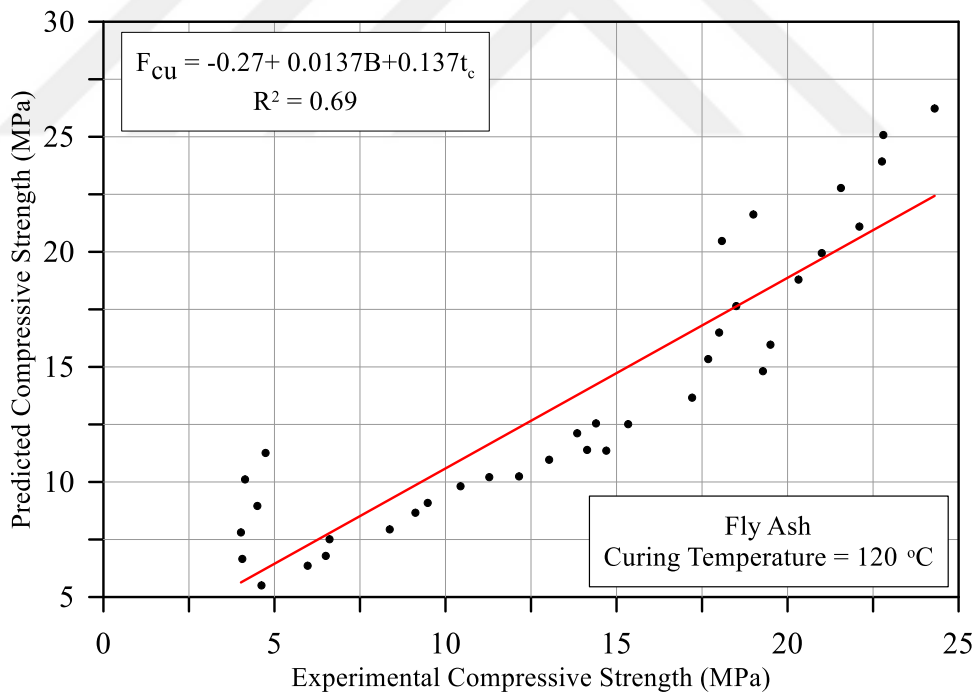


Figure 7.20 Step-wise regression model for compressive strength of FA based LWGMs exposed to 120 °C of curing temperature.

7.4 Step-Wise Regression Relationships of Compressive Strength vs. Binder, Curing Temperature, and Curing Time

In the previous sections, regression equations for compressive strength of geopolymer mortar based on only two independent variables were obtained using linear step-wise regression. In this section, the compressive strength is correlated with the three independent variables at once. Thus, compressive strength is correlated to binder content, curing temperature, and curing time. Figure 7.21 shows the experimental versus predicted compressive strength values for all experimental data of the fly ash-based geopolymer mortar. The coefficient of determination of this equation is approximately 0.78, which is quite good. On the other hand, for the GGBFS-based LWGMs, the step-wise regression showed that curing temperature was insignificant with probability value greater than 0.05. Therefore, the equation was in terms of binder content and curing time only. However, the R^2 was as low as 0.43.

In order to make a broad comparison of the prediction performance all of the derived step-wise regression formulas are presented in table 7.1.

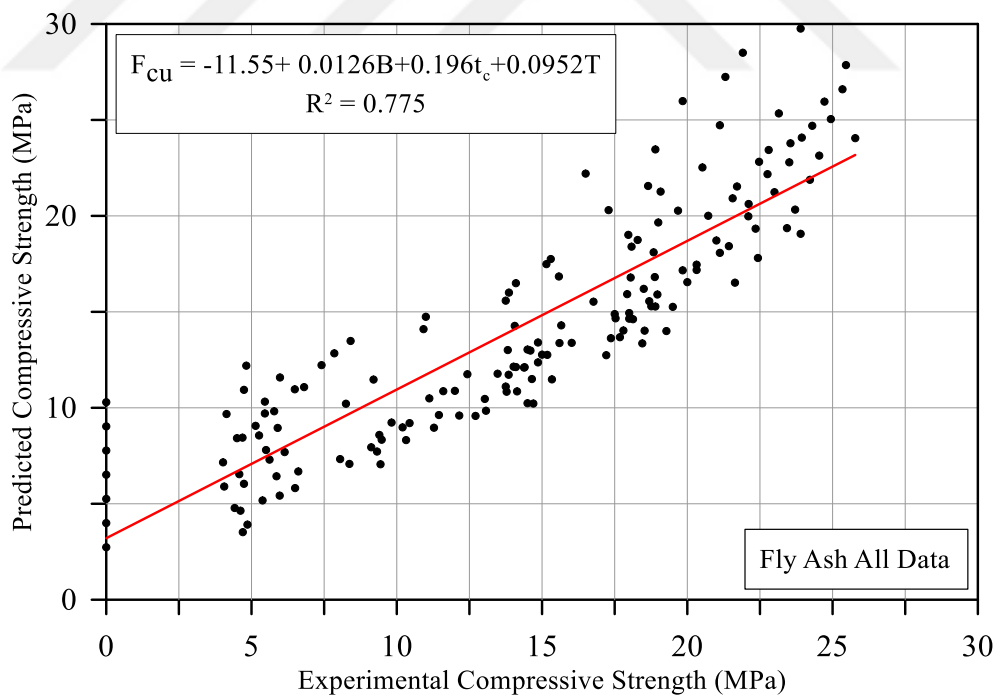


Figure 7.21 Step-wise regression model for compressive strength of FA based LWGMs at different binder content, curing temperature, and curing time.

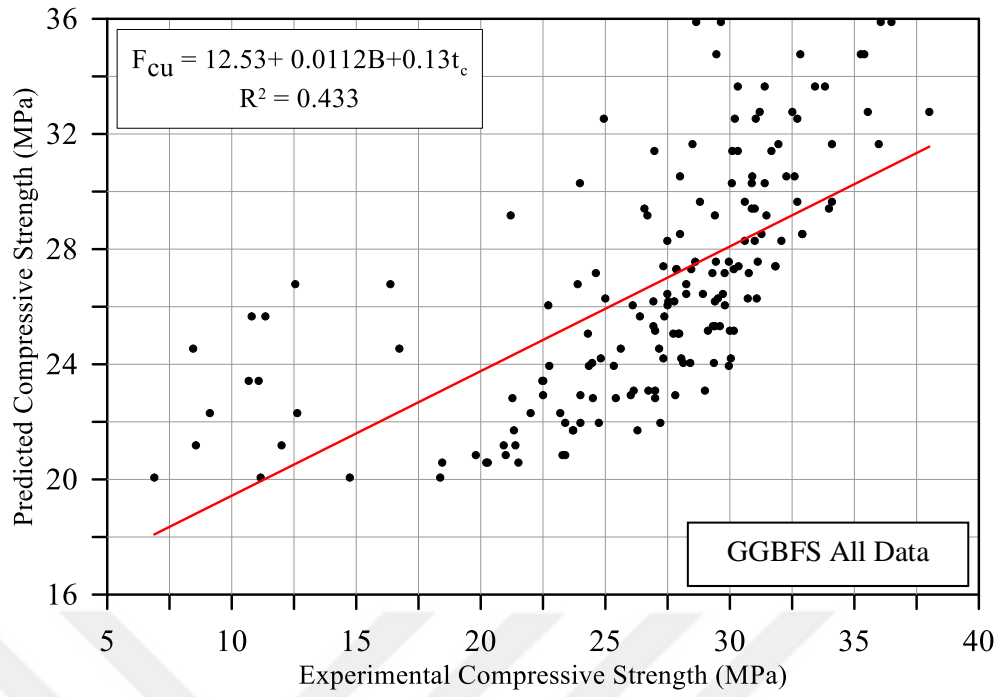


Figure 7.22 Step-wise regression model for compressive strength of GGBFS based LWGMs at different binder content, curing temperature, and curing time.

Table 7.1 Comparison of step-wise regression formulations.

Mix ID	Definition	Step-wise regression formulas	R ²
GGBFS based LWGMs	Curing time = 2 hrs.	$F_{cu}=17.19+0.0113B+0.263T$	0.88
	Curing time = 6 hrs.	$F_{cu}=10.04+0.0129B+0.034T$	0.721
	Curing time = 8 hrs.	$F_{cu}=15.8+0.0117B$	0.679
	Curing time = 24 hrs.	$F_{cu}=25.89+0.01B+0.0695T$	0.788
	Curing time = 48 hrs.	$F_{cu}=28.4+0.0114B+0.0968T$	0.881
	Curing time = 72 hrs.	$F_{cu}=31.06+0.0097B+0.108T$	0.796
	Curing temperature=60 °C	$F_{cu}=7.69+0.0129B+0.229 t_c$	0.557
	Curing temperature=80 °C	$F_{cu}=11.94+0.01B+0.186 t_c$	0.535
	Curing temperature=100 °C	$F_{cu}=17.07+0.009B+0.077 t_c$	0.531
	Curing temperature=120 °C	$F_{cu}=13.42+0.012B+0.28 t_c$	0.791
	All data	$F_{cu}=12.53+0.0112B+0.13 t_c$	0.433
FA based LWGMs	Curing time = 2 hrs.	$F_{cu}= -12.91+0.006B+0.133T$	0.811
	Curing time = 6 hrs.	$F_{cu}= -13.56+0.0123B+0.14T$	0.847
	Curing time = 8 hrs.	$F_{cu}= -14.2+0.0135B+0.148T$	0.899
	Curing time = 24 hrs.	$F_{cu}= - 6.37+0.0156B+0.0958T$	0.944
	Curing time = 48 hrs.	$F_{cu}= 2.36+0.0145B+0.039T$	0.845
	Curing time = 72 hrs.	$F_{cu}= 8.05+0.0137B$	0.775
	Curing temperature=60 °C	$F_{cu}= -5.98+0.01B+0.25 t_c$	0.831
	Curing temperature=80 °C	$F_{cu}= -2.4+0.011B+0.214 t_c$	0.813
	Curing temperature=100 °C	$F_{cu}= -3.29+0.015B+0.177 t_c$	0.80
	Curing temperature=120 °C	$F_{cu}= - 0.27+0.0137B+0.137 t_c$	0.69
	All data	$F_{cu}= - 11.55+0.0126B+0.196 t_c +0.0952T$	0.775

7.5 Compressive Strength Modeling of Geopolymer Mortar Based on Gene Expression Programming

In this section, the Gene Expression Programming (GEP) is used to evaluate the effects of the studied three parameters (binder content, curing temperature, and curing time) on compressive strength of geopolymer mortar. As in the previous section, the evaluation is in the form of a regression formula based on the type of binder. Thus, two formulas are to be conducted in this section, one for the fly ash-based geopolymer, while the second is for GGBFS-based geopolymer mortar.

7.5.1 Brief Review of GEP

Going back to the end of 1980's and the beginning of 1990's, the Genetic Algorithms (GAs) and later the Genetic Programming (GP) were developed as new evolutionary techniques. The GP is simply the evolution and optimum solving of computer programs (research problems) of domain-independent-problems based on the Darwinian principles of gene survival, reproduction, and evolution. Both GAs and GP techniques use only single type of individuals or entity to formulate both the genome and phenome types of the problem. In biology, the genome refers to the chromosome that carries all features of the entity, while the phenome is the visualized shape of that entity (the body). In GPs, the chromosomes are the individuals, which are fixed-length strings of linear form, while the individuals of GP are parse-trees of nonlinear different shapes and different lengths (Ferreira C., 2001). The GEP on the other hand, uses the two forms, where fixed-length linear-strings are used to encode the individuals during the processing phase. These codes are then translated to nonlinear entities of different shapes and sizes in the post processing phase, which are simplified expression trees. Thus, GEP translates the language of chromosomes into a simple language of expression trees (Ferreira C., 2001).

In GEP, different numbers of different-length and shape and multi-gene chromosomes are used to code the variables of the problem need to be solved. In addition to the main variables of the problems, the program defines constants and mathematical expressions as parts of these chromosomes. The mathematical expressions include all types of possible mathematical operations such as addition, subtraction, multiplication, division, square or higher order roots, squaring or higher

powers, logarithms, exponentials, trigonometric functions, and others. In the start of the evolution process, a fitness function is chosen to evaluate the accuracy of the solution and the errors. This fitness is evaluated at the first step for a random generation. In the subsequent steps, the individuals with best fitness are selected (survived individuals) for reproduction and development of the next generation. The development of each next generation carried out by carrying some or all of several randomly selected operations on the survived (selected based on best fitness) chromosomes and genes from the previous generation. These reproduction operations include replication of survived genes, mutation, partial or gene transportation, and partial or gene recombination. This process continues one generation by another for several hundreds, thousands, or millions of generations until the best fitness of the solution is obtained. Figure 7.23 shows the flowchart of the GEP processing.

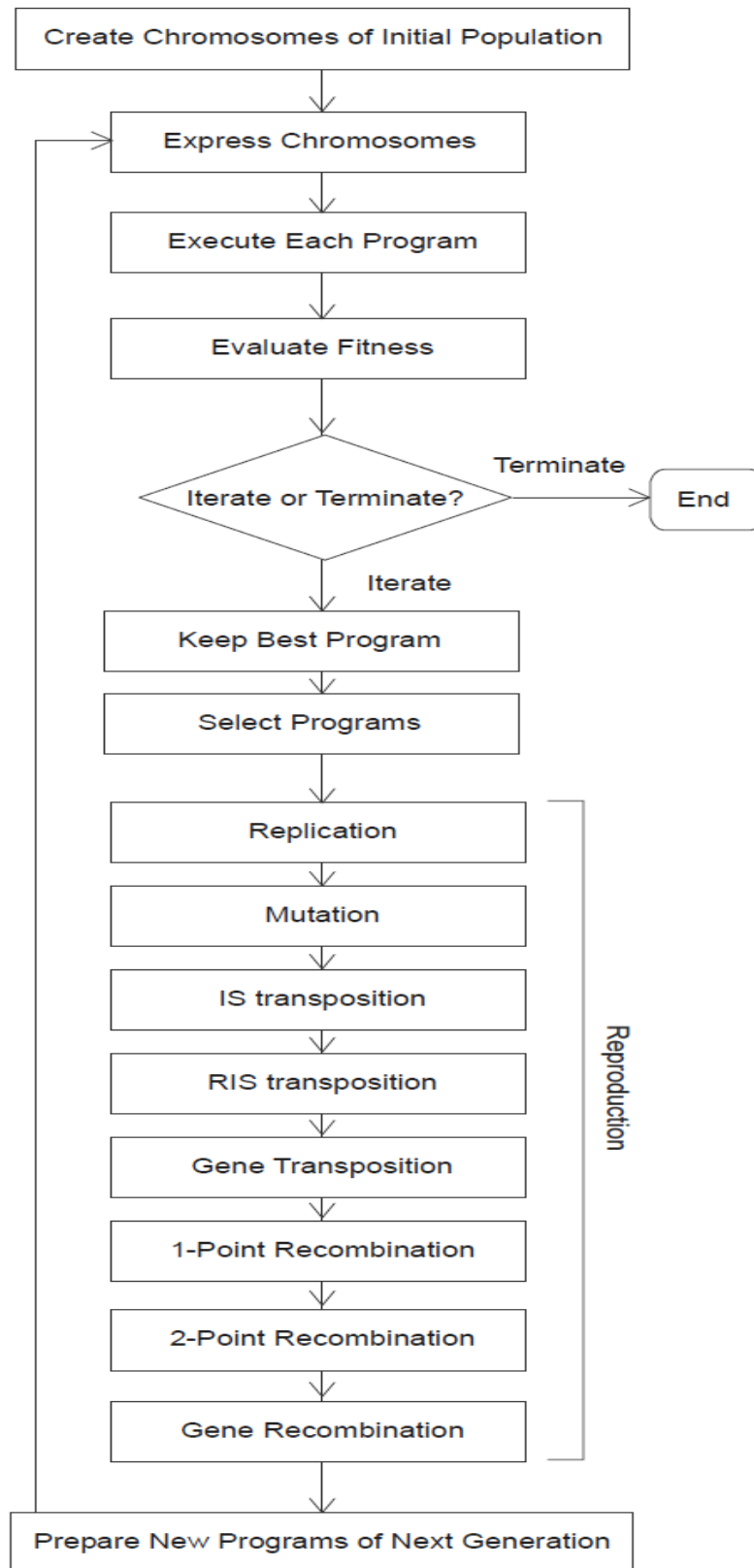


Figure 7.23 Flowchart of GEP (Ferreira C., 2001).

7.5.2 Numerical Application of GEP

In this section, the GEP is used for formulation-based modeling of the compressive strength of the geopolymers mortar based on the experimental results of this study. This formulation is carried out based on the binder type, while binder content, curing temperature, and curing period are kept variables. Thus, two formulas are obtained using GEP. The first is for the compressive strength of fly ash-based geopolymers mortar, while the second is for the GGBFS-based geopolymers mortar. In both of which, the compressive strength is nonlinearly evaluated based on the binder content, the curing temperature, and the curing period as expressed in Equation (7.1). The total number of compressive strength results (samples) used in GEP for each binder was 168. The fitness function used in the GEP in this study is the coefficient of determination (R^2), which was also used in the step-wise regression in this chapter.

$$F_{cu} = f(B, T, t_c) \quad (7.1)$$

In the GEP carried out in this study, thirty chromosomes each of 3 genes and head length of 7 were used, while the addition was used as the linking function to link the resulted expression trees. Thus, each resulted equation will be composed of three expression trees linked by addition. To simplify the resulted functions, only a limited set of mathematical operations were selected. These operations include addition, subtraction, multiplication, division, square root, cubic root, squaring, cubing, natural logarithm, exponential, sin, and cosine.

7.5.3 GEP-Based Formulas of Compressive Strength

Figure 7.24 shows the resulted expression trees of the compressive strength of fly ash-based samples, while Figure 7.25 shows the expression trees of that of GGBFS samples. In these figures and the following equations, the parameters d_0 , d_1 , d_2 refer to the variables of the equation, which are the binder content (B), the curing temperature (T), and the curing time (t_c), respectively, while C_0 and C_1 are constants of each sub-equation.

Equation (7.2) is the GEP predicted formula for the fly ash-based mortar, which is derived from expression trees given in Figure 7.24. This equation has a coefficient of determination $R^2 = 0.95$. As shown in Figure 7.25, which is much better than that of

stepwise regression, which was 0.775. This reveals the power of GEP to predict regression formulas.

$$F_{cu} = F_1 + F_2 + F_3 \quad (7.2)$$

$$F_1 = C_1 \ln[(\sin d_1)^2 + d_2] \quad (7.3)$$

Where $C_0 = 4.00769$ and $C_1 = 4.87732$

$$F_2 = \cos d_o \ln \left[\frac{d_1}{C_1} \ln d_2 \right] \quad (7.4)$$

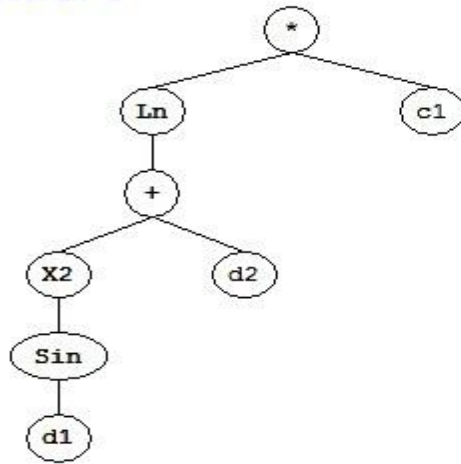
Where $C_0 = -5.881989$ and $C_1 = 6.77649$

$$F_3 = \cos d_1 \left[C_1 + \frac{d_2/C_0}{C_1} \right] \quad (7.5)$$

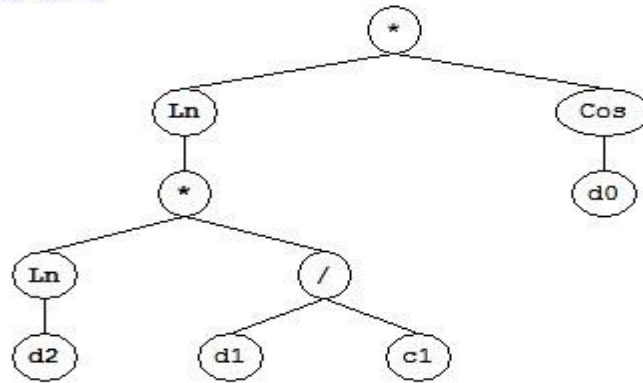
Where $C_0 = -4.005798$ and $C_1 = 4.376678$

Where F_1 , F_2 , and F_3 are the sub-function resulted from each sub-expression trees shown in Figure 7.24, respectively, and connected by the addition linking function.

Sub-ET 1



Sub-ET 2



Sub-ET 3

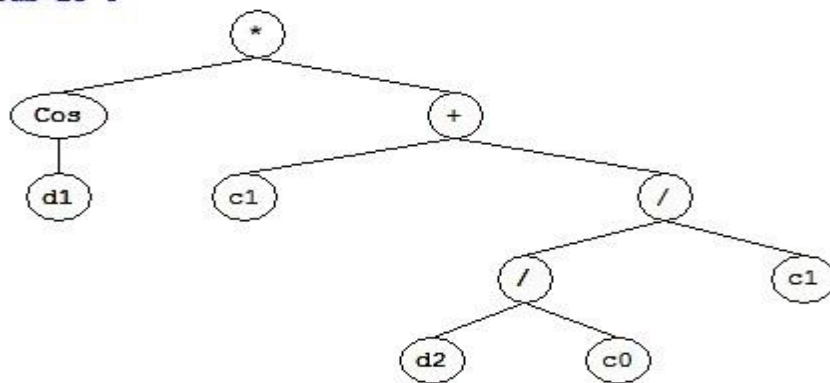


Figure 7.24 Expression trees of compressive strength prediction of fly ash-based geopolymer samples.

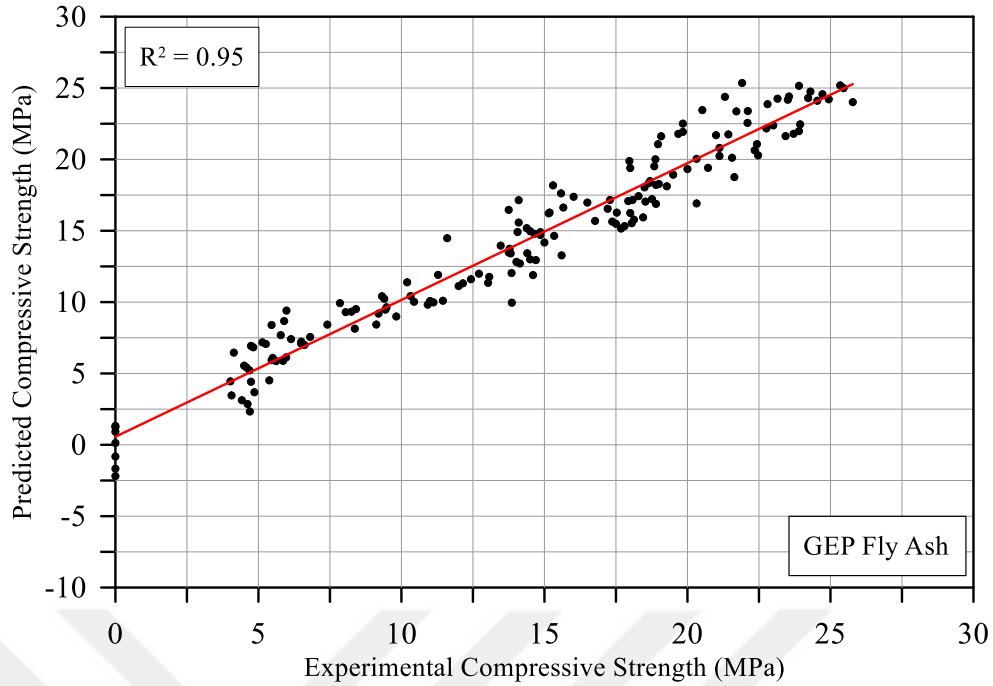


Figure 7.25 GEP predicted vs experimental compressive strength of fly ash based LWGMs compressive strength of 168 specimens.

Equation (7.6) gives the predicted formula of compressive strength of the GGBFS mortar, which is derived from expression trees given in Figure 7.26. This equation has a coefficient of determination $R^2 = 0.866$. This coefficient of determination is highly superior to that predicted from linear step-wise regression (0.433), which assures that GEP is much powerful than traditional statistical regression tools. Figure 7.27 shows the linear correlation between the GEP predicted and the experimental compressive strength of the GGBFS-based geopolymer mortar.

$$F_{cu} = F_1 + F_2 + F_3 \quad (7.6)$$

Where F_1 , F_2 and F_3 are given by Equations (7.7), (7.8), and (7.9), respectively.

$$F_1 = d_o / [(C_o + C_1 - d_2^3) - (d_1 - C_1)] \quad (7.7)$$

Where $C_o = 7.316192$ and $C_1 = 7.221954$

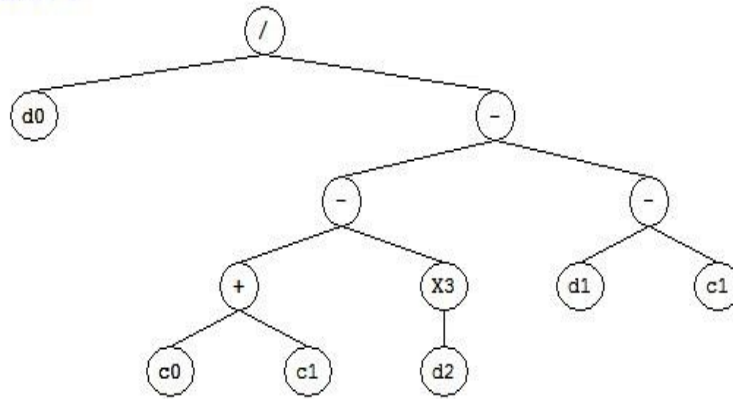
$$F_2 = \sqrt[3]{2d_o \left(C_o + \frac{C_o}{d_2} \right) + d_o} \quad (7.8)$$

Where $C_o = 9.992737$ and $C_1 = -5.524353$

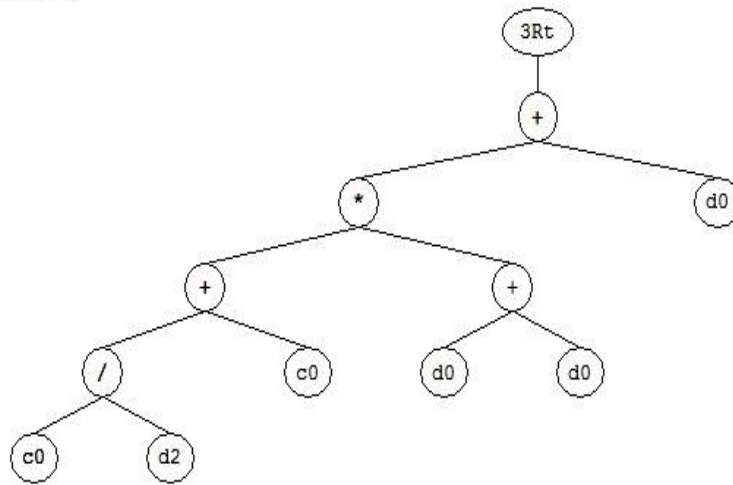
$$F_3 = [d_2 / (\sin d_2 - C_1)] \sin C_o d_1 \quad (7.9)$$

Where $C_o = 7.880677$ and $C_1 = -9.897583$

Sub-ET 1



Sub-ET 2



Sub-ET 3

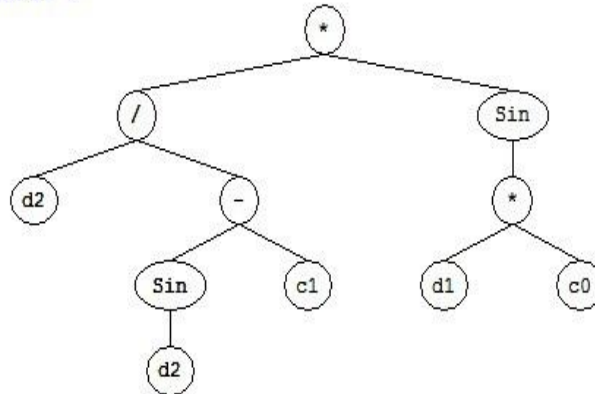


Figure 7.26 Resulted expression trees of compressive strength of GGBFS-based geopolymer samples.

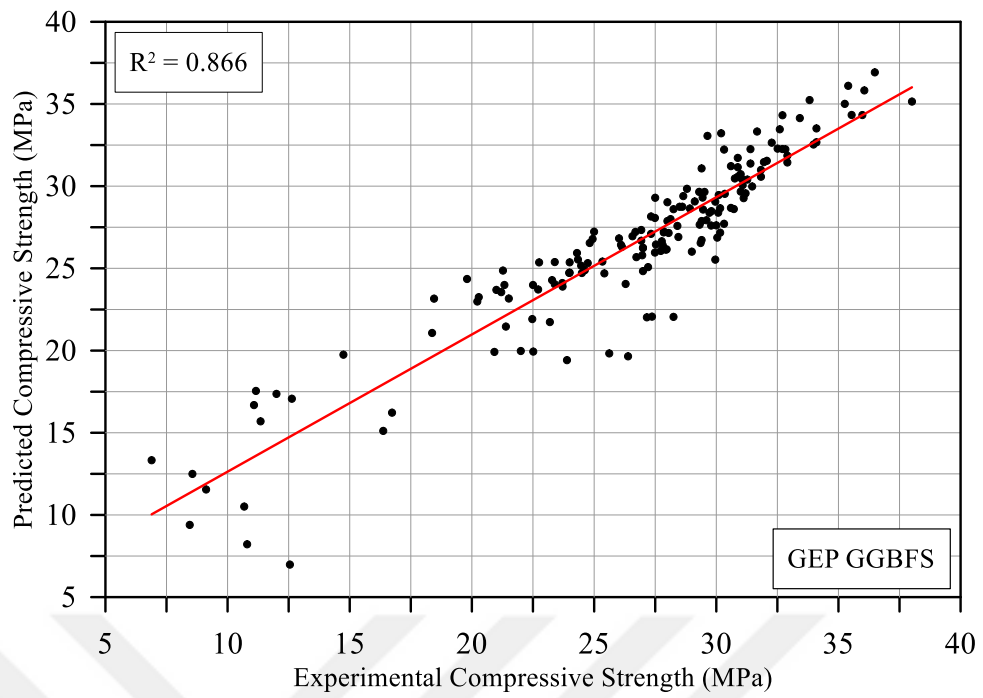


Figure 7.27 GEP predicted vs experimental compressive strength of GGBFS based LWGMs compressive strength of 168 specimens.

CHAPTER 8

CONCLUSIONS AND RECOMMENDATIONS

8.1 Conclusions

Based on the materials used and the test results obtained from the experimental program and the interpretation of the results, the following conclusions can be drawn:

1. The increment in the binder content increased the compressive strength of the LWGM. However, the increment in the compressive strength is not proportional to the increase of the binder content. Since the LWFA has high porosity, it is the weak component of the LWGM. Therefore, it can be concluded that the more the LWFA in a unit volume the less the compressive strength is obtained.
2. Curing temperature and curing duration are also significant in the activation of LWGM. Compressive strength raised with the increment of curing period, the strength increased up to 48 h for GGBFS-based LWGM and up to 72 h for FA-based LWGM. However, the strength decreased beyond 48 h curing at 120 °C in FA-based LWGM. It can be attributed to internal crack development as a result of expansion of LWFA due to excessive heating.
3. Curing temperature relies on the curing duration. Curing for 2 hrs at 60°C didn't make notable difference in strength developed in FA-based LWGM but longer curing caused noticeable acceleration of the reaction rate and increased the strength. However, the compressive strength of FA-based LWGM raised with the increment of curing temperature to 120°C for 2 to 24 hours curing and 100°C for 48 to 72 hours curing.

4. The compressive strength of GGBFS-based LWGM rose with the increment of curing temperature to 120°C for 2 hours curing and 100°C for 6 to 8 hours curing. Specimens activated at 48 hours observed to have the optimum curing temperature and the highest compressive strength values when cured at 60 °C.
5. GGBFS-based LWGM had lower workability than FA-based LWGM. The flow decreased with an increase of the NaOH concentration and Na₂SiO₃ to NaOH ratio from 1 to 2.5 in FA and GGBFS geopolymer mortar.
6. The fresh unit weight of LWGM raised with the increment of NaOH concentration and Na₂SiO₃ to NaOH ratio.
7. The compressive and splitting tensile strengths raise up to an optimal value as the alkali activator concentration raises in LWGM.
8. The highest 7-day compressive strength (31.2 and 21.08 MPa) was achieved from oven-cured LWGM when the SS/NH ratio was 2.0 and 1.0 with 12 M for GGBFS and FA respectively.
9. The effect of mix variables on the tensile strength development was similar to that of compressive strength development.
10. LWGM with higher alkali activator concentration resulted in lower water absorption.
11. The study revealed that the sorptivity depended essentially on the content of silica and alkali. Strong alkali solution is required to dissolve GGBFS and FA during the geopolymerization. Anyhow, there was a reduction in the sorptivity and absorption with the increment in compressive strength.

8.2 Recommendation for Future Study

It was observed that there are various parameters affecting the compressive strength development of LWGM. The recommendations for future studies can be as follows;

1. It is recommended that effects of some other critical parameters such as different type of light-weight aggregate with less porosity, properties of base material such as fineness and chemical compositions can be studied.
2. Soft computing based prediction models can be derived by using the presented data in this study and the collected ones from the literature.
3. An experimental research on durability and thermal properties of LWGM is highly recommended as a future study.
4. In a future study some companion normal weight mortars may be included to compare with the strength and failure patterns of the two types of geopolymer mortars.

REFERENCES

- Abdulkareem, O. A., Al Bakri, A. M., Kamarudin, H., Nizar, Khairul, I., Saif Ala'eddin, A. (2014). Effects of elevated temperatures on the thermal behavior and mechanical performance of fly ash geopolymer paste, mortar and lightweight concrete, *Construction and Building Materials*, **50**, 377–387.
- ACI Committee 363. (1992). State-of-the-art report on high-strength concrete (ACI 363R-92), *American Concrete Institute*, Farmington Hills, Mich., 55 pp.
- Aguilar, R., BurciagaDíaz, O., Escalante García, J. (2010). Lightweight concretes of activated metakaolin-Fly ash binders, with blast furnace slag aggregates, *Construction and Building Materials*, **24**, 1166–1175
- Al Bakri, A. M., Kamarudin, H., Bnhussain, M., Nizar, I.K., Rafiza, A.R. Zarina, Y. (2012).The processing, characterization and properties of fly ash based geopolymer concrete, *Reviews on advanced materials science*, **30**, 90 -97.
- Algin, H. M. (2016). Optimised design of jet-grouted raft using response surface method, *Computers and Geotechnics*. **74**, 56–73.
- Ariffin, N. F., Hussin, M.W., Sam, A. R., Bhutta, M.A., Khalid, N. H. Mirza, A. J. (2015). Strength properties and molecular composition of epoxy-modified mortars, *Construction and Building Materials*, **94**, 315–322.
- ASTM C 109/C 109M. (2005). standard test method for compressive strength of hydraulic cement mortars (Using 2-in. or [50-mm] Cube Specimens), *American Society for Testing and Materials*.
- ASTM C138/C 138M. (2001). Standard test method for density (unit weight), yield, and air content (gravimetric) of concrete, *American Society for Testing and Materials*.
- ASTM C1585 (2004). Standard test method for measurement of rate of absorption of water by hydraulic-cement concretes. *American Society for Testing and Materials*.

ASTM C496 (2004), Standard test method for splitting tensile strength for cylindrical concrete specimens, *American Society for Testing and Materials*.

ASTM C618 (2002). Standard specification for coal fly ash and raw or calcined natural pozzolan for use in concrete, *American Society for Testing and Materials*.

Bondar, D. (2013). Geo-polymer concrete as a new type of sustainable construction materials, *Third International Conference on Sustainable Construction Materials and Technologies*, Kyoto, Japan.

CEB-FIP Model Code for Concrete Structures (1990). Evaluation of the time dependent behavior of concrete, *Bulletin d'Information No. 199*, Comite European du Béton/Fédération Internationale de la Precontrainte, Lausanne, 1991, 201 pp.

Davidovits, J. (1991). Geopolymers: inorganic polymeric new materials, *Journal of Thermal Analysis*, **37**, 1633-1656.

Davidovits, J. (1995). Global warming impact on the cement and aggregate industrie, *World Resource review*, **6**, 263-278.

Davidovits, J. (2011). Geopolymer chemistry and applications, 3rd edition, Institut Géopolymère, France.

De Vargas, A. S., Dal Molin, D. C., Vilela, A. C., Da Silva, F. J., Pavao, B., Veit, H. (2011). The effects of Na₂O/SiO₂ molar ratio, curing temperature and age on compressive strength, morphology and microstructure of alkali-activated fly ash-based geopolymers, *Cement and Concrete Composite*, **33**, 653–660.

Deb, P. S., Sarker, P. K., Barbhuiya, S. (2016). Sorptivity and acid resistance of ambient-cured geopolymer mortars containing nano-silica, *Cement and Concrete Composites*, **72**, 235-245.

Duxson, P.A., Jimenez, A.F., Provis, J.L., Lukey, G.C., Palomo, A., Van Deventer J.S.J. (2007). Geopolymer technology: the current state of the art, *Journal of Materials Science*, **42**, 2917–2933.

Fernández-Jiménez, A., Palomo, A., Sobrados, I., Sanz, J. (2006). The role played by the reactive alumina content in the alkaline activation of fly ashes. *Microporous and Mesoporous Materials*, **91**, 111-119.

Fernandez-Jimenez, A., Paloma, A. (2003). Characterisation of fly ashes. Potential reactivity as alkaline cements, *Fuel*, **82**, 2259-2265.

Fernandez-Jimenez, A., Palomo, A. (2005). Composition and microstructure of alkali activated fly ash binder: effect of the activator, *Cement and Concrete Research*, **35**, 1984–1992.

Fernandez-Jimenez, A., Palomo, A. (2006). Engineering properties of alkali-activated fly ash concrete, *ACI Material Journal*, **103**, 106–112.

Fernandez-Jimenez, A., Puertas F. (2001). Setting of alkali-activated slag cement Influence of activator nature, *Advance Cement Research*, **13**, 115-121.

Ferreira, C. (2001). Gene Expression Programming: A new adaptive algorithm for solving problems, *Complex Systems*, **13**, 87-129.

Ghosh, K., Ghosh, P. (2012). Effect of %Na₂O and %SiO₂ on apparent porosity and sorptivity of fly ash based geopolymer, *IOSR Journal of Engineering (IOSRJEN)* ISSN: 2250-3021, **2**, 96-101.

Ghosh, K., Ghosh, P. (2012). Effect of Na₂O/Al₂O₃, SiO₂/Al₂O₃ and W/B ratio on setting time and workability of fly ash based geopolymer, *International Journal of Engineering Research and Applications (IJERA)* ISSN: 2248-9622, **2**, 2142-2147.

Glukhovsky, V. (1994). Alkaline Cements and Concretes, *Frist International Conference 1*, 1-8, Kiev. Ukraine.

Gorhan, G. and Kurklu, G. (2014).The influence of the NaOH solution on the properties of the fly ash-based geopolymer mortar cured at different temperatures, *Composites, Part B*, **58**, 371–377.

Hall, C. (1989). Water sorptivity of mortars and concretes: a review, *Mag Concert Research*, **41**, 51–61.

Hanjitsuwan, S., Hunpratub, S., Thongbai, P., Maensiri, S., Sata, V., Chindaprasirt, P. (2014). Effects of NaOH concentrations on physical and electrical properties of high calcium fly ash geopolymer paste, *Cement & Concrete Composites*, **45**, 9-14.

Hardjito, D. and Fung, S. S. (2010). Parametric Study on the Properties of Geopolymer Mortar Incorporating Bottom Ash, *Concrete Research Letters* **1**, 115-124.

Hardjito, D., Cheak, C.C., Ing, C.H.L. (2008). Strength and setting times of low calcium fly ash-based geopolymer mortar, *Modern Applied Science*, **2**, 3-11.

Hardjito, D., Rangan, B.V. (2005). Development and properties of low-calcium fly ash-based geopolymer concrete, *Research Report GCI*, Faculty of Engineering, Curtin University of Technology, Perth, available at espace@curtin or www.geopolymer.org, 01/11/2016.

Hardjito, D., Wallah, S. E., Sumajouw, D.M., Rangan, B. V. (2004). On the Development of Fly Ash-Based Geopolymer Concrete, *Materials Journal*, **101**, 467-472.

Helmy A. (2016). Intermittent curing of fly ash geopolymer mortar, *Construction and Building Materials*, **110**, 54–64.

Huseien, G. F., Mirza, J., Ismail, M., Hussin, M. W. (2016). Influence of different curing temperatures and alkali activators on properties of GBFS geopolymer mortars containing fly ash and palm-oil fuel ash, *Construction and Building Materials*, **125**, 1229–1240.

Islam, A., U. Alengaram, M. Z. Jumaat, Bashar, I. I. (2014). The development of compressive strength of ground granulated blast furnace slag-palm oil fuel ash-fly ash based geopolymer mortar, *Materials & Design*, **56**, 833-841.

Javier, C., Dale, B., Jason, W. (2011). Effect of sample conditioning on the water absorption of concrete, *Cement and Concrete Composites*, **33**, 805–813.

Jimenez, F., Palomo, A., Criado, M. (2005). Microstructure development of alkali-activated fly ash cement: a descriptive model, *Cement and Concrete Research*, **35**, 1204-1209.

Komnitsas, K., Zaharaki, D. (2007). Geopolymerisation: a review and prospects for the minerals industry, *Miner Eng.* **20**, 1261–77.

Kong, D. L., Sanjayan, J. G., Sagoe-Crentsil, K. (2008). Factors affecting the performance of metakaolin geopolymers exposed to elevated temperatures, *Journal of Materials Science*, **43**(3), 824-831.

- Kumar, S., Kumar, R., Mehrotra, S. P. (2010). Influence of granulated blast furnace slag on the reaction, structure and properties of fly ash based geopolymer, *Journal of Materials Science* **45**, 607–615.
- Lee, W. K., van Deventer, J. S. (2002). The effects of inorganic salt contamination on the strength and durability of geopolymer, *Colloids and Surfaces A: Physicochemical and Engineering Aspects*, **211**, 115–126.
- Liew, Y.M., Kamarudin, H., Bakri A.M., Binhussain, M., Luqman, M., Nizar, I.K., (2011). Influence of solids-to-liquid and activator ratios on calcined kaolin cement powder, *Physics procedia*, **22**, 312–317.
- Lloyd, N., Rangan, V. (2009). Geopolymer concrete-sustainable cementless concrete, *Paper presented at the Proceedings of the 10th ACI International Conference on Recent Advances in Concrete Technology and Sustainability*, Issues, 33-54.
- Manware, A. K., .Chouhan, R. K., Mudgal, M., Joshi, R., Amritphale, S. S. (2016). Effect of Curing Conditions and Molarity on Compressive Strength of Fly ash based Geopolymer Mortar, *International Journal of Innovative Research in Science, Engineering and Technology*, **5**, 18410-18416.
- Mazumder, M. D., Ghosh, P. (2016). Effect of blast furnace slag and concentration of sodium hydroxide on different parameters of fly ash based geopolymer mortar, *American Research Thoughts*, **2**, 3583-3593.
- Mijarsh, M. J., Megat J. M., Ahmad, Z. A. (2015). Effect of delay time and Na_2SiO_3 concentrations on compressive strength development of geopolymer mortar synthesized from TPOFA, *Construction and Building Materials*, **86**, 64–74.
- Morsy, M. S., Alsayed, S. H., Al-Salloum, Y., Almusallam, T. (2014). Effect of sodium silicate to sodium hydroxide ratios on strength and microstructure of fly ash geopolymer binder, *Arabian Journal for Science and Engineering*, **39**, 4333-4339.
- Myers, R. H., Montgomery, D. C., Anderson-Cook, C. M. (2009). Response surface methodology: process and product optimization using designed experiments, Wiley.
- Neville A.M., Properties of concrete, fourth ed., Pearson education limited, Essex, UK, 2004.

- Panias, D., Giannopoulou, I. P., Perraki, T. (2007). Effect of synthesis parameters on the mechanical properties of fly ash-based geopolymers, *Colloids and Surfaces A: Physicochemical and Engineering Aspects*, **301**, 246-254.
- Partha, S. D., Pradip, N., Prabir, K. S. (2014). The effects of ground granulated blast-furnace slag blending with fly ash and activator content on the workability and strength properties of geopolymer concrete cured at ambient temperature, *Materials and Design*, **62**, 32–39.
- Patcharapol, P., Charoenchai, R. , Chatchavan, E. , Duangchai, C. , Khuanchai, J., Prinya, C. (2015). Properties of lightweight high calcium fly ash geopolymer concretes containing recycled packaging foam, *Construction and Building Materials*, **94**, 408–413.
- Petermann, J., Saeed, A., Hammons, M. (2010). Alkali-activated geopolymers, *A Literature Review. Materials and Manufacturing Directorate*.
- Pradeep G. (2008). Response surface method. Saarbrücken, Germany: VDM Verlag Publishing.
- Rangan, B. V. (2011). Fly Ash-based geopolymer concrete, proceedings of the international workshop on geopolymer cement and concrete, *Allied Publishers Private Limited, Mumbai, India*, December, 68-106.
- Rattanasak, U. and Chindaprasirt, P. (2009). Influence of NaOH solution on the synthesis of fly ash geopolymer, *Minerals Engineering*, **22**, 1073-1078.
- Salih, M. A Farzadnia, N., Ali, A. A., Demirboga, R. (2015). Effect of different curing temperatures on alkali activated palm oil fuel ash paste, *Construction and Building Materials*, **94**, 116-125.
- Sanni, S. H., Khadiranaikar, R. B. (2013). Performance of alkaline solutions on grades of Geopolymer concrete, *International Journal of Research in Engineering and Technology*, **45**, 607–615.
- Sindhunata, V. D., Llukey, G., Xu, H. (2006). Effect of curing temperature and silicate concentration on fly-ash-based geopolymerization, *Industrial and Engineering Chemistry Research*, **45**, 3559–3568.

- Sinha, D. K., Kumar, A., Kumar, S. (2013). Reduction of pollution by using Fly ash, bottom ash and granulated blast furnace slag in geopolymer building materials, *Scholars Journal of Engineering and Technology*, **1**, 177-182.
- Somna, K, Jaturapitakkul, C, Kajitvichyanukul, P., Chindaprasirt, P. (2011). NaOH-activated ground fly ash geopolymer cured at ambient temperature, *Fuel*, **90**, 2118–2124.
- Temuujin, J., Williams, R. P., van Riessen, A. (2009). Effect of mechanical activation of fly ash on the properties of geopolymer cured at ambient temperature , *Journal of Materials Processing Technology*, **209**, 5276-5280.
- Thokchom, S., Dutta, D., Ghosh, S. (2011). Effect of incorporating silica fume in fly ash geopolymers, *International Journal of Civil, Environmental, Structural, Construction and Architectural Engineering*, **5**, 750-754.
- Thokchom, S., Ghosh P., Ghosh S. (2009). Effect of water absorption, porosity and sorptivity on durability of geopolymer mortars, *Journal of Engineering and Applied Sciences*, **4**, 28-32.
- TS500 (2000). Requirements for design and construction of reinforced concrete structures, *Turkish Standards Institution*, Ankara, Turkey.
- Van Jaarsveld, J. & van Deventer, J., (1999). The effect of metal contaminants on the formation and properties of waste-based geopolymers, *Cement and Concrete Research*, August, **29**, 1189-1200.
- Van Jaarsveld, J., Van Deventer, J., Lukey, G. (2002). The effect of composition and temperature on the properties of fly ash-and kaolinite-based geopolymers, *Chemical Engineering Journal*, **89**, 63–73.
- Villa, C., Pecina, E. T., Torres, R., Gomez, L. (2010). Geopolymer synthesis using alkaline activation of natural zeolite, *Construction and Building Materials*, **24**, 2084–2090.
- Wang, S. D and Scrivener, K. L. (1995). Hydration products of alkali activated slag cement, *Cement and Concrete Research*, **25**, 561-571.

Whitcomb, P. J., Anderson, M. J. (2004). RSM simplified: optimizing processes using response surface methods for design of experiments, New York: Taylor & Francis.

Yahya, Z., Al Bakri, A. M., Hussin, K. (2015). Effect of solids to liquids, Na_2SiO_3 to NaOH and curing temperature on the palm oil boiler ash (Si + Ca) geopolymerisation system, *Materials*, **8**, 2227-2242.

Yellaiah, P., Sanjay, K. S., .and Gunneswara Rao, T. D. (2014). Tensile strength of fly ash based geopolymer mortar, *ARPJ Journal of Engineering and Applied Sciences*, **9**, 2297-2301.

Zhang, H. Y., Kodur, V., Wua, B., Cao, L., Wanga, F. (2016). Thermal behavior and mechanical properties of geopolymer mortar after exposure to elevated temperatures, *Construction and Building Materials*, **109**, 17-24.

PERSONAL INFORMATION

Name and Surname : Safie Mahdi Oleiwi
Nationality : Iraq
Birth place and date : Diyala/1968
Marital status : Married – 4 kids
Mobile number : +90 5347382598 in Turkey
+964 7702370192 in Iraq
E-mail : safiemahdi@yahoo.com

EDUCATION

Degree	Graduate School	Year
Master	University of Al-Mustansiriya	2001
Bachelor	Salahaddin University-Erbil	1990
High School	Haddin High School	1985

WORK EXPERIENCE

Year	Place	Enrollment
1990-1995	Ministry of Industrial Military	Roads Department
2002-2008	Ministry of Transport	Project Implementation
2008-2014	University of Diyala	Assistant Lecturer
2014-	University of Diyala	Lecturer

PUBLICATIONS

Ali H. Hameed, safie M. Oleiwi, Shakir M. Mohmmmed, Ameer M Ibrahim, (2010).The effect of reinforcement on the ultrasonic pulse velocity for concrete, First Conference of Engineering Scientific, college of Engineering, Diyala university, 79-92.

Safie M. Oleiwi, (2014). Evaluate the depth of destroyed layer for reinforcement concrete samples exposed to fire, Diyala Journal of Engineering Sciences, 7 (3),1-18.

Kasım Mermerdas, Zeynep Algin , Safie Mahdi Oleiwi, Dia Eddin Nassani,(2017). Optimization of lightweight GGBFS and FA geopolymer mortars by response surface method, Construction and Building Materials, 139, 159-171.